PB-232 453

ADSORPTION FROM AQUEOUS SOLUTION

W. J. Weber, et al

Michigan University

Prepared for:

Environmental Protection Agency

June 1974

DISTRIBUTED BY:

NTIS
National Technical Information Service
U. S. DEPARTMENT OF COMMERCE
5285 Port Royal Road, Springfield Va. 22151

SELECTED WATER RESOURCES ABSTRACTS

INPUT TRANSACTION FORM

1. Report No.

2.

PB 232 453

W 74-07739

4. Title

ADSORPTION FROM AQUEOUS SOLUTION,

5. Report Date

6.

8. Performing Organization Report No.

7. Author(s)

W. J. Weber, Jr., and P. J. Usinowics

10. Project No.

EPA Project 17020 EPF

9. Organization

Michigan University, Ann Arbor, Environmental and Water Resources Engineering

11. Contract/Grant No.

12. Sponsoring Organization

13. Type of Report and Period Covered

15. Supplementary Notes --Environmental Protection Agency, Cincinnati, Ohio, Report EPA-670/2-74-012, June 1974. 236 p, 130 ref, 4 append.

Reproduced from best available copy.

16. Abstract

A model based on material balance concepts and second-order reaction kinetics is presented for prediction of the performance of expanded-bed adsorption systems for treatment of complex mixtures of dissolved organic materials in aqueous solution. The model utilizes system parameters measured or calculated from bench-scale batch experiments, correlative techniques, and hydrodynamic considerations. The major focal point of these investigations is the description of the mixtures as composite solutes by using an overall concentration parameter (chemical oxygen demand, COD) and mathematic treatment of the mixtures as single-solute systems for prediction of continuous flow adsorber breakthrough profiles. (EPA)

17a. Descriptors --*Waste water treatment, *Mathematical models, *Activated carbon, *Kinetics, *Adsorption, *Forcasting, Model studies, Chemical oxygen demand, Mixing.

ⓔ

17b. Identifiers

Reproduced by
NATIONAL TECHNICAL
INFORMATION SERVICE
U S Department of Commerce
Springfield VA 22151

17c. COWRR Field & Group 05D

18. Availability

Available from the National Technical Information Service as PB $ 15.00 in ~~paper copy, $1.45 in microfiche.~~

19. Security Class. (Report)

20. Security Class. (Page)

21. No. of Pages 238

22. Price 15.00

Send To:

WATER RESOURCES SCIENTIFIC INFORMATION CENTER
U.S. DEPARTMENT OF THE INTERIOR
WASHINGTON, D.C. 20240

Abstractor

Institution

ABSTRACT

A model based on material balance concepts and second-order reaction kinetics is presented for prediction of the performance of expanded-bed adsorption systems for treatment of complex mixtures of dissolved organic materials in aqueous solution. The model utilizes system parameters measured or calculated from bench-scale batch experiments, correlative techniques, and hydrodynamic considerations. The major focal point of these investigations is the description of the mixtures as composite solutes by using an overall concentration parameter (chemical oxygen demand, COD) and mathematic treatment of the mixtures as single-solute systems for prediction of continuous flow adsorber breakthrough profiles.

Twelve mixtures varying in composition and adsorption characteristics are used to determine the applicability of the model. The mixtures were composed of compounds selected to exhibit a wide range of adsorption behavior. The experimental results demonstrate that the adsorption parameters required as input to the model can be developed for the mixtures based on the overall concentration parameter. Non-adsorbing fractions of the total concentration may be determined through examination of experimental adsorption isotherms.

The model was tested for prediction of continuous flow column performance for the twelve mixtures and found to correspond well to experimentally-generated breakthrough curves up to at least 50% breakthrough. Continued operation beyond this point commonly results in better-than-predicted removal of solute.

The kinetic model is compared to a mathematically-simpler mass-transfer model and found to be a more accurate predictive tool for the breakthrough profiles.

Experimental investigations of the adsorption behavior of individual components of two binary mixtures are reported. The individual components were examined as pure solutions, as a mixture, and as sequentially added components following prior exposure of the adsorbent to the other mixture compound. Asymmetric profiles were experimentally generated for the pure solutions, resulting in similar deviations between predicted and measured breakthrough curves. Reasons for these deviations are postulated and discussed.

This report was submitted in fulfillment of Project Number 17020 EPF under the sponsorship of the Environmental Protection Agency. Only the initial stages of the work reported herein was performed under this EPA sponsorship; the remainder of the work was completed under Grant Number GK-35060 from the National Science Foundation. The work, which is presented in its entirety for the benefit of the reader, was performed by the University of Michigan, Environmental and Water Resources Engineering Program, College of Engineering, Ann Arbor, Michigan 48104

TABLE OF CONTENTS

CONCLUSIONS i

RECOMMENDATIONS viii

LIST OF TABLES x

LIST OF ILLUSTRATIONS xi

NOMENCLATURE xvi

I. INTRODUCTION 1

2. MATHEMATIC MODEL DEVELOPMENT 7

Second-order Kinetic Approach of Thomas.. 11

Material Balance Relationships for Expanded-Bed System 13

Mass-Transfer Relationships 23

3. EXPERIMENTAL MATERIALS AND ANALYTIC PROCEDURES 33

Complex Solute Mixtures 33

Active Carbon 40

Analytic Methods 42

Experimental Column System 44

4. PARAMETER DETERMINATIONS FOR UTILIZATION OF PREDICTIVE MATHEMATIC MODEL 50

Fixed Parameters 50

Hydrodynamic Parameters 51

Adsorption Equilibrium Constants 54

Diffusional Mass-Transfer Coefficients .. 81

5. CONTINUOUS FLOW EFFLUENT - CONCENTRATION HISTORY PROFILES 121

TABLE OF CONTENTS (continued)

Predicted Profiles and Experimental Verification for Sorbate Mixture System 124

Predicted Profiles and Experimental Verification for Adsorber/Non-Adsorber Systems 134

Comparison of Mathematic Models 142

6. MIXTURE COMPONENT ANALYSIS 145

General Considerations 145

Experimental Investigations 151

Results of Batch Experiments 153

Concentration-History Profile of Individual Components in Competitive Adsorption 159

Phenol 162

Phenol: Mix 1 162

Phenol: Mix 2 165

Dodecyl Sodium Sulfate 166

Dodecyl Sodium Sulfate: Mix 1 166

Dodecyl Sodium Sulfate: Mix 2 170

Elution of Compounds 172

Discussion of Component Analysis Results 175

Secondary Adsorption Phenomena 177

TABLE OF CONTENTS (continued)

REFERENCES 180

APPENDICES

Appendix 1: Laplace Transform A1-1

Appendix 2: COD Determination Using Technicon$_R$ Autoanalyzer ... A2-1

Appendix 3: Computer Program for Kinetic Model A3-1

Appendix 4: Michaels Equilibrium Mathematic Model A4-1

Computer Program Solution for the Michaels Equilibrium Model A4-11

CONCLUSIONS

The complexity of analytic measurement techniques and of mathematic formulations for evaluation of individual compounds in multicomponent systems subject to adsorption phenomena dictates the desirability of simplification techniques for delineation of total system behavior. A simplification procedure investigated in this research utilized an overall description parameter based on chemical oxygen demand to characterize complex mixtures of dissolved organic compounds ranging in individual sorption properties. The sorption properties of the mixtures based on the overall description parameter subsequently permitted the use of mathematic models formulated for single component sorption systems. The applicability of this simplifying technique was the principal focal point of this research.

The adaptation of the second-order surface-reaction-controlled kinetic formulations of Thomas by Hiester and Vermeulen for prediction of packed-bed adsorber column performance and the subsequent extension of these works by Keinath and Weber to expanded-bed adsorber systems provided the primary mathematic model for evaluation. This mathematic model incorporates the use of the generalized Langmuir isotherm for description of equilibrium distribution of sorbate between fluid- and solid-phases. Hiester and Vermeulen have related the diffusional mass-transfer rate expressions to the second-order surface-reaction expression given in the development of Thomas. These adsorption isotherm and mass-transfer parameters are available from bench-scale batch experiments or correlative techniques. Hydrodynamic descriptions of the expanded-bed adsorber system provide the remaining input parameters for the use of the predictive mathematic model.

The use of an overall description parameter to develop the adsorption isotherm and mass-transfer rate constants essentially yields effective average adsorption behavior measurements of a complex sorbate system. The experimental portion of this research related to the determination of these adsorption constants demonstrated that the adsorption isotherms for complex mixtures could be successfully generated on a COD basis and then adequately described by the Langmuir adsorption isotherm relationship. Furthermore, the experimental adsorption isotherm development provided a simple procedure for effectively measuring non-adsorbing fractions of dissolved materials which are included in the overall description parameter concentration but which are not indicative of adsorber-bed performance. In systems in which only adsorption phenomena contribute to the removal of dissolved materials, non-adsorbing components will remain unchanged, and hence must not be included in evaluation of the adsorption performance of a system. This is not to negate the potential importance of such non-adsorbing fractions because an overall reduction of dissolved organic material concentrations based on the overall description parameter may be of primary interest. However, in evaluation of the adsorption process as a means of accomplishing a reduction of part of the total dissolved organics concentration as one step in a series of unit operations, exclusion of the non-adsorbing fraction clarifies the performance of the adsorber bed.

Correlation techniques based on the work of Resnick and White provide a method for determination of external diffusion mass-transfer rate constants. In order to utilize this approach, it is necessary to provide an effective molecular volume for the complex mixture based on the equivalent molecular weight of one COD unit. An approach based on Kopp's Law for determination of the effective molecular volume has been presented and found to be adequate for use in the predictive mathematic model.

Internal diffusion mass-transfer rate constants were determined for rapidly-agitated bench-scale batch experiments. The internal pore-surface diffusion constant formulation was found to be controlling internal mass-transfer mechanism due to the magnitude of the solid-fluid phase distribution constant. However, due to the magnitude of this distribution constant, external diffusion was found to be the overall rate-limiting mechanism. Hiester and Vermeulen related these diffusional mass-transfer rate constants, using a linear driving-force relationship after Michaels, to the second-order kinetic surface-reaction controlled rate expression proposed by Thomas. Thus an overall rate constant, assuming series addition of diffusional mass-transfer effects, may be determined.

The hydrodynamic formulations for the parameter determinations of a given expanded-bed system have been set forth by Keinath and Weber. These concepts allow the computation of expanded-bed porosity, volume, and height which are needed in application of the predictive mathematic model.

The adsorption isotherm and diffusional mass-transfer rate constants, and the hydrodynamic characterizations of the expanded-bed adsorber systems provided the necessary input measurements for evaluation of the applicability of the predictive mathematic model to complex mixtures of dissolved organic compounds classified by an overall description concentration measurement parameter as a single solute system. Twelve mixtures of organic compounds were used, eight of which contained only sorbable constituents, and four of which had non-sorbable fractions included. The results of comparisons of the mathematically predicted effluent concentration-history profiles and the experimentally-generated data illustrated that for all systems, there was good agreement between the two profiles up to 0.5 C_o effluent concentration. One system exhibited a symmetrical experimental profile in complete accord with the mathematic prediction, but all other systems indicated better-than-predicted adsorber performance, deviating from the predicted profiles after 0.5 - 0.8 C_o effluent concentration.

The second-order kinetic model was compared to the mathematically-simpler equilibrium model of Michaels to determine if the increased complexity of the former mathematic model resulted in better prediction of adsorber bed performance. This comparison justified the use of the more complex mathematic model because the equilibrium model demonstrated inability to adequately describe any portion of the actual experimental effluent concentration-history profile. Obviously, therefore, the kinetic model is by far preferred over the equilibrium model.

Several possible explanations may be postulated with respect to the demonstrated inability of the kinetic mathematic model to predict the latter stages of the effluent concentration-history profiles. The mathematic model is formulated using a simplified rate law to define the diffusional mass-transfer processes, with constant diffusional mass-transfer rate coefficients. This results in a symmetric sigmoidal-shaped profile. The asymmetry of the experimental systems indicate that the simplified rate expression is a probable source for the deviations between the predicted and experimental profiles observed. However, this cannot be ascertained a priori because complex mixtures of sorbates were used in these experimental investigations, and the behavior of such systems must also be considered. Several effects, not simulated in batch experimental investigations, present themselves in flow through adsorber-bed operations. One effect is chromatographic separation, wherein a less readily adsorbed compound comprises the total effluent concentration of an adsorber-bed for a period of time before other more-adsorbable compounds begin to pass through. Another effect is the noted increase in capacity when a slow reaction follows an initial fast reaction. The possibility of this occurring has been illustrated. Displacement phenomena can further complicate the adsorption process. Secondary adsorption phenomena, including multilayer adsorption effects and micelle production within the porous adsorbent, may also be contributing factors to the apparently better adsorption observed in the experimental systems than that predicted by the mathematic model.

Component analyses were performed with batch and continuous-flow adsorption systems to provide information concerning the reasons for the discrepancies observed with respect to the effluent concentration-history profiles. The batch experiments illustrated competitive effects on the rate-of-uptake of individual sorbates when in a mixture versus in pure solution. The rates were retarded in the former situation. When a pure solution of sorbate was sequentially exposed to the adsorber, the rate of uptake approximated that of the sorbate in the mixture.

The continuous-flow adsorber-bed component analyses yielded several important results. The effluent concentration-history profiles for the pure solutions were asymmetrical and generated the same general deviations from their mathematically predicted profiles. The adsorber bed, although saturated by a pure solution of one compound of the same concentration as in its mixture, still exhibited a capacity for the second compound sequentially added to it. The individual effluent concentration-history profiles for the sorbates added as a mixture developed more rapidly than for the pure solution cases.

There is evidence of competition for adsorption and also of unavailability of adsorption sites for all compounds of a mixture as a result of these component experiments. But perhaps the most significant result of the component analysis lies in the fact that the effluent concentration-history profiles for the pure sorbate solutions, introduced to a full-adsorption capacity adsorber bed,

was asymmetrical. This strongly suggests that the simplified diffusional mass-transfer rate law does not hold for the total operation period of the continuous-flow system.

It has been demonstrated in this research that a complex mixture of dissolved organics may be simplified by classifying it by an overall description parameter which can be used to develop adsorption isotherm and diffusional mass-transfer rate constants. The adsorption isotherm development provides a means for determining non-adsorbing fractions of the overall description parameter, thereby clarifying the effectiveness of sorption operations for the portion of the complex mixtures subject to removal by the physicochemical process. The mathematic model based on reaction-kinetics after Thomas utilizing the adsorption isotherm parameters and diffusional mass-transfer rate constants developed for twelve complex mixtures based on an overall description parameter predicted effluent concentration-history profiles in good agreement with all respective mixture experimentally-generated profiles for at least 0.5 C_o effluent concentration, which is well within the critical region of interest. When compared to the Michaels equilibrium mathematic model, it is evident that the more complex second-order reaction kinetic mathematic model is more realistic in describing the actual experimental profile data.

RECOMMENDATIONS

Although the second-order kinetics mathematic model successfully predicts at least fifty percent of the effluent concentration-history profiles for complex mixtures simplified to "single solute" systems, the descrepancies found between the mathematically-predicted and the experimentally-generated profiles for pure components suggest re-evaluation of the basic simplifying assumptions used to formulate the mathematic model. The most obvious starting point for this is the formulation of the diffusional mass-transfer rate equation. In order to achieve more complete mathematic prediction ability, the rate equation may have to be redefined by a more 'exact' description of the concentration gradient which controls diffusion. Although an analytic solution would probably be impossible, numerical techniques are available, and the tedium of such methods of analysis is lessened considerably by the use of computers. The major consideration of the usefulness of such a model will be the evaluation of added accuracy of prediction versus the additional expenditure of effort for utilization of that mathematic model in comparison to less-accurate but mathematically-easier models.

The ultimate aim of mathematic modelling of continuous-flow adsorber-bed systems with respect to wastewater treatment is to develop a model which will predict the performance of an adsorber bed in which all major effects of contaminant removal are incorporated. This will require the mathematic description of biological enhancement of adsorption processes as has been noted in pilot- and full-scale demonstration plants. This requires accurate predictive models for the adsorption processes alone. It may be possible to extend the second-order kinetic model to include the effects of uptake of sorbates by biological activity within the adsorber-bed, with good correlative results obtaining. Such an approach should be taken only after evaluation of a more "exact" expresion for the rate of diffusional mass-transfer has been investigated in developing a predictive mathemathic model. If the latter approach yields better correlations to experimental effluent concentration-history profiles, then that model should be expanded to include biological activity effects.

LIST OF TABLES

Table	Title	Page
3-1	Physical and Chemical Characteristics of Mixture Components	35
3-2	Chemical Oxygen Demand of Mixture Components	36
3-3	Binary Mixture Composition	38
3-4	Ternary Mixture Composition	39
3-5	Adsorber / Non-Adsorber Mixture Composition	41
4-1	Langmuir Isotherm Constants for Pure Compounds Used in Mixtures	62
4-2	Langmuir Isotherm Constants for Sorbate Mixtures	73
4-3	Langmuir Isotherm Constants for Adsorber/ Non Adsorber Mixtures	80
4-4	Parameters for Determination of External Diffusion Rate Constant	85
4-5	Internal Mass Transfer Rate Constants	114
5-1	Hydrodynamic Properties of Columnar System	122
5-2	Adsorption Parameters for Model Utilization	123

LIST OF ILLUSTRATIONS

Figure	Title	Page
2-1	Typical Adsorption Wave in Adsorber Column	8
2-2	Material Balance for Adsorption Column	14
3-1	Calibration Curve for Chemical Oxygen Demand	43
3-2	Absorb Spectrum for Phenol	45
3-3	Calibration Curve for Phenol	46
3-4	Schematic Representation of Experimental Column Setup	47
4-1	Adsorption Isotherm: Phenol	58
4-2	Adsorption Isotherm: Dodecyl Sodium Sulfate	59
4-3	Adsorption Isotherm: n-Hexanol	60
4-4	Adsorption Isotherm: Mix 1	65
4-5	Adsorption Isotherm: Mix 2	66
4-6	Adsorption Isotherm: Mix 3	67
4-7	Adsorption Isotherm: Mix 4	68
4-8	Adsorption Isotherm: Mix 5	69
4-9	Adsorption Isotherm: Mix 6	70
4-10	Adsorption Isotherm: Mix 7	71
4-11	Adsorption Isotherm: Mix 8	72
4-12	Adsorption Isotherm: Mix 9	75
4-13	Adsorption Isotherm: Mix 10	76
4-14	Adsorption Isotherm: Mix 11	77
4-15	Adsorption Isotherm: Mix 12	78
4-16	Experimental Rate Study: Mix 1	89
4-17	Experimental Rate Study: Mix 2	90

LIST OF ILLUSTRATIONS (continued)

Figure	Title	Page
4-18	Experimental Rate Study: Mix 3	91
4-19	Experimental Rate Study: Mix 4	92
4-20	Experimental Rate Study: Mix 5	93
4-21	Experimental Rate Study: Mix 6	94
4-22	Experimental Rate Study: Mix 7	95
4-23	Experimental Rate Study: Mix 8	96
4-24	Experimental Rate Study: Mix 9	97
4-25	Experimental Rate Study: Mix 10	98
4-26	Experimental Rate Study: Mix 11	99
4-27	Experimental Rate Study: Mix 12	100
4-28	Rate Data for Determination of Internal Diffusion Rate Constant: Mix 1	101
4-29	Rate Data for Determination of Internal Diffusion Rate Constant: Mix 2	102
4-30	Rate Data for Determination of Internal Diffusion Rate Constant: Mix 3	103
4-31	Rate Data for Determination of Internal Diffusion Rate Constant: Mix 4	104
4-32	Rate Data for Determination of Internal Diffusion Rate Constant: Mix 5	105
4-33	Rate Data for Determination of Internal Diffusion Rate Constant: Mix 6	106
4-34	Rate Data for Determination of Internal Diffusion Rate Constant: Mix 7	107
4-35	Rate Data for Determination of Internal Diffusion Rate Constant: Mix 8	108
4-36	Rate Data for Determination of Internal Diffusion Rate Constant: Mix 9	109

LIST OF ILLUSTRATIONS (continued)

Figure	Title	Page
4-37	Rate Data for Determination of Internal Diffusion Rate Constant: Mix 10	110
4-38	Rate Data for Determination of Internal Diffusion Rate Constant: Mix 11	111
4-39	Rate Data For Determination of Internal Diffusion Rate Constant: Mix 12	112
4-40	Sensitivity of Kinetic Mathematic Model to Variations in Langmuir Ultimate Capacity, Q	115
4-41	Sensitivity of Kinetic Mathematic Model to Variations in Langmuir Energy Constant, b	117
4-42	Sensitivity of Kinetic Mathematic Model to Variations in External Diffusion Rate Constant, $k_f a$	119
5-1	Expanded-Bed Adsorber Effluent Concentration-History Profile: Mix 1	125
5-2	Expanded-Bed Adsorber Effluent Concentration-History Profile: Mix 2	126
5-3	Expanded-Bed Adsorber Effluent Concentration-History Profile: Mix 3	127
5-4	Expanded-Bed Adsorber Effluent Concentration-History Profile: Mix 4	129
5-5	Expanded-Bed Adsorber Effluent Concentration-History Profile: Mix 5	130
5-6	Expanded-Bed Adsorber Effluent Concentration-History Profile: Mix 6	131
5-7	Expanded-Bed Adsorber Effluent Concentration-History Profile: Mix 7	132
5-8	Expanded-Bed Adsorber Effluent Concentration-History Profile: Mix 8	133

LIST OF ILLUSTRATIONS (continued)

Figure	Title	Page
5-9	Expanded-Bed Adsorber Effluent Concentration-History Profile: Mix 9	136
5-10	Expanded-Bed Adsorber Effluent Concentration-History Profile: Mix 10	137
5-11	Expanded-Bed Adsorber Effluent Concentration-History Profile: Mix 11	138
5-12	Expanded-Bed Adsorber Effluent Concentration-History Profile: Mix 12	139
6-1	Types of Column Effluent Concentration-History Profiles	146
6-2a	Illustration of Chromotographic Effect	149
6-2b	Illustration of Chromotographic Effect	150
6-3	Component Rate Studies for Phenol: Mix 1	154
6-4	Component Rate Studies for Phenol: Mix 2	155
6-5	Component Rate Studies for Dodecyl Sodium Sulfate: Mix 1	157
6-6	Component Rate Studies for Dodecyl Sodium Sulfate: Mix 2	158
6-7	Expanded-Bed Adsorber Effluent Concentration-History Profile: Mix 1	160
6-8	Expanded-Bed Adsorber Effluent Concentration-History Profile: Mix 2	161
6-9	Component Effluent Concentration-History Profiles in Expanded Bed Operation: Phenol, Mix 1	163
6-10	Component Effluent Concentration-History Profiles in Expanded Bed Operation: Phenol, Mix 2	164

LIST OF ILLUSTRATIONS (continued)

Figure	Title	Page
6-11	Component Effluent Concentration-History Profiles in Expanded Bed Operation: Dodecyl Sodium Sulfate, Mix 1	167
6-12	Component Effluent Concentration-History Profiles in Expanded Bed Operation: Dodecyl Sodium Sulfate, Mix 2	168
6-13	Desorption of Phenol	173
6-14	Desorption of Dodecyl Sodium Sulfate	174
A2-1	Chemical Oxygen Demand Auto Analyzer System	192
A4-1	Idealized Effluent Concentration-History Profile	199
A4-2	Idealized Counter Current Adsorption	203
A4-3	Adsorption Isotherm and Operating Line	205

NOMENCLATURE

ROMAN

Symbol	Description and Units
a	Effective area for mass transfer through the film surrounding the adsorbent particle, (cm^2/cm^3)
a'	$a\gamma$ (cm^2/cm^3)
A	Dummy variable
A_c	Cross sectional area of adsorber column (cm^2)
b	Langmuir equilibrium energy constant $(cm^3/gram)$
B	Dummy variable
C	Concentration of solute in bulk solution at a specified point in the column, $(grams/cm^3)$
C_1	Dummy variable
C_b	Concentration of solute in bulk solution at breakthrough $(grams/cm^3)$
C_e	Concentration of solute in the fluid phase in equilibrium with adsorbed amount in the solid phase $(grams/cm^3)$
C_j	Internal or pore concentration of solute in the fluid phase, $(grams/cm^3)$
C_o	Influent concentration of solute, $(grams/cm^3)$
C_R	Quantity of solute removed from the solution within the primary adsorption zone, (grams)
C_x	Solute concentration at adsorber bed exhaustion, $(grams/cm^3)$
d_p	Diameter of adsorbent particle, (cm)
D_ℓ	Free-liquid diffusivity of solute, (cm^3/sec)

NOMENCLATURE (continued)

Symbol	Description and Units
D_G	Ratio of solid-phase and fluid-phase concentrations of solute at saturation, ($q_\infty \rho / C_0 \varepsilon$), (dimensionless)
D_p	Intraparticle or pore diffusivity of the solute in the fluid phase, (cm^2/sec)
D_s	Intraparticle or pore diffusivity of the solute in the solid phase, (cm^2/sec)
f	Fractional capacity of adsorbent remaining at breakpoint, (dimensionless)
F	Volumetric flow rate through column, (cm^3/min)
$F(\varepsilon)$	Function of void ratio, (dimensionless)
g	Gravitational acceleration term, (cm/sec^2)
h	Height of primary adsorption zone, (cm)
H	Height of adsorber bed in expanded state, (cm)
j_d	Mass transfer factor, (dimensionless)
k	Second-order surface-reaction-controlled adsorption rate constant, ($cm^3/gram/min$)
k_r	First-order surface-reaction-controlled desorption rate constant, (min^{-1})
k_f	External-diffusion controlled mass transfer rate constant, (cm/min)
k_p	Intraparticle fluid-phase pore diffusion controlled mass transfer rate constant, (cm/min)
k_s	Intraparticle solid-phase pore diffusion controlled mass transfer rate constant, (cm/min)
K	Overall mass transfer rate coefficient for equilibrium model (cm/min)
L	Length of expanded bed, (cm)
m_s	Superficial rate of saturation of adsorbent ($gram/min/cm^2$)

NOMENCLATURE (continued)

Symbol	Description and Units
M	Molecular weight of solvent (grams/mole)
N_{Gr}	Grashof number, ($N_{Gr} = dp^3\rho_\ell(\rho_s-\rho_\ell)g/\mu^2$), (dimensionless)
N_{Re}	Reynolds number, ($N_{Re} = d_p v_p \rho_\ell/\mu$), (dimensionless)
N'_{Re}	Modified Reynolds number, ($N'_{Re} = d_p v_p \rho_\ell/\mu(1-\varepsilon)$), (dimensionless)
N_{Sc}	Schmidt number, ($N_{Sc} = \nu/D_\ell$), (dimensionless)
p	Dummy variable
q	Dummy variable
q	Amount of solute adsorbed per unit weight of adsorbent averaged over the entire particle at a specified time and position in the column, (grams/gram)
q_b	Amount of solute adsorbed per unit weight of adsorbent at breakpoint, (grams/gram)
q_e	Amount of solute adsorbed per unit weight of adsorbent in equilibrium with the coexisting liquid phase concentration, (grams/gram)
q_j	Internal solid-phase concentration of adsorbed solute, (grams/gram)
q_x	Amount of solute adsorbed per unit weight of adsorbent at exhaustion of adsorber bed, (grams/gram)
q_∞	Saturation capacity, amount of solute adsorbed per unit weight of adsorbent in equilibrium with influent concentration, C_o, (grams/gram)
Q	Ultimate capacity of the adsorbent, Langmuir monolayer ultimate capacity, (grams/gram)
r	Equilibrium modulus, ($r = 1/(1+bC_o)$), (dimensionless)
R	Radial distance from center of spherical particle, (cm)

NOMENCLATURE (continued)

Symbol	Description and Units
R_p	Total radius of spherical particle, (cm)
S	Degree of saturation at breakpoint, (dimensionless)
S_b	Amount of solute accumulated in the adsorber bed per unit cross sectional area at breakpoint, (grams/cm^2)
S_s	Total amount of solute which will accumulate in the adsorber bed per unit cross sectional area (grams/cm^2)
t	Dummy variable
T	Absolute temperature, (degrees Kelvin)
t_f	Time of formation of primary adsorption zone, (min)
t_h	Time for primary adsorption zone to travel its own height, (min)
t_x	Time required for exhaustion of adsorber bed, (min)
v	Bulk volume of expanded bed, (cm^3)
$(v_{p_o})_I$	Terminal particle velocity for Intermediate Law regime, (cm/sec)
$(v_{p_o})_N$	Terminal particle velocity for Newton's Law regime, (cm/sec)
$(v_{p_o})_S$	Terminal particle velocity for Stokes' Law regime, (cm/sec)
V	Total volume of solution fed to column, (cm^3)
V_a	Total effluent volume flowing through the adsorber bed during the appearance of the primary adsorption zone in the effluent, (cm^3)
V_b	Total volume passed through adsorber bed up to breakpoint, (cm^3)
V_e	Total effluent volume passing through adsorber bed, (cm^3)

NOMENCLATURE (continued)

Symbol	Description and Units
V_p	Volume of adsorbent particle, (cm^3)
V_o	Molecular volume of solute molecule at normal boiling point, (cm^3/mole)
V_{o_m}	Effective molecular volume of mixture, (cm^3/gram-mole COD)
V_x	Total volume of solution passed through adsorber bed at exhaustion, (cm^3)
$\overline{V}$	Superficial velocity of flow through adsorber bed, (cm/min)
x	Dummy variable
x_c	Concentration of adsorbent, (grams/cm^3)
X	Association parameter for the solvent in the Wilke-Chang correlation, (dimensionless)
y	Dummy variable
z	Dummy variable
GREEK	
α	Dummy variable
β	Dummy variable
γ	Intraparticle void ratio, (dimensionless)
ε	Interparticle void ratio in expanded bed, (dimensionless)
η	Variable of integration
κ	General rate coefficient for combined resistances, (min^{-1})
κ_f	External-diffusion mass transfer rate coefficient, (min^{-1})
κ_I	Internal-diffusion mass transfer rate coefficient, (min^{-1})

NOMENCLATURE (continued)

Symbol	Description and Units
κ_p	Intraparticle fluid-phase pore-diffusion mass transfer rate coefficient, (min^{-1})
κ_s	Intraparticle solid-phase pore-diffusion mass transfer rate coefficient, (min^{-1})
λ	Wavelength, (millimicrons)
μ	Absolute viscosity, (centipoise)
ν	Kinematic viscosity, (stokes)
ξ	Variable of integration
π	3.1416
ρ	Density of adsorbent in the expanded bed, ($grams/cm^3$)
ρ_ℓ	Density of solvent, ($grams/cm^3$)
ρ_s	Density of adsorbent, ($grams/cm^3$)
σ	Dummy variable
τ	Time from first entry of solution to column, (min)
θ	Dummy variable
ω	Dummy variable

Chapter 1

INTRODUCTION

The population growth and industrial expansion that has occurred in the United States in the last quarter century has exerted serious demands on the natural water resource. This same growth and industrialization has contributed also to degradation of available water sources as a result of increased quantities and complexities of waste products discharged into these waters. The natural purification or assimilation capacities of waterways in most population and industrial centers has been far exceeded, so that previous concepts of using these waterways as waste purifiers are untenable (42). Conventional water and waste water treatment schemes are only partially effective against the expanding list of refractory compounds, and stream self-purification is unlikely for compounds which have resisted waste treatment.

The Advanced Waste Treatment Research program was initiated in 1960 in response to recognition of the need for more complete treatment of waste waters than afforded by conventional methods. The objectives of this program were to evaluate and develop additional and alternative treatment methods to produce a satisfactory effluent for discharge into receiving waters or for direct subsequent reuse as a water supply (76). A primary consideration for the development of this program pertained to the fact that an estimated forty per cent of the population was using water which in part had previously been discharged as a sewage effluent (76). The need for such evaluations of wastewater treatment processes takes on added significance when future projected total water demands for the United States are considered. It is estimated that by the year 2000, total water requirements for the United States will exceed the supply presently regarded as useable surface water (12). It thus appears that wastewater will of necessity be considered as a water resource in the future.

Currently, wastewater reuse - both indirect and direct - is recognized as requiring more complete removal of pollutant materials from waters than is achieved by conventional biologic treatment (97). Stephen (95) indicated in a survey of U.S. cities that, after both conventional primary and secondary treatment of sewage, approximately 50 milligrams per liter (mg/l) of organic contaminants and 300-400 mg/l of dissolved inorganic materials were present in the effluents. In order to protect receiving waters and subsequent users of the waters into which these effluents are discharged, it is evident that further reduction in the levels of these contaminants is necessary.

Of the various methods of wastewater treatment examined within the AWTR program, one of the most promising to emerge for the removal of perdurable dissolved organic contaminants is adsorption (77) with active carbon (129). There are several systems of application for this process (15), but the one which has been shown to be the most advantageous is the continuous-flow columnar system (49, 50, 78, 114, 121), operated in either a fixed-bed (49, 50) or an expanded-bed (78, 114, 121) mode.

Applications of active carbon for treatment of secondary effluents from conventional biological wastewater-treatment operations have indicated definite improvement in effluent quality (48, 79, 80, 85, 130), with small residual fractions of organic content in the effluents from 'tertiary' active carbon treatment consisting primarily of partially oxidized substrates and metabolites of microorganisms((78).

Perhaps the biggest drawback in utilizing active carbon in a tertiary treatment scheme is economic. The additional cost involved often equals the cost of conventional primary/secondary treatment (84) and the additional benefits may not be economically justifiable. However, the direct treatment of wastewater by physicochemical methods of chemical coagulation and adsorption has been found to afford the benefit of superior quality effluents and more stable operation while being economically competitive with conventional wastewater treatment alone (9, 33, 84, 88, 119). The potential for industrial reuse of physicochemically treated wastewater is being investigated in a 2.0 million gallons per day demonstration plant in Colorado Springs, Colorado (36), and numerous demonstration and pilot plant studies concerning physicochemical treatment schemes are continuing throughout the country (96).

Contact systems for application of granular active carbon, as previously noted, are usually columns or beds operated in either fixed-bed or expanded-bed mode. In wastewater treatment, expanded-bed operation has been shown to involve fewer operational difficulties and freedom from problems commonly experienced in packed-bed treatment (123). Problems of clogging, severe head loss and air binding due to particulate matter, microbial growth, and dissolved gases are minimized in expanded beds. While the adsorption process has been found equally effective for both packed- and expanded- beds of active carbon, the lower power and maintenance requirements and advantages of relatively uninterrupted operation indicate that the expanded-bed mode is to be preferred (43, 116).

It is evident that the physicochemical wastewater-treatment process of adsorption is gaining prominence as a means for producing quality effluents which are low in concentrations of dissolved organic material. However, to design adsorption columns, it usually has been necessary to generate reasonably long-term performance data for a specific waste from pilot-plant studies. Such experimental systems are relatively complex, their construction and operation both costly and time consuming. If prediction of adsorption performance for that waste were available from equilibrium and mass-transfer parameters obtained from simple bench-scale batch experiments, then the design of adsorption columns would be greatly facilitated, as bench-scale batch experiments have the advantage of ease of adaptability to small volume work, ease of investigation of variation in parameters, and general facility of operation.

Keinath and Weber (55) have proposed a mathematic model for prediction of expanded-bed adsorber performance for single solute systems utilizing data obtained from batch experiments and correlative techniques. They have proposed further that this predictive model could be extended to predict adsorber performance for individual solutes in complex mixtures, provided appropriate individual equilibrium and rate parameters could be evaluated (55).

The investigations reported herein deal with the application of the Keinath-Weber model to predict concentration-history profiles for expanded-bed adsorbers for complex sorbate mixtures. An important aspect of this work lies in an attempt to mathematically and experimentally treat complex multicomponent sorbate mixtures in the same manner as single solute systems, characterizing them by an overall concentration parameter rather than by identifying and developing parameters for each of the individual components. The single-solute approach to complex mixtures, if applicable, could have several advantages beside relative mathematic and experimental simplicity, since the individual components of a wastewater are commonly in such small concentrations and/or so numerous as to render identifications and measurements for each extremely difficult, if not impossible, in application situations. Although reasonably sophisticated analytical techniques (65) are available for identification of many wastewater components, even many of these available techniques will need to be simplified before routine use can be made of them, as they generally require specialized procedures developed for specific situations. Additionally, the composition of domestic sewage consists of organic components which are even yet largely (60-70%) unidentified (76) and generally reported only according to rather broad categories (46).

The overall descriptive concentration parameter chosen for this research is chemical oxygen demand (COD). This parameter is commonly used for classification of the strength of a wastewater and generally includes dissolved organic compounds which are biologically inactive or resistant as well as those compounds which are biologically degradable. The research also illustrates and discusses a method for adequately handling non-adsorbing compounds which are measured in the overall concentration parameter. This is a necessary consideration in utilizing the single-solute approach to complex mixtures, as non-adsorbing fractions will appear in the effluent concentration-history curve from initial operation of the adsorption column and can result in misinterpretation of adsorber performance.

The results of this research will ultimately provide a method for developing design criteria for expanded-bed adsorbers to meet effluent-quality criteria. The ability to predict the critical regions of the concentration-history profile also provides a basis for continued efforts to expand the mathematic model to account for the apparent enhancement of wastewater treatment due to biological activity as noted in many earlier investigations on actual sewage (33,78,82,115). It may be desirable to seek a more exact solution for the total concentration-history curve in developing a mathematic model with biological activity included, depending on the complexity of the numerical procedure needed to generate solutions for such a model. However, the reported research represents a good starting point for comparison of the benefits of additional accuracy versus the increased difficulty of solution of more complex mathematic relationships.

CHAPTER 2

MATHEMATIC MODEL DEVELOPMENT

The removal of sorbate material in adsorption beds results in a variable concentration distribution curve of the sorbate within the bed. A typical sorbate concentration distribution curve for this situation is shown in Figure 2-1. The movement of the distribution curve within an adsorbent bed during exposure of the bed to the continuous passage of sorbate-laden solution is generally termed the adsorption wave (60). As the adsorption wave extends past the height of the adsorber bed, the sorbate effluent concentration-history profile is generated. The general purpose of the study of the adsorption wave is to obtain an understanding of the various mechanisms which determine the changes in the sorbate effluent concentrations. Mathematic descriptions incorporating these adsorption mechanisms in an overall analysis would effect several important consequences including: 1) the prediction of the performance of a particular adsorber bed from a minimum amount of experimental data and without exhaustive tests on the bed itself; 2) design of the best test procedures for column scale-up from small- to large-scale beds; 3) optimization of reactor design.

The mechanisms for removal of a sorbate passing through a bed of porous adsorbent are generally recognized as involving one or more of the following effects: 1) diffusional mass-transfer of the sorbate from solution to the gross surface of the adsorbent particle; 2) diffusion of the sorbate into, or along the surface of, the pores

FIGURE 2-1. TYPICAL ADSORPTION WAVE IN ADSORBER COLUMN

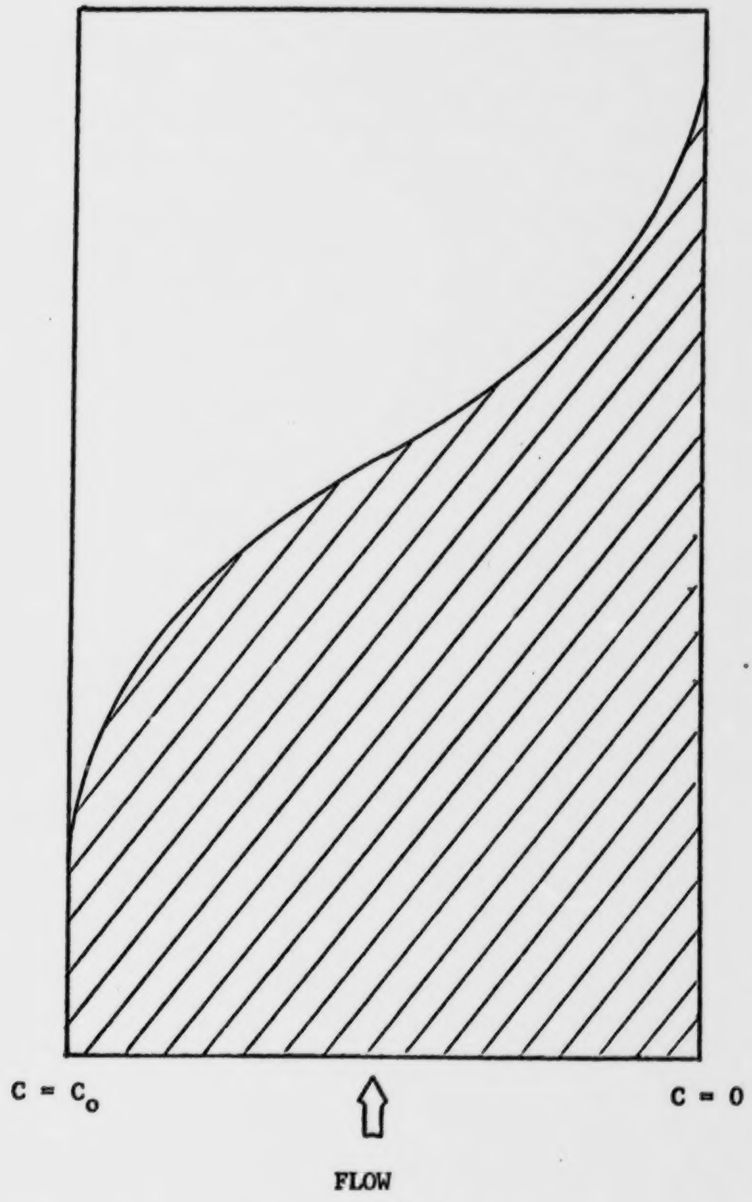

of the adsorbent particle; 3) adsorption of the diffusing material on the internal pore surface of the adsorbent; and, 4) chemical reaction between the sorbate and the adsorbent. The rate at which these individual steps proceed directly affects the adsorption process. The relative importance of each of these mechanisms may vary widely with the conditions of operation. In the most general case, all four steps may occur at approximately the same rate, resulting in an extremely complex mathematical problem.

The simplest model is that in which there is no mass transfer. De Vault (19) and Glueckauf (28) developed this case for gas chromatography. The merit of this model lies in the basic understanding that the effluent concentration-history profile always has a leading and trailing end.

In many situations, one particular mechanism may be considered as the rate controlling step because it occurs at a much slower rate than any of the others. For the special case of single mechanism rate-controlled adsorption processes, a number of mathematic models have been proposed for fixed-bed column operations. Hougen and Marshall (44) presented a solution for the case of external-diffusion-controlled resistance to mass transfer. Rosen (87) and Thomas (101) solved the case in which internal pore diffusion controlled the rate of mass transfer. Vermeulen (109) has presented a solution for the case in which solid-phase pore diffusion controls. Furnas (26) and Goldstein (30) have treated the case for systems in which either external diffusion or surface adsorption controls the rate of mass transfer, and Bohart and Adams (11) and Masamune and

Smith (70,71) have solved the case for surface adsorption controlling.

The three possible two-resistance cases have also been solved by Masamune and Smith (70), Rosen (87), and Amundson (6). Tien and Thodos (106) have provided solutions for the problem of combined external and pore diffusion controlling. For the general case of three-resistance-controlled mass transfer, Masamune and Smith (69) have presented a solution in integral form.

The models presented by the above-mentioned authors were based on simplifying assumptions relative to the equilibrium distribution of sorbate between solution and solid phases. Because of mathematic expediency, a linear isotherm has been used in these mathematic models. However, compounds typical of dissolved wastewater components have been found to exhibit adsorption isotherms of the favorable type (20, 104, 118, 122) and in some cases approach irreversibility. Thus, the use of a linear type of isotherm for wastewater systems would be inadequate.

The solution of the material balance equation for column adsorber performance leads to increased mathematic complexity when other than linear adsorption is used to describe the sorbate distribution. Tien and Thodos (104) have presented a numerical technique for solution of the material balance equation using a Freundlich isotherm to describe the equilibrium relationship. T. Weber and Meyer (112) utilized an empirical equilibrium relationship to develop a mathematic model for solution by numerical techniques. Thomas (100) has developed a mathematic model based on reaction-kinetics, which allows the use of the Langmuir isotherm equilibrium relationship. The Langmuir isotherm defines favorable equilibrium distribution of sorbate between the two phases, and, in the limit, will provide a description of irreversible and linear isotherm equilibria. Hiester and Vermeulen (39, 110) have related the second-order kinetics of the Thomas mathematic development to diffusional mass-transfer relationships for packed bed adsorbers. Keinath and Weber (56, 57) have utilized the development of Hiester and Vermeulen based on the fundamental work of Thomas and have extended it for use as a predictive model for expanded-bed adsorber systems. The mathematic model presented herein illustrates the basic developments of these investigators and provides the tool for prediction of the effluent concentration-history profiles for the complex waste mixtures investigated in this study.

SECOND-ORDER KINETIC APPROACH OF THOMAS

Thomas (100) presented the following schematic representation of physical adsorption:

$$\text{Sorbate} + \text{Sorbent} \underset{k_r}{\overset{k}{\rightleftarrows}} \text{Sorbate} \cdot \text{Sorbent} \tag{2-1}$$

A general expression for the rate of adsorption at the solid surfaces, assuming Langmuir-type adsorption equilibria (38, 100) may be given as

$$\left[\frac{d(\text{Sorbate} \cdot \text{Sorbent})}{d\tau}\right]_{\text{reaction}} = k(\text{Sorbate})(\text{Sorbent}) - k_r(\text{Sorbate} \cdot \text{Sorbent}) \tag{2-2}$$

where τ is time, k is the adsorption rate constant for second-order surface-reaction-controlled kinetics, and k_r is the rate constant for the desorption reaction.

If Q is defined as the ultimate monolayer capacity of the adsorbent for the adsorbate, and q is representative of the amount of monolayer adsorption achieved, then (Q-q) will be equivalent to the amount of unused capacity of the adsorbent. By defining the ratio of the adsorption rate constant to the desorption rate constant, k/k_r, as equivalent to b, the Langmuir equilibrium constant, relating to the energy of adsorption, Equation 2-2 may be expressed as

$$\frac{\partial q}{\partial \tau} = k\left[C(Q-q) - (1/b)q\right] \qquad (2\text{-}3)$$

At equilibrium $\partial q/\partial \tau = 0$, and Equation 2-3 may be written:

$$q = \frac{QbC}{1 + bC} \qquad (2\text{-}4)$$

in accord with the Langmuir definition for adsorption equilibria.

In column operation, the saturation capacity of the adsorbent, q_∞, may be defined as the total amount of adsorbate which has been removed from solution when the adsorbent has reached equilibrium with the solution influent concentration, C_o. Equation 2-4, written in terms of the saturation capacity, is

$$q_\infty = \frac{QbC_o}{1 + bC_o} \qquad (2\text{-}5)$$

MATERIAL BALANCE RELATIONSHIPS FOR EXPANDED-BED SYSTEM

The conservation of mass equation, written for an infinitesimal thickness of bed at a given cross-section dictates that the difference between the amount of adsorbate entering that section and exiting that section must be equivalent to the amount retained by the adsorbent within that section. A schematic of the column cross-section being considered is shown in Figure 2-2. It is assumed that the bed consists of uniformly sized particles, uniform bed porosity exists, and only linear flow is present within the bed. Furthermore, axial diffusion within the bed is assumed to be negligible with respect to convection, as supported by investigations by Acrivos (3), Aris and Amundson (7), and Amundson (5), and that concentration gradients in the radial direction, treated by Lapidus and Amundson (61) and Amundson (6) are insignificant.

The material balance for an infinitesmal cross-section of expanded bed may proceed as follows. The following parameters are used in formulating the material balance relationship: τ denotes the time of first entry of solution to the column cross-section; C equals the concentration of sorbate in the solution entering the section; F is the volumetric flow rate; v is the bulk volume of the expanded adsorber bed; ρ equals the density of the adsorbent in the expanded bed; and ϵ represents the interparticle void ratio of the expanded bed. Schematically, the material balance relationship is given by

FIGURE 2-2. MATERIAL BALANCE FOR ADSORPTION COLUMN

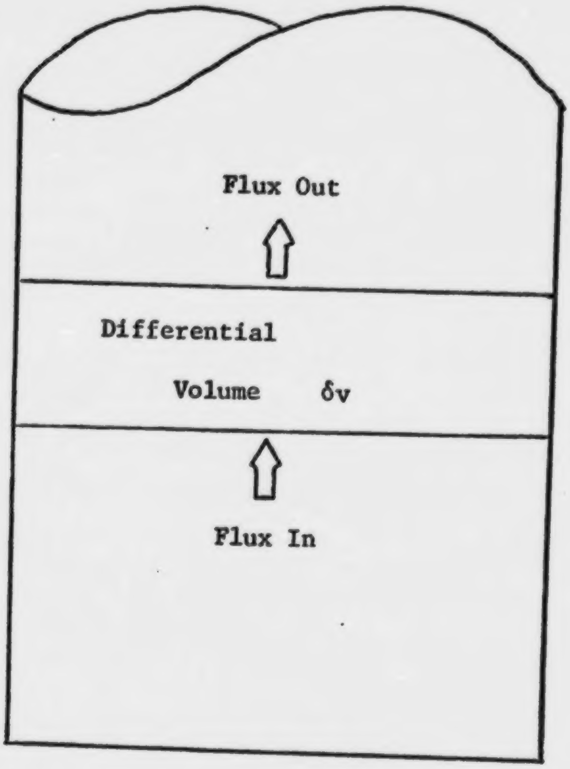
Flux Out
Differential
Volume δv
Flux In

$$C \cdot F \cdot \delta\tau - \left(C + \frac{\delta C}{\delta v} \cdot dv\right) \cdot F \cdot \delta\tau - \rho \frac{\delta q}{\delta\tau} \cdot dv \cdot \delta\tau = \varepsilon \frac{\delta C}{\delta\tau} \cdot dv \cdot \delta\tau$$

$$\left[\begin{array}{l}\text{convective flow of}\\ \text{mass into the}\\ \text{differential element}\end{array}\right] - \left[\begin{array}{l}\text{convective flow}\\ \text{of mass out of}\\ \text{the differential}\\ \text{element}\end{array}\right] - \left[\begin{array}{l}\text{amount of mass ad-}\\ \text{sorbed on the solid}\\ \text{phase within the}\\ \text{differential}\\ \text{element}\end{array}\right]$$

$$= \left[\begin{array}{l}\text{Accumulation of mass within}\\ \text{the differential volume}\end{array}\right] \qquad (2\text{-}6)$$

Or, in terms of the given parameters, the material balance relationship taken over a differential time $\delta\tau$, can be expressed as

$$\left[C \cdot F \cdot \delta\tau\right] - \left[\left(C + \frac{\partial C}{\partial v} \cdot dv\right) \cdot F \cdot \delta\tau\right] - \left[\rho \frac{\partial q}{\partial \tau} \cdot dv \cdot \delta\tau\right]$$

$$= \left[\varepsilon \frac{\partial C}{\partial \tau} \cdot dv \cdot \delta\tau\right] \qquad (2\text{-}7)$$

in which the bracketed terms of Equation 2-7 correspond exactly to those given schematically by Equation 2-6.

Equation 2-7 reduces to

$$\frac{\partial C}{\partial v} + \frac{\varepsilon}{F}\frac{\partial C}{\partial \tau} + \frac{\rho}{F}\frac{\partial q}{\partial \tau} = 0 \qquad (2\text{-}8)$$

which for constant flow rate becomes

$$\left(\frac{\partial C}{\partial v}\right)_V + \varepsilon\left(\frac{\partial C}{\partial V}\right)_v + \rho\left(\frac{\partial q}{\partial V}\right)_v = 0 \qquad (2\text{-}9)$$

Equation 2-9 may be simplified by replacing the influent volume, V, by that volume which has passed through the cross sectional element, equal to $V - v\varepsilon$. Utilizing a fundamental property of derivatives for functions of functions or implicit functions (53), we may write

$$\left(\frac{\partial c}{\partial v}\right)_V = \left[\left(\frac{\partial c}{\partial v}\right)_V\left(\frac{\partial v}{\partial v}\right)_v + \left(\frac{\partial c}{\partial V}\right)_v\left(\frac{\partial V}{\partial v}\right)_V\right] \qquad (2\text{-}10)$$

which becomes upon substitution of V-vε for V

$$\left(\frac{\partial c}{\partial v}\right)_V = \left[\left(\frac{\partial c}{\partial v}\right)_V\left(\frac{\partial v}{\partial v}\right)_v + \left(\frac{\partial c}{\partial (V-v\varepsilon)}\right)_v \cdot \left(\frac{\partial (V-v\varepsilon)}{\partial v}\right)_V\right] \qquad (2\text{-}11)$$

Equation 2-11 simplifies to

$$\left(\frac{\partial c}{\partial v}\right)_V = \left(\frac{\partial c}{\partial v}\right)_{V-v\varepsilon} - \varepsilon\left(\frac{\partial c}{\partial (V-v\varepsilon)}\right)_v \qquad (2\text{-}12)$$

which upon substitution into Equation 2-9, simplification, and rearrangement, results in

$$\left(\frac{\partial c}{\partial v}\right)_{V-v\varepsilon} + \rho\left(\frac{\partial q}{\partial (V-v\varepsilon)}\right)_v = 0 \qquad (2\text{-}13)$$

Equation 2-13 is the necessary and sufficient condition for the existence of a function, f(v, V-vε) such that

$$df = Cd(V-v\varepsilon) - \rho q\, dv \qquad (2\text{-}14)$$

in which f(v,V-vε) is a perfect differential. If the integration

$$f = \int_{v=0}^{v,V-v\varepsilon} \left[\rho q dv - Cd(V-v\varepsilon)\right] \qquad (2\text{-}15)$$

can be extended to a point (v, V-vε) beyond which both C and q remain zero, then f(v, V-vε) is the total amount of sorbate in the column.

In terms of f(v, V-vε), the relations for the calculation of the concentrations are

$$\left.\begin{aligned} C &= \frac{\partial f}{\partial(V-v\varepsilon)} && \text{(a)} \\ q &= -\frac{1}{\rho}\frac{\partial f}{\partial v} && \text{(b)} \end{aligned}\right\} \qquad (2\text{-}16)$$

The fundamental differential equation for the performance of the adsorber column governed by a mass transform te law as given in Equation 2-3 and utilizing the relationship given in Equations 2-16 can be derived. Expressing Equation 2 in terms of $(V-v\varepsilon)$ we have

$$\frac{\partial q}{\partial \tau} = F\frac{\partial q}{\partial V} = F\frac{\partial q}{\partial(V-v\varepsilon)}\frac{\partial(V-v\varepsilon)}{\partial V} = \frac{\partial q}{V-v\varepsilon)} \qquad (2\text{-}17)$$

which becomes, in terms of Equation 2-16b,

$$F\frac{\partial q}{\partial(V-v\varepsilon)} = -\frac{F}{\rho}\frac{\partial^2 f}{\partial(V-v\varepsilon)} \qquad (2\text{-}18)$$

Also from Equation 2-16a

Reproduced from best available copy.

$$\frac{\partial C}{\partial v} = \frac{\partial\left(\frac{\partial f}{\partial(V-v\varepsilon)}\right)}{\partial v} = \frac{\partial^2 f}{\partial v\partial(V-} \qquad (2\text{-}19)$$

Expanding Equation 2-3 in terms of Equation simplifying and relating the expansion to Equation 2-19, Equation -13 becomes

$$\frac{\partial^2 f}{\partial v\partial(V-v\varepsilon)} + A\frac{\partial f}{\partial v} + B\frac{\partial f}{\partial(V-v\varepsilon)} + \frac{\partial f}{\partial(V-v\varepsilon)}$$

$$= 0 \qquad (2\text{-}20)$$

in which

$$A = \frac{k}{Fb}$$

$$B = \frac{kQ\rho}{F}$$

$$C_1 = \frac{k}{F} \qquad (2\text{-}21)$$

In order to solve Equation 2-20, the following logarithmic expression containing a new function of v and (V-vε), Φ(v, V-vε) is given by Thomas (99).

$$C_1 f = \ell n \left[\left(e^{-(Bv + A(V-v\varepsilon))}\right) \Phi(v, V-v\varepsilon) \right] \qquad (2\text{-}22)$$

Upon substitution of Equation 2-22 into Equation 2-20, and simplification, the linear equation

$$\frac{\partial^2 \Phi(v, V-v\varepsilon)}{\partial v \partial (V-v\varepsilon)} = AB\Phi(v, V-v\varepsilon) \qquad (2\text{-}23)$$

obtains.

Recalling the relationships for C and q as given by Equation 2-16, differentiation of Equation 2-22 will yield

$$\left.\begin{aligned} C &= \frac{1}{C_1} \left(\frac{\partial \ell n \Phi}{\partial V-v\varepsilon} - A \right) \\ q &= -\frac{1}{C_1} \left(\frac{\partial \ell n \Phi}{\partial v} - B \right) \end{aligned}\right\} \qquad (2\text{-}24)$$

The boundary condition of Φ(v, V-vε) are specified by the initial conditions within the column. For

$$\left.\begin{aligned} v &= 0,\ V-v\varepsilon \geq 0,\ C = C_o \\ v &\geq 0,\ V-v\varepsilon = 0,\ q = 0 \end{aligned}\right\} \qquad (2\text{-}25)$$

Thus, for $\Phi(v, V-v\varepsilon)$, we obtain the following corresponding boundary conditions,

$$\left.\begin{aligned} \frac{\partial[\ell n(0,\ V-v\varepsilon)]}{\partial(V-v\varepsilon)} &= C_1\ C_o + A = \alpha \\ \frac{\partial[\ell n(v,0)]}{\partial v} &= B \end{aligned}\right\} \qquad (2\text{-}26)$$

and let $\alpha\beta = AB$.

Integrating Equation 2-26 yields

$$\left.\begin{aligned} \Phi(0,\ V-v\varepsilon) &= e^{\alpha(V-v\varepsilon)} \\ \Phi(v,0) &= e^{Bv} \end{aligned}\right\} \qquad (2\text{-}27)$$

The solution of Equation 2-23 under the boundary conditions of Equation 2-27 may be found by the method of the Laplace transform. Some of the details of the calculation can be found in Appendix 1. This procedure results in the following equation for $\Phi(v, V-v\varepsilon)$

$$\begin{aligned} \Phi(v,\ V-v\varepsilon) = {} & J_o\{2i\sqrt{ABv(V-v\varepsilon)}\ \} + \\ & \int_0^v Be^{B\xi} J_o\{2i\sqrt{AB(V-v\varepsilon)(v-\xi)}\ \}d\xi\ + \\ & \int_0^{V-v\varepsilon} \alpha e^{\alpha\eta} J_o\{2i\sqrt{\alpha\beta v(V-v\varepsilon-\eta)}\ \}d\eta \end{aligned} \qquad (2\text{-}28)$$

in which ξ and η are the variables of integration around the boundary of the region determined by the characteristics and the axes.

Recognizing (31) that $I_n(z) = i^{-n}J_n(iz)$, then

$$I_o(z) = J_o(iz) \tag{2-29}$$

Therefore Equation 2-28 becomes

$$\Phi(v,V-v\varepsilon) = I_o\{2\sqrt{ABv(V-v\varepsilon)}\} + \int_0^v Be^{B\xi}I_o\{2\sqrt{AB(V-v\varepsilon)(v-\xi)}\}\, d\xi + \int_0^{V-v\varepsilon} \alpha e^{\alpha\eta}I_o\{2\sqrt{\alpha\beta v(V-v\varepsilon-\eta)}\}\, d\eta \tag{2-30}$$

By making the following substitutions

$$\left.\begin{aligned} B(v-\xi) &= t_1 \\ A(V-v\varepsilon) &= \omega \end{aligned}\right\} \tag{2-31}$$

a new function $\Psi(Bv,A(V-v\varepsilon))$ may be written to define the first integral in Equation 2-30 as

$$\Psi(Bv, A(V-v\varepsilon)) = e^{Bv}\int_0^{Bv} e^{-t_1}I_o\{2\sqrt{\omega t_1}\}\, dt_1 \tag{2-32}$$

Similarly

$$\Psi(\alpha(V-v\varepsilon),\beta v) = \int_0^{V-v\varepsilon} \alpha e^{\alpha\eta}I_o\{2\sqrt{\alpha\beta v(V-v\varepsilon-\eta)}\}\, d\eta \tag{2-33}$$

Thus Equation 2-30 becomes

$$\Phi(v,V-v\varepsilon) = I_o\{2\sqrt{ABv(V-v\varepsilon)}\} + \Psi(Bv,A(V-v\varepsilon))$$

$$+ \Psi(\alpha(V-v\varepsilon),\beta v) \qquad (2\text{-}34)$$

By series expansion of $\Psi(\sigma,\theta)$, it can be shown (102) that

$$\Psi(\sigma,\theta) + \Psi(\theta,\sigma) = e^{(\sigma+\theta)} - I_o\{2\sqrt{\sigma\theta}\} \qquad (2\text{-}35)$$

and differentiating $\Psi(\sigma,\theta)$

$$\frac{\partial\Psi(\sigma,\theta)}{\partial\sigma} = \Psi(\sigma,\theta) + I_o\{2\sqrt{\sigma\theta}\} \qquad (2\text{-}36)$$

$$\frac{\partial\Psi(\sigma,\theta)}{\partial\theta} = \Psi(\sigma,\theta) + \frac{\partial}{\partial\theta} I_o\{2\sqrt{\sigma\theta}\} \qquad (2\text{-}37)$$

with the limiting values

$$\Psi(0,\theta) = 1$$

$$\Psi(\sigma,0) = e^{\sigma}-1$$

$$\lim_{\sigma\to\infty} e^{-(\sigma+\theta)}\,\Psi(\sigma,\theta) = 1 \qquad (2\text{-}38)$$

Differentiating Equation 2-22 with respect to $(V-v\varepsilon)$ and recalling Equation 2-16a yields

$$C = \frac{1}{C_1}\left(\frac{\left[\dfrac{\partial\Phi(v,\ V-v\varepsilon)}{\partial(V-v\varepsilon)}\right]}{\Phi(v,\ V-v\varepsilon)} - A\right) \qquad (2\text{-}39)$$

From Equations 2-34, 2-36, and 2-37, we can evaluate $\partial\Phi(v,\ V-v\varepsilon)/\partial(V-vc)$, and upon simplification, write

$$C = \frac{1}{C_1}\frac{1}{\Phi}(\alpha-A)\left[\Psi(\alpha(V-v\varepsilon),\beta v) + I_o\{2\sqrt{ABv(V-v\varepsilon)}\}\right] \qquad (2\text{-}40)$$

Recalling that $\alpha = C_1C_o+A$, then $\alpha-A = C_1C_o$, hence,

$$C = \frac{C_o}{\Phi(v,V-v\varepsilon)}\left[\Psi(\alpha(V-v\varepsilon),\beta v) + I_o\{2\sqrt{ABv(V-v\varepsilon)}\}\right] \qquad (2\text{-}41)$$

or

$$\frac{C}{C_o} = 1 - \left[\frac{\Psi(Bv,A(V-v\varepsilon)}{\Phi(v,\ V-v\varepsilon)}\right] \qquad (2\text{-}42)$$

Hiester and Vermeulen (39) have related the function $J(\sigma,\theta)$ as derived by Furnas (26) and Schumann (89) to the Thomas function $\Psi(\sigma,\theta)$ such that

$$J(\sigma,\theta) = 1 - e^{-(\theta+\sigma)}\Psi(\sigma,\theta) \qquad (2\text{-}43)$$

In order to use Equation 2-43 for the solution of Equation 2-42, the function $J(\sigma,\theta)$ must be evaluated very accurately. Using an asymptotic expansion due to Osanger and given by Thomas (102) the $J(\sigma,\theta)$ function reduces to

$$\left.J(\sigma,\theta) = \tfrac{1}{2}\{1-\mathrm{erf}(\sqrt{\sigma}-\sqrt{\theta}) + \frac{e^{-(\sqrt{\sigma}-\sqrt{\theta})^2}}{\sqrt{\pi}\ \ [\sqrt{\theta}\ \ \sqrt[4]{\sigma\theta}]}\right\} \qquad (2\text{-}44)$$

Therefore,

$$\left.\begin{aligned}\Psi(\sigma,\theta) &= \left[1 - J(\sigma,\theta)\right] e^{(\sigma+\theta)}\\ \Psi(\theta,\sigma) &= \left[1 - J(\theta,\sigma)\right] e^{(\sigma+\theta)}\end{aligned}\right\} \qquad (2\text{-}45)$$

Thomas (102) also gives an approximation for $I_o(z)$ as

$$I_o(z) \simeq \frac{e^z}{\sqrt{2\pi z}} \qquad (2\text{-}46)$$

Hence, Equation 2-42 can be solved using the relationships for Φ, as given in Equation 2-34, and for Ψ as given in Equation 2-45. Therefore, Equation 2-42 for the solution of the concentration-history profile is readily solvable using functions which are tabulated with high accuracy (40, 47).

MASS-TRANSFER RELATIONSHIPS

In order to utilize Equation 2-42 for the prediction of effluent concentration-history profiles for adsorber columns, it is necessary to relate the second-order kinetic equations of Thomas (100) to the controlling mass-transfer equations. Recall that the rate of adsorption can be limited by diffusional mass transfer of the sorbate from solution to the gross surface of the adsorbent particle ('film' diffusion), or diffusion of the sorbate into, or along the surface of, the pores of the adsorbent particle, adsorption of the diffusing material on the internal pore surface of the adsorbent, or chemical reaction between the sorbate and the adsorbent. The effective rate of adsorption will thus be controlled by the step exhibiting the greatest resistance to mass-transfer. Neglecting all but the rate-limiting resistance or combining the resistances into one step with a single effective rate parameter present two alternative procedures to facilitate the use of mathematic relationships for the mass-transfer process. The diffusional equations to be presented in this section will be shown to be closely related to the kinetic equations and that an effective mass-transfer coefficient is obtainable. The diffusional mechanisms for adsorption, as indicated by Juda and Carron (52) in batch experiments, do not alter the basic nature of adsorption as second-order-kinetic processes. In adsorption, the materials adsorbed upon the solid surfaces may be said to have become closely associated to the solid phase or to have undergone chemical reaction with it.

Adsorption and Chemical Reaction

Although the earliest analysis of the adsorption wave was made considering adsorption or chemical reaction as rate controlling (11), for all but a few isolated cases, these steps will be extremely rapid, and the resistance due to them will be negligible. For most practical cases, then, the effects of these resistances can be neglected as confirmed by the data provided by Vassiliou and Dranoff (108) and Weber and Morris (123). Furthermore, indications that the adsorption process itself is not rate-limiting are given by investigations (2, 66, 75) of the rates at which interfacial tensions are lowered by chemical compounds representative of organic pollution materials.

External Diffusion

Mass transfer in the region separating the bulk solution and the solid surface has been treated utilizing film, boundary layer, and penetration theories (10). However, the fluid-mechanics of this region are not well-defined. 'Film diffusion' will be used to refer to the resistance to mass transfer through the region separating the external bulk solution from the external solid surface of adsorbent.

If it is assumed that the concentration of sorbate at the point in the hydrodynamic boundary layer immediately adjacent to the external surface of the adsorbent is in equilibrium with the average solid-phase concentration on the internal surfaces, this condition may be expressed as

$$\left(\frac{dq}{d\tau}\right)_F = k_f a \frac{\varepsilon}{\rho} (C-C_e) \tag{2-46}$$

in which k_f is the mass-transfer coefficient for the case in which film diffusion controls the overall mass-transfer process; a is the effective area for mass transfer across the boundary region per unit volume of bed; and C_e is the concentration of sorbate in equilibrium with the coexisting solid-phase concentration. This equilibrium concentration for column operation can be given by expressing Equation 2-3 in terms of the influent concentration, C_o, and setting the net rate of reaction equal to zero. This yields

$$C_e = \frac{qC_o}{q_\infty(1+bC_o) - bqC_o} \tag{2-47}$$

Defining r, the equilibrium modulus (39) by

$$r = \frac{1}{1 + bC_o} \tag{2-48}$$

and substituting Equations 2-47 and 2-48 into 2-46 yields

$$\left(\frac{dq}{d\tau}\right)_F = \frac{k_f a \frac{\varepsilon}{\rho}}{q_\infty \left[1+(r-1)\frac{q}{q_\infty}\right]} \left[C(q_\infty-q)-rq(C_o-C)\right] \tag{2-49}$$

Noting that Equation 2-3, expressed in terms of q_∞ and r, becomes

$$\frac{dq}{d\tau} = \frac{kQ}{q_\infty}\left[C(q_\infty - q) - rq(C_o - C)\right] \tag{2-50}$$

and comparing Equation 2-49 with Equation 2-50 we can relate a rate coefficient, κ_f, for external diffusion to the second-order surface-reaction-controlled rate constant, k, such that

$$\frac{kQ}{q_\infty} = \frac{\kappa\varepsilon}{q_\infty \rho} \tag{2-51}$$

From Equation 2-51 and comparison of Equations 2-49 and 2-50, a relationship for the effective external-diffusion rate constant obtains, and is given by

$$\kappa_f = \frac{k_f a}{1+(r-1)(q/q_\infty)} \tag{2-52}$$

When the complete concentration-history profiles are to be calculated, the average value of q/q_∞ may be taken as 0.5 for r less than 1 (39), for the favorable equilibrium condition. Thus, for r less than 1,

$$\kappa_f = \frac{2k_f a}{r+1} \tag{2-53}$$

Internal Diffusion

Internal diffusion is the mass-transfer controlling mechanism which controls the movement of sorbate from the exterior surface of the adsorbent to the internal surfaces of the adsorbent particle. Internal diffusion may be of two types: 1) the sorbate may enter an adsorbent particle by diffusing through the fluid phase in the pores; or 2) by movement in a condensed or adsorbed phase along the solid pore surfaces. The first type, termed pore diffusion, occurs before any phase change, whereas the second type, termed pore-surface diffusion occurs after the sorbate becomes part of the solid phase. Pore-surface diffusion is visualized as a two-dimensional diffusion along the pore boundaries of a particle consisting of impervious crystallites separated by pore spaces that are accessible to the sorbate(29). These two diffusional mechanisms act in a physically parallel method, thus the more rapid will control the rate of mass transfer. The fluid-phase pore diffusion will be favored if the concentration level in the pore-fluid is high, and pore-surface diffusion will be favored if that concentration level is low (34).

Fluid-Phase Pore Diffusion

A material balance taken over a differential spherical shell for a particle of radius R and thickness dR can be shown to simplify to

$$\left[\frac{dq}{d\tau}\right]_{\text{pore}} = \frac{3D_p R^2 \gamma}{\rho R_p{}^3} \frac{\partial C_j}{\partial R} \qquad (2\text{-}54)$$

after Kasten and Amundson (54). D_p is the diffusivity in the pore fluid; γ is the intraparticle void ratio; R_p is the total radius of the particle; and the subscript j signifies the subscripted parameter is determined at the interior of the particle. Equation 2-54 relates the rate of uptake to the radial concentration gradient of the sorbate within the pore fluid. By averaging the extent of saturation over the entire particle, one can express the concentration gradient in terms of the difference between the bulk solution concentration, C, and the fluid-phase concentration of sorbate, C_e, which is in equilibrium with the average solid-phase concentration on the internal pore surfaces. The rate of uptake may then be written as

$$\left[\frac{dq}{d\tau}\right]_{pore} = k_p a \, \frac{\gamma}{\rho} \, (C-C_e) \tag{2-55}$$

in which k_p is the mass-transfer rate constant for the fluid-phase pore-diffusion controlled case.

Equation 2-55 may be rearranged using Equation 2-47 to yield

$$\left[\frac{dq}{d\tau}\right]_{pore} = \frac{k_p a \, \frac{\gamma}{\rho}}{q_\infty(1+(r-1)q/q_\infty)} \left[C(q_\infty-q)-rq(C_o-C)\right] \tag{2-56}$$

As in the case of external-diffusion-controlled mass-transfer, given by Equation 2-49, Equation 2-56 is in similar form to the second-order kinetic rate expression, Equation 2-50. With reference to Equation 2-50 and 2-51, an expression for a fluid-phase pore diffusion rate constant, κ_p, may be determined. Thus,

$$\kappa_p = \frac{k_p a}{1+(r-1)q/q_\infty} \tag{2-57}$$

If r is less than 1, we may again take the value of q/q_∞ as 0.5 when the entire effluent concentration-history profile is of interest (39), yielding

$$\kappa_p = \frac{2k_p a}{r+1} \tag{2-58}$$

Pore-Surface Diffusion

A material balance relationship for solid-phase pore-surface diffusion, has been developed in a similar manner as that for pore fluid diffusion (Equation 2-54) and is given, after Masamune and Smith (70) as

$$D_s \left[\frac{\partial^2 q_j}{\partial R^2} + \frac{2}{R} \frac{\partial q_j}{\partial R} \right] = \frac{\partial q_j}{\partial \tau} \qquad (2\text{-}59)$$

in which D_s is the solid-phase diffusivity of the sorbate along the surface of the pore. An approximation to Equation 2-59 has been given by Michaels (73) and Glueckauf and Coates (29). Using a linear-driving-force relationship as giving the rate of approach to complete saturation of the adsorbent being proportional to the difference between the extent of saturation at the outer surface of the adsorbent particle and the average extent of saturation within the particle. The rate expression is given as

$$\left[\frac{dq}{d\tau} \right]_s = k_s a' \, (q_e - q) \qquad (2\text{-}60)$$

in which q_e is the local concentration of sorbate in the solid phase at the exterior surface of the particle and is assumed to be in equilibrium with the coexisting liquid phase concentration, C. For a zero net rate of reaction, Equation 2-50 yields

$$q_e = \frac{q_\infty C}{(1-r)C + rC_o} \qquad (2\text{-}61)$$

which, upon substitution into Equation 2-60, and rearrangement yields

$$\left[\frac{dq}{d\tau}\right]_s = \frac{k_s a'}{(1-r)C+rC_o}\left[C(q_\infty-q)-rq(C_o-C)\right] \tag{2-62}$$

With reference to Equations 2-49 and 2-56, we see that Equation 2-62 is of the same general form. Thus all three diffusional cases have been related to the surface-reaction kinetic controlled rate expression, given by Equation 2-50. Thus an effective diffusional rate constant for pore-surface controlled diffusions, κ_s, may be determined by examination of Equations 2-62, 2-50, and 2-51. Writing

$$\frac{\kappa_s \varepsilon}{q_\infty \rho} = \frac{k_s a'}{(1-r)C + rC_o} \tag{2-63}$$

and defining

$$D_G = \frac{q_\infty \rho}{C_o \varepsilon} \tag{2-64}$$

after Hiester and Vermeulen (39), one can write

$$\kappa_s = \frac{k_s a' D_G}{(1-r)(C/C_o) + r} \tag{2-65}$$

D_G is a dimensionless coefficient, termed the distribution coefficient. From its ratio relationship, it can be seen that D_G represents the limiting distribution of sorbate between solid and solution phases.

If the entire effluent-concentration-history profile is of interest, 0.5 C_o is a permissible value for C (39), yielding

$$\kappa_s = \frac{2k_s a' D_C}{(r + 1)} \tag{2-66}$$

The developments for diffusional mass-transfer relationships just presented provide relationships between diffusional mass-transfer coefficients and the second-order kinetic rate constant. Since the second-order kinetic rate constant is required in the solution of Equation 2-42, Equations 2-53, 2-56, and 2-66 provide a method of replacing the kinetic rate constant with diffusional rate constants when external, internal pore-fluid, or internal pore-surface diffusion controls, respectively.

Combining External and Internal Resistances

For cases in which external and internal diffusion occur in series, King (59) has demonstrated that the respective mass transfer coefficients, measured individually under conditions in which the alternative resistance is either absent or has been effectively suppressed, may be added

$$\frac{1}{\kappa} = \frac{1}{\kappa_f} + \frac{1}{\kappa_I} \tag{2-67}$$

where κ_I represents the controlling internal diffusion. Since fluid-phase pore diffusion and solid-phase pore diffusion occur in parallel, only one of these two resistances will enter into the series relationship governing combined external and internal diffusion, except when both occur at comparable rates. Otherwise, the more rapid of the internal diffusion mechanisms will control. Thus κ_I will be represented by either κ_p as given in either Equation 2-57 or Equation 2-58 (for r less than 1), or by κ_s as given in Equation 2-65 or Equation 2-66 (for r less than 1). Likewise, κ is given by Equation 2-52 or 2-53 (for r less than 1).

Di Giano and Weber (20) have found in studies of adsorption kinetics in finite and infinite bath systems that a dependence of diffusion resistance on adsorption behavior seems to exist. Strongly adsorbed solutes demonstrated a mass transfer dependence on internal pore diffusion mechanisms, whereas less strongly adsorbed solutes made application of irreversible immobilization and quasi-steady state approximations very difficult. For the latter type adsorbers, a simplified film diffusion model was found adequate to describe the initial rates of uptake. The weaker adsorbers were generally smaller in molecular size, suggesting that internal resistance becomes more prominent in controlling the rate of mass transfer with increasing molecular size. Extension of these batch system adsorption behavior observations to flow through adsorber systems cannot be made *a priori*. In the approach taken here for determination of the overall diffusional mass transfer coefficient, comparison of the external diffusion mass transfer coefficient to the controlling internal diffusion mass transfer coefficient indicates the overall controlling mechanism.

CHAPTER 3

EXPERIMENTAL MATERIALS AND ANALYTIC PROCEDURES

COMPLEX SOLUTE MIXTURES

General Considerations

Synthetic wastewaters were designed for use in testing the applicability of the Keinath-Weber model for prediction of effluent concentration-history profiles for complex mixtures. This approach was selected so as to provide controlled mixture composition in all experimental investigations and also to inhibit biological activity which could distort the interpretation of adsorber column performance. This approach to initial testing of the mathematic model is preferred to the use of an actual wastewater because of the accuracy, reproducibility and control of variables which the former method affords.

Selection of the individual components in designing the complex synthetic mixtures must be done judiciously. It is necessary to design complex mixtures from components which exhibit a relatively broad range of physical and adsorption characteristics and which can be measured by the overall description parameter of choice. Such mixtures should simulate the wide range of adsorbable compounds often found in wastewaters and provide a basis for examining the generality of the mathematic model.

Sorbate Compounds

The selection of sorbate compounds was based on the above criteria and a desire to utilize dissolved organic compounds which are typical of those commonly found in wastewaters. The organic compounds chosen were phenol, a cyclical aromatic compound; dodecyl sodium sulfate (commonly called sodium lauryl sulfate), a 12-carbon aliphatic surfactant; and n-hexanol, a moderate-weight primary alcohol. The physical characteristics of these compounds are illustrated in Table 3-1. The adsorption characteristics of these compounds are discussed in Chapter 4 and are noted to differ significantly in the Langmuir capacity and energy parameters.

Reagent grade phenol was obtained in loose-crystalline form from the Mallinckrodt Chemical Works. USP dodecyl sodium sulfate was obtained as a mixture of sodium alkyl sulfates, consisting chiefly of the dodecyl sodium salt, from the Fisher Scientific Company. USP n-hexanol was obtained from the Aldrich Chemical Company.

The theoretical oxygen demand, which is numerically equal to the amount of oxygen that would be required to effect total oxidation of an organic compound in the hypothetical reaction with a given concentration of that organic compound, was determined for the individual organic species and is shown for each component in Table 3-2. Table 3-2 also lists the actual chemical oxygen demand (COD) as determined in the analytical test for COD that was utilized in this research.

Complex Sorbate Mixture Composition

The complex mixtures were designed so that a given compound contributed a predetermined fraction of the total mixture COD. A total of eight mixtures of sorbate compounds were devised and investigated in this research. These mixtures include five binary

TABLE 3-1

PHYSICAL AND CHEMICAL CHARACTERISTICS OF MIXTURE COMPONENTS

COMPOUND	FORMULA	MOLECULAR WEIGHT	SOLUBILITY IN GRAMS PER 100 ml OF WATER
Dodecyl Sodium Sulfate	$CH_3(CH_2)_{11}OSO_3N_2$	288.39	very soluble
n-Hexanol	$CH_3(CH_2)_4CH_2OH$	102.17	0.59 (20°C)
Phenol	C_6H_5OH	94.11	6.7 (16°C)
Sodium Acetate	CH_3COON_2	82.04	119 (0°C)
D-Glucose (dextrose)	$C_6H_{12}O_6$	180.16	82.0 (25°C)

TABLE 3-2

CHEMICAL OXYGEN DEMAND OF MIXTURE COMPONENTS

COMPOUND	THEORETICAL COD (mg COD/mg compound)	MEASURED COD (mg COD/mg compound)
Dodecyl Sodium Sulfate	2.03	1.43
n-Hexanol	2.51	0.969
Phenol	2.03	1.88
Sodium Acetate	0.683	0.70
D-Glucose	1.067	1.067

mixtures and three ternary mixtures, each differing from the others in composition of individual species. A summary of the composition of the binary mixtures is shown in Table 3-3, and a summary of the ternary mixtures is shown in Table 3-4. These tables illustrate that the sorbate compounds were combined so as to provide a large variation of mixture compositions with which to check the mathematic model.

Non-Adsorbing Organic Compounds

It has been noted in Chapter 1 that the use of an overall description parameter must be carefully approached when examining adsorber performance due to the possible interference of non-adsorbing components which contribute to the total composition as determined by the overall description parameter. Therefore, it was deemed essential to investigate the problems presented by such non-adsorbing fractions and to determine methods of accounting for these fractions.

The organic compounds chosen for use in combination with the sorbing organic compounds were sodium acetate and dextrose. Sodium acetate was chosen because it is the salt of acetic acid, which in turn is representative of low molecular weight acids commonly found in wastewaters. Dextrose (D-glucose) is a monosaccharide which is representative of low molecular weight carbohydrates also characteristically found in wastewaters. Experimental investigations confirmed the non-adsorptive behavior of both of these organic substances.

The physical characteristics of these two compounds are listed in Table 3-1. The theoretical oxygen demand and the experimentally

TABLE 3-3

BINARY MIXTURE COMPOSITION

MIXTURE	COMPOUNDS	FRACTIONAL CONTRIBUTION TO MIXTURE COD
1	Phenol	0.50
	Dodecyl Sodium Sulfate	0.50
2	Phenol	0.25
	Dodecyl Sodium Sulfate	0.75
3	Phenol	0.75
	Dodecyl Sodium Sulfate	0.25
4	n-Hexanol	0.50
	Dodecyl Sodium Sulfate	0.50
5	n-Hexanol	0.75
	Dodecyl Sodium Sulfate	0.25

TABLE 3-4

TERNARY MIXTURE COMPOSITION

MIXTURE	COMPOUNDS	FRACTIONAL CONTRIBUTION TO MIXTURE COD
6	Phenol	0.25
	n-Hexanol	0.25
	Dodecyl Sodium Sulfate	0.50
7	Phenol	0.50
	n-Hexanol	0.25
	Dodecyl Sodium Sulfate	0.25
8	Phenol	0.333
	n-Hexanol	0.333
	Dodecyl Sodium Sulfate	0.333

determined chemical oxygen demand are listed in Table 3-2. Reagent grade sodium acetate was obtained as anhydrous powder from the J. T. Baker Company. Reagent grade dextrose was obtained from the General Chemical Division of Allied Chemical Company.

Adsorber/Non-adsorber Mixtures

In order to investigate the contribution of non-adsorbing organic fractions, four additional mixtures were incorporated in this research. The composition of these mixtures are shown in Table 3-5. The mixtures were composed of the three sorbate organics - phenol, dodecyl sodium sulfate, n-hexanol - and varying amounts of the non-adsorbing compounds, ranging from 6.8% to 60% of total mixture COD.

ACTIVE CARBON

The active carbon used in all the experimental investigations reported herein was Filtrasorb 400 activated carbon, a granular coal-base active carbon, which was obtained from Calgon Corporation. The carbon was thoroughly sieved into uniform size fractions with a set of United States Standard Sieves. Two different size fractions were used in these experiments - particles passing a 30 mesh sieve and retained on a 40 mesh sieve (30/40) corresponding to an arithmetic mean diameter of 0.503 mm, and particles passing an 80 mesh sieve and retained on a 100 mesh sieve (80/100), corresponding to an arithmetic mean diameter of 0.161 mm. These size fractions of carbon were then thoroughly washed in glass distilled water to remove fine carbon material and leachable substances. The final wash water was checked to assure that the active carbon was not a source of any substances contributing to COD. The active carbon was then dried to constant weight at 120°C.

TABLE 3-5

ADSORBER/NON-ADSORBER MIXTURE COMPOSITION

MIXTURE	COMPOUNDS	FRACTIONAL CONTRIBUTION TO MIXTURE COD
9	Phenol	0.550
	n-Hexanol	0.101
	Dodecyl Sodium Sulfate	0.149
	Sodium Acetate	0.200
10	Phenol	0.182
	n-Hexanol	0.304
	Dodecyl Sodium Sulfate	0.446
	Sodium Acetate	0.068
11	Phenol	0.200
	n-Hexanol	0.121
	Dodecyl Sodium Sulfate	0.179
	Sodium Acetate	0.500
12	Phenol	0.200
	n-Hexanol	0.200
	Dodecyl Sodium Sulfate	0.200
	Sodium Acetate	0.200
	D-Glucose	0.200

ANALYTIC METHODS

Chemical Oxygen Demand

Chemical oxygen demand determinations for the experimental work were performed utilizing a Technicon Auto Analyzer. Details of the COD procedure can be found in Appendix 2. The principle of the COD test using the Auto Analyzer is in accordance with that outlined in Standard Methods for the Examination of Water and Wastewater (4). The organic materials are oxidized by a potassium dichromate-sulfuric acid mixture with appropriate catalytic reagents and interference reducing reagents. The chemical composition of this oxidizing mixture can also be found in Appendix 2.

The Auto Analyzer technique employs a photometric method to determine the response to reduction of potassium dichromate by chemical oxygen demand. The change in transmittance resulting from a positive response, i.e. a decrease in the color intensity of the dichromate oxidizing mixture, results in a peak on the continuous strip chart recorder. The change in transmittance, or the peak height, was found to be linearly proportional to the chemical oxygen demand, as shown in the calibration curve, Figure 3-1. The results of the COD determinations utilizing the Auto Analyzer were found to be in excellent agreement with COD evaluations utilizing the Standard Methods (4) procedure.

Phenol

Phenol was analyzed separately in the component experiments discussed in Chapter 6 and in the isotherm development for single components. Phenol exhibits an absorption spectrum in the ultra-

FIGURE 3-1. CALIBRATION CURVE FOR CHEMICAL OXYGEN DEMAND

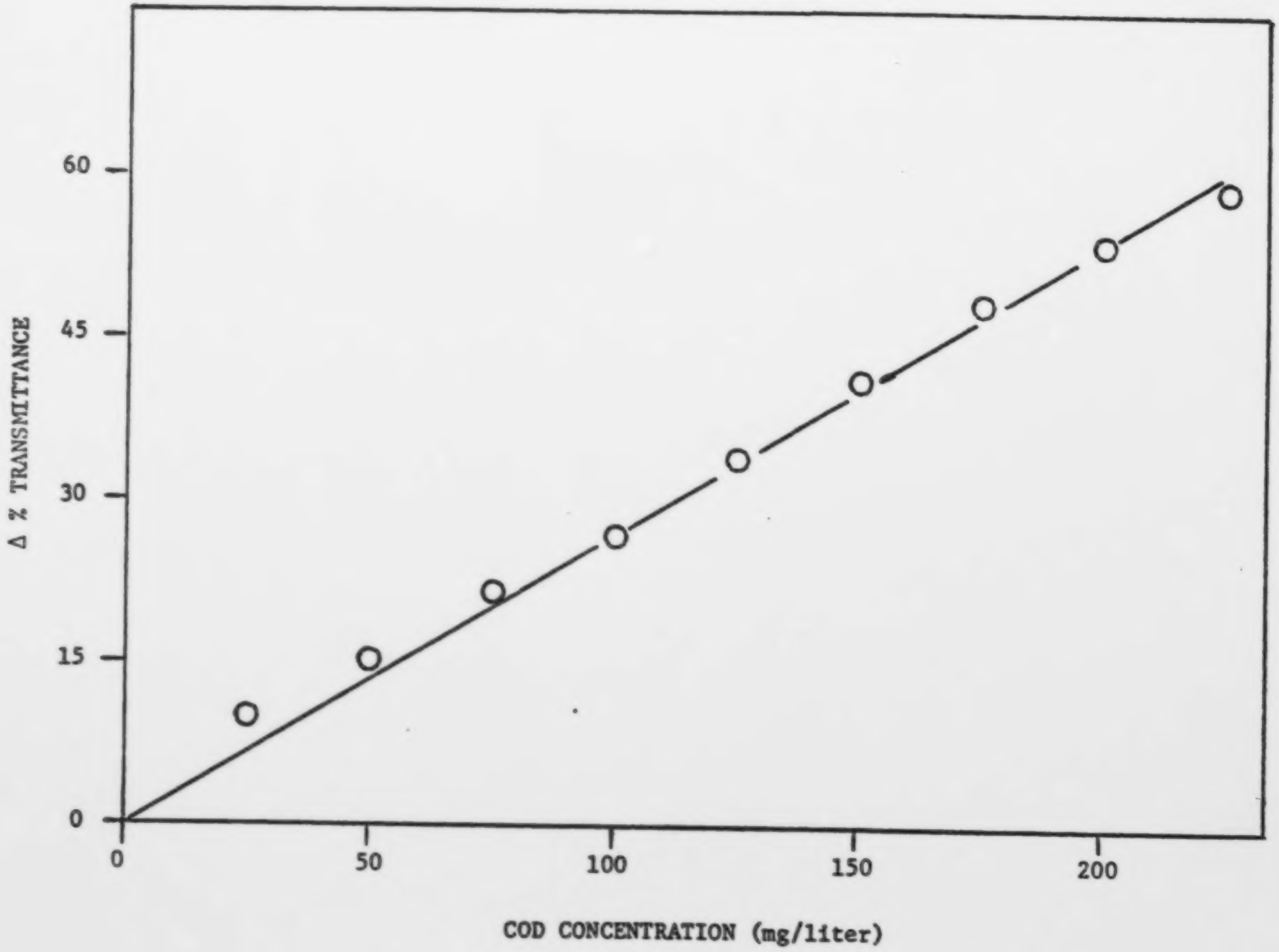

violet light wavelength range, and can be directly measured by photometric methods. A phenol absorbance spectrum for the ultraviolet wavelengths was run using a Perkin-Elmer Model PE-202 UV-Visible Spectrophotometer and is shown in Figure 3-2. Maximum absorbance for phenol is at 274 mμ for the neutral molecule and 287 mμ for the anion. Analysis for the concentrations of individual samples were performed using a Beckman Model DU-2 Spectrophotometer. A linear dependence of absorbance with concentration of phenol is exhibited, as demonstrated in the calibration curve, Figure 3-3.

EXPERIMENTAL COLUMN SYSTEM

A schematic representation of the experimental continuous-flow column system used to generate the concentration-history profiles for verification of the mathematic model predictions is shown in Figure 3-4. The columns utilized were 2.0 inch inside-diameter plexiglass cylinders, 0.375 inch wall thickness, and 76 inches long. The inlet sections of the columns were designed to dissipate the velocity head at that section, so as to assure one-dimensional, steady-state flow in the columns. This was achieved by providing a 1.5 inch deep distribution chamber filled with 2.0 mm glass beads at the base of the column. A brass tube carrying the feed solution was inserted into the distribution chamber so that it extended across the radius of the chamber. Twelve equally spaced 0.125 inch holes in two equal rows separated by 90° were drilled into this brass tubing. The holes pointed downward into the distribution chamber and this inlet condition helped provide good dissipation of the velocity head.

FIGURE 3-2. ABSORB SPECTRUM FOR PHENOL

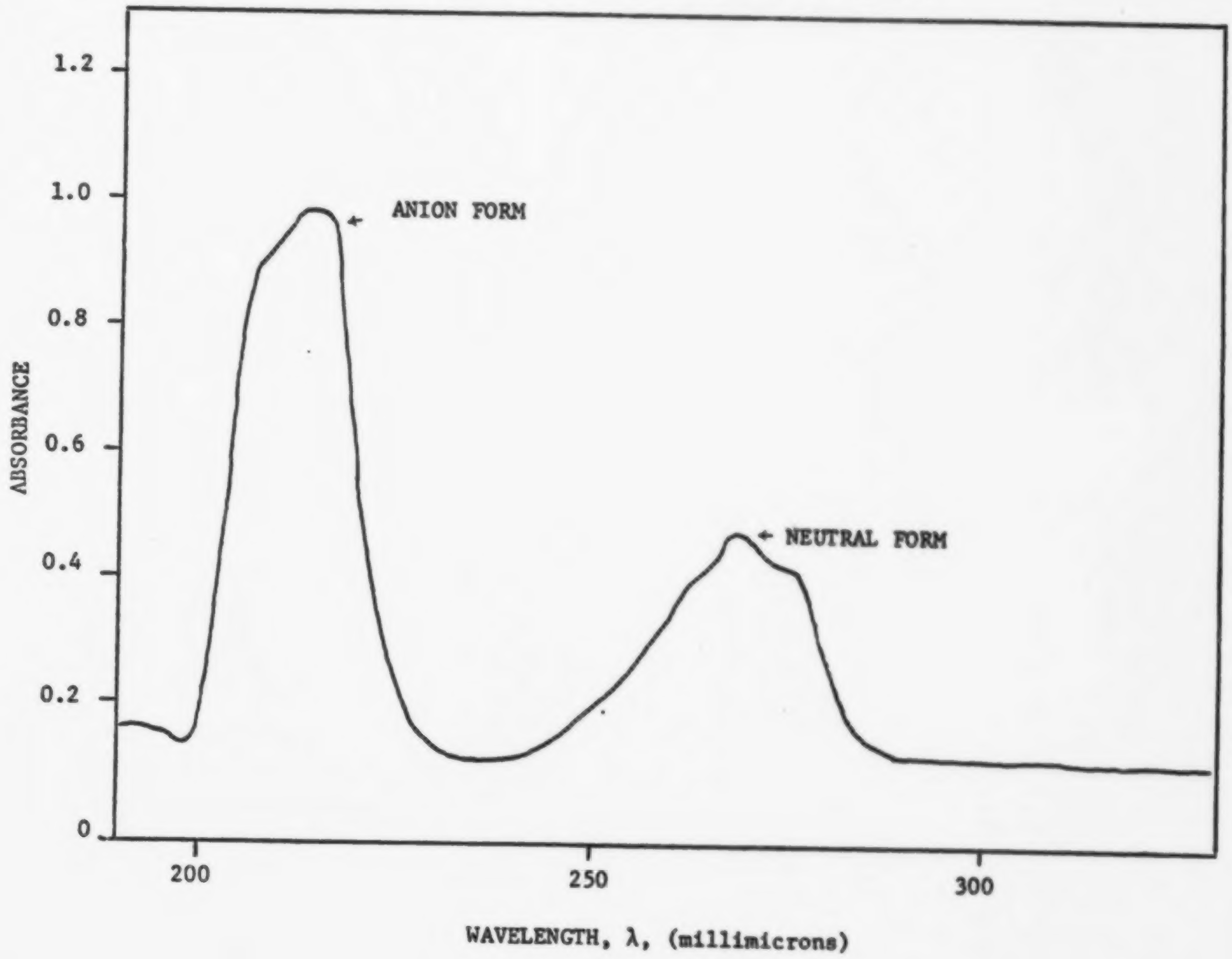

FIGURE 3-3. CALIBRATION CURVE FOR PHENOL

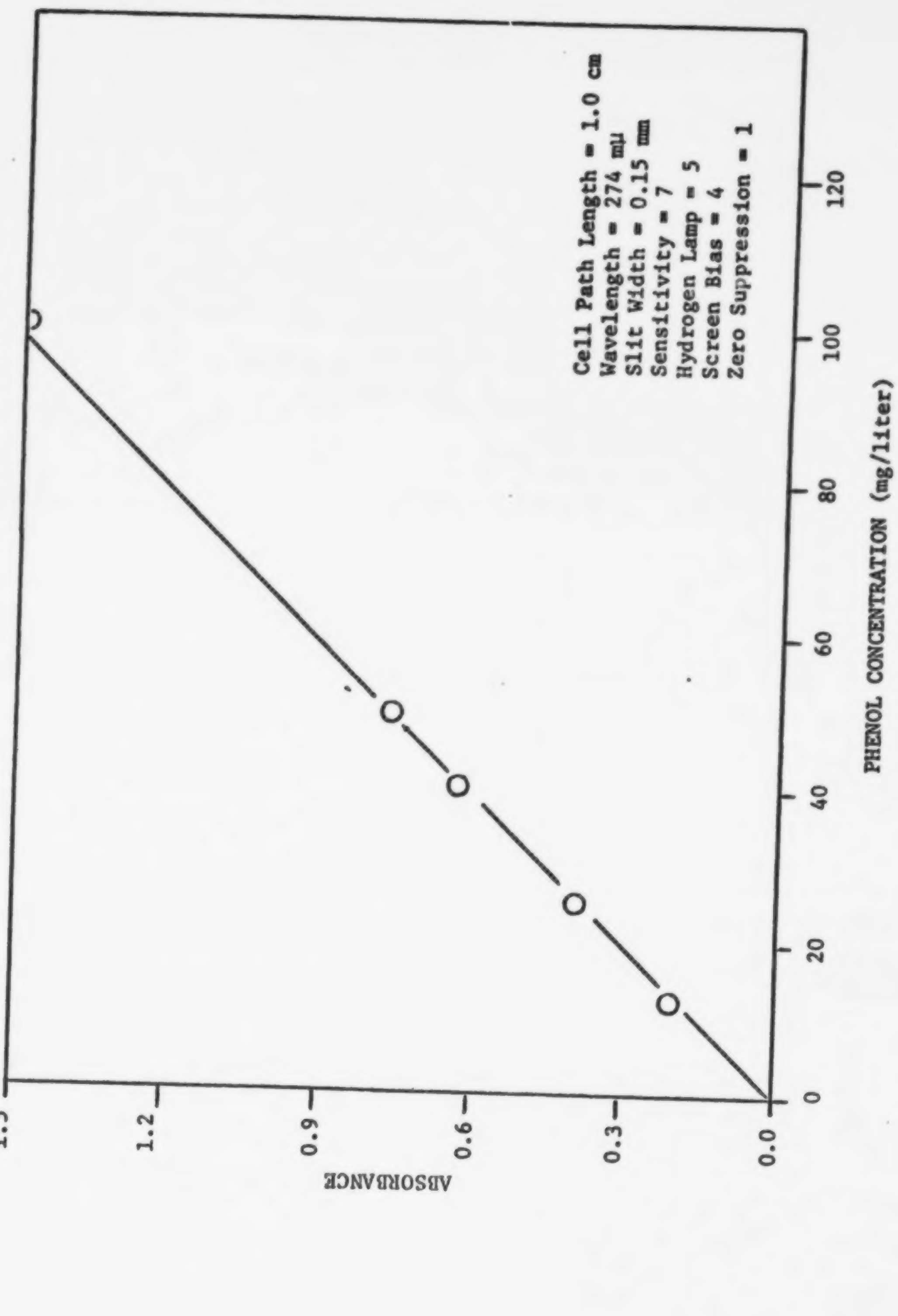

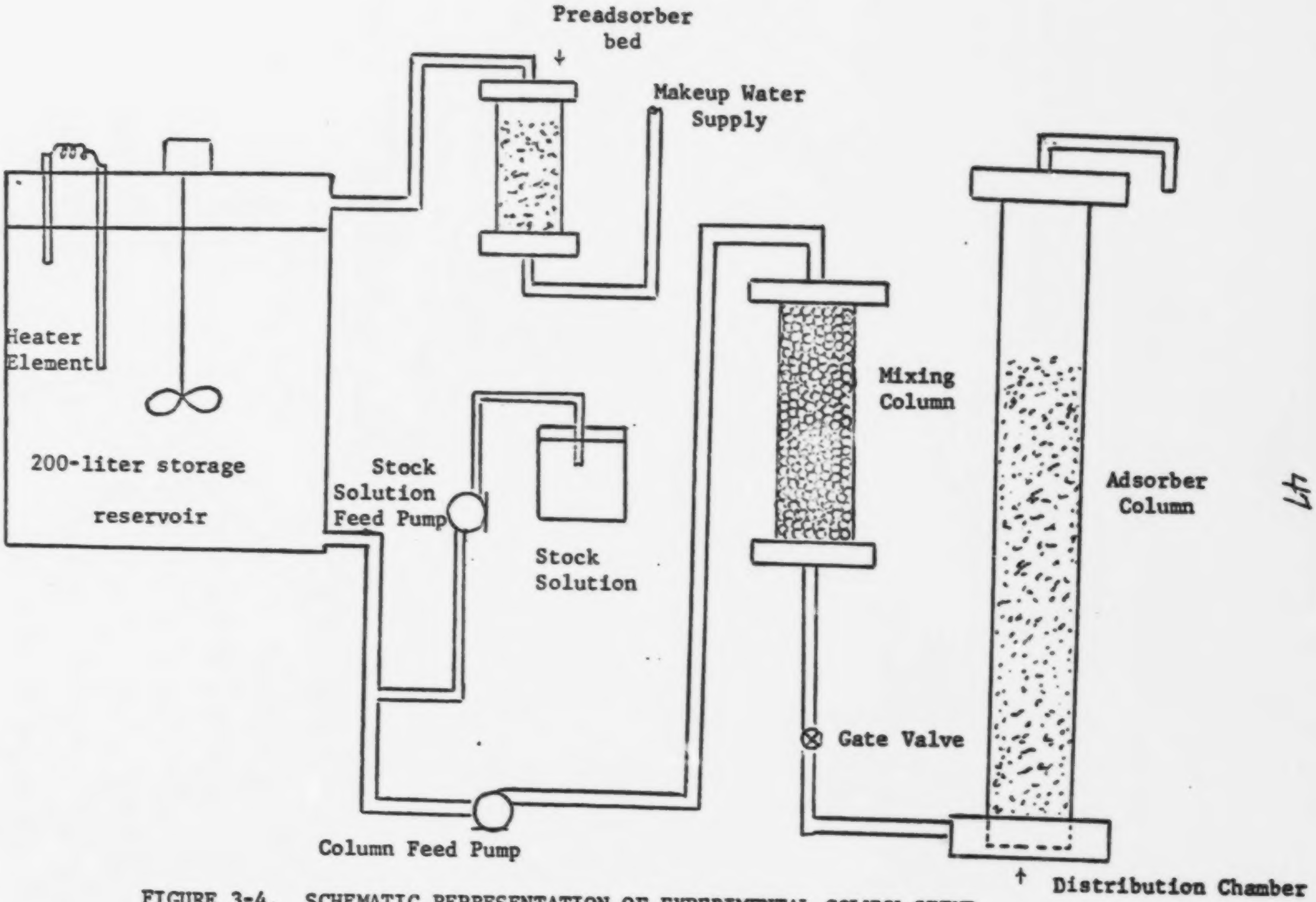
Preadsorber
bed
Makeup Water
Supply
Heater
Element
200-liter storage
reservoir
Stock
Solution
Feed Pump
Stock
Solution
Mixing
Column
Adsorber
Column
Gate Valve
Column Feed Pump
Distribution Chamber

FIGURE 3-4. SCHEMATIC REPRESENTATION OF EXPERIMENTAL COLUMN SETUP

Tap water from the Ann Arbor Municipal System served as a supply for solution make-up water. The tap water flowed through a pretreatment active carbon bed containing 2.0 kilograms of Filtrasorb carbon. This water was then stored in a stirred 200-liter polyethylene tank which contained a thermostatically-controlled heater element to provide temperature control during generation of the experimental concentration-history profiles.

The pretreated, temperature-equilibrated water was connected to four separate feed channels by polyethylene tubing. Each channel was supplied with concentrated mixture solution by means of a T-connection fitted with a one-way valve on the stock solution feed line. The feed solution was transported from polyethylene storage tanks by a four-channel polystaltic pump (Buchler Instrument Model No. 2-6100). The concentration of the stock mixture solution was determined by measuring the flow of the feed through 0.062 inch inside-diameter, 0.0655 inch wall medical-grade silicone tubing and knowing the total flow rate and desired concentration for each column.

Flow rate was provided and controlled by using a four-channel constant proportioning pump (Hills McCanna Co., Model No. 122C). Each channel was set for the desired flow rate and maintained that rate for the duration of experimental operation.

To assure adequate mixing of solution make-up water and stock solution, a 24-inch plexiglass column filled with 10 mm glass beads was provided in line between the proportioning pump and the adsorber column. A gate valve was inserted in order to sample and check the influent concentration, thus going to the adsorption bed. The feed solution then proceeded into the distribution chamber. Above the distribution chamber was an 80-mesh nickel screen supporting the adsorption bed of active carbon. The solution mixture passed through this bed and exited at the top of the column. The effluent line provided the sampling port for the concentration-determination in solution exposed to the adsorber bed. The data acquired by periodic sampling of the influent and effluent sections generated the desired concentration-history profiles for verification of the mathematic model predictions.

CHAPTER 4

PARAMETER DETERMINATIONS FOR UTILIZATION OF PREDICTIVE MATHEMATIC MODEL

The Thomas solution to the material balance equation given by Equation 2-42 and the formulation of diffusional mass-transfer coefficient relationships to the second-order kinetic rate constant (Equations 2-51, 2-53, 2-56, and 2-66) provide a mathematic tool for prediction of effluent-concentration-history profiles for expanded adsorber beds. In order to utilize this mathematic model, the column adsorber system must be described by physical, hydrodynamic, and adsorption equilibrium and kinetic constants. In this section, the specification and determination of the requisite parameters for utilization of the mathematic model are presented and discussed.

FIXED PARAMETERS

The mathematic model was developed on the basis of a material balance relationship with the volumetric flow rate and the influent concentration of sorbate fixed at constant values. For experimental purposes, the volumetric flow rate was set and maintained at a constant rate. For design purposes, optimization procedures may be employed to determine the best volumetric flow rate in conjunction with other adsorber column parameters.

The influent concentration of the sorbate in the mixtures was also chosen and introduced to the adsorber columns at a constant concentration value utilizing the experimental column arrangement discussed in Chapter 3.

HYDRODYNAMIC PARAMETERS

Three parameters which relate to the hydrodynamics of the fluid-particle expanded-bed adsorber system need to be determined for utilization of the predictive mathematic model. These parameters are: 1) porosity of the adsorber bed in the expanded state; 2) volume of the expanded adsorber bed; and, 3) density of the expanded adsorber bed. The hydrodynamics of fluidization have been reviewed and the important relationships for calculation of these hydrodynamic parameters have been illustrated by Keinath and Weber (56). A brief summary of the important relationships for determination of the requisite hydrodynamic parameters is presented herein.

Porosity of Expanded Bed

A force balance performed on a free-falling sphere in a liquid medium results in an expression relating the drag coefficient to particle velocity and physical characteristics of the fluid-particle system (25,35). A standard drag curve (90) represents the relationships between the drag coefficient and the dimensionless Reynolds number, N_{Re}. From these basic considerations, three relationships for various Reynolds number regimes, termed Stoke's regime, the intermediate regime, and Newton's regime (90), can be expressed for determination of particle velocity for the respective regimes.

For low values of the Reynolds number, ($N_{Re} < 2$), the Stoke's law expression for the particle velocity results (56). This is given by

$$(v_{p_o})_S = \frac{d_p{}^2(\rho_s - \rho_\ell)\ g}{18\mu} \qquad (4\text{-}1)$$

in which v_{P_o} is the particle velocity, d_p is the diameter of the particle, ρ_s is the density of the solid particle, ρ_ℓ is the density of the liquid, g is the universal gravitational constant, μ is the absolute viscosity of the liquid medium.

For intermediate values of the Reynolds number, $(2<N_{Re}<500)$, an approximation of the drag coefficient (10) results in

$$(v_{P_o})_I = \frac{0.153\, d_p^{1.14} \left[g(\rho_s-\rho_\ell)\right]^{0.71}}{\rho_\ell^{0.29}\ \mu^{0.43}} \tag{4-2}$$

For high Reynolds number values $(500 < N_{Re} < 2 \times 10^5)$, Newton's law for the evaluation of the drag coefficient holds (90), resulting in

$$(v_{P_o})_N = 3.03 \left[\frac{d_p(\rho_s-\rho_\ell)}{\rho_\ell}\right]^{\frac{1}{2}} \tag{4-3}$$

For the case of densely associated particles, which obviously prevails in expanded-bed adsorber systems, there is mutual interference of particle motion which is not accounted for in the force balance. Lewis and Bowerman (63) have proposed a relationship between the ratio of steady-state liquid velocity through the expanded bed to the terminal particle velocity and a power function of the void ratio, expressed by

$$\frac{\overline{V}}{\overline{v}_{P_o}} = F(\varepsilon) \tag{4-4}$$

where $\overline{V}$ is the superficial fluid velocity.

For the intermediate Reynolds number regime, Keinath and Weber (56) experimentally found that

$$\varepsilon = \left[\frac{\bar{V}}{(v_{Po})_I}\right]^{0.256} \qquad (4\text{-}5)$$

which can be used to predict void ratios for expanded bed systems.

Another approach by Wen and Yu (125) related the ratio of drag forces yields an expression for prediction of the void ratio. This can be expressed as

$$\varepsilon = \left[\frac{18\, N_{Re} + 2.70\, N_{Re}^{1.687}}{N_{Gr}}\right]^{0.192} \qquad (4\text{-}6)$$

$$\text{for } 10^{-3} < N_{Re} < 10^{3} \qquad (4\text{-}6)$$

in which N_{Gr} is the Grashof number and is equated to $d_p^{\,3}\rho_\ell(\rho_s-\rho_\ell)\, g/\mu^2$. Keinath and Weber (56) have found good agreement with actual void ratios and those predicted by Equations 4-5 and 4-6. Their results are in good agreement with other investigations (63,83,125) which were performed using a wide variety of experimental systems. Thus Equation 4-5 in conjunction with Equation 4-2 may be used for prediction of the void ratio when the Reynolds number for the system of interest is in the intermediate regime, or the generalized void ratio expression given by Equation 4-6 may be used within its Reynolds number limitations.

Expanded-bed Volume

With the value of the porosity of the expanded bed determined from Equation 4-5 or 4-6, it becomes a simple matter of determining the volume of the expanded bed for a given total mass of adsorbent of known solid density.

Density of the Expanded Bed

For a given total mass of adsorbent, the density of the expanded bed can be readily calculated from the aforementioned considerations for determination of the expanded-bed volume.

ADSORPTION EQUILIBRIUM CONSTANTS

The mathematic model developed by Thomas was based on the Langmuir isotherm development. In order to use that model, the equilibrium distribution between the sorbate in the fluid- and solid-phase must therefore be experimentally developed and mathematically described by the Langmuir isotherm, as given by Equation 2-4.

Experimental Technique

The equilibrium isotherm phase distribution of sorbate was determined for each mixture system by application of the bottle-point method after Weber and Morris (122). Specifically, for each mixture, measured amounts of carefully-sized and -prepared Filtrasorb active carbon were added to individual 0.120-liter glass bottles containing 0.100 liter of mixture solution. The bottles were tightly sealed using polyethylene-lined plastic caps, and were then placed on a laboratory-designed roller system, which provided continuous agitation for the duration of the experimental isotherm development. Blank samples, i.e. solution aliquots containing no adsorbent, were included in the experimental isotherm development. They provided information of the initial concentration of each solute mixture and served as a check on degradation of organic material by comparison of the solute concentrations at the commencement and at the termination of the agitation period.

In order to determine whether or not equilibrium had been reached, samples containing identical amounts of active carbon and mixture solution were incorporated in the experimental work. Periodically one such sample was removed from the agitator and the remaining sorbate fluid-phase concentration was analyzed. When this residual concentration was determined to be unchanging, equilibrium phase distribution of sorbate was assumed to have been achieved.

The equilibrium sorbate concentration in the fluid phase subtracted from the initial sorbate concentration, (C_o-C_e), yields the amount of sorbate removed by the active carbon for a given bottle-point sample, and after normalization generates a point on the adsorption isotherm. An adsorption isotherm is given by a plot of the amount of sorbate removed per unit weight of adsorbent, $(C_o-C_e)/x_c = q$, versus the equilibrium fluid-phase concentration of sorbate, C_e.

The Langmuir constants of interest for use in the predictive mathematic model are the ultimate capacity of the adsorbent for the sorbate, Q, and the Langmuir energy constant, b. These constants may be calculated by linearizing Equation 2-4, the mathematic expression for the Langmuir adsorption isotherm. By inverting the Langmuir isotherm formulation, the linear form of Equation 2-4 results, and is expressed as

$$\frac{1}{q} = \frac{1}{Qb} \cdot \frac{1}{C_e} + \frac{1}{Q} \qquad (4\text{-}7)$$

It is obvious that a plot of 1/q versus $1/C_e$ will yield a linear trace with a slope equal to 1/Qb and an intercept of 1/Q. This approach has been applied, in conjunction with a least-squares linear-regression analysis for best fit of linearized data points, for the interpretation of the experimental isotherm data and determination of the requisite Langmuir isotherm constants. The values of Q and b obtained in this manner were substituted into Equation 2-4, and the calculated Langmuir adsorption isotherms which resulted were compared to the respective experimental isotherm data points.

Experimental adsorption isotherms determinations were performed to generate the sorbate equilibrium distribution profile for pure solutions of the individual components of the complex mixtures and for each of the twelve complex mixture systems. The active carbon used in all the isotherm developments was the 0.503 mm Filtrasorb carbon. Additional adsorption isotherm experiments were conducted with a smaller size (0.161 mm) Filtrasorb carbon to confirm for the mixtures the observations by Keinath and Weber (56) and Dedrick and Beckman (17) with single solute systems that particle size did not significantly affect the ultimate equilibrium distribution of the sorbate between the solid- and fluid-phase. The results of the isotherm experiments are reported below.

Single Solute Isotherms

The complex mixtures used in the experimental portion of this research were composed of sorbate compounds which differed in their respective adsorption equilibria. In this manner, the generality of the predictive mathematic model could be tested. Therefore, individual isotherms for pure solutions of the individual mixture components were experimentally generated to ascertain that a range of equilibrium adsorption behavior was provided by the individual components. It was recognized that the adsorption behavior for an individual component in pure solution would differ from behavior exhibited in competitive sorbate mixtures, with a probable decrease in capacity for the individual sorbates (113). No extrapolation of the results of pure sorbate components to behavior of any given sorbate in a complex mixture is assumed.

Dextrose and Sodium Acetate

Adsorption isotherm experiments for pure solutions of dextrose and sodium acetate indicated that essentially no adsorption of either component occurred even with dosages of active carbon as high as 15.0 grams per liter. These compounds were thus classified as non-adsorbable organics and were used as such in four complex mixtures.

Phenol, Dodecyl Sodium Sulfate, and n-Hexanol

The experimental isotherms developed for pure solutions of phenol, dodecyl sodium sulfate, and n-hexanol are shown in Figures 4-1, 4-2, and 4-3 respectively. The solid line in these figures indicates the calculated Langmuir isotherms, determined by application of Equation 2-4 utilizing the experimentally determined ultimate capacity and adsorption energy constants, Q and b, respectively.

Comparison of the calculated Langmuir adsorption isotherm to the experimental data points indicates good correlation for each of the respective compounds. Thus, the Langmuir adsorption isotherm

FIGURE 4-1. ADSORPTION ISOTHERM: PHENOL

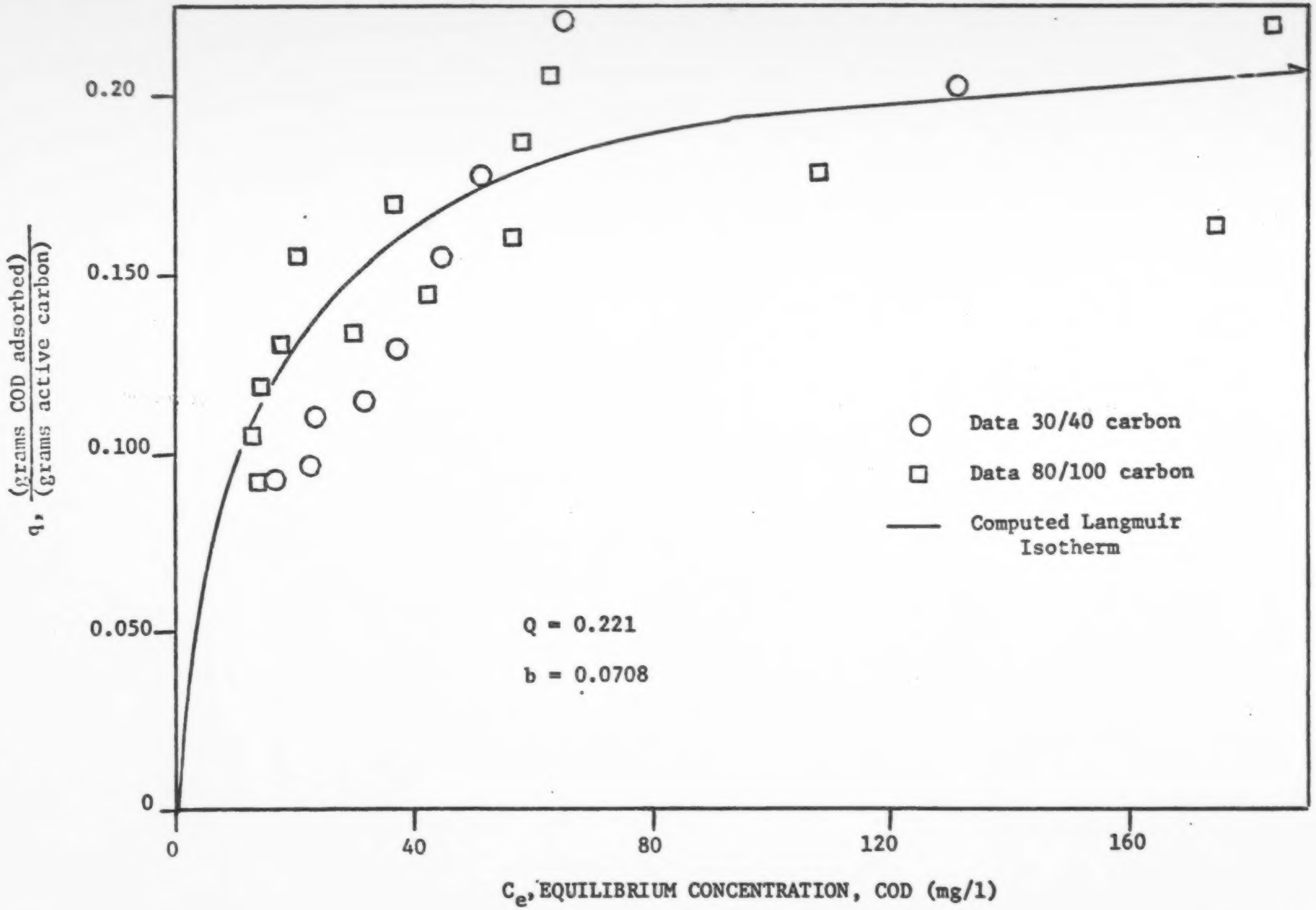

FIGURE 4-2. ADSORPTION ISOTHERM: DODECYL SODIUM SULFATE

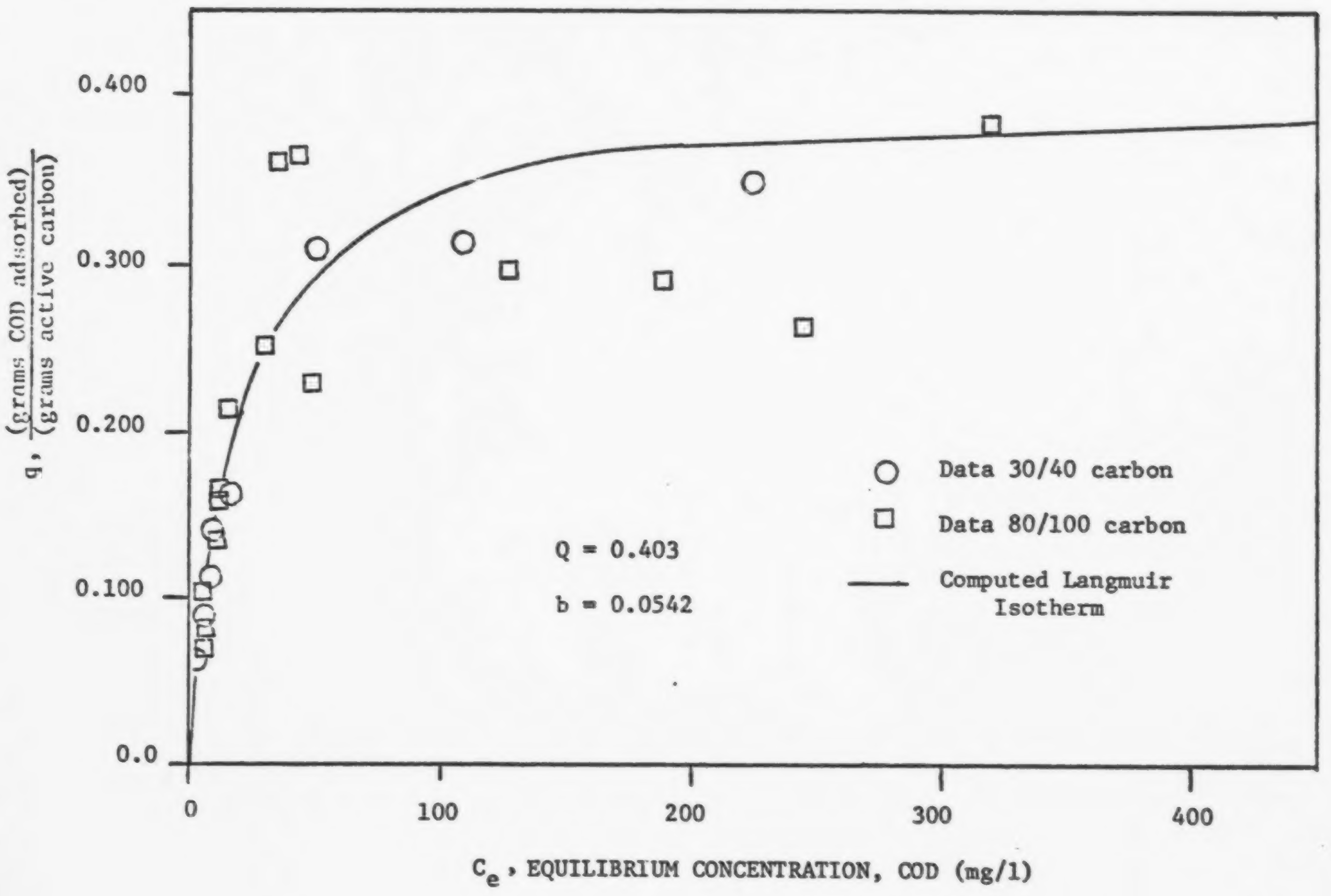

FIGURE 4-3. ADSORPTION ISOTHERM: n-HEXANOL

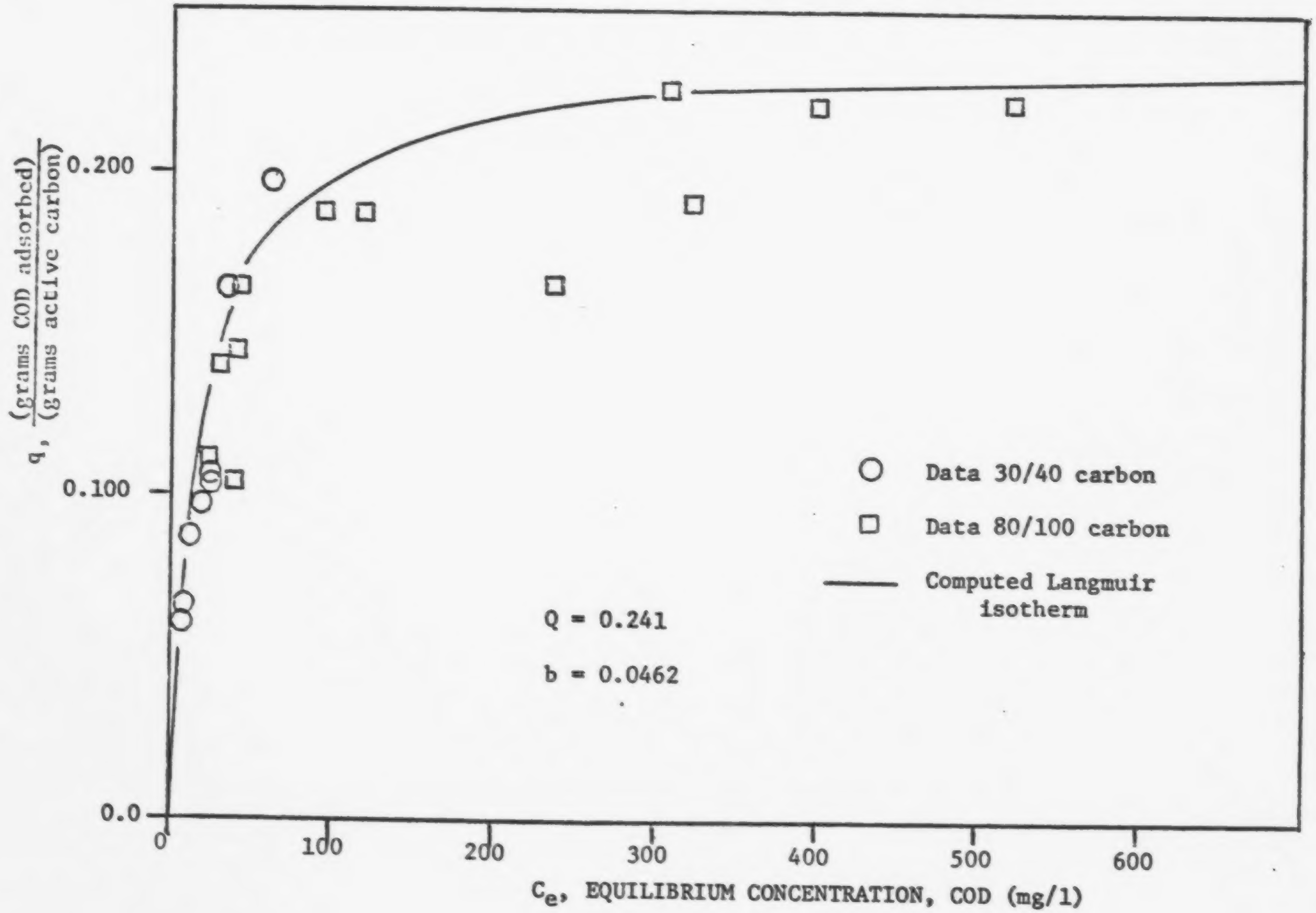

definition appears to adequately describe the sorbate equilibrium distribution for these compounds. The adsorption isotherms are all of the favorable type, and, upon inspection, indicate that the use of a linear equilibrium relationship would be a gross approximation of sorbate distribution.

The experimentally determined Langmuir ultimate adsorption capacity and energy constant for each of the sorbates in pure solution can be found in Table 4-1. Comparison of the individual Langmuir isotherm values for each component based on COD indicate that phenol had the lowest ultimate adsorption capacity, with that for n-hexanol only slightly higher, whereas dodecyl sodium sulfate exhibited an ultimate adsorption capacity almost double that of phenol. However, on a COD basis, phenol exhibited the highest Langmuir energy constant value and n-hexanol had the lowest. These comparisons indicate that a variety of adsorption behavior could logically be expected from mixtures of these three compounds, and hence such mixtures would provide a suitable basis for determining the generality of the predictive mathematic model for effluent concentration-history profiles.

The adsorption isotherms for each of the three sorbate compounds in pure solution were generated using both size fractions of active carbon. The results of these studies indicate that no difference in ultimate capacity or the Langmuir isotherm energy constant resulted for the active carbon used in these experiments. This is in agreement with other investigations (17, 56). This result has practical implications in that smaller size adsorbent particles proposed for use in column operations can be used in experimental isotherm developments.

TABLE 4-1

LANGMUIR ISOTHERM CONSTANTS FOR PURE COMPOUNDS USED IN MIXTURES

COMPOUND	LANGMUIR ULTIMATE CAPACITY CONSTANT, Q (mg COD adsorbed/mg active carbon)	LANGMUIR ENERGY CONSTANT, b (liter/mg COD)
Phenol	0.221	0.0708
n-Hexanol	0.241	0.0462
Dodecyl Sodium Sulfate	0.403	0.0542
Sodium Acetate	*	*
D-Glucose	*	*

(*) indicates nonadsorbing compound.

The advantage of using smaller adsorbent particles in isotherm experiments lies in the fact that if the same isotherm obtains for all particle sizes of a given adsorbent-sorbate system, then equilibrium will be attained more rapidly using small size particles. Since b, the Langmuir energy constant, is equal to the ratio of the forward (adsorption) reaction rate constant to the reverse (desorption) reaction rate constant, isotherm developments fitting the above-mentioned criteria require that this reaction-rate-constant ratio be constant. However, adsorption rates have been shown to vary inversely with $d_p^{1.6}$,(32, 39); therefore, faster equilibrium is expected for smaller particle experimental adsorption equilibria systems.

Sorbate Mixtures

Experimental adsorption isotherm developments were performed using the complex sorbate mixtures composed of the individual sorbate compounds (as detailed previously). The concentrations of the complex sorbate mixtures were expressed in terms of the overall description parameter, COD, in accordance with the aims of this research to treat complex mixtures as single component systems. The Langmuir ultimate adsorption capacity and energy constants for the respective mixtures were developed on a COD basis. The active carbon used for the experimental adsorption isotherms was the 0.503 mm size fraction for all complex mixtures, Mix 1 through Mix 8, and the 0.161 mm size fraction was also used for the experimental adsorption isotherms for Mix 2, Mix 4, and Mix 8. These three complex sorbate mixtures represented binary mixtures of dodecyl sodium sulfate and phenol, dodecyl sodium sulfate and n-hexanol, and a ternary mixture of these three sorbate compounds, respectively.

The experimental adsorption isotherm results for Mix 1 through Mix 8 are shown in Figures 4-4 through 4-11, respectively. The solid line in each of these figures represents the Langmuir adsorption isotherm calculated from Equation 2-4, utilizing the ultimate adsorption capacity constant and Langmuir adsorption energy constant derived from the linearized experimental data for each mixture. Examination of Figures 4-4 through 4-11 indicate that the experimental adsorption isotherm data points are well-described by the Langmuir formulation for each of the complex mixtures. All of the experimental isotherms are of the favorable type.

The experiments incorporating the 0.161 mm active carbon confirmed the results for the pure solution isotherm developments that there was no apparent dependence of ultimate adsorption capacity on particle size. Figures 4-5, 4-7, and 4-11 indicate that identical adsorption isotherms obtained for a given mixture composition with both particle size fractions.

The experimentally determined Langmuir adsorption isotherm constants for Mixtures 1 through 8 are given in Table 4-2. Comparison of these constants show a wide range of equilibrium adsorption behavior for these sorbate mixtures. For example, Mix 4 has the highest ultimate adsorption capacity and the lowest adsorption energy constant. Mix 3, on the other hand, has the lowest ultimate adsorption capacity, but the Langmuir adsorption energy constant is approximately two orders of magnitude greater than that of Mix 4.

FIGURE 4-4. ADSORPTION ISOTHERM: MIX 1

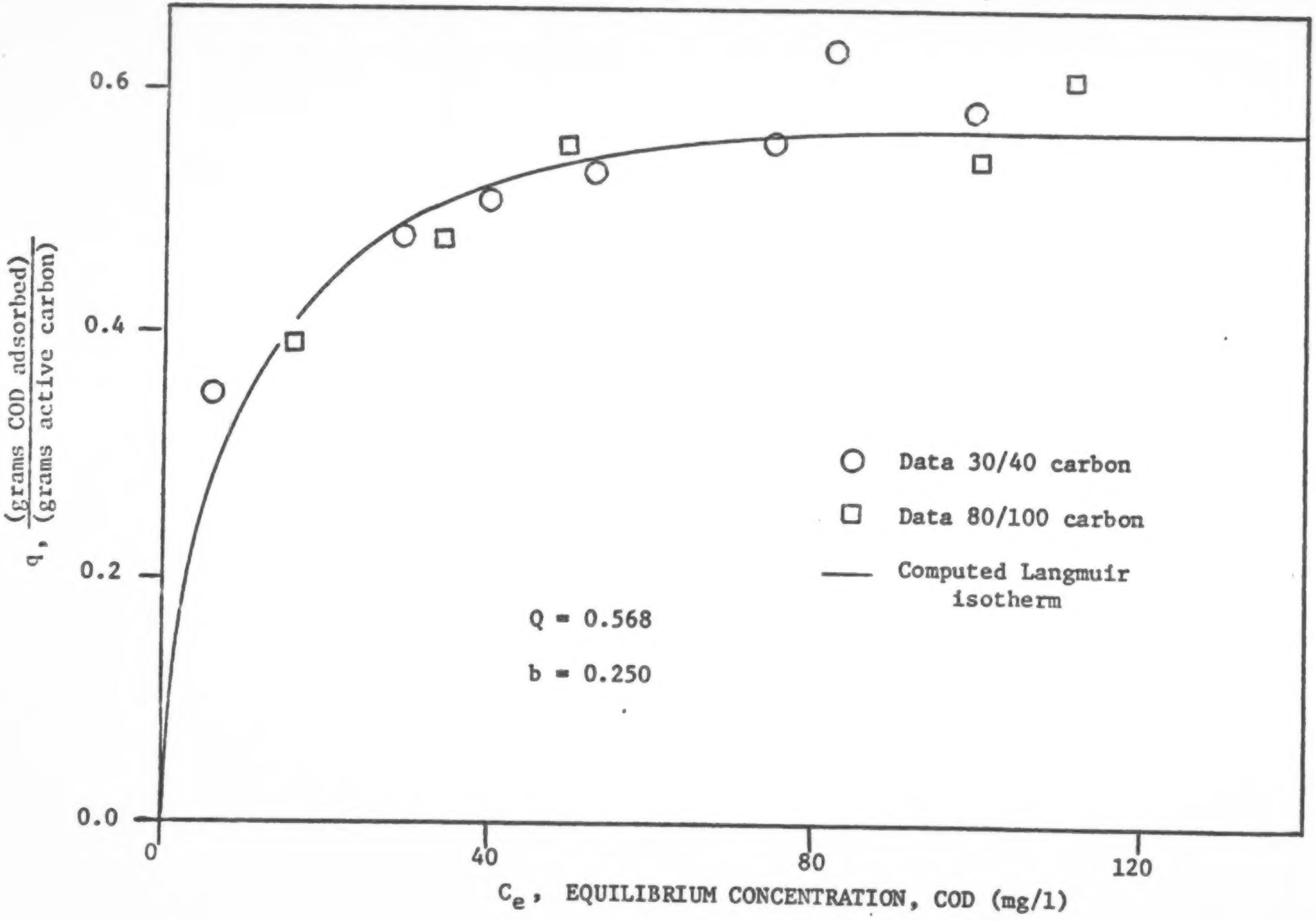

FIGURE 4-5. ADSORPTION ISOTHERM: MIX 2

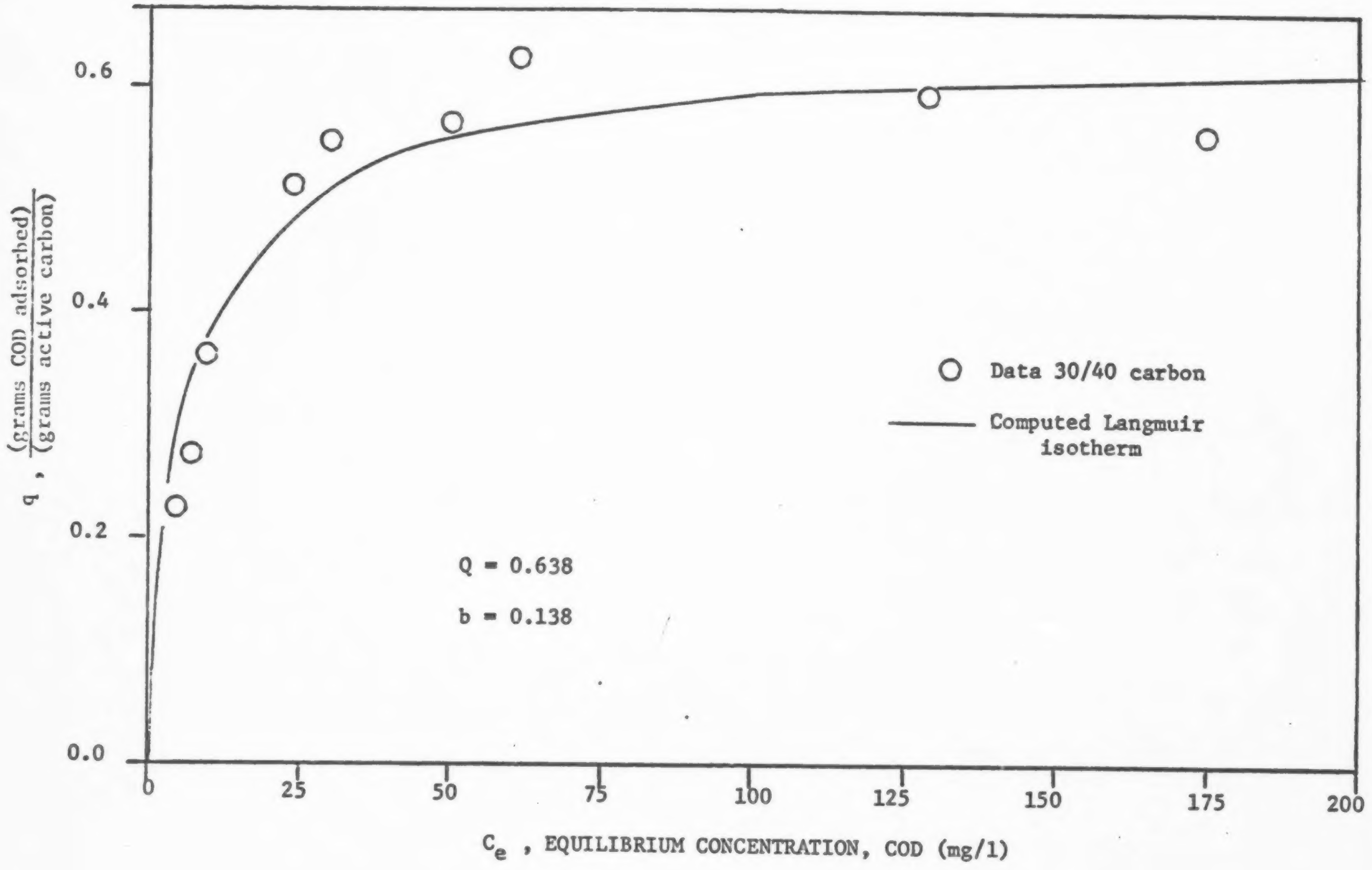

FIGURE 4-6. ADSORPTION ISOTHERM: MIX 3

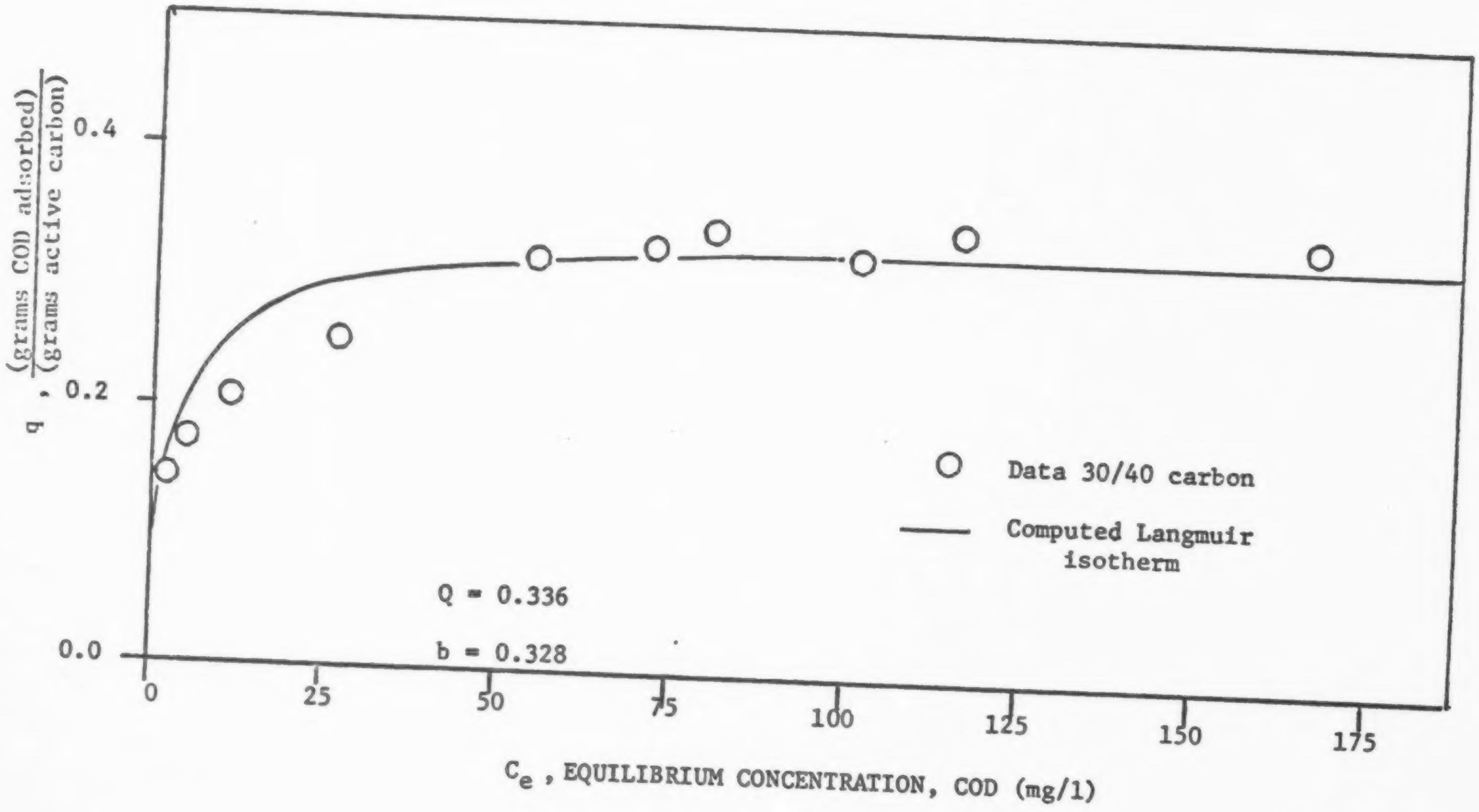

FIGURE 4-7. ADSORPTION ISOTHERM: MIX 4

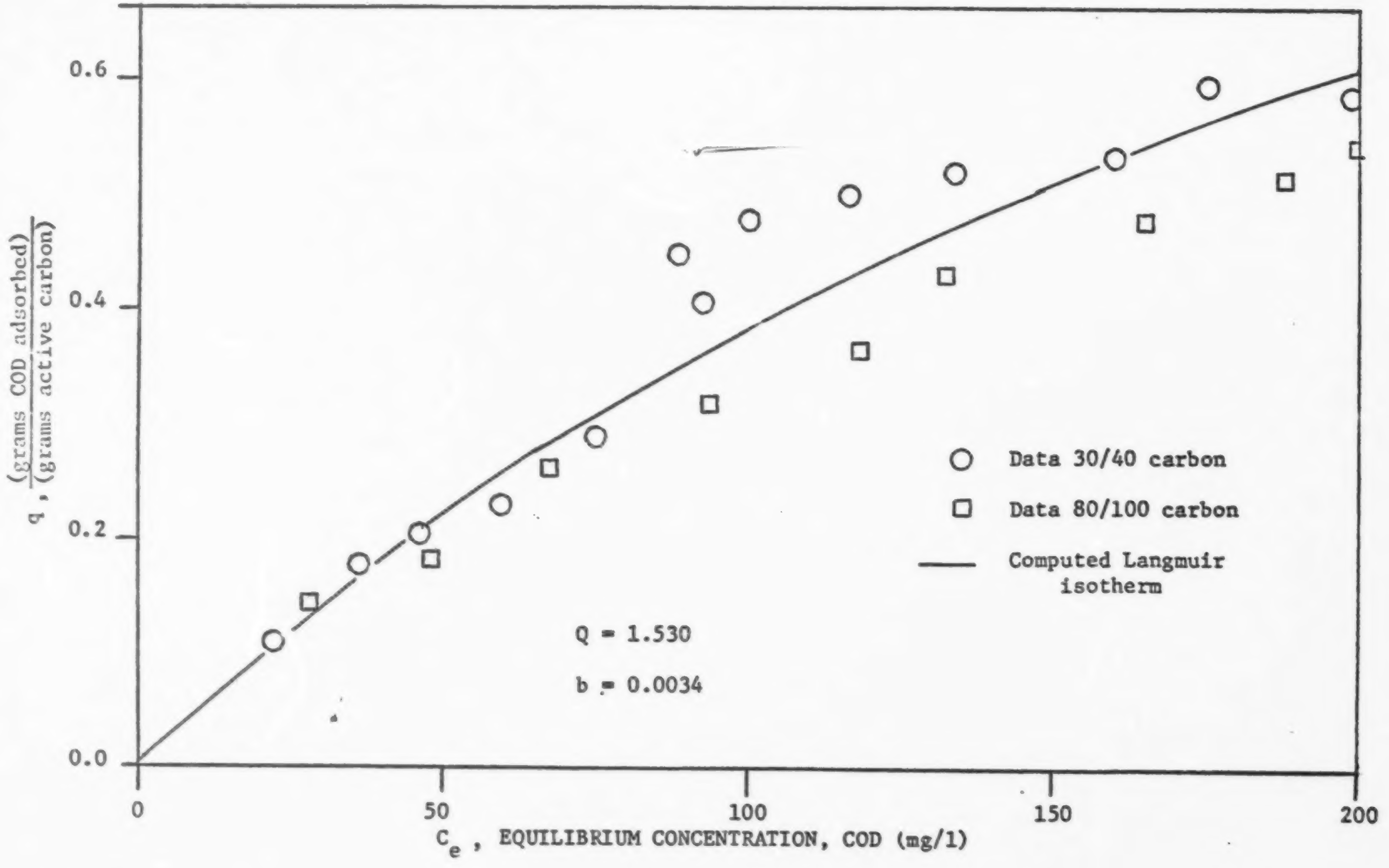

FIGURE 4-8. ADSORPTION ISOTHERM: MIX 5

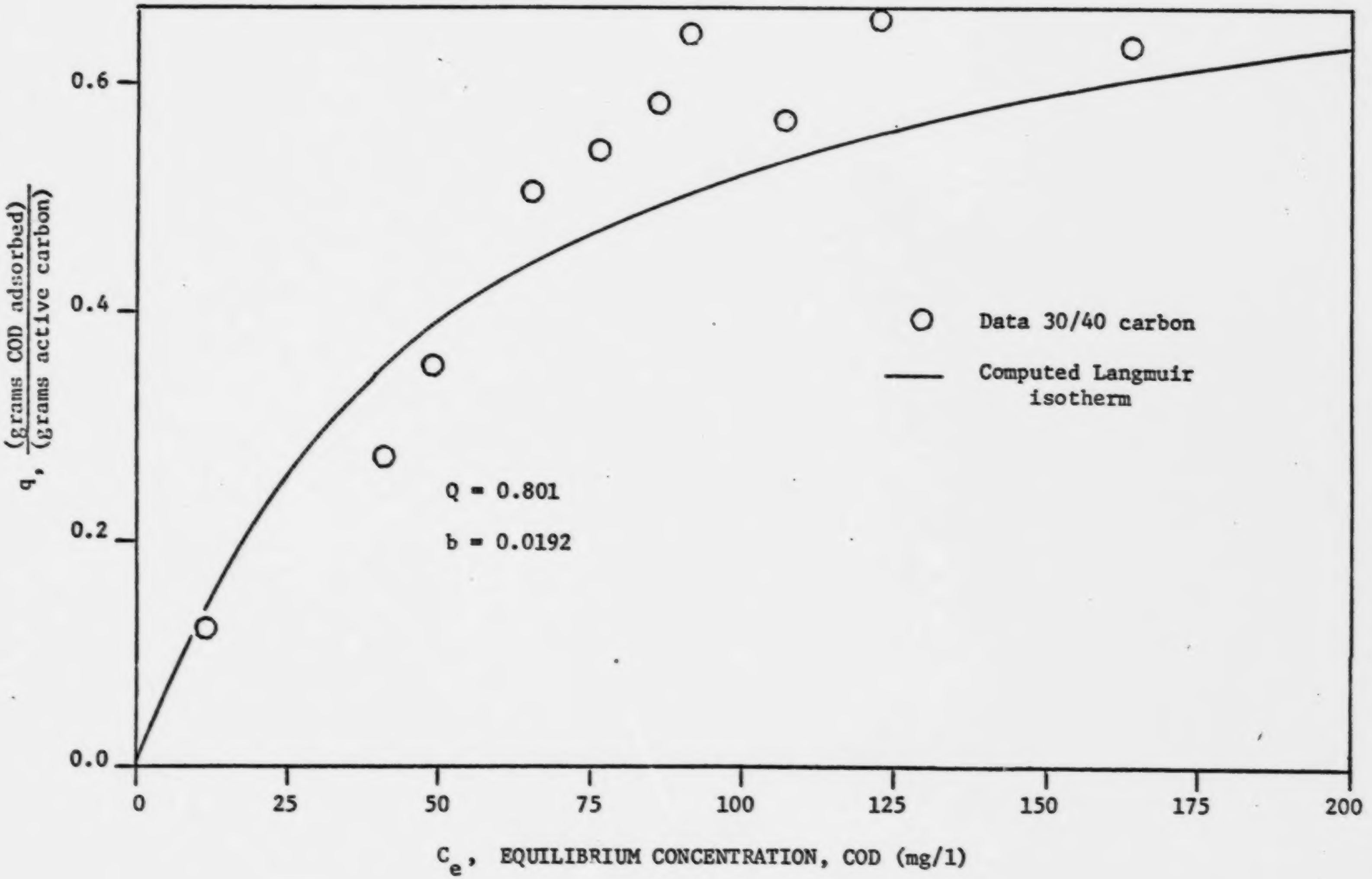

FIGURE 4-9. ADSORPTION ISOTHERM: MIX 6

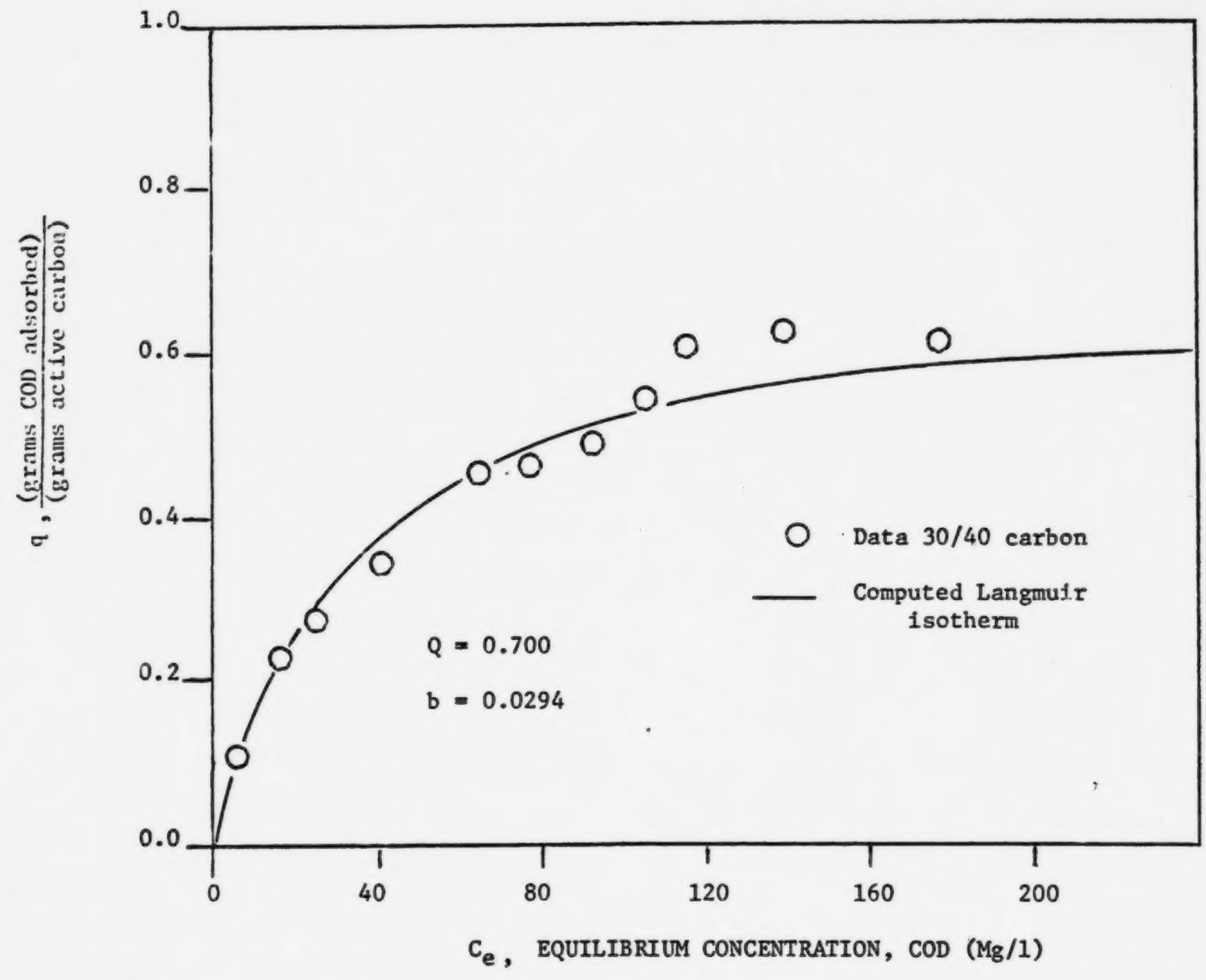

FIGURE 4-10. ADSORPTION ISOTHERM: Mix 7

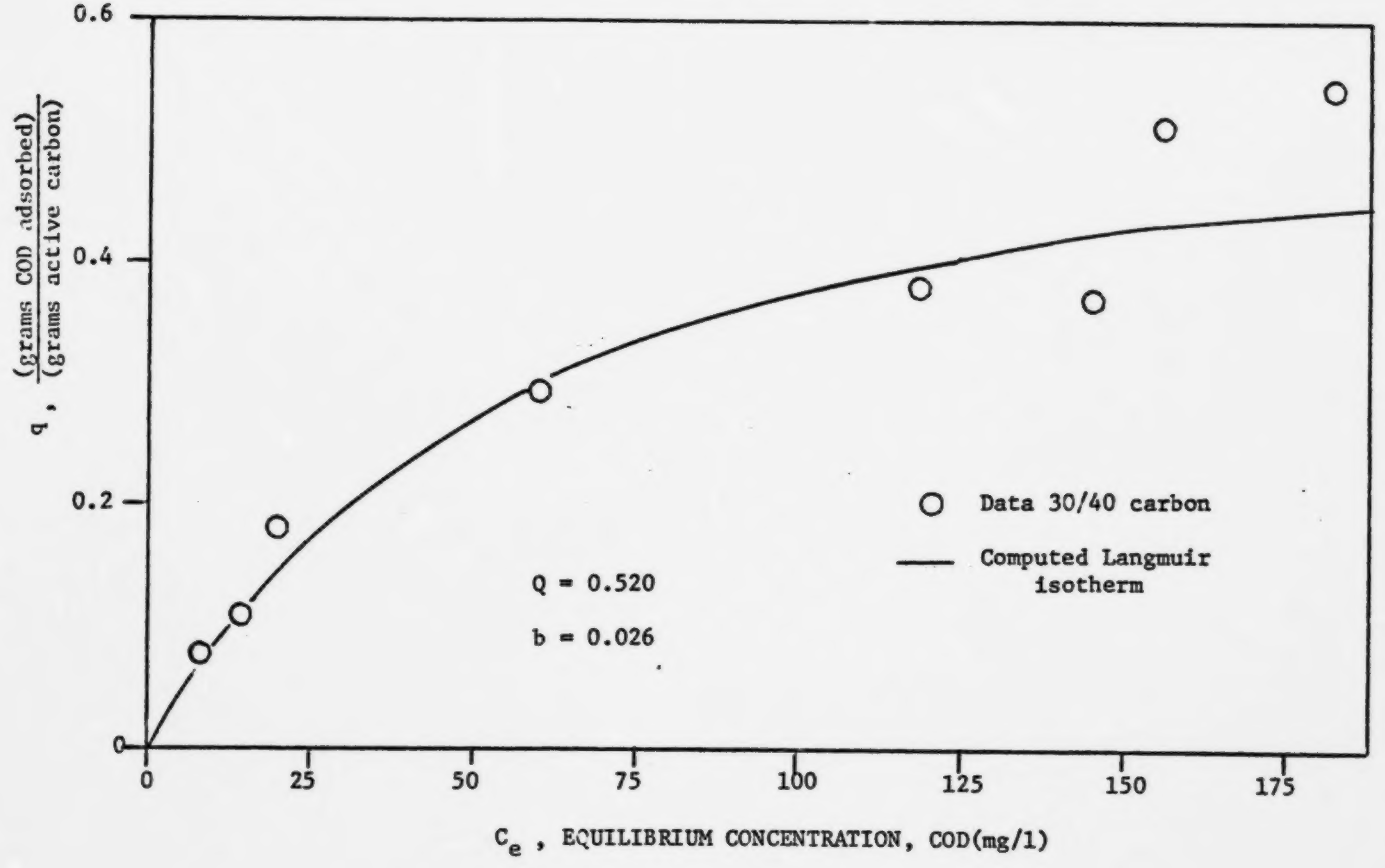

FIGURE 4-11. ADSORPTION ISOTHERM: MIX 8

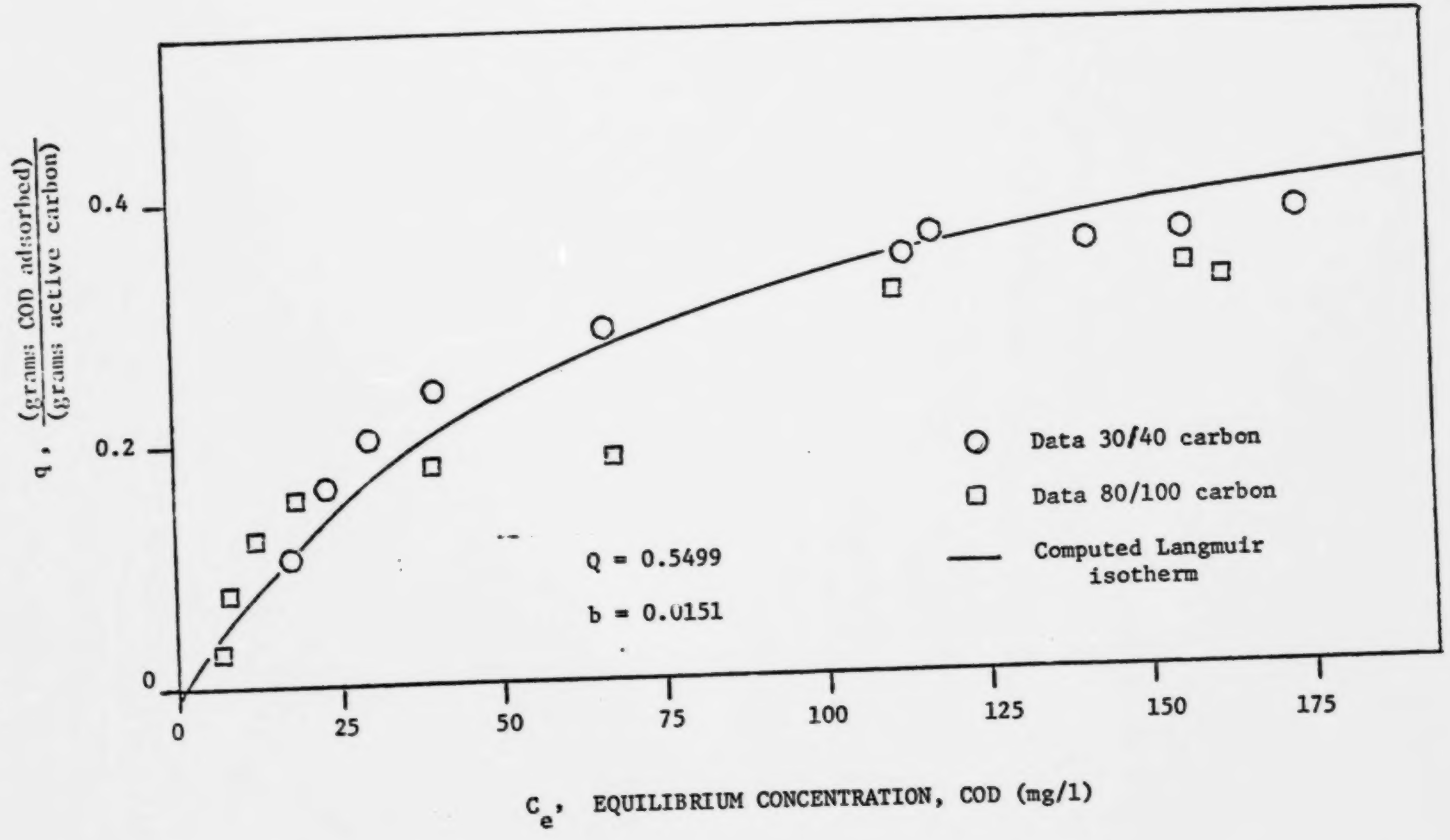

TABLE 4-2

LANGMUIR ISOTHERM CONSTANTS FOR SORBATE MIXTURES

MIXTURE	LANGMUIR ULTIMATE CAPACITY CONSTANT, Q (mg COD adsorbed/ mg active carbon)	LANGMUIR ENERGY CONSTANT, b (liter/mg COD)
1	0.568	0.250
2	0.336	0.328
3	0.638	0.138
4	1.530	0.0034
5	0.801	0.0192
6	0.700	0.0294
7	0.549	0.0151
8	0.520	0.026

Further examination of Table 4-2 indicates that based on the variety of Langmuir adsorption isotherm values, the mixtures as developed should provide a good test for the general applicability of the predictive adsorption mathematic model.

Adsorber/Non-Adsorber Mixtures

Adsorption isotherms were experimentally generated for the four complex mixtures containing non-adsorbing fractions of dissolved organic compounds. The concentrations of the complex mixtures were again expressed as COD and the mixtures were treated as single component systems. The active carbon used for the adsorption isotherm developments was the 0.503 mm size fraction for all adsorber/non-adsorber mixtures, Mix 9 through Mix 12, and the 0.161 mm size fraction was used in an adsorption isotherm experiment for Mix 9.

The results of these experiments can be found in Figures 4-12 through 4-15 for Mix 9 through Mix 12, respectively. Examination of these figures indicate that the adsorption isotherm data points form a curve representative of a favorable adsorption isotherm for all mixture cases, but with one very important difference. The difference can be seen to be that the adsorption isotherm data points do not approach an equilibrium concentration of zero as q, the amount adsorbed per unit amount of carbon, approaches zero, but remain at a distinctly measurable equilibrium concentration.

A very important consequence of this behavior is that the experimental adsorption isotherm development provides a means for determining non-adsorbing fractions of materials which contribute to the overall description parameter used to characterize a complex

FIGURE 4-12. ADSORPTION ISOTHERM: MIX 9

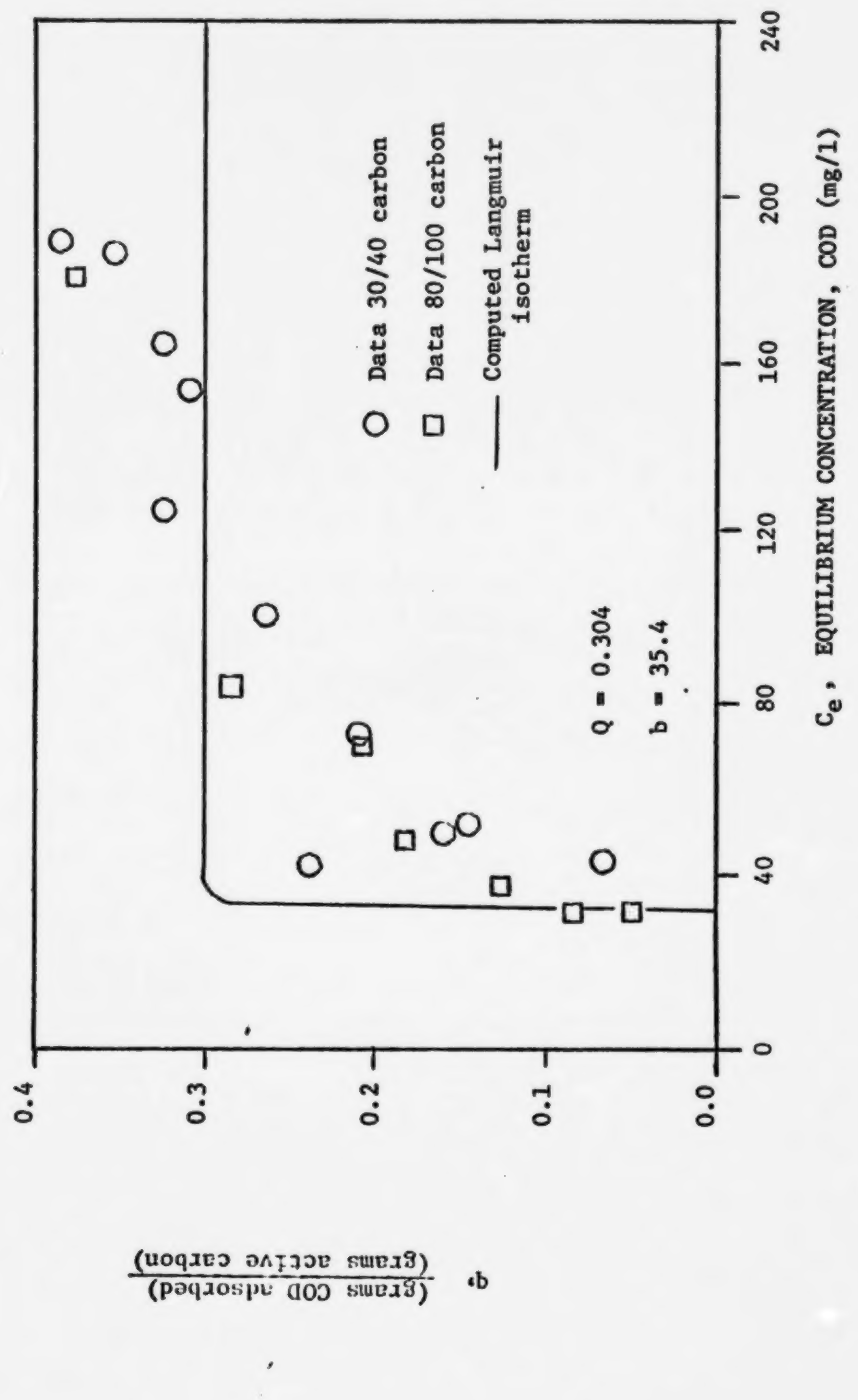

FIGURE 4-13. ADSORPTION ISOTHERM: MIX 10

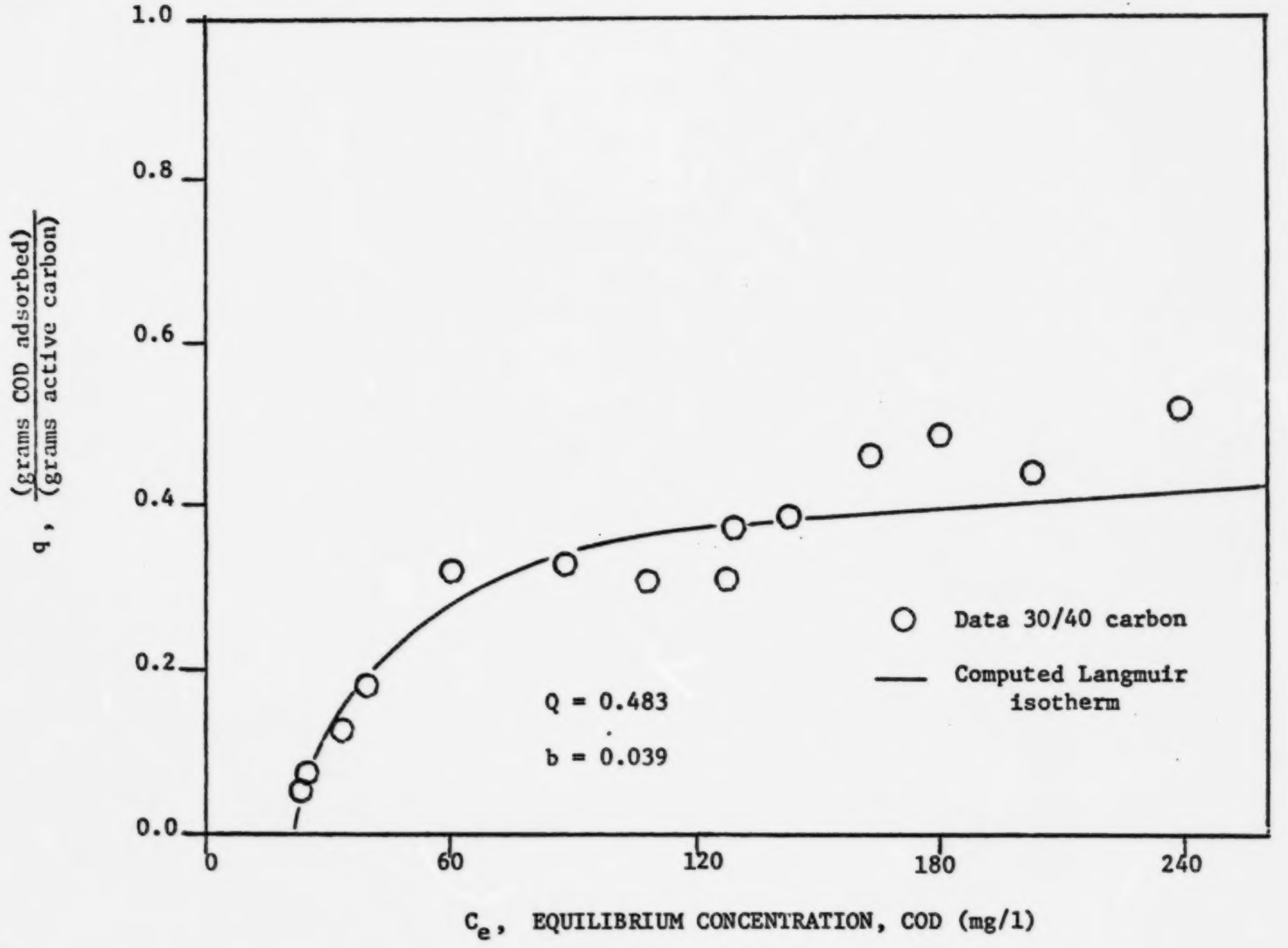

FIGURE 4-14. ADSORPTION ISOTHERM: MIX 11

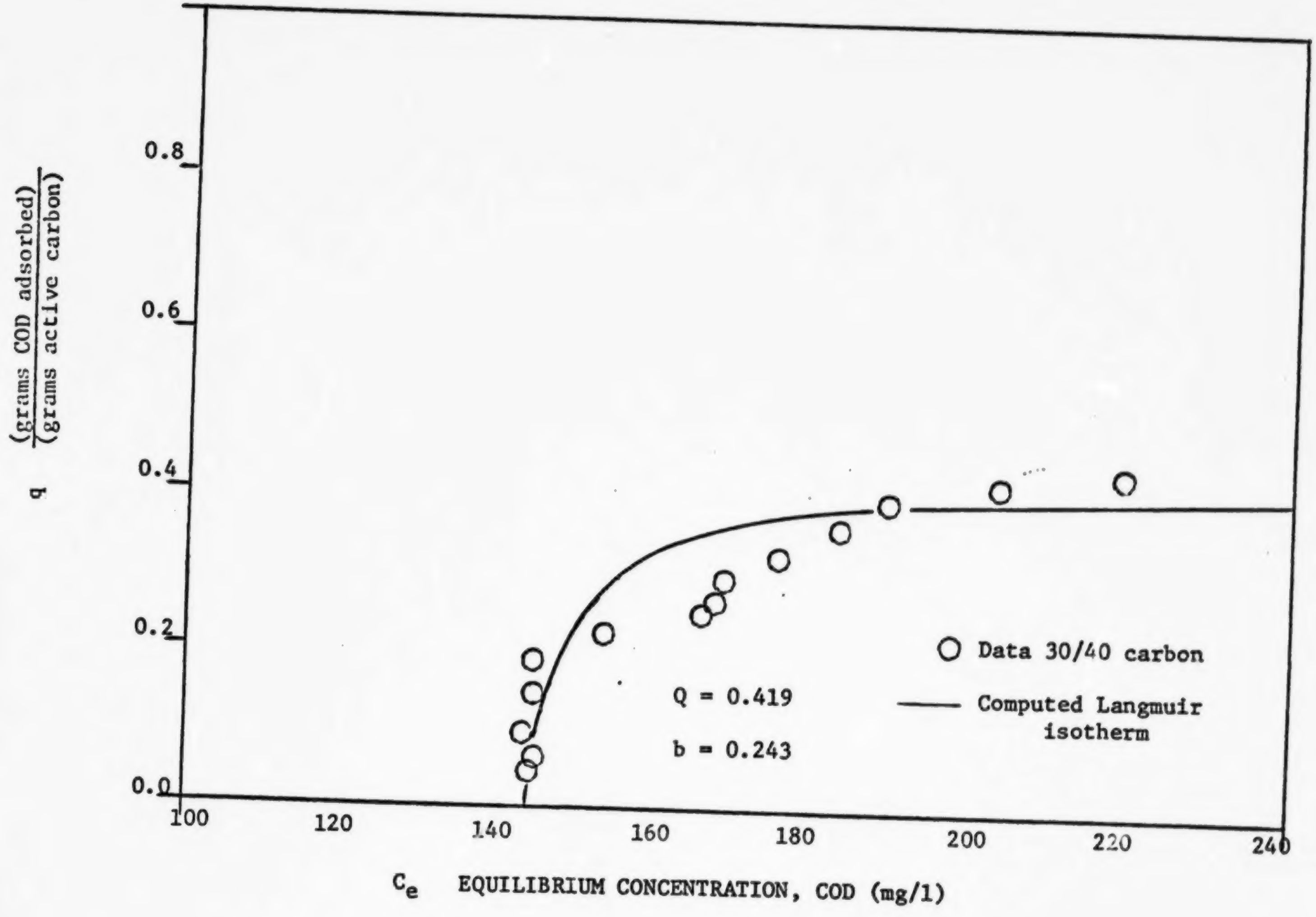

FIGURE 4-15. ADSORPTION ISOTHERM: MIX 12

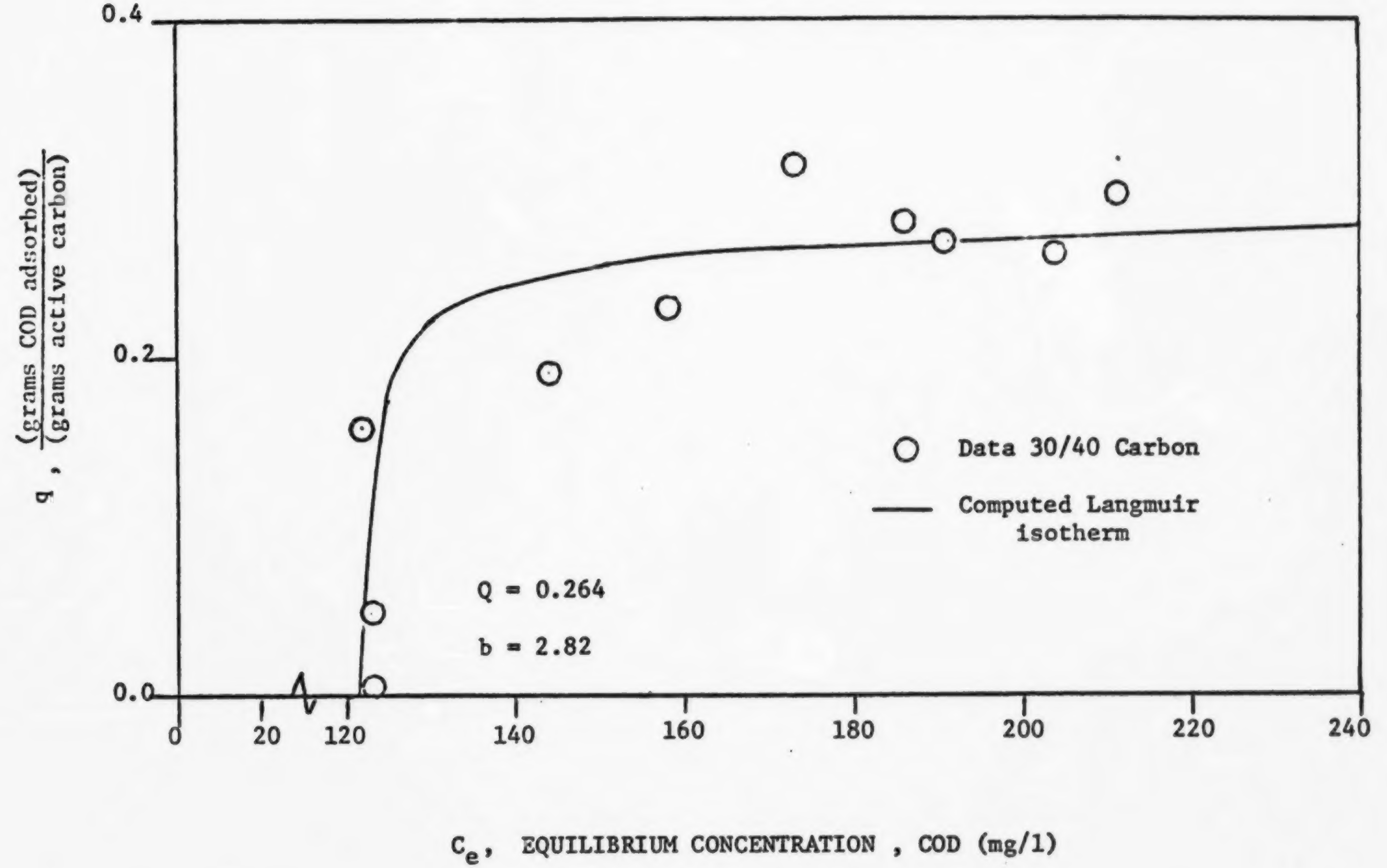

mixture as a single component system. This is most easily accomplished by recognizing that the measurable amount of equilibrium concentration, taken as q approaches zero, must therefore represent the concentration of non-adsorbing components in the mixture which contribute to the overall description parameter.

In order to use the Langmuir adsorption isotherm development (Equation 2-4), a new equilibrium concentration must be established such that C_e will approach zero as q tends toward zero. The identification of this new C_e is easily done by defining the equilibrium concentration zero point to be that point on the total equilibrium concentration at which q approximately equals zero. Simply stated, the equilibrium concentrations corresponding to given q values would be defined as the adsorbable equilibrium concentrations, i.e. the total equilibrium concentration as measured minus the non-adsorbable solution concentration determined to be the equilibrium concentration remaining at q equal to zero.

The Langmuir adsorption isotherm constants were determined by using the above concepts to redefine the equilibrium concentration data. The solid lines in Figures 4-12 through 4-15 represent the calculated Langmuir adsorption isotherms based on the experimentally obtained ultimate adsorption capacity and adsorption energy constants. Good agreement between the experimental and calculated adsorption isotherms is evident.

The Langmuir constant values for Mix 9 through Mix 12 are given in Table 4-3. The values for the ultimate adsorption capacity ranged from 0.264 grams COD/grams active carbon for Mix 12 to 0.483 grams

TABLE 4-3

LANGMUIR ISOTHERM CONSTANTS FOR ADSORBER/NON-ADSORBER MIXTURES

MIXTURE	LANGMUIR ULTIMATE CAPACITY CONSTANT, Q (mg COD adsorbed/mg active carbon)	LANGMUIR ENERGY CONSTANT, b (liter/mg COD)
9	0.304	35.4
10	0.483	0.039
11	0.419	0.243
12	0.264	2.82

COD/grams active carbon for Mix 10. The adsorption energy constant was 35.4 per milligram per liter COD for Mix 9 and 0.039 per milligram per liter for Mix 10.

Figure 4-12 indicates that essentially the same adsorption isotherm was obtained using either size adsorbent particle, in agreement with all similar experiments reported in this research.

DIFFUSIONAL MASS-TRANSFER COEFFICIENTS

The use of Equation 2-42 to predict effluent concentration-history profiles requires the determination of diffusional mass-transfer coefficients which can be related to the second-order surface-reaction controlled kinetic formulation which constitutes the basis for the predictive mathematic model. The diffusional mass-transfer coefficients of interest are the external diffusion coefficient and the internal fluid-phase pore diffusion or solid-phase pore-surface diffusion coefficient. The external diffusion coefficient quantifies the resistance to mass-transfer across the hydrodynamic boundary layer separating the bulk solution and the solid phase. The internal diffusion coefficients measure the resistances due to either fluid-phase diffusion mechanisms or to solid-phase surface diffusion mechanisms within the internal pores of the adsorbent particles.

External Diffusion Coefficients

Practicable methods for the measurement of external diffusion coefficients from non-flow experimental systems are not available. Correlation techniques have been developed and are applicable for determination of these coefficients. Chu, *et al*. (16), have correlated a mass-transfer factor, j_d, with the modified Reynolds number, N'_{Re}, by modifying the Chilton-Colburn (14) momentum-transfer correlation to pressure-drop for flow in a conduit to flow in granular beds. A plot of the natural log of j_d versus the natural log of N'_{Re} provided the correlation. Good results for both fixed- and fluid-beds were obtained for particle sizes of 0.07 centimeters to 1.87 centimeters. The mass-transfer function, j_d, is given by

$$j_d = \frac{k_f (N_{Sc})^{2/3}}{\overline{V}} \tag{4-7}$$

in which N_{Sc} is the Schmidt number. The other terms in Equation 4-7 have been previously defined. The modified Reynolds number is expressed by

$$N'_{Re} = \frac{d_p \overline{V}}{\nu(1-\varepsilon)} \tag{4-8}$$

in which ν is the kinematic viscosity of the fluid.

Resnick and White (82) found that the correlation of the natural log of N'_{Re} versus the natural log of j_d for systems involving particles with diameters less than 0.10 centimeters was inadequate. They were able to correlate the natural log of the j_d mass-transfer factor to the natural log of the ratio of the modified Reynolds number to the Grashof number, N_{Gr}. The Grashof number is expressed as

$$N_{Gr} = \frac{d_p^{\,3} \rho_\ell (\rho_s - \rho_\ell) g}{\mu^2} \tag{4-9}$$

The Resnick-White correlation was experimentally verified by Keinath and Weber (56) to be adequate and to be represented by the relationship

$$j_d = 7.95 \times 10^{-2} \left[N'_{Re}/N_{Gr} \right]^{-0.345} \qquad (4\text{-}10)$$

for bed depths less than 55.5 centimeters. For bed depths greater than this value, however, a regular variation in j_d was noted and quantified by Keinath and Weber (56) as

$$j_d = \frac{3.15}{L} \left[N'_{Re} / N_{Gr} \right]^{-0.345} \qquad (4\text{-}11)$$

in which L is the height of the expanded-bed in centimeters. Depending upon operating conditions, the j_d mass-transfer factor can be calculated from Equation 4-9 or Equation 4-10 using only physical and hydrodynamic parameters of the column system.

With the j_d mass-transfer factor determined, k_f, the external diffusion rate constant may be determined by rearrangement of Equation 4-7. The Schmidt number is given by

$$N_{Sc} = \nu/D_\ell \qquad (4\text{-}12)$$

in which D_ℓ is the free liquid diffusivity of the solute in the solution bulk. The free liquid diffusivity may be calculated from the Wilke-Chang (128) relationship for associated solvents, given by

$$D_\ell = 7.4 \times 10^{-8} \left[\frac{T\sqrt{X \cdot M}}{\mu v_o^{0.6}} \right] \qquad (4\text{-}13)$$

in which D_ℓ is given as the coefficient for the solute in bulk solution (cm ^{2}/second); T is the absolute temperature (degrees

Kelvin); X is the association parameter for the solvent (X = 2.6 for water); M is the molecular weight of the solvent (grams/mole); μ is the absolute viscosity of the solvent (centipoise); and V_o is the molecular volume of the solute molecule.

In order to calculate a value for the free liquid diffusivity using the Wilke-Chang relationship, the molecular volume of the solute must be known. In order to use Equation 4-13 for the complex mixtures used in this research, an effective molecular volume for the mixture as a single sorbate component must be proposed. This was accomplished by utilizing concepts set forth by Le Bas (62) based on Kopp's Law (27). Kopp's Law states that the sum of the volumes of atomic species composing a molecular compound is equal to the molecular volume of that compound. Le Bas has provided a method of evaluating the atomic volumes for atoms associated in molecular compounds of different natures. Based on these concepts, the molecular volumes of the individual sorbate compounds were first determined. These values were then used in the following proposed general formula for effective molecular volumes of complex mixtures classified as a single component.

$$V_{o_m} = \sum \left[\frac{\text{gram-moles of compound}}{\text{gram-moles of COD}} \cdot V_o \cdot \begin{array}{l}\text{fractional}\\ \text{contribution}\\ \text{of compound}\\ \text{to total COD}\end{array} \right] \qquad (4\text{-}14)$$

V_{o_m} is the effective molecular volume of the mixture. The calculated effective molecular volumes for the twelve mixtures are shown in Table 4-4. The effective molecular volume calculated for the mixtures

TABLE 4-4

PARAMETERS FOR DETERMINATION OF EXTERNAL DIFFUSION RATE CONSTANT

MIXTURE	$\underline{V}_o$	$D_\ell \times 10^5$ (cm^2/sec)	$k_f \times 10$ (cm/mm)	$k_f a$ (min^{-1})
1	123.5	0.890	0.823	1.839
2	88.8	1.085	0.939	2.098
3	158.02	0.768	0.746	1.666
4	167.3	1.024	0.904	2.018
5	179.9	0.711	0.708	1.582
6	145.32	0.807	0.771	1.723
7	110.7	0.951	0.860	1.921
8	129.49	0.865	0.807	1.804
9	92.2	1.061	0.925	2.066
10	152.2	0.786	0.752	1.691
11	127.4	0.874	0.813	1.816
12	133.8	0.849	0.797	1.781

ρ_s = 1.387 grams/cc

ρ_ℓ = 0.997 grams/cc

μ = o.9358 centipoise

containing non-sorbate fractions were determined using the sorbate fraction only, since the diffusion of the non-adsorbing components should have negligible effects in dilute solutions (10), such as in the case for the mixtures used herein.

The free liquid diffusivities calculated for the mixtures are given in Table 4-4. These values were substituted into Equation 4-7 and the resulting external rate constants, k_f, are listed in Table 4-4 for the respective mixtures. This constant may then be equated to the effective external rate constant κ_f by Equation 2-52 or Equation 2-53.

Internal Diffusion Coefficients

Rapidly-agitated batch experiments were performed to determine the internal diffusion coefficients for use in the predictive mathematic model. The agitation in such systems minimizes the resistance of mass-transfer across the hydrodynamic boundary separating the solid phase from the bulk solution, thus establishing internal pore diffusion mechanisms as the rate limiting factor (124). Such systems provide a means of determining the internal diffusion rate constants and the corresponding mass-transfer coefficients for application of the mathematic model given by Equation 2-42.

Experimental Materials and Methodology

Adsorption experiments to determine diffusion mass-transfer rates were conducted in the following manner. Three liters of mixture solution of concentration equal to that used in the continuous flow-through column experiments were placed in a baffled four-liter glass reactor. All mixtures were prepared by carefully weighing the proportional amount of individual compounds to be added to the solution. The make-up water was active-carbon-treated Ann Arbor tap water. The solution was allowed to stand for a period of twenty-four hours in the covered reactors to allow it to equilibrate with room temperature, which remained relatively constant at 23°C, and to come to adsorption equilibrium with the reactor surfaces.

The active carbon used was the 0.503 mm size fraction, the same as was used in the columns. It is necessary that the same size active carbon particles be used in the rate studies because a definite dependence of adsorption rates in rapidly-agitated systems has been noted. Weber and Morris (121) found these adsorption rates to vary with the inverse square of the adsorbent particle diameter. Hiester and Vermeulen (39) and Griffin and Dranoff(32) have found rates of sorbate uptake to vary inversely with $d_p^{2.56}$, and Keinath and Weber (56) have found the relationship of the rate of sorbate uptake to be proportional to the reciprocal of $d_p^{1.96}$.

The reactor solution was agitated using a polyethylene coated stirring blade with power supplied by a T-line stirrer (Cole Palmer Instrument and Equipment Company). The T-line stirrers were rated at 1550 rpm but were slowed down to 1000 rpm using a Powerstat Variable Autotransformer (Superior Electric Company) to prevent foam formation due to the presence of the surfactant dodecyl sodium sulfate and the powerful agitation produced at full power. A carefully measured amount of the 0.503 mm active carbon was added to the rapidly-agitated reactor. Sampling was accomplished by briefly stopping the stirring and removing 20 milliliters of solution. An initial sample was also taken before introduction of the active carbon. Analysis of the concentrations of the sorbate with respect to time yielded data for determination of the adsorption uptake rate, taking into account the volume decrease due to sampling.

Experimental Results

The concentration-decay curves for Mixtures 1 through 12 are given in Figures 4-16 through 4-27, respectively. From the concentration-decay curves and the initial value of sorbate concentration, the amount of sorbate removed by the active carbon was easily determined. If pore diffusion is the rate limiting factor for adsorption, then the amount of sorbate adsorbed per unit weight of carbon should vary linearly with the square root of time (121). Figures 4-16 through 4-27 indicate that such a linear trace results for the rate experiments performed for Mix 1 through Mix 12, respectively. Normalization of the uptake rate data was achieved by utilizing the equivalent plot of the square of the amount adsorbed per unit amount of adsorbent versus time. The slope of these plots can then be used in conjunction with Equations 2-55 and 2-60 to determine the fluid-phase pore diffusion rate constant and the solid-phase pore-surface diffusion rate constant, respectively. Figures 4-28 through 4-39 represent the normalized plots for the uptake rate experiments for Mixtures 1 through 12, respectively, with the solid lines representing a linear regression least squares analysis for best fit of the data points. The slopes of these best fit lines were used in calculating the adsorption rate constants.

FIGURE 4-16. EXPERIMENTAL RATE STUDY: MIX 1

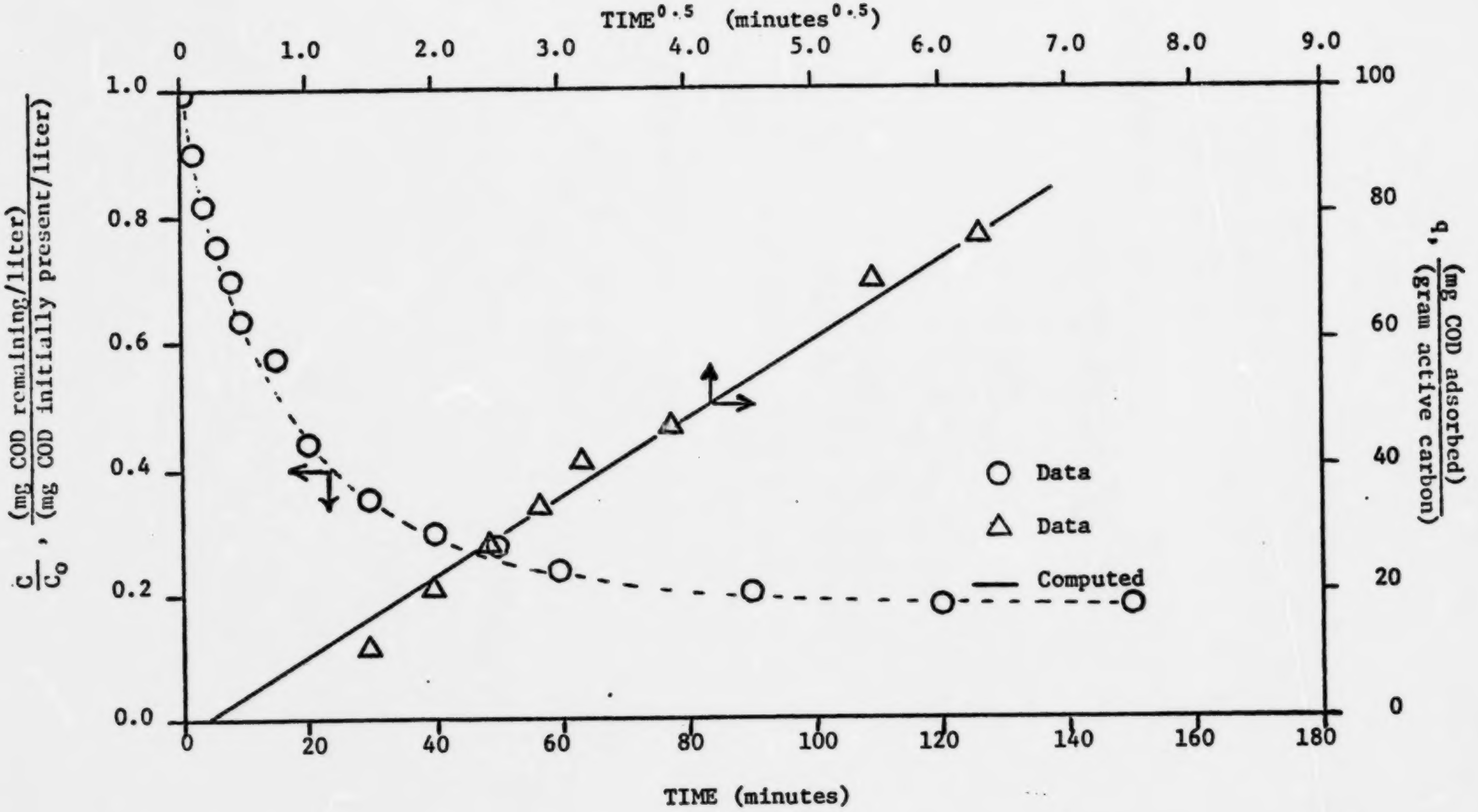

FIGURE 4-17. EXPERIMENTAL RATE STUDY: MIX 2

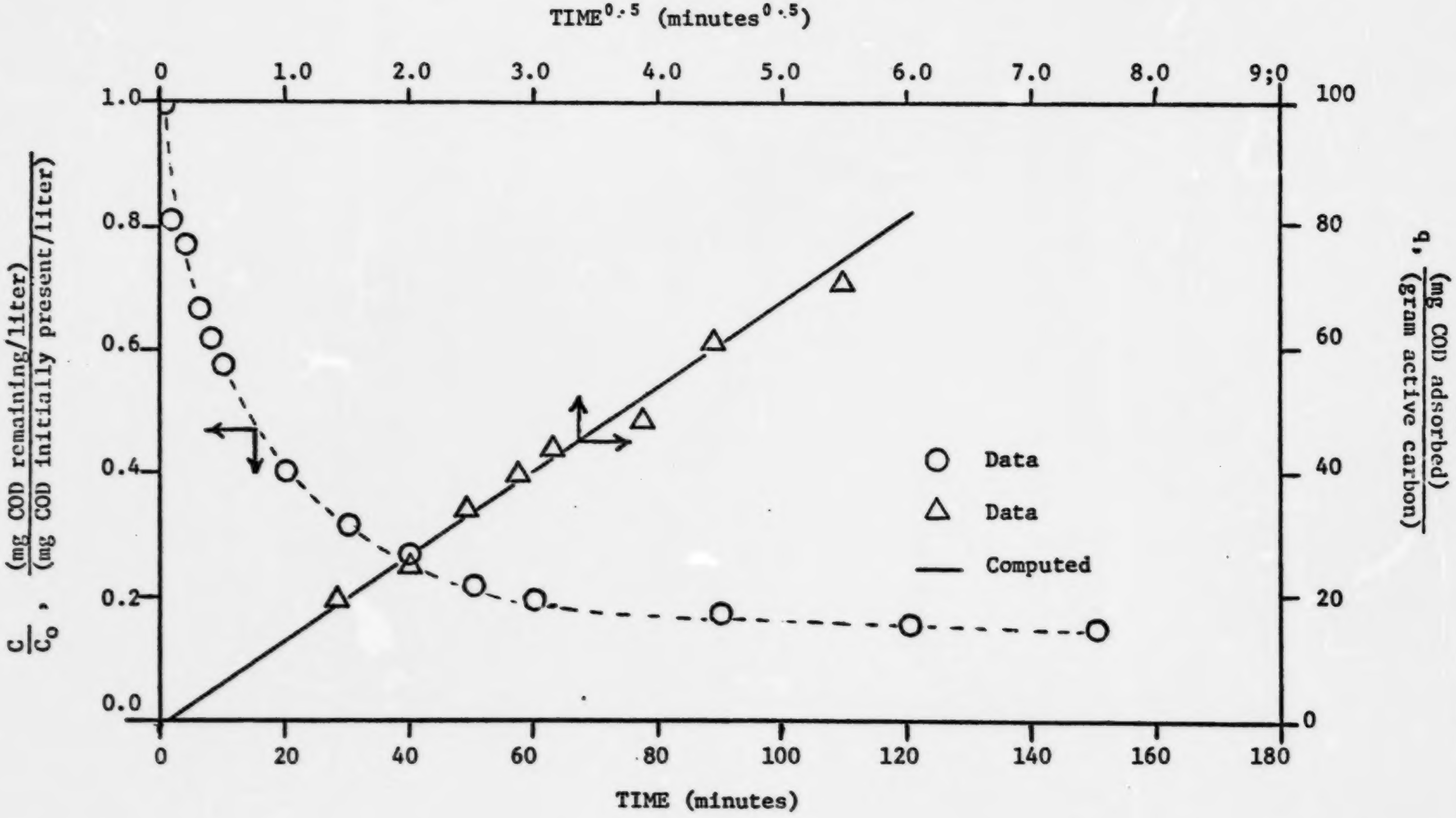

FIGURE 4-18. EXPERIMENTAL RATE STUDY: MIX 3

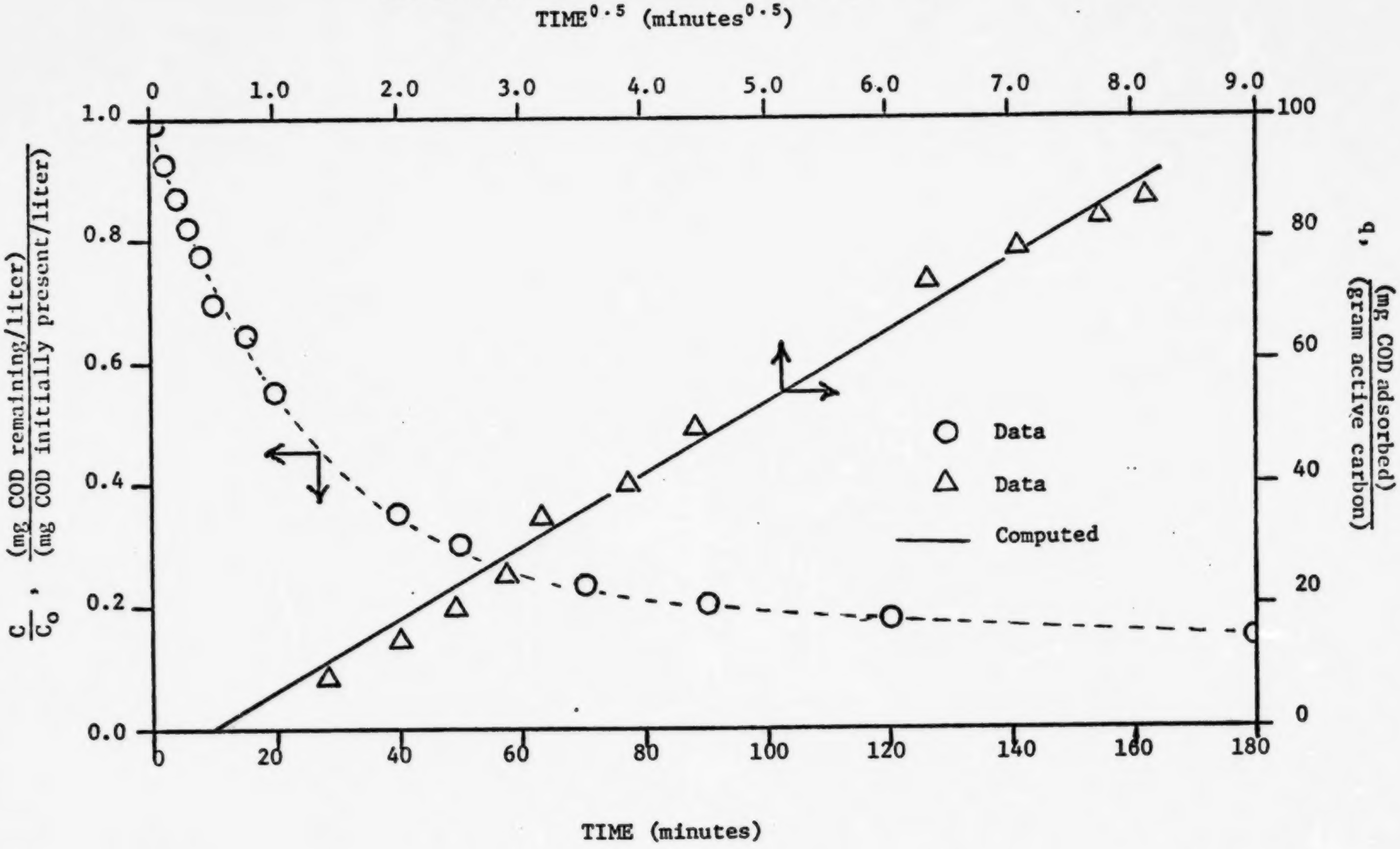

FIGURE 4-19. EXPERIMENTAL RATE STUDY: MIX 4

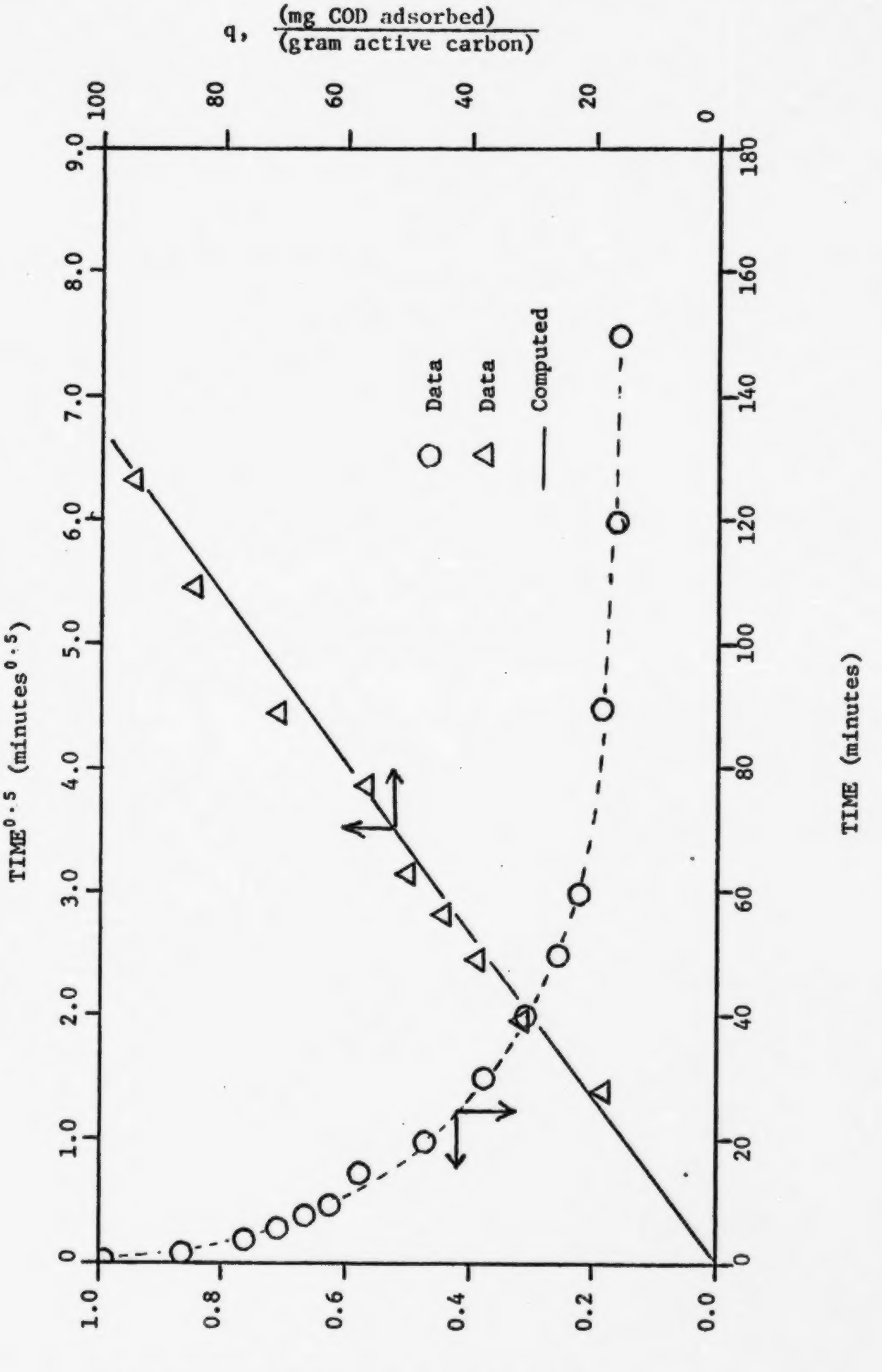

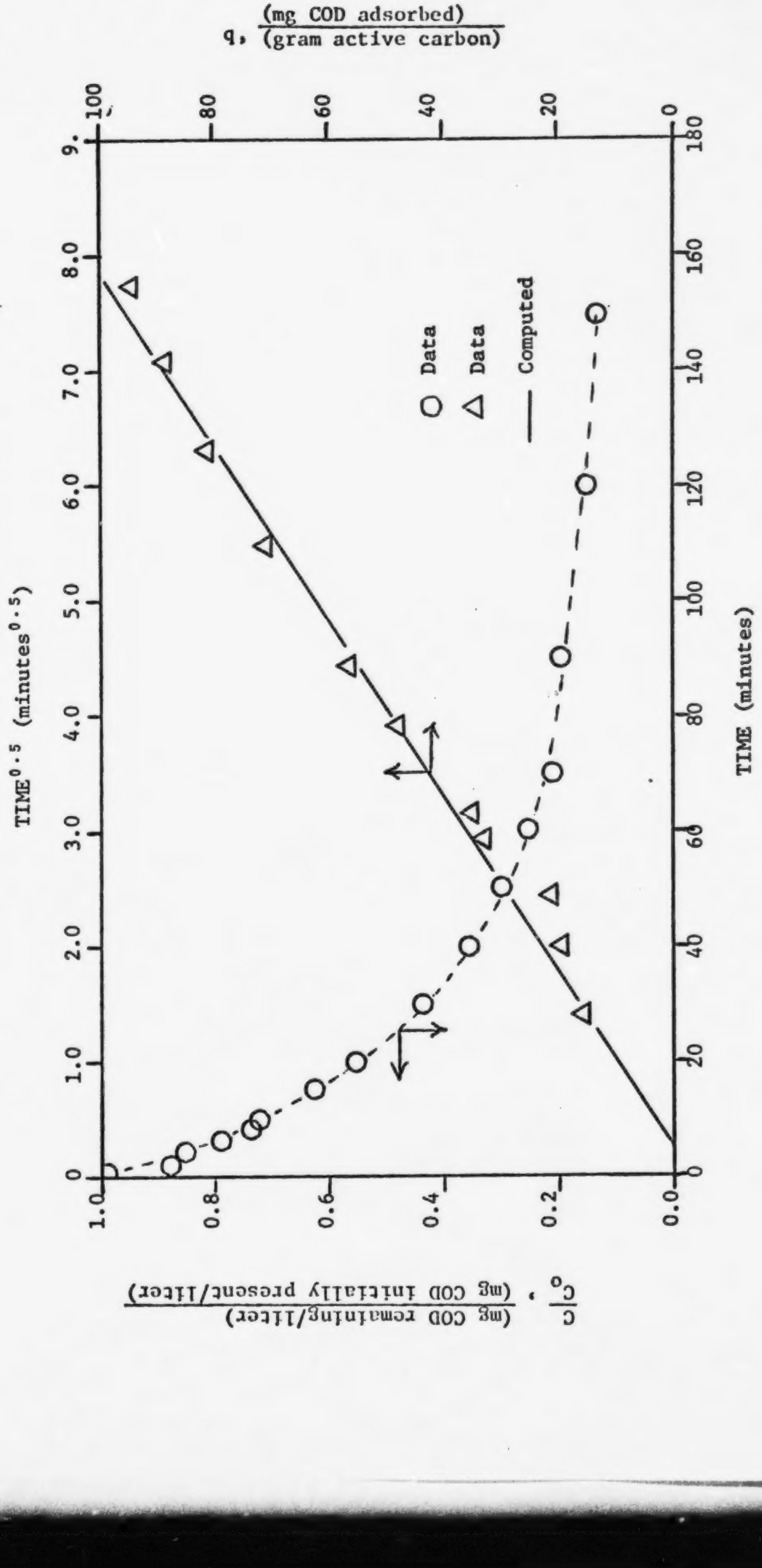

FIGURE 4-20. EXPERIMENTAL RATE STUDY: MIX 5

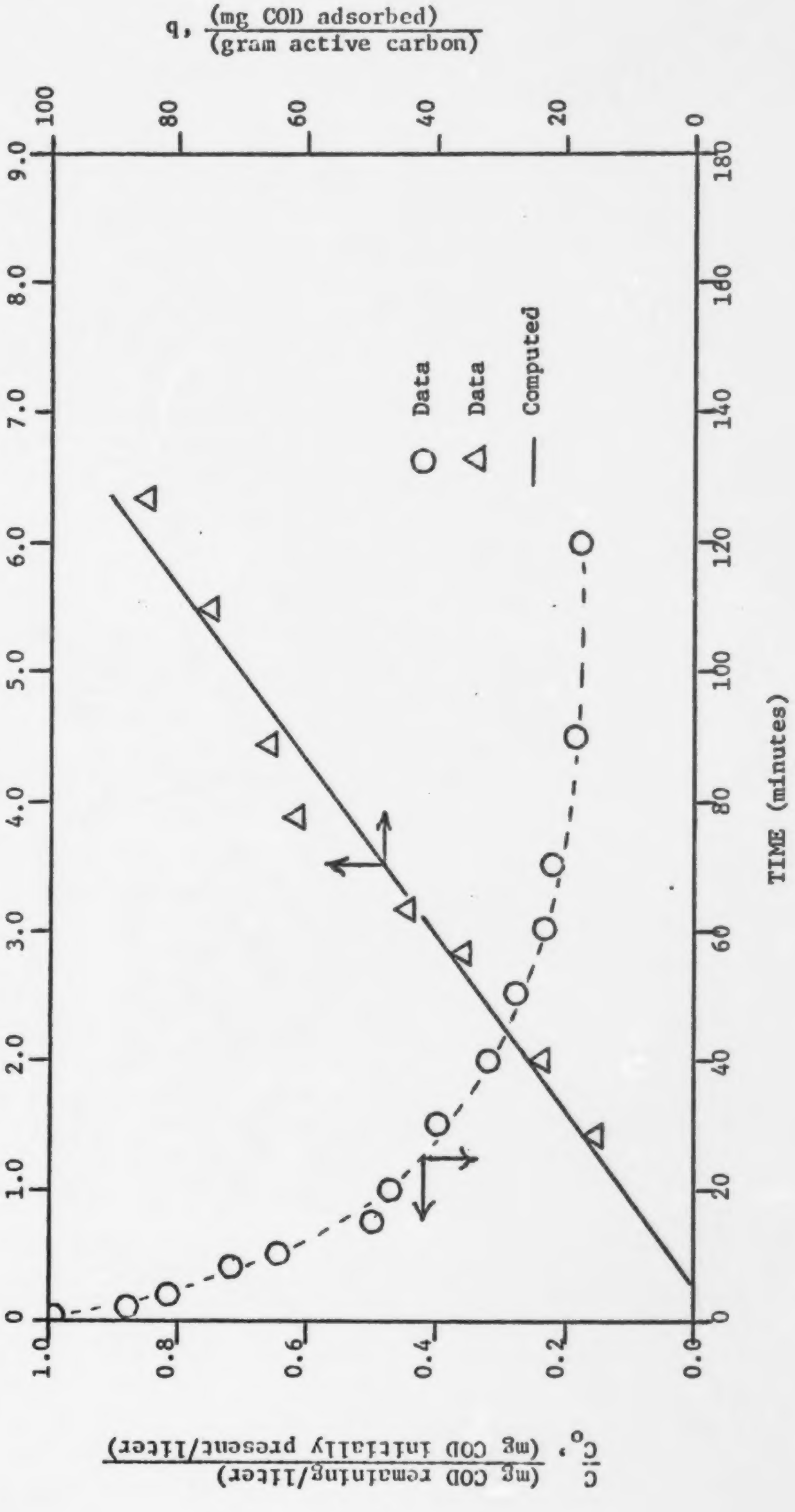

FIGURE 4-21. EXPERIMENTAL RATE STUDY: MIX 6

FIGURE 4-22. EXPERIMENTAL RATE STUDY: MIX 7

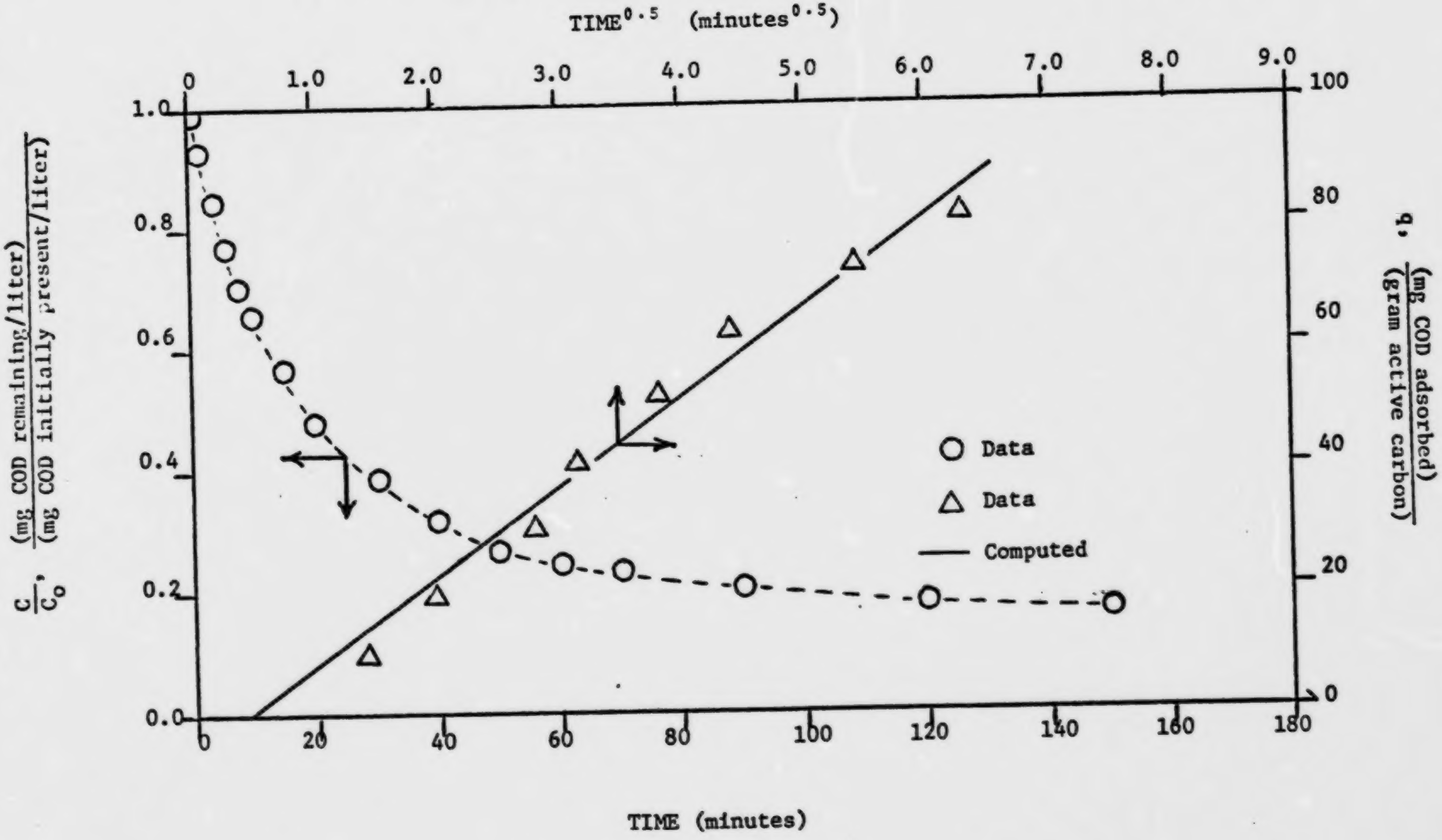

FIGURE 4-23. EXPERIMENTAL RATE STUDY: MIX 8

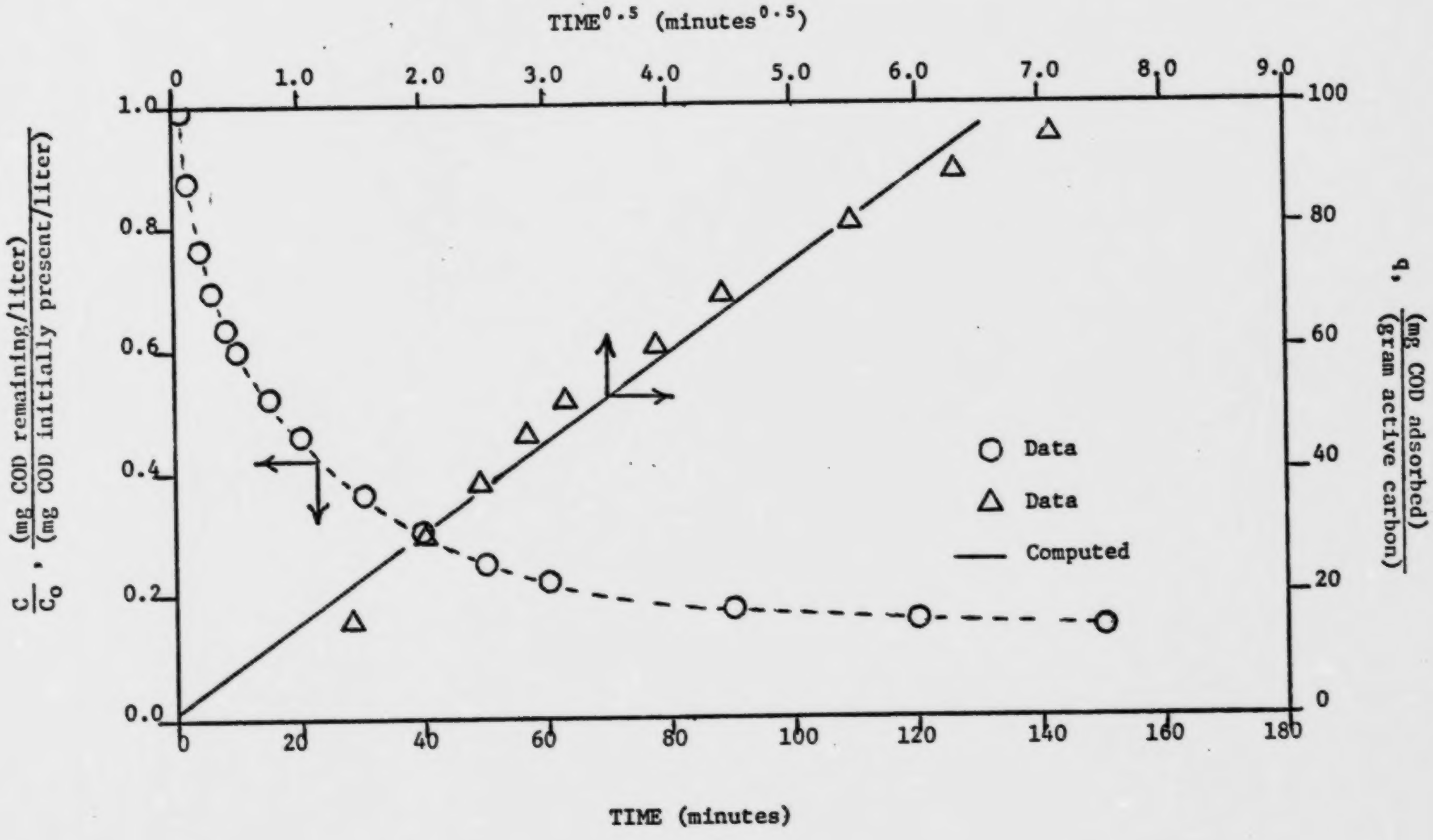

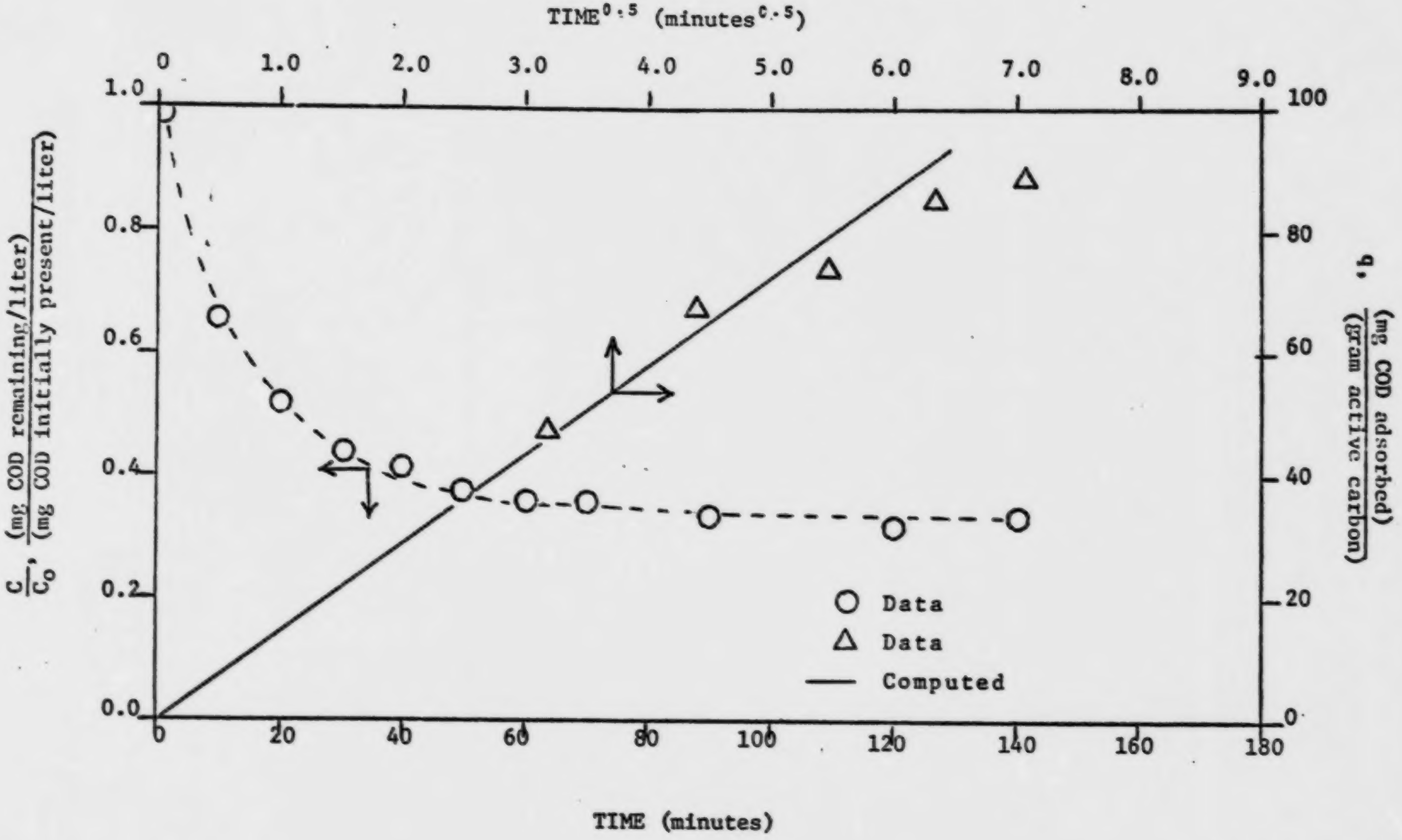

FIGURE 4-24. EXPERIMENTAL RATE STUDY MIX 9

FIGURE 4-25. EXPERIMENTAL RATE STUDY: MIX 10

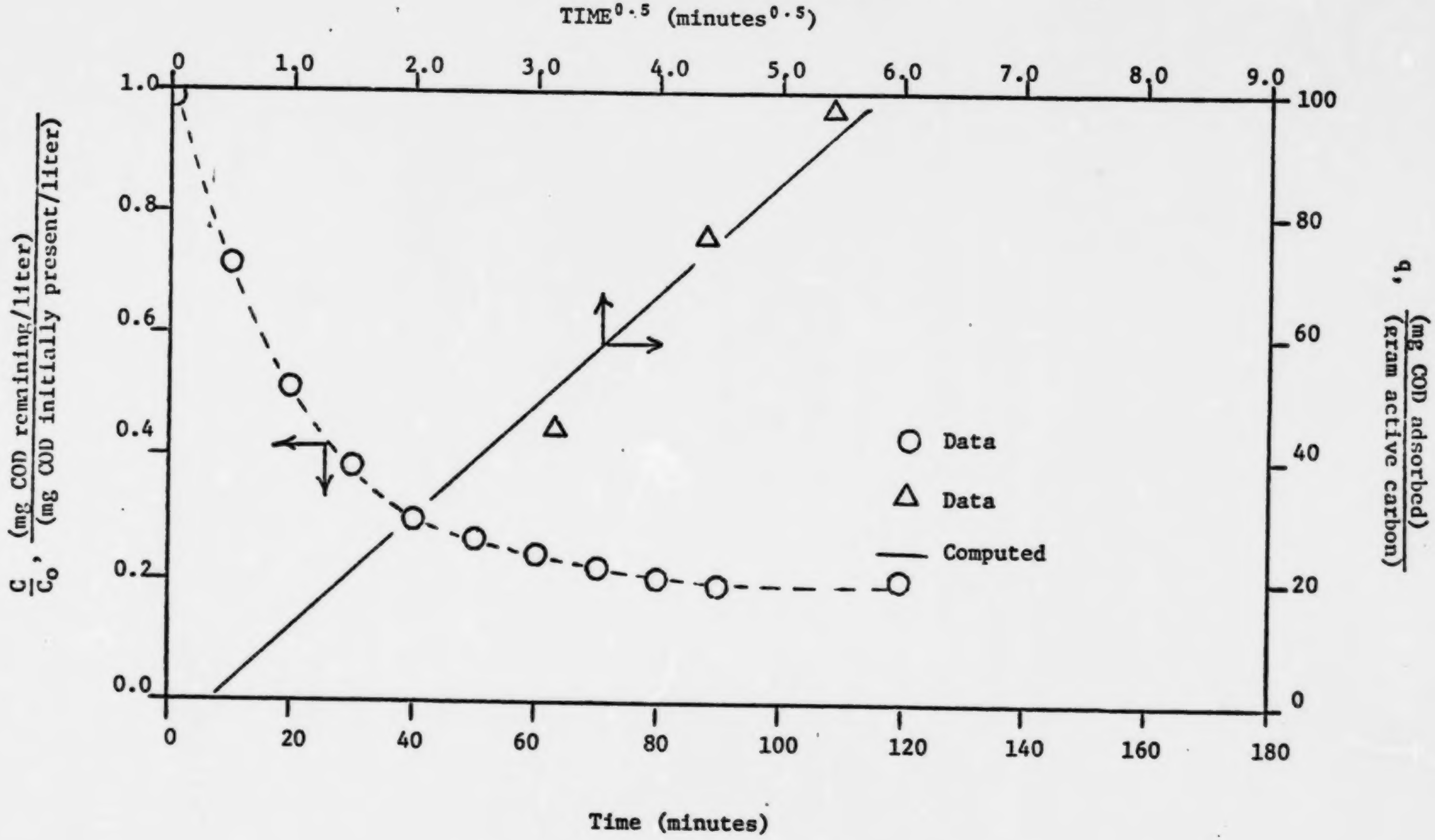

FIGURE 4-26. EXPERIMENTAL RATE STUDY: MIX 11

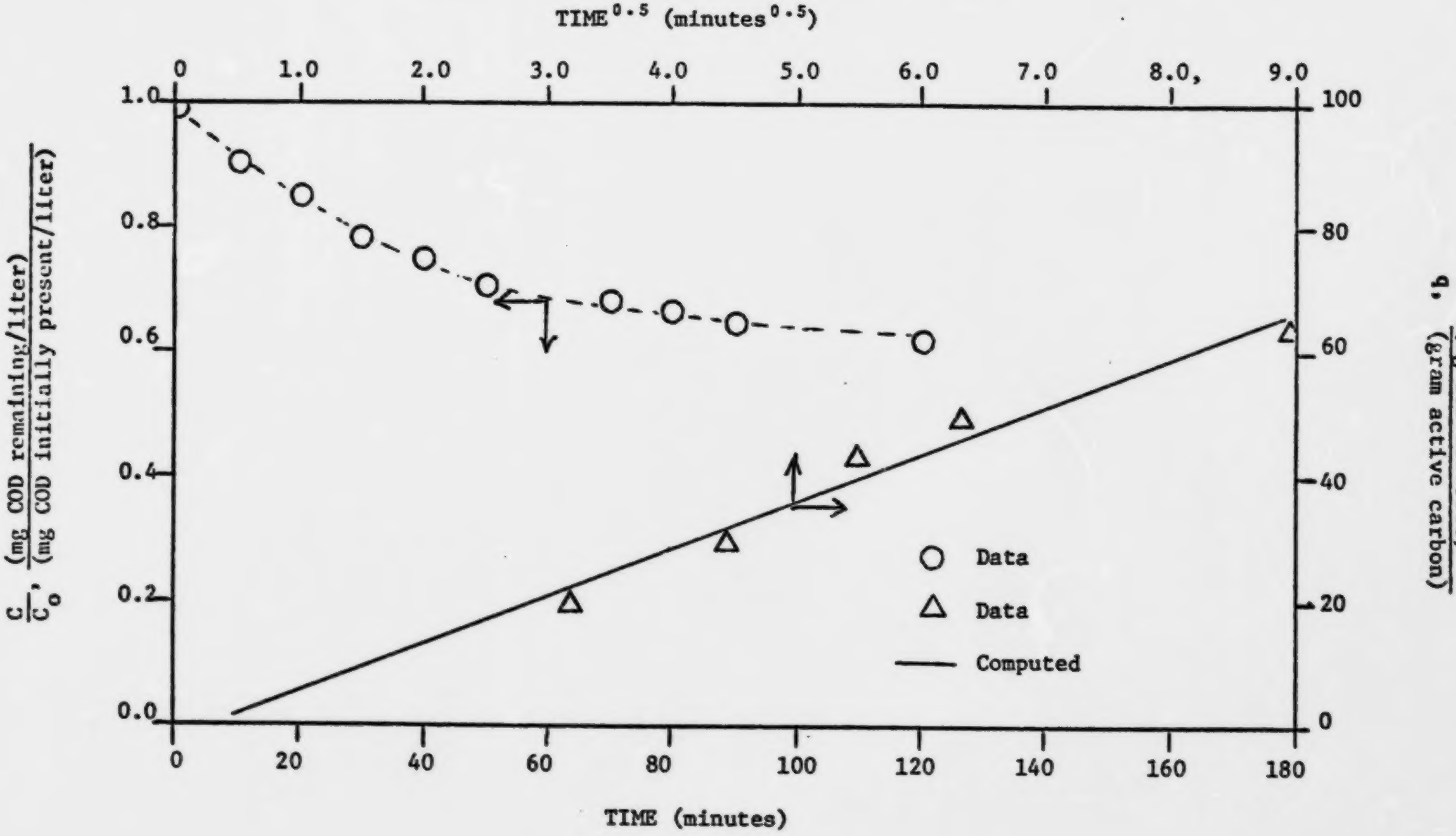

FIGURE 4-27. EXPERIMENTAL RATE STUDY: MIX 12

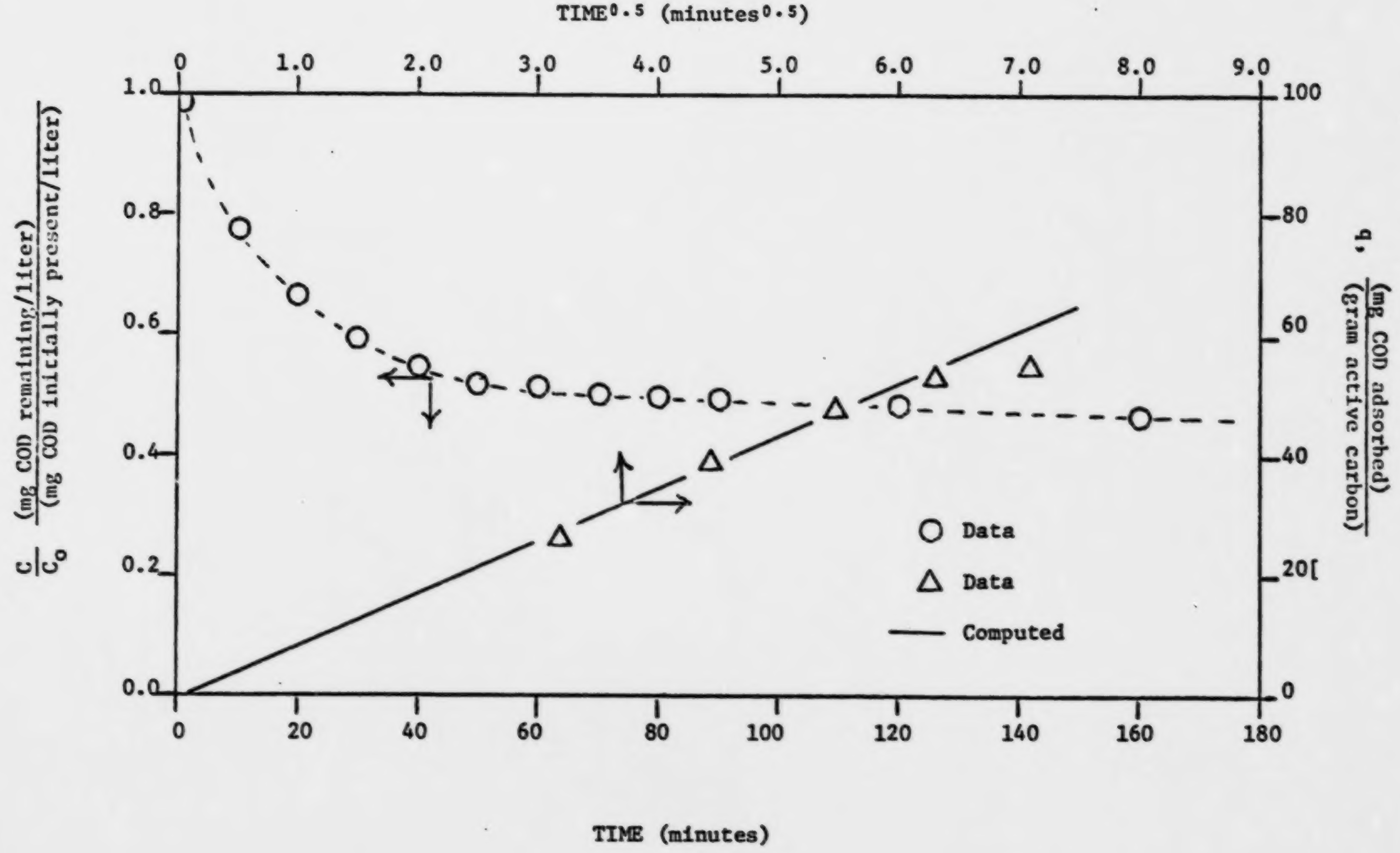

FIGURE 4-28. RATE DATA FOR DETERMINATION OF INTERNAL DIFFUSION RATE CONSTANT: MIX 1

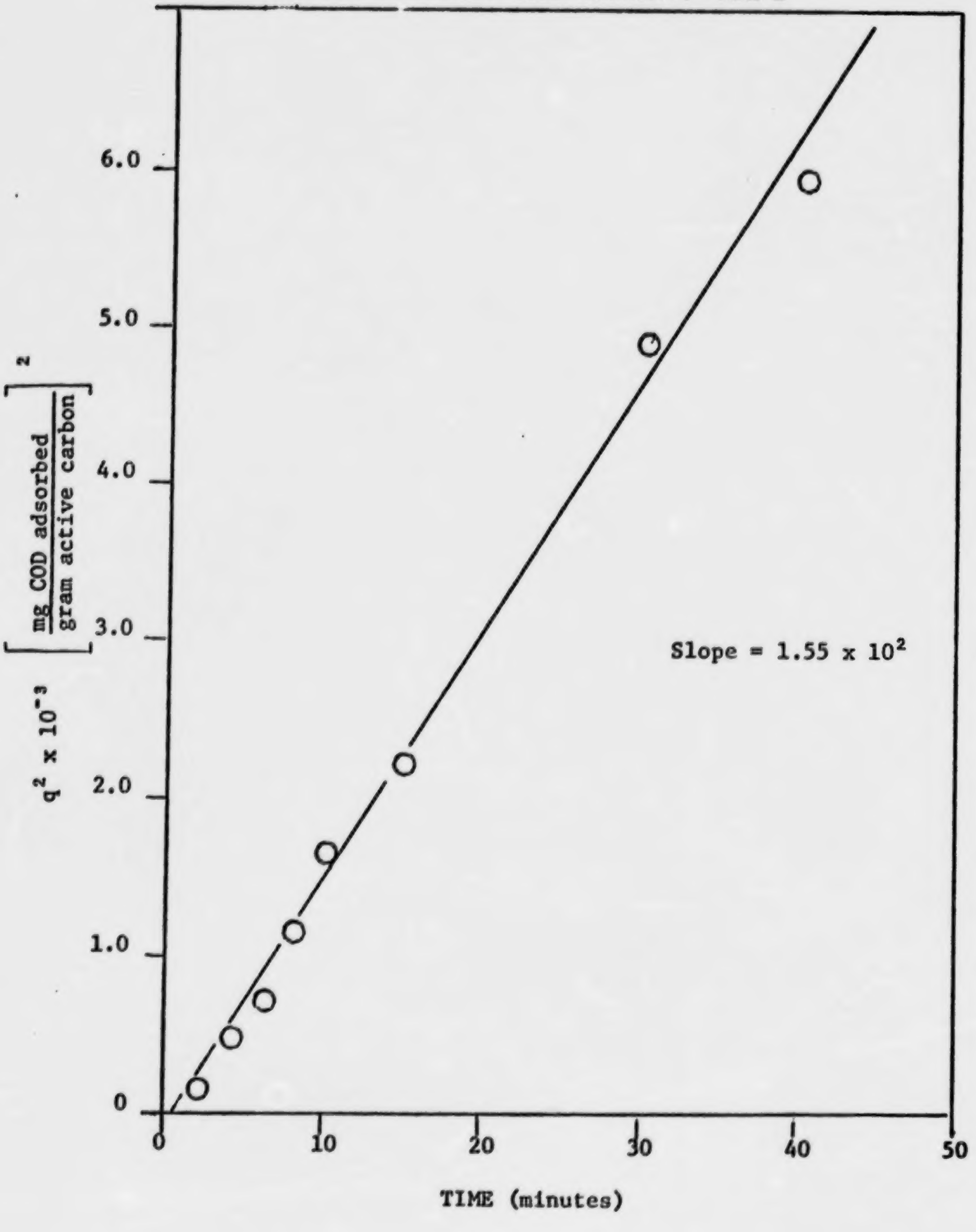

FIGURE 4-29. RATE DATA FOR DETERMINATION OF INTERNAL DIFFUSION RATE CONSTANT: MIX 2

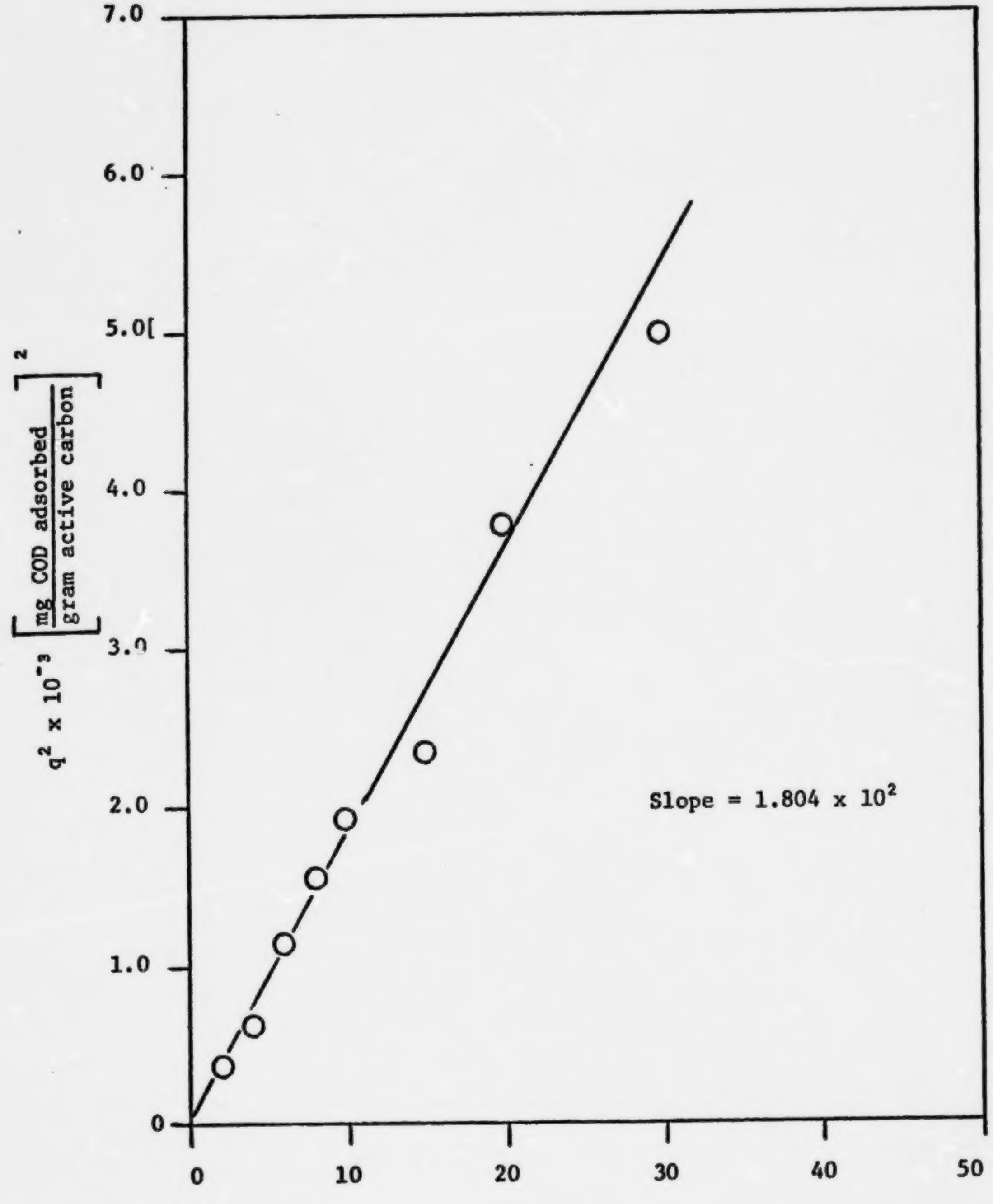

TIME (minutes)

FIGURE 4-30. RATE DATA FOR DETERMINATION OF INTERNAL DIFFUSION RATE CONSTANT: MIX 3

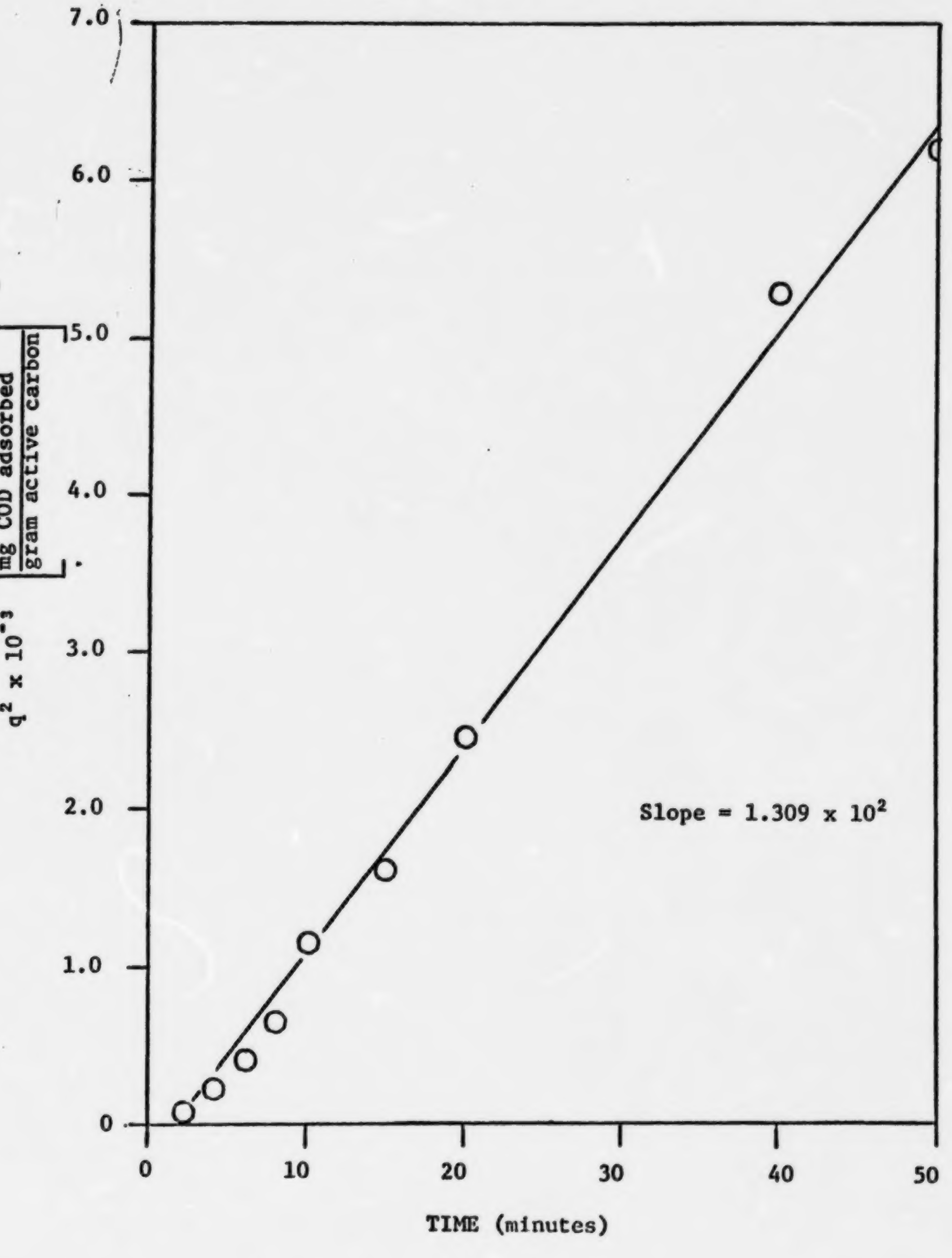

FIGURE 4-31. RATE DATA FOR DETERMINATION OF INTERNAL DIFFUSION RATE CONSTANT: MIX 4

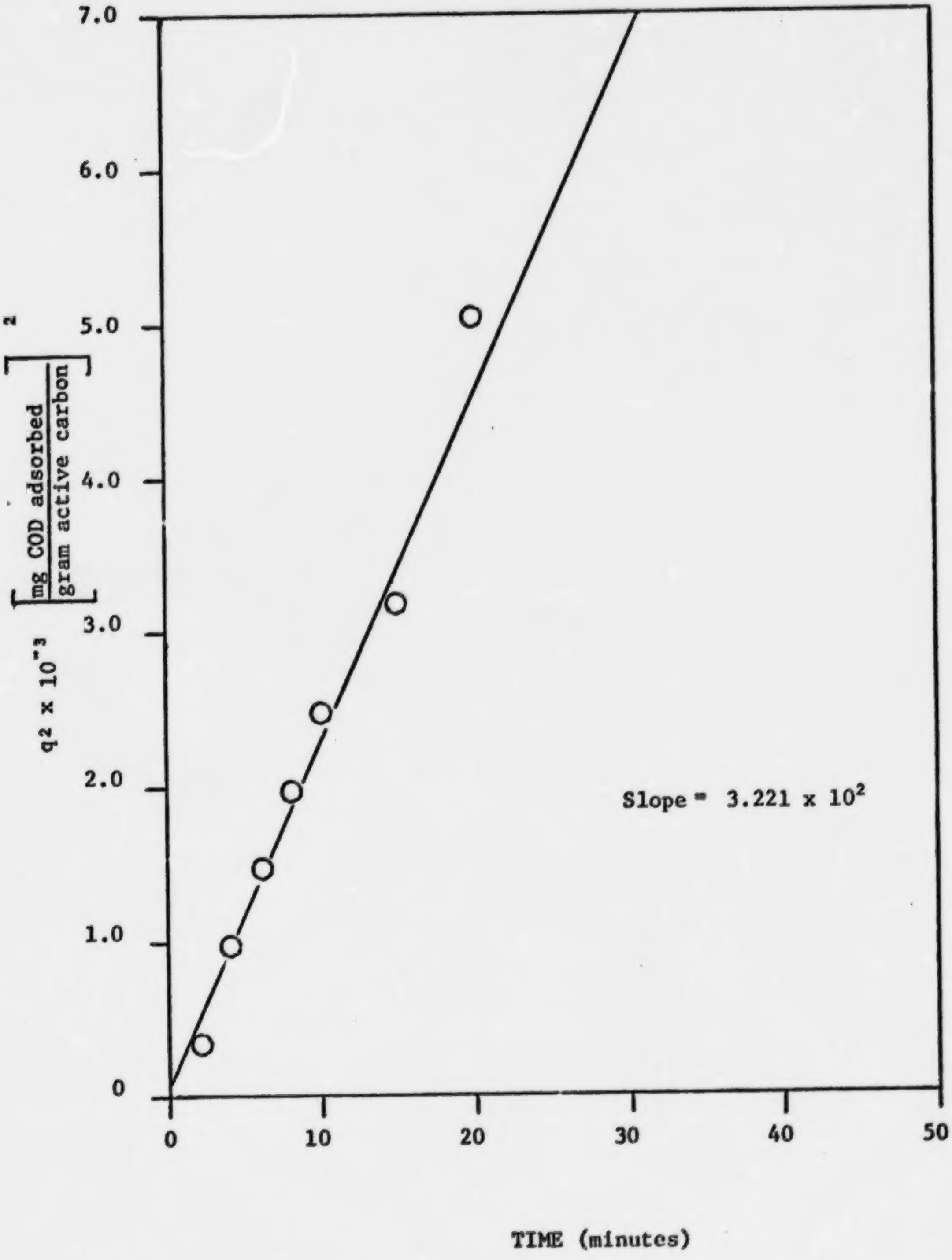

FIGURE 4-32. RATE DATA FOR DETERMINATION OF INTERNAL DIFFUSION RATE CONSTANT: MIX 5

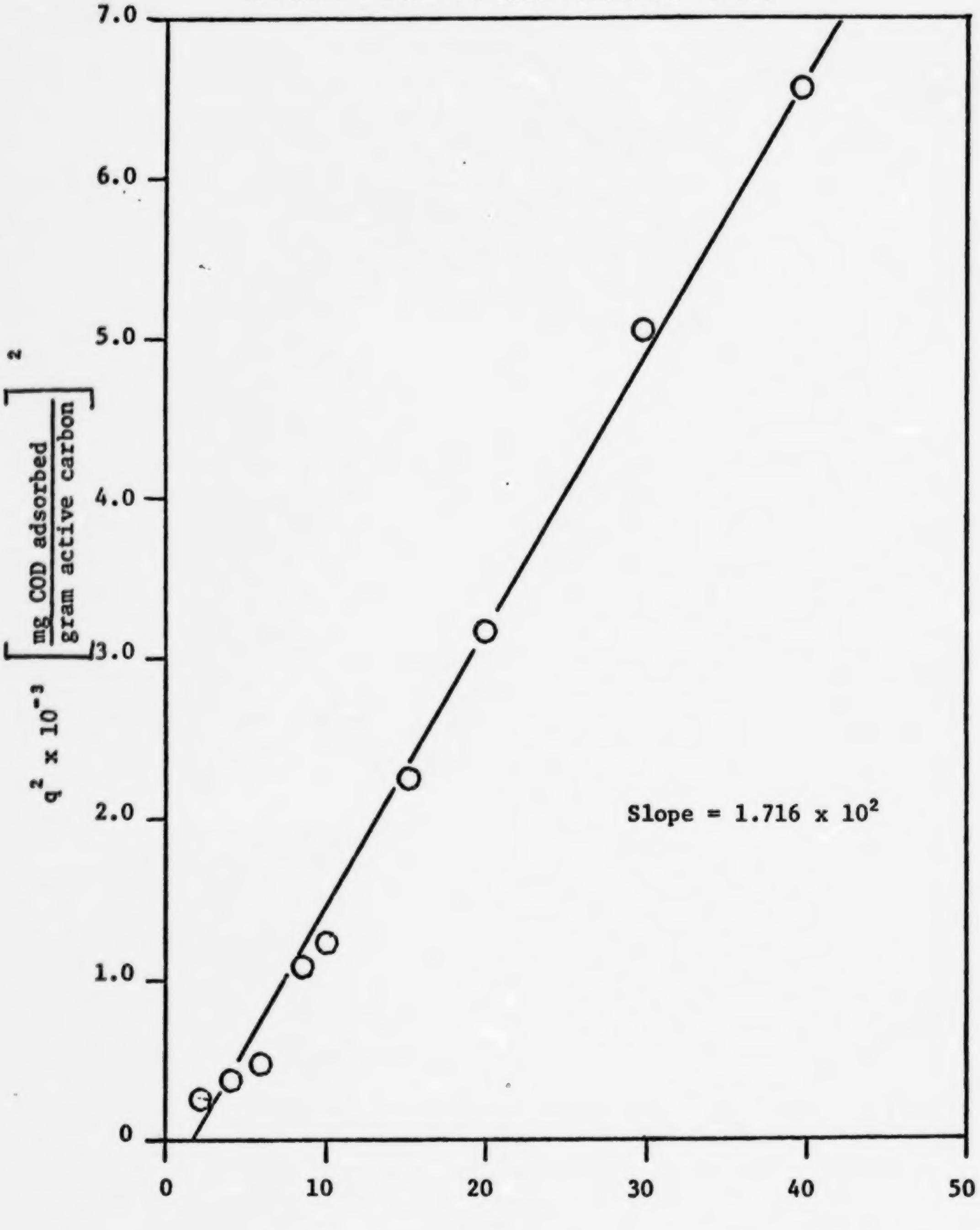

FIGURE 4-33. RATE DATA FOR DETERMINATION OF INTERNAL DIFFUSION RATE CONSTANT: MIX 6

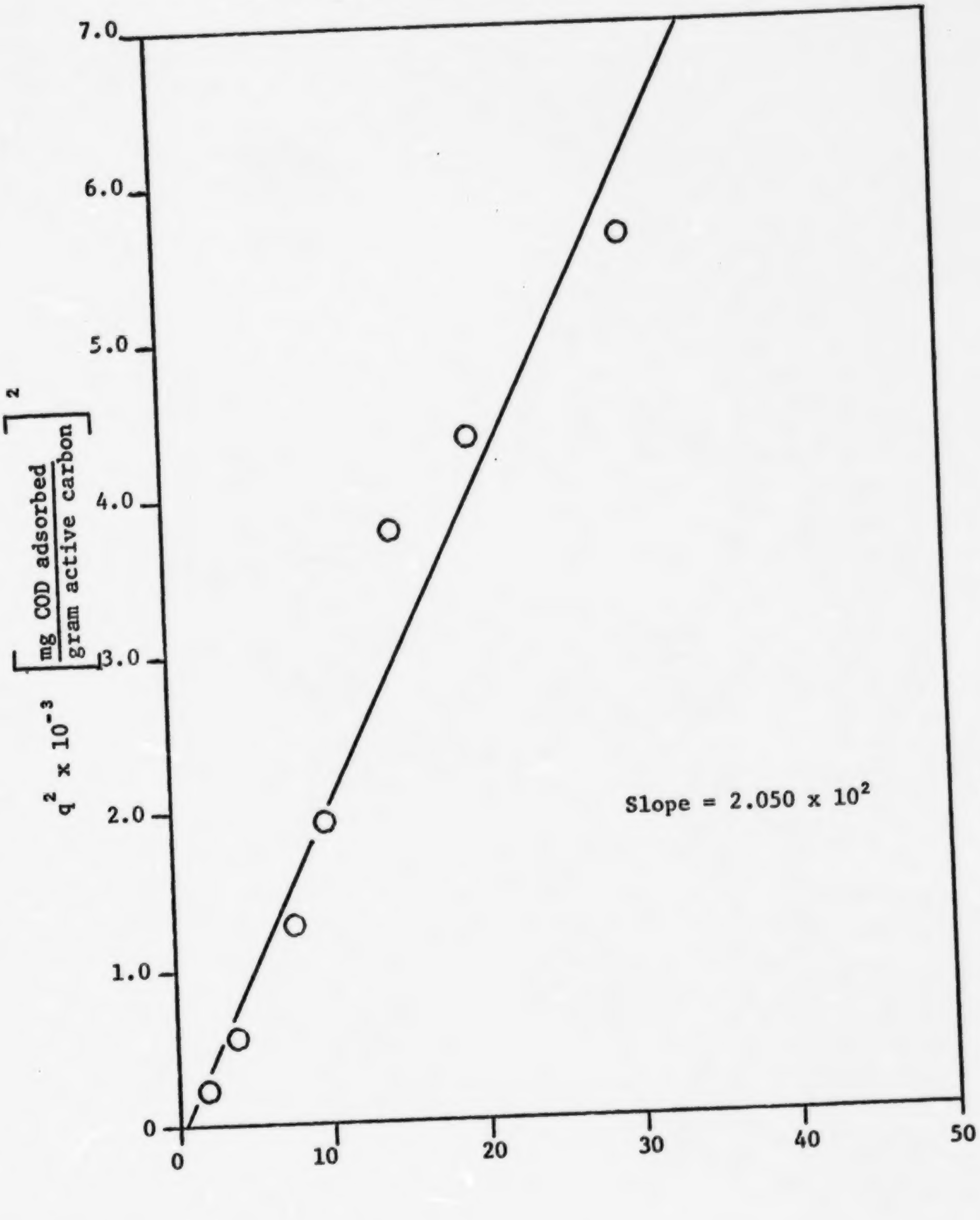

FIGURE 4-34. RATE DATA FOR DETERMINATION OF INTERNAL DIFFUSION RATE CONSTANT: MIX 7

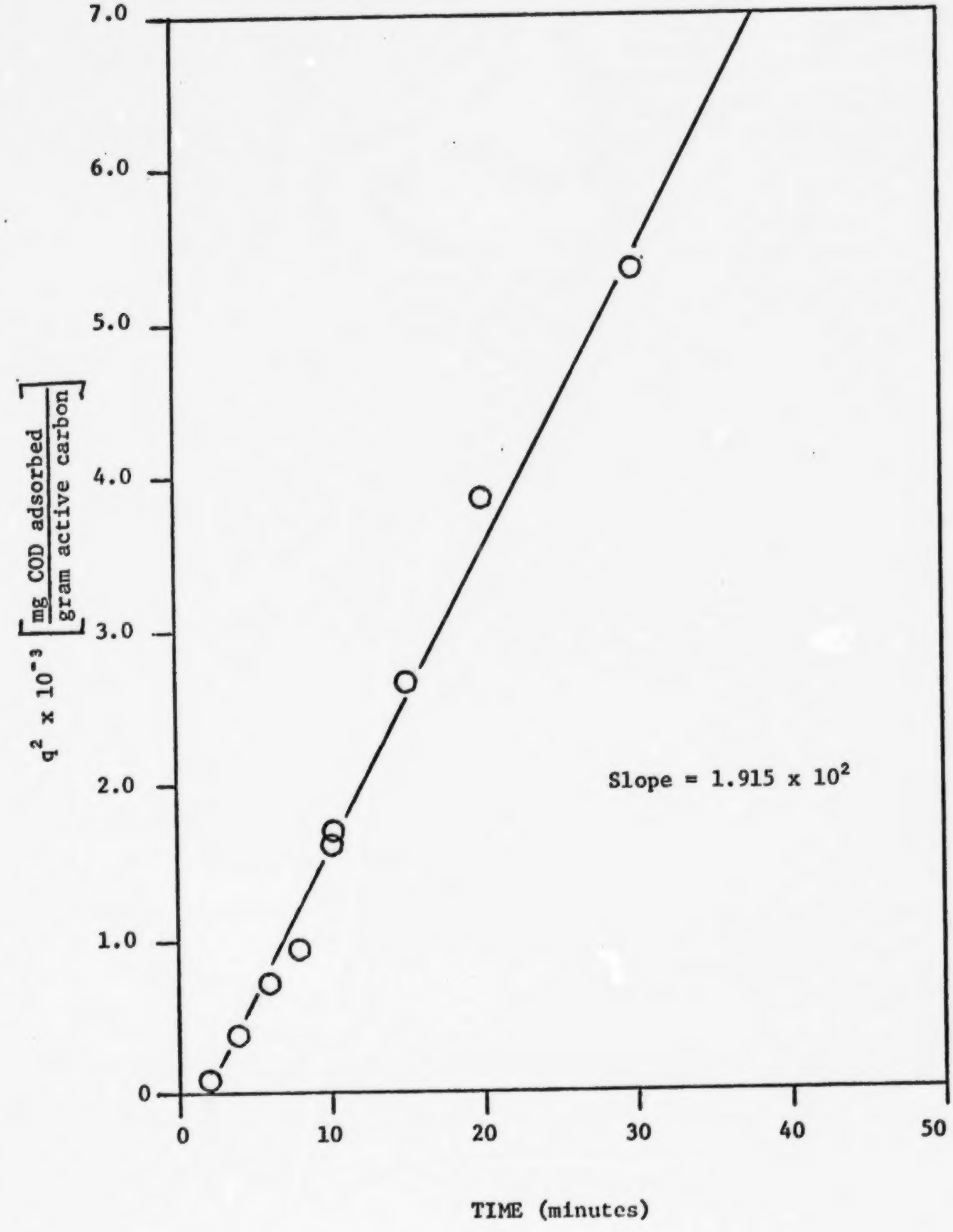

FIGURE 4-35. RATE DATA FOR DETERMINATION OF INTERNAL DIFFUSION RATE CONSTANT: Mix 8

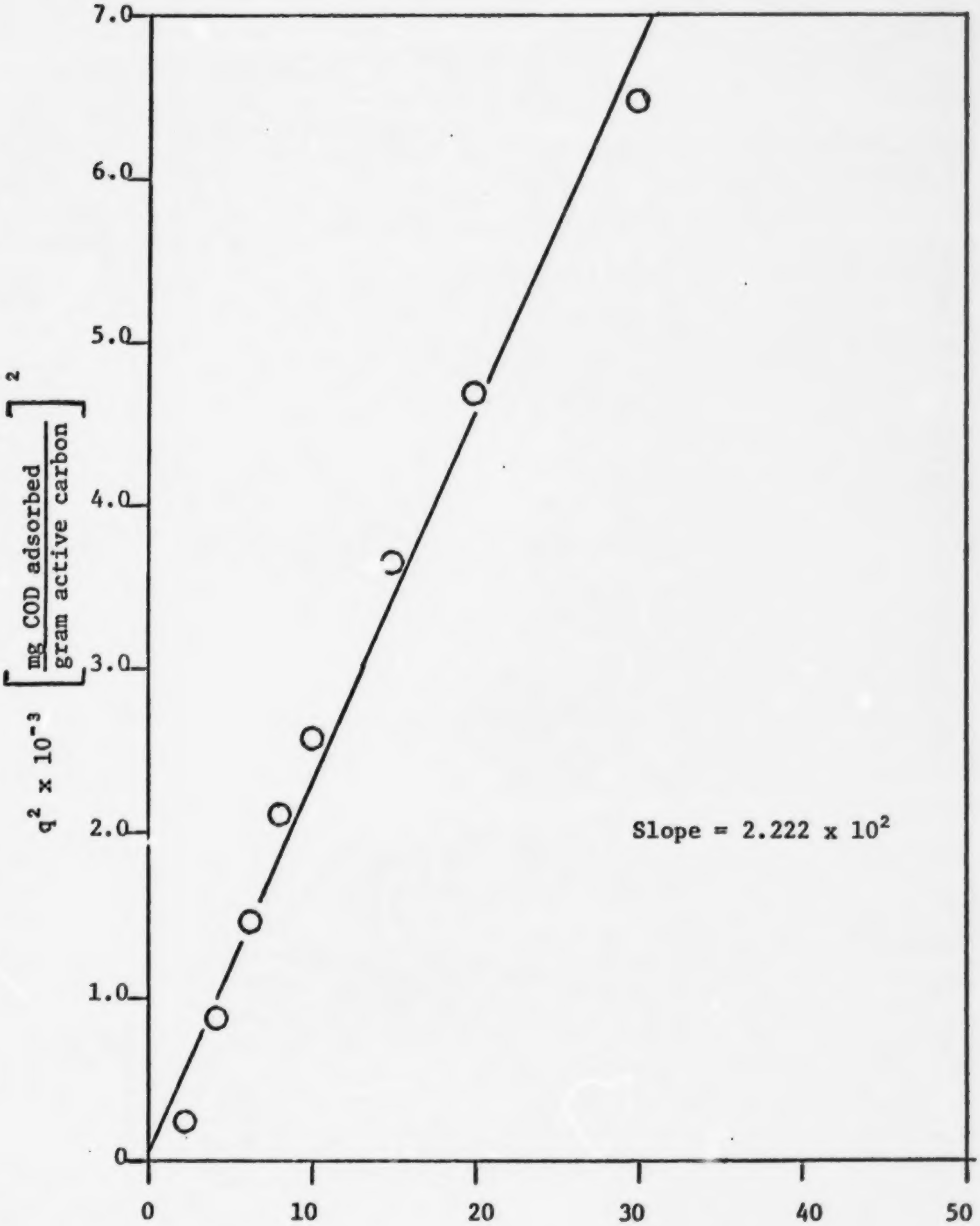

FIGURE 4-36. RATE DATA FOR DETERMINATION OF INTERNAL DIFFUSION RATE CONSTANT: MIX 9

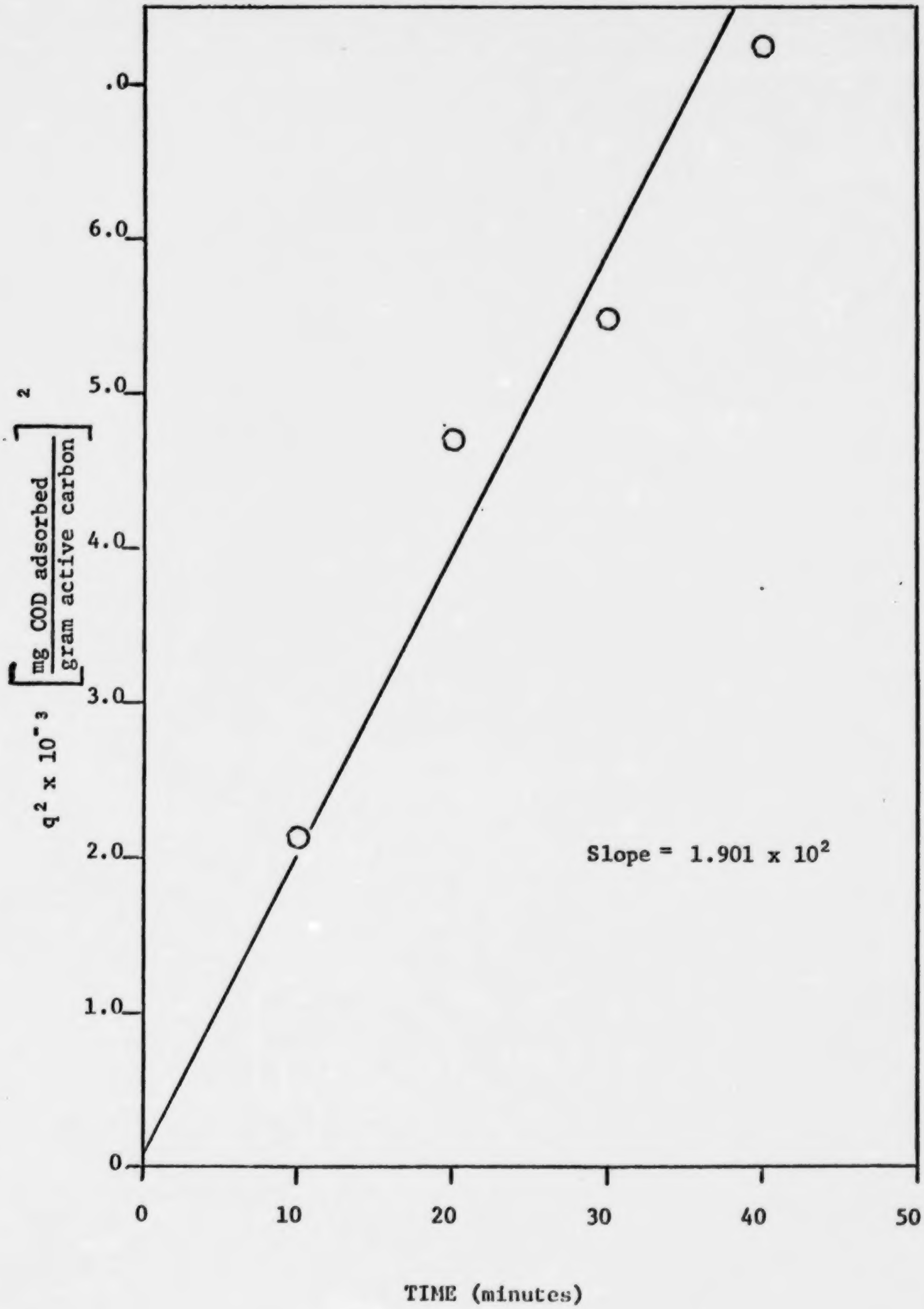

FIGURE 4-37. RATE DATA FOR DETERMINATION OF INTERNAL DIFFUSION RATE CONSTANT: MIX 10

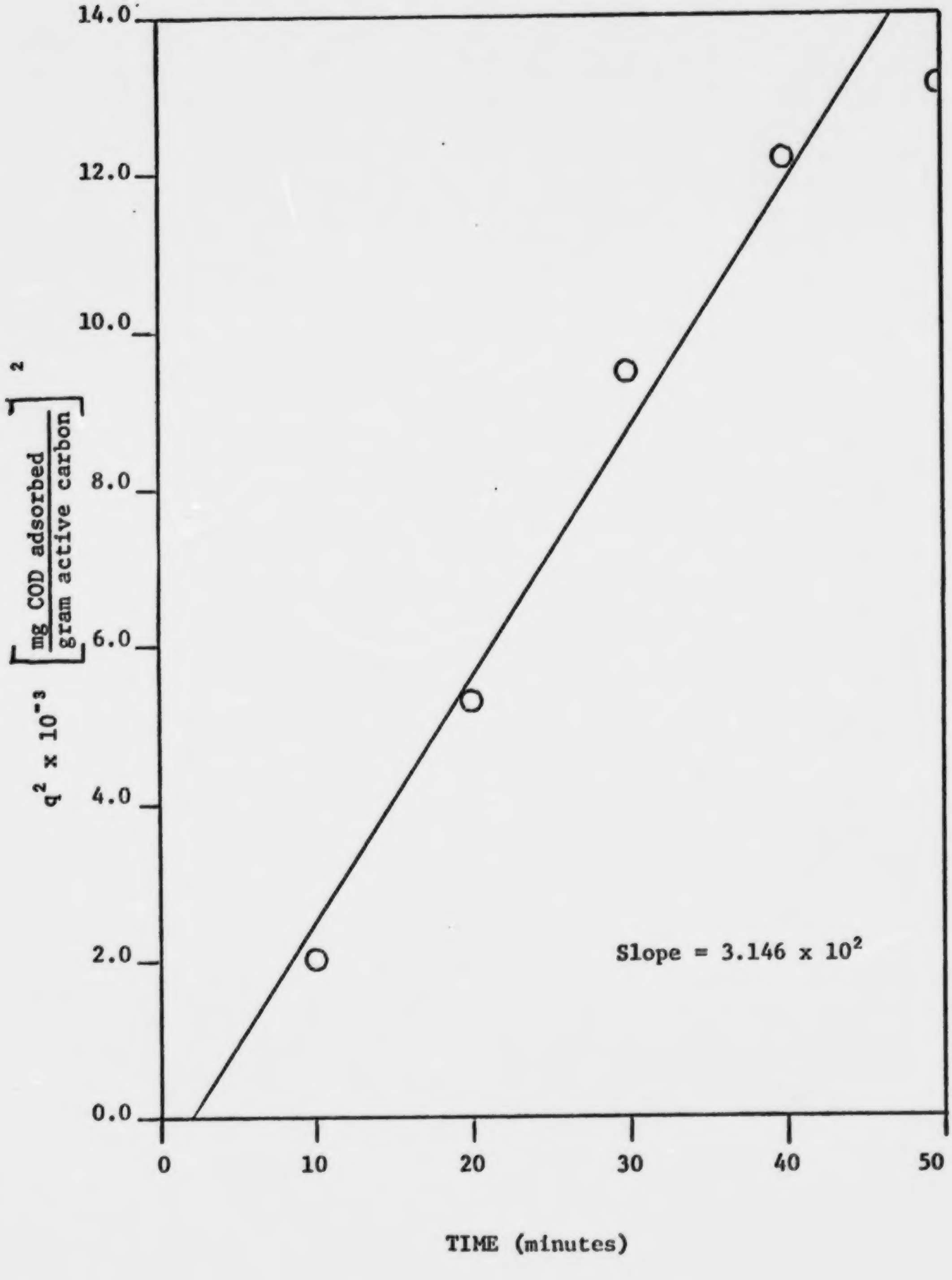

FIGURE 4-38. RATE DATA FOR DETERMINATION OF INTERNAL DIFFUSION RATE CONSTANT: MIX 11

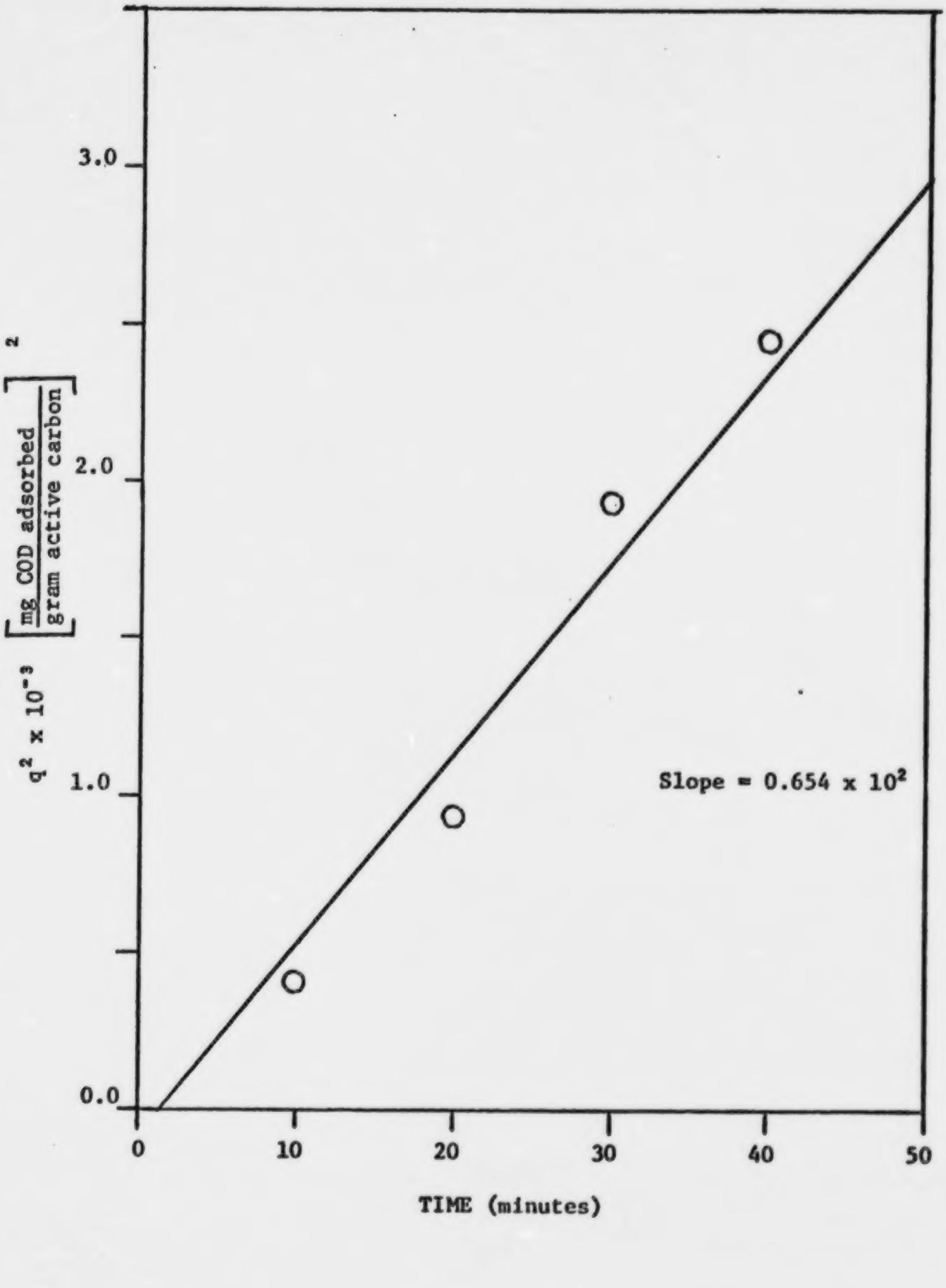

FIGURE 4-39. RATE DATA FOR DETERMINATION OF INTERNAL DIFFUSION RATE CONSTANT: MIX 12

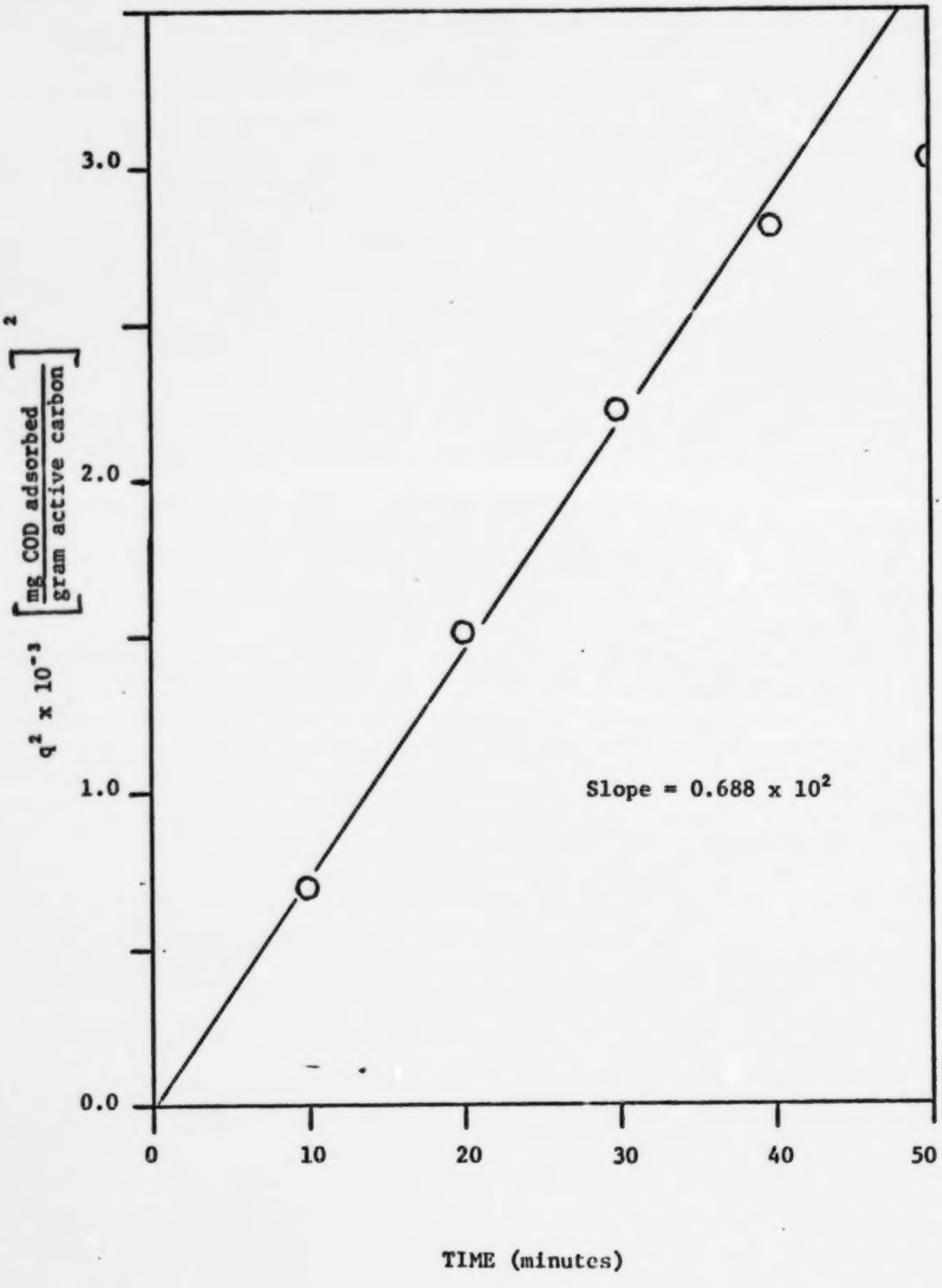

Table 4-5 gives the values for k_pa and k_sa' as calculated by relating the slopes of the normalized curves $(d(q^2)/d\tau = 2q\ dq/d\tau)$ to Equations 2-55 and 2-60, respectively, for each of the mixtures. It can be noted that the rate constant for fluid-phase pore diffusion is larger than the rate constant for solid-phase pore-surface diffusion, ranging from four to approximately ten times larger. Conversely, since the values of the distribution coefficient, D_G, are all approximately 10^3, the mass-transfer solid-phase pore-surface diffusion coefficient, κ_s, was found to be approximately 2 orders of magnitude greater than κ_p, the fluid-phase pore diffusion coefficient. This indicates that the internal rate-controlling diffusion mechanism is solid-phase pore-surface diffusion. The solid-phase pore-surface mass-transfer resistance series combination given by Equation 2-67.

Sensitivity Analyses

The sensitivity of the mathematic model to the adsorption equilibrium constants and to the mass-transfer rate constants was determined by choosing a hypothetical set of column and adsorption parameters and generating a family of curves by varying one adsorption parameter while holding all other system parameters constant. The relative importance of the adsorption parameters can be evaluated in this manner.

Figure 4-40 shows the effect of varying the Langmuir ultimate adsorption capacity constant. As logically would be predicted, an increase in the ultimate adsorption capacity results in a longer period of column operation before complete exhaustion of the hypothetical adsorber bed is achieved. For higher adsorption capacities, more sorbate material has to be introduced into the adsorber system before

TABLE 4-5

INTERNAL MASS TRANSFER RATE CONSTANTS

MIXTURE	k_pa (min^{-1})	k_sa' (min^{-1})	$D_G \times 10^{-2}$
1	2.549	0.358	8.881
2	2.797	0.710	6.428
3	2.767	0.451	11.03
4	2.128	0.354	11.63
5	2.354	0.518	11.38
6	2.632	0.455	11.79
7	3.059	0.767	8.62
8	2.559	0.433	7.638
9	3.415	0.724	7.800
10	4.477	0.988	8.578
11	9.23	1.044	17.56
12	2,176	0.507	10.93

FIGURE 4-40. SENSITIVITY OF KINETIC MATHEMATIC MODEL TO VARIATIONS IN LANGMUIR ULTIMATE CAPACITY, Q

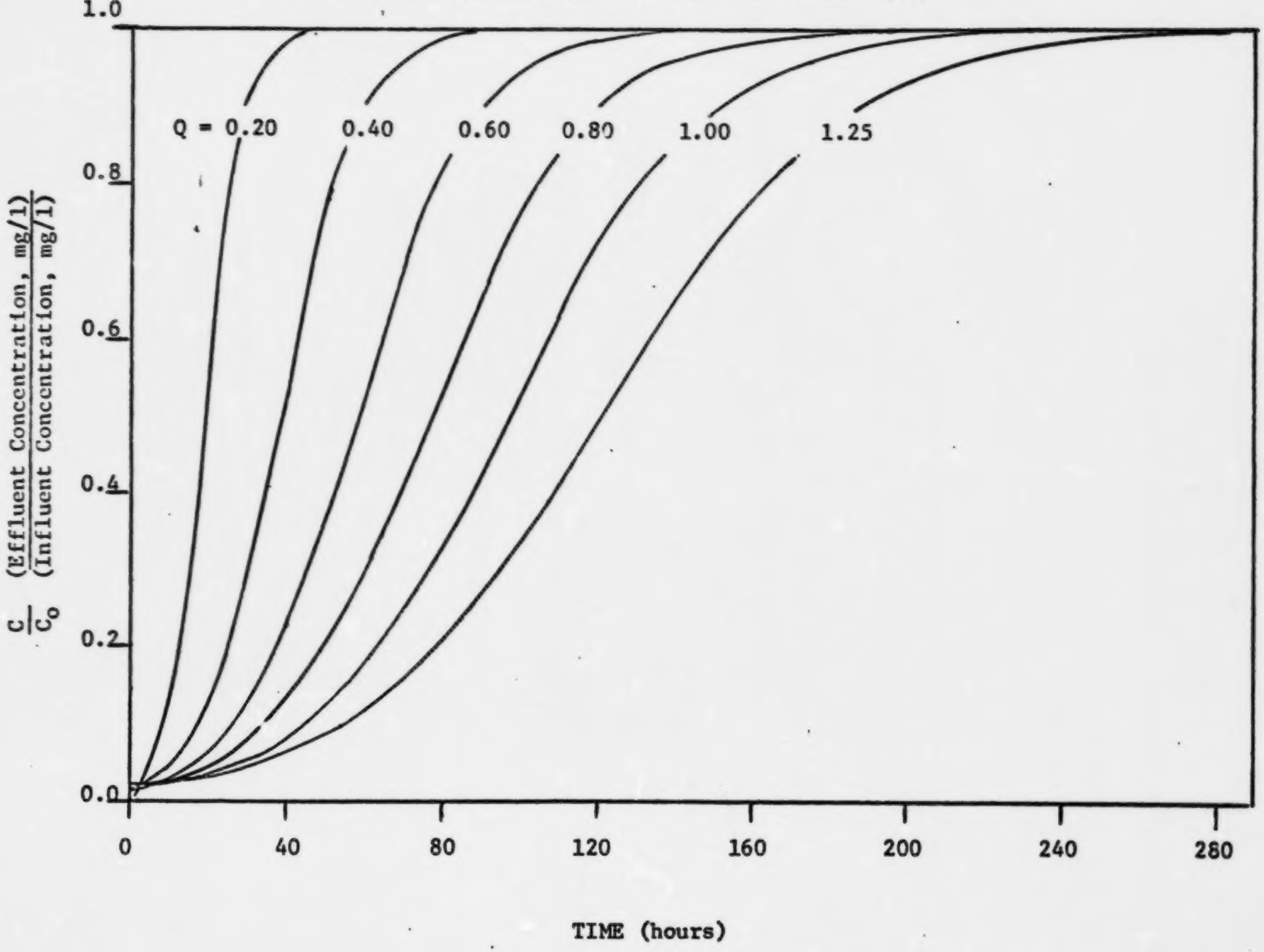

saturation can occur and satisfy the adsorber capacity. Therefore, sorbate compound systems exhibiting a high adsorption affinity capacity can be expected to be better adsorbed and to be absent from column adsorber effluents for a longer operation time period than those systems with a low adsorption capacity, all other parameters being equal.

The predictive mathematic model exhibited interesting behavior with variations in the Langmuir adsorption energy constant. Figure 4-41 illustrates the family of curves generated for different values of the adsorption energy constant. As the adsorption energy constant increases, there is a marked increase in sorbate removal within the adsorber column. This logically follows from the fact that an increase in the adsorption energy constant relates to more favorable adsorption, or, simply stated, an increase in the adsorption energy constant implies the adsorption reaction rate constant increases with respect to the desorption rate constant, and the adsorption reaction is favored. As the adsorption energy constant continues to increase, negligible increase in adsorption can be observed in Figure 4-41, as illustrated by the curve on the extreme right hand side. Examination of the hypothetical isotherm indicates that the condition represented by the increase in the adsorption energy constant represents an approach to irreversibility. The mathematic model therefore demonstrates that as adsorption becomes more favorable, based on adsorption isotherm developments, the approach to irreversible adsorption reaches a point at which increased values of the Langmuir adsorption energy have no significant effect on the model predictions for adsorber performance.

FIGURE 4-41. SENSITIVITY OF KINETIC MATHEMATIC MODEL TO VARIATIONS IN LANGMUIR ENERGY CONSTANT, b

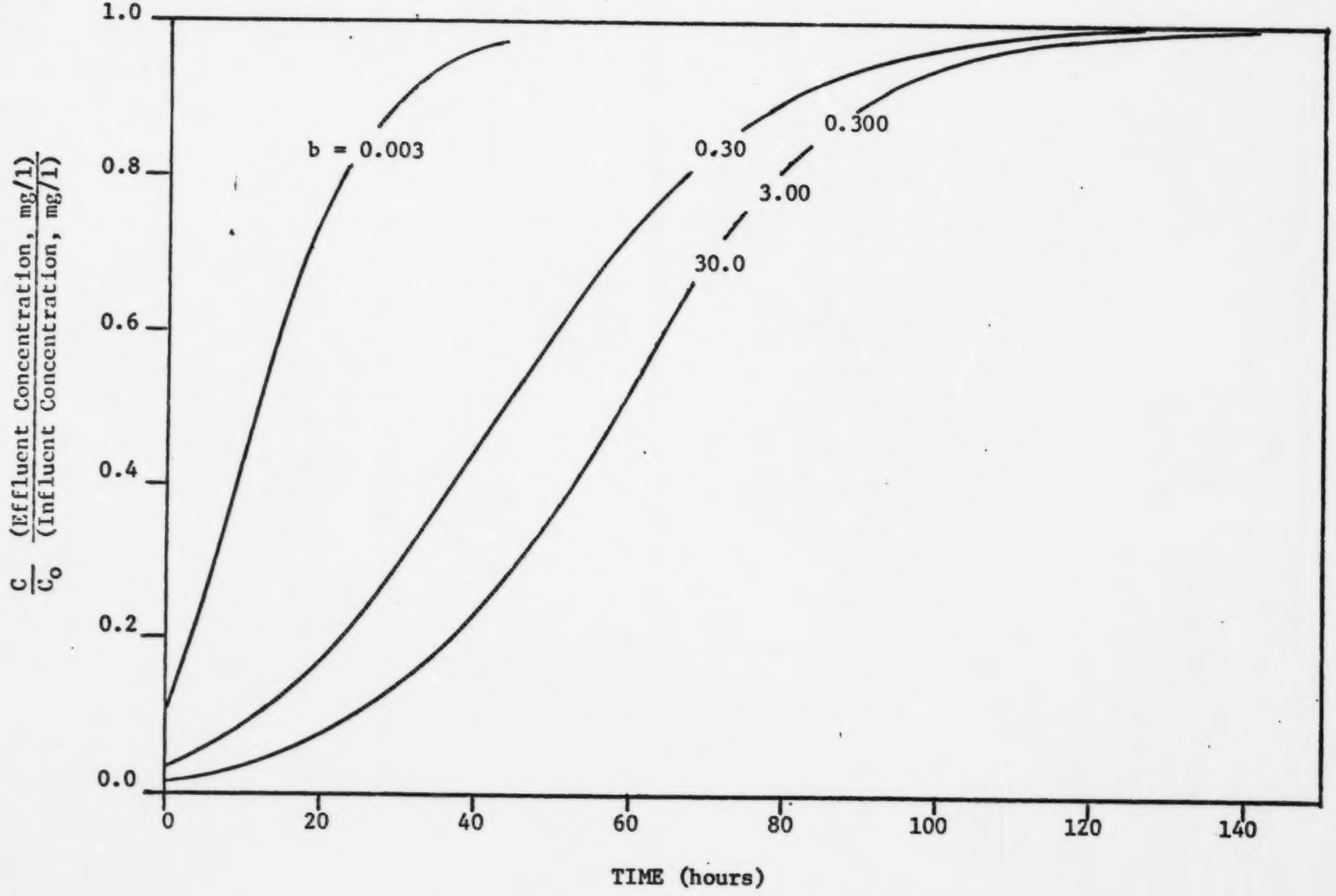

Furthermore, ultimate adsorption capacity alone is not sufficient to predict adsorber performance.

The family of curves given in Figure 4-42 illustrates the effect of varying external diffusion rate constant, $k_f a$, and, hence, the related external diffusion coefficient, κ_f. From this family of curves, it can be seen that as the rate of transfer across the hydrodynamic boundary from the bulk solution to the solid phase increases, i.e. as $k_f a$ increases, better adsorption occurs with less sorbate showing up in the effluent. The period of better adsorption extends for a longer time with higher mass-transfer rates and then the effluent concentration rapidly increases, developing a very sharp profile. The sharpness of the profile is due to the fact that just prior to this time, and from the beginning of the adsorber bed operation, most of the sorbate had been removed from the solution, yielding a high quality effluent. The ultimate adsorption capacity of the active carbon was then approached and hence only a small fraction of the sorbate was further removed before saturation of the adsorber occurred.

Variation of the solid-phase pore-surface rate constant resulted in negligible changes in predicted effluent concentration-history profiles for the hypothetical systems. The reason for this can best be explained by examining Equation 2-67 for combining external diffusion and internal diffusion coefficients. Substituting Equations 2-53 and 2-66 for κ_f and κ_s, respectively, into Equation 2-67, yields

$$\kappa = \frac{2}{(r+1)\left[\frac{1}{k_f a} + \frac{1}{k_s a' D_G}\right]} \qquad (4\text{-}15)$$

$r < 1$

FIGURE 4-42. SENSITIVITY OF MATHEMATIC MODEL

TO VARIATIONS IN EXTERNAL DIFFUSION RATE CONSTANT, $k_f a$

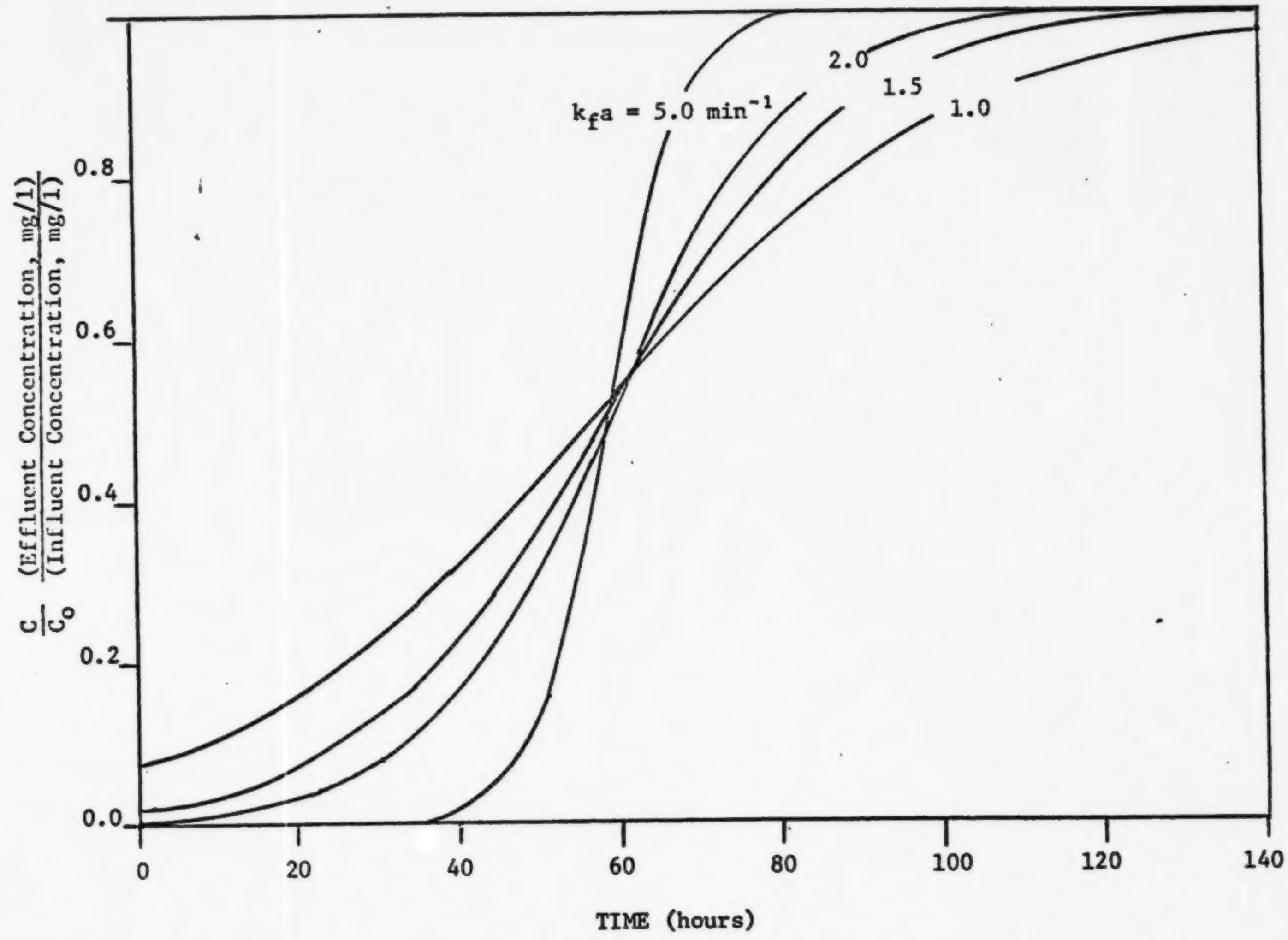

It is obvious that external diffusion will control the overall value of κ, given by Equation 4-15, when $1/k_f a$ is larger than $1/(k_s a' D_G)$. As $k_s a'$ is always somewhat less than $k_f a$ (38), internal diffusion will become the controlling resistance as the distribution coefficient, D_G, approaches unity, in agreement with experimental results (13).

The adsorption equilibrium constants and the adsorption mass-transfer diffusion coefficients reported in this section were used in the solution of the predictive mathematic model for effluent concentration-history profiles. The mathematic concepts presented in Chapter 2 and the experimental approaches presented in this chapter for evaluation of the required adsorber column parameters represent the basis for utilization of the predictive mathematic model.

CHAPTER 5

CONTINUOUS FLOW EFFLUENT CONCENTRATION-HISTORY PROFILES

The mathematic model developed in Chapter 2 provides a means for predicting effluent concentration-history profiles for expanded-bed adsorber systems. The application of this mathematic model requires the specification of nine distinct parameters, the determinations of which have been illustrated in Chapter 4. The adequacy of the mathematic model for predicting effluent concentration-history profiles for complex mixtures of dissolved organic material which have been characterized by a single concentration parameter is evaluated herein by comparison of mathematically-predicted to experimentally-generated effluent concentration-history profiles.

The experimental profiles were generated for each of the twelve complex mixtures given in Tables 3-4 and 3-5 by use of the continuous-flow expanded bed column system described in Chapter 3 and illustrated in Figure 3-4. The 0.503 mm particle size Filtrasorb active carbon was used in all continuous-flow experiments. The hydrodynamic characteristics based on 250.0 grams of active carbon and a flow rate of 5.0 gallons per minute per square foot, as used in all experiments, were determined from the concepts set forth in Chapter 4 and are given in Table 5-1.

The adsorption parameters required for application of the predictive mathematic model are given in Table 5-2 for the respective mixture systems. Determination methods for each of these parameters may be found in Chapter 4.

TABLE 5-1

HYDRODYNAMIC PROPERTIES OF COLUMNAR SYSTEM

POROSITY OF EXPANDED BED (dimensionless)	DENSITY OF EXPANDED BED (grams/carbon cc)	VOLUME OF EXPANDED BED (cc)	HEIGHT OF EXPANDED BED (cm)
0.5953	0.2597	962.7	47.6

TABLE 5-2

ADSORPTION PARAMETERS FOR MODEL UTILIZATION

MIXTURE	LANGMUIR Q (gram COD adsorbed/ gram active carbon)	Langmuir b (liter/mg)	$k_f a$ (min^{-1})	$k_s a'$ (min^{-1})
1	0.568	0.250	1.839	0.358
2	0.336	0.328	2.098	0.710
3	0.638	0.138	1.666	0.451
4	1.530	0.0034	2.018	0.354
5	0.801	0.0192	1.582	0.518
6	0.700	0.0294	1.723	0.455
7	0.5499	0.0151	1.921	0.767
8	0.520	0.026	1.804	0.433
9	0.304	35.4	2.066	0.724
10	0.483	0.039	1.691	0.988
11	0.419	0.243	1.816	1.044
12	0.264	2.82	1.781	0.507

The mathematically-predicted profiles were produced by numerical solution of Equation 2-42. The use of an IBM 360/70 digital computer facilitated the solution of the mathematic model. The computer program providing the numerical solutions is given in Appendix 3. The mathematically predicted effluent concentration-history profiles are depicted by the solid lines in Figures 5-1 through 5-12 for Mixtures 1 through 12, respectively.

PREDICTED PROFILES AND EXPERIMENTAL VERIFICATON FOR SORBATE MIXTURE SYSTEMS

Binary Mixtures

Figures 5-1 through 5-3 represent comparisons between experimentally-generated and mathematically-predicted effluent concentration-history profiles for the binary mixtures of phenol and dodecyl sodium sulfate, given as Mixtures 1 through 3, respectively. The solid line in these Figures represents the computed numerical solution of Equation 2-42, predicting the adsorber bed performance. Comparison of the mathematically predicted profile to the actual experimental data illustrates good correspondence for all three systems in the initial stages of column operation. However, in all three cases discrepancies between the predicted profiles and the experimental profiles develop in later stages of the adsorber-bed performance. The experimental data starts to deviate from the symmetrical-shape predicted profile at approximately 0.7 C_0 for Mixes 1-3. In all cases, the observed effluent concentration-history profile resulted in better adsorption of organic material than predicted by Equation 2-42.

FIGURE 5-1. EXPANDED-BED ADSORBER EFFLUENT CONCENTRATION-HISTORY

PROFILE: MIX 1

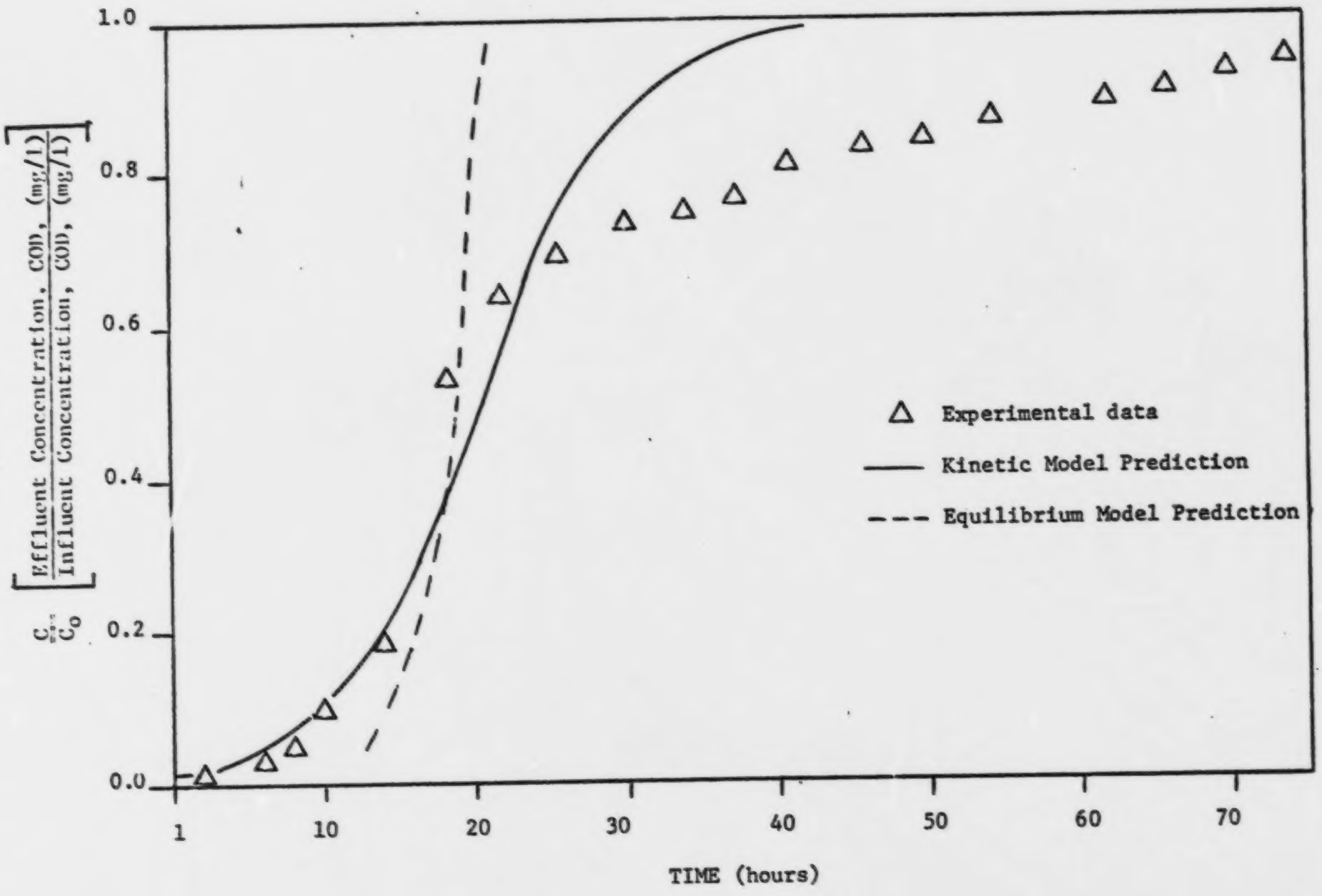

FIGURE 5-2. EXPANDED-BED ADSORBER EFFLUENT CONCENTRATION-HISTORY

PROFILE: MIX 2

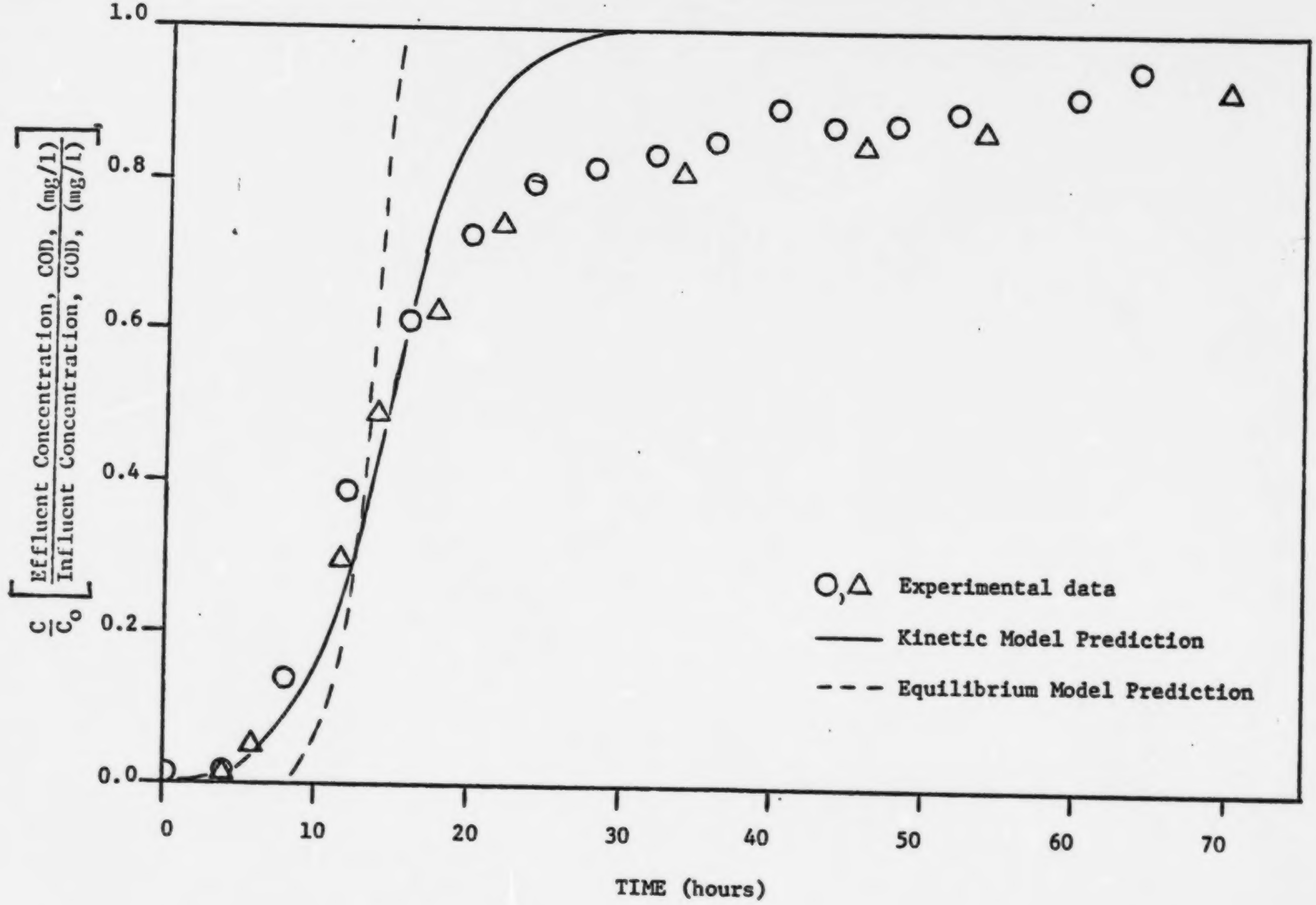

FIGURE 5-3. EXPANDED-BED ADSORBER EFFLUENT CONCENTRATION-HISTORY

PROFILE: MIX 3

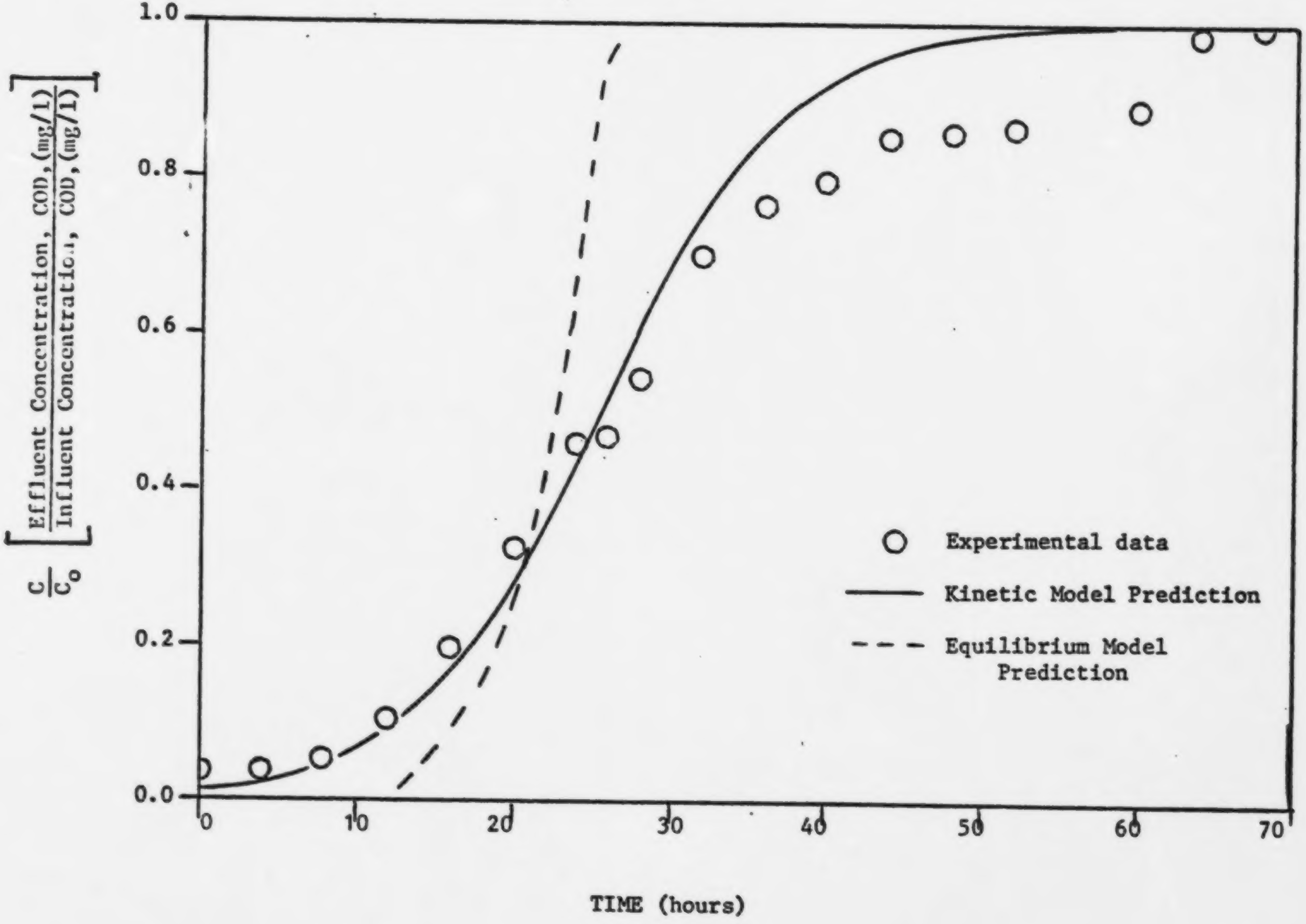

The mathematically predicted effluent concentration-history profiles for Mixtures 4 and 5, binary mixtures of dodecyl sodium sulfate and n-hexanol, are compared to the experimental data in Figures 5-4 and 5-5, respectively. For Mixture 4, the mathematically-predicted profile corresponds to the experimental data, but, at approximately 0.6 C_o, the experimental profile again shows better adsorption operation than predicted, and then rapidly approaches saturation capacity at approximately the same time as predicted by the mathematic model. The experimental effluent concentration-history data for Mixture 5 does not correspond as well initially to the mathematically-predicted profile; the predicted profile indicates better adsorption than obtained initially. During later stages of operation, the reverse occurs - the predicted profile indicates less adsorption than occurs in the experimental system. The mathematic model in this case seems to generate an 'average' curve for the total experimental effluent concentration-history profile. An interesting observation indicates that if the predicted curve were to fit the initial data more accurately, then the experimental data would again deviate from the predicted profile at approximately 0.6 C_o as noticed previously for Mixtures 1 through 4.

Ternary Mixtures

A comparison for the effluent concentration-history profiles for the experimental ternary mixtures systems of phenol, dodecyl sodium sulfate, and n-hexanol, which constitute Mixtures 6 through 8, to their respective predicted profiles may be made using Figures 5-6 through 5-8. Figure 5-6 indicates almost perfect agreement between

FIGURE 5-4. EXPANDED-BED ADSORBER EFFLUENT CONCENTRATION-HISTORY PROFILE: MIX 4

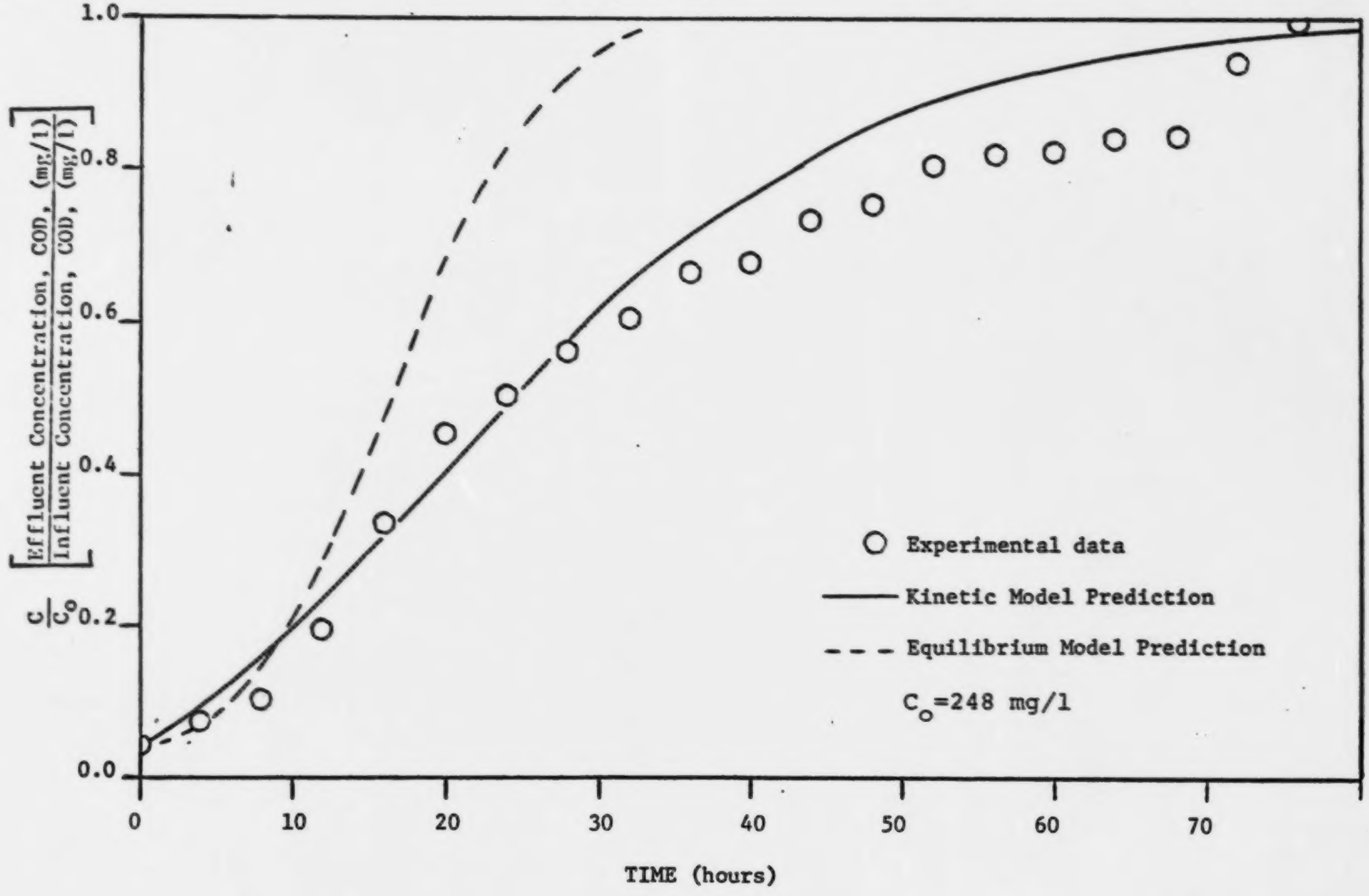

FIGURE 5-5. EXPANDED-BED ADSORBER EFFLUENT CONCENTRATION-HISTORY PROFILE: MIX 5

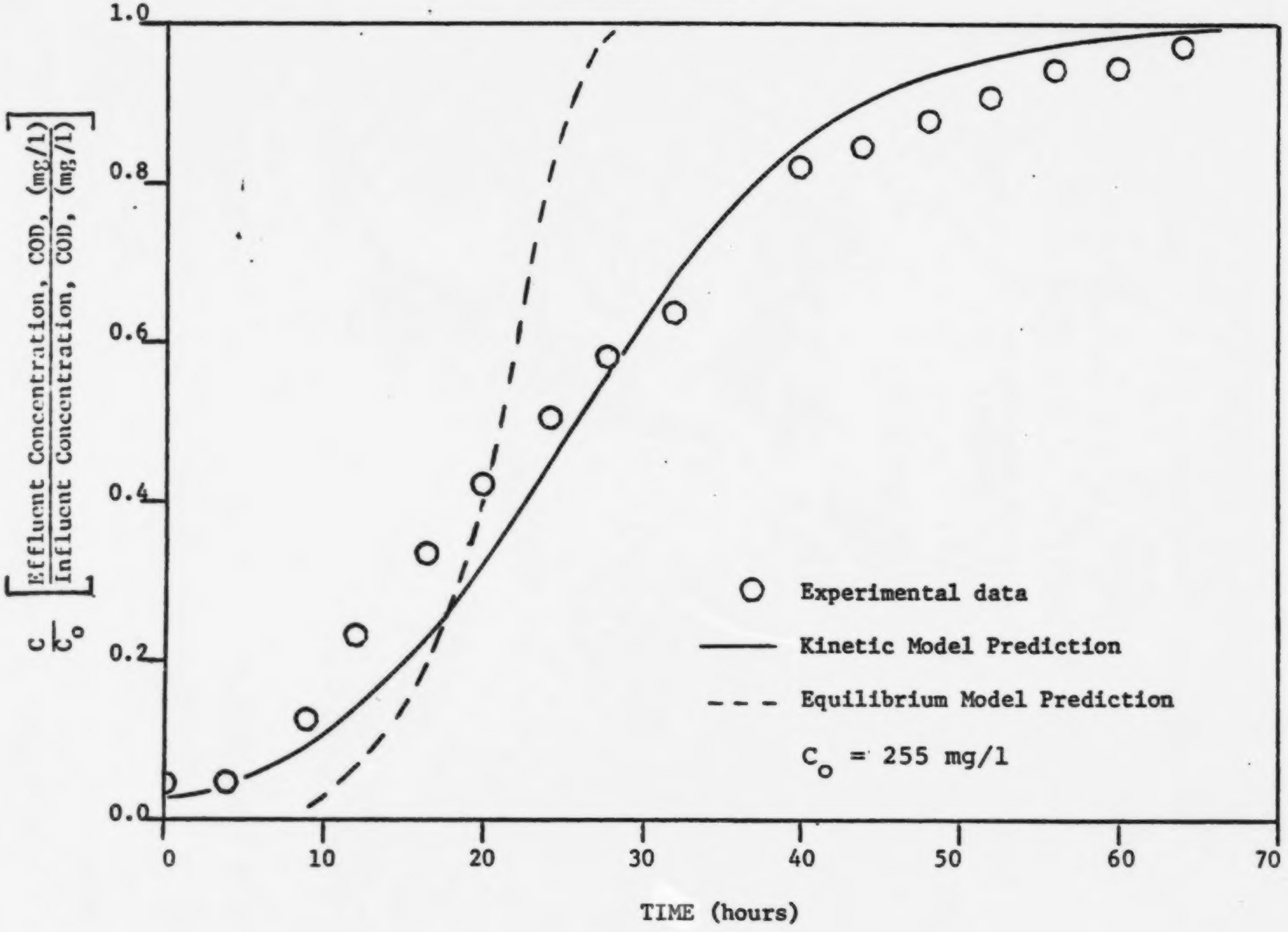

FIGURE 5-6. EXPANDED-BED ADSORBER EFFLUENT CONCENTRATION-HISTORY PROFILE: MIX 6

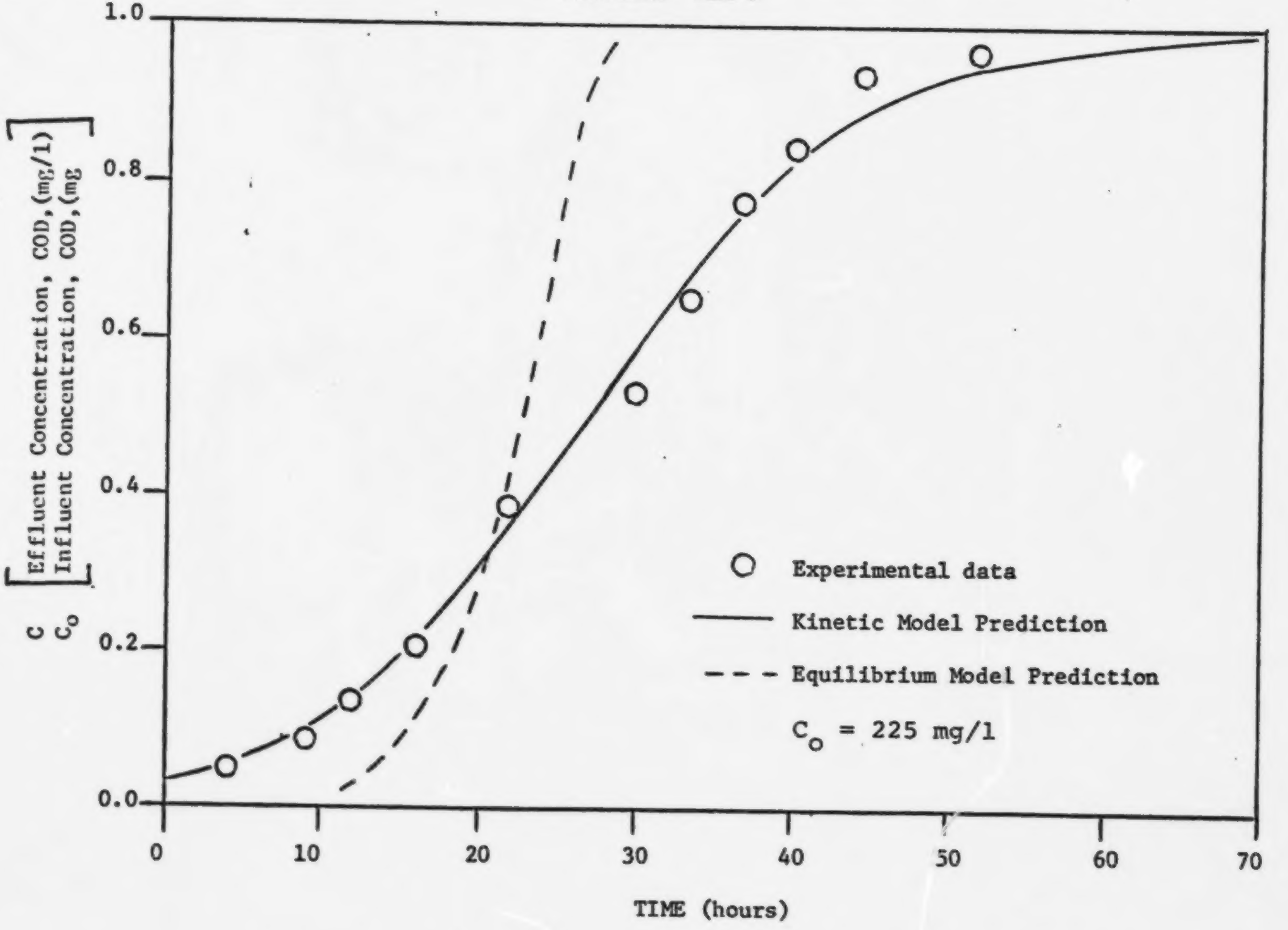

FIGURE 5-7. EXPANDED-BED ADSORBER EFFLUENT CONCENTRATION-HISTORY PROFILE: MIX 7

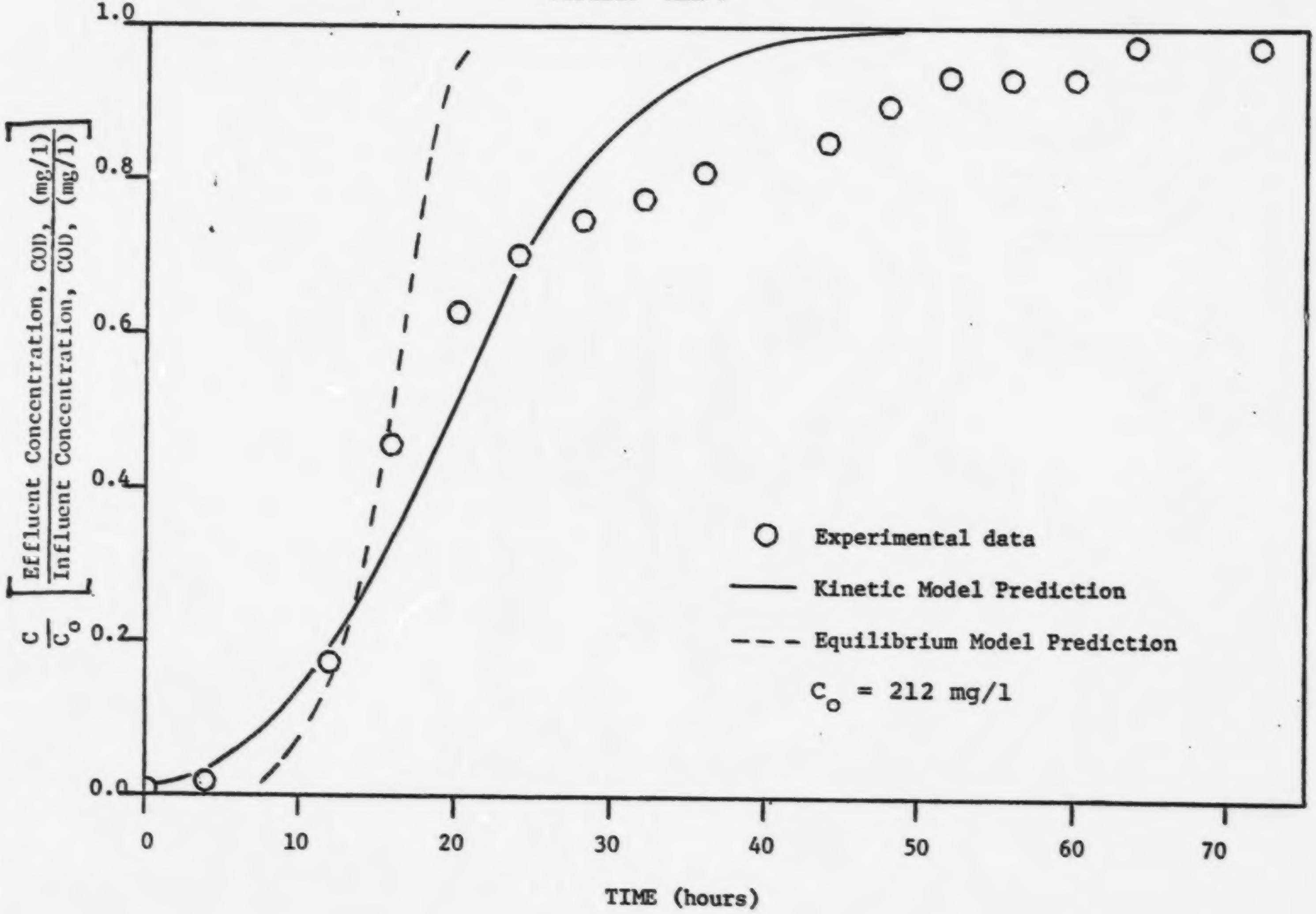

FIGURE 5-8. EXPANDED-BED ADSORBER EFFLUENT CONCENTRATION-HISTORY PROFILE: MIX 8

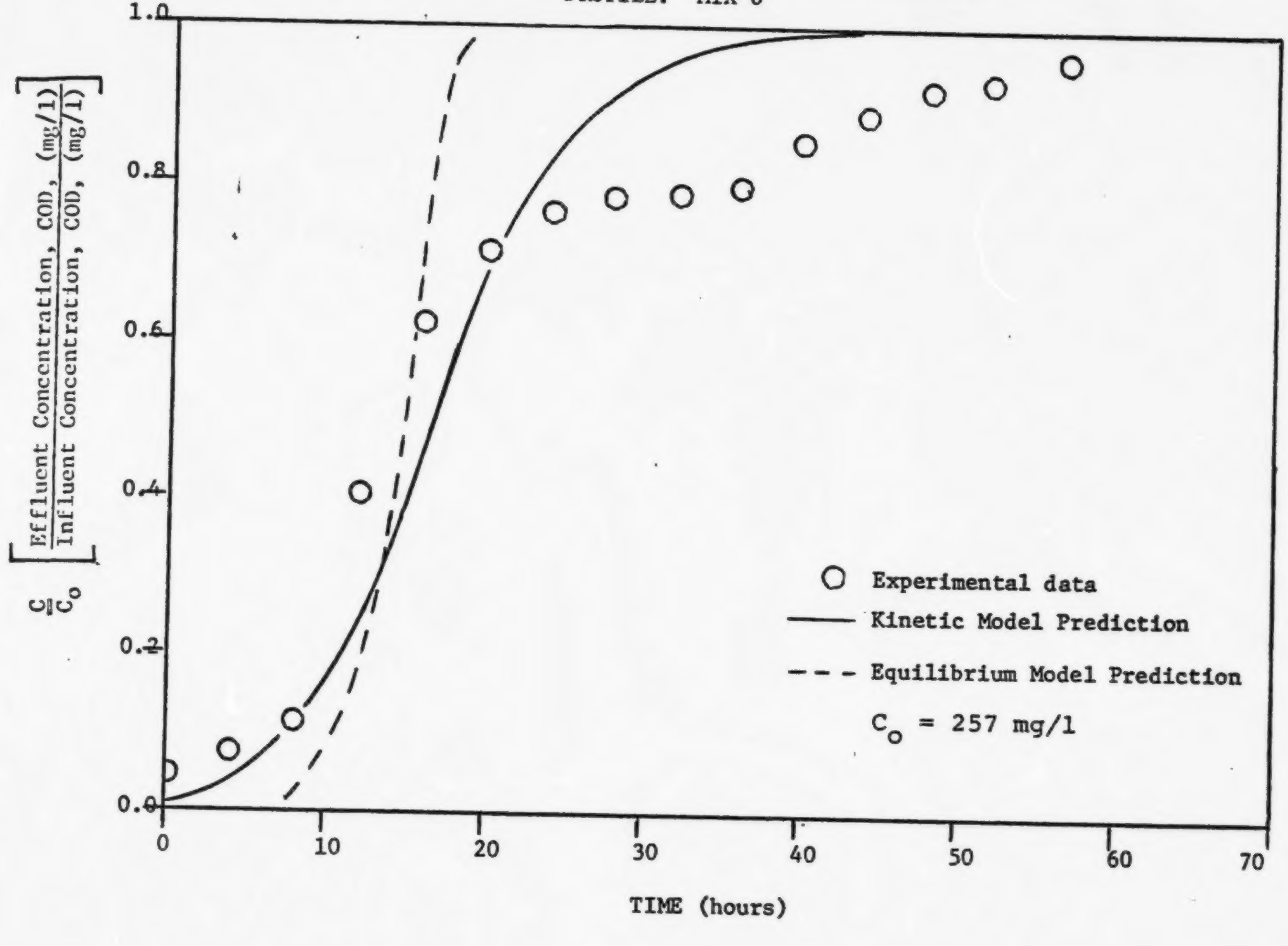

the experimental data and the predicted effluent concentration-history profile throughout the entire range of column operation. This is the only system which showed such excellent agreement.

The mathematically predicted profile for Mixture 7, given in Figure 5-7, demonstrates reasonably good correlation with the experimental data up to approximately 0.7 C_o. The experimental system then indicates better adsorption than the mathematic model predicts. The same general pattern obtains in comparing the predicted versus experimental profiles for Mixture 8, as illustrated in Figure 5-8.

The sorbate systems investigated for determination of the ability of the mathematic model to predict adsorber performance generally developed asymmetric effluent concentration-history profiles which agreed reasonably well with the predicted profiles up to 0.6 to 0.7 C_o effluent concentration. Then, better adsorption occurred than was predicted. The mathematic model thus seems to be adequate to describe the initial stages of the expanded-bed effluent concentration-history profile, which is the region of interest for design calculations. However, the mathematic model generally breaks down in the later stages of adsorption, as previously indicated.

PREDICTED PROFILES AND EXPERIMENTAL VERIFICATION FOR ADSORBER/NON-ADSORBER SYSTEMS

When non-adsorbing compounds which contribute to the overall description parameter for characterizing a waste as a single component system are present in the influent solution to an adsorber bed, they should appear in the effluent from that bed in unchanged concentration. This of course assumes only adsorption affects in the column. Therefore, the prediction of effluent concentration-history profiles for adsorber bed performance depends on excluding the non-adsorbing fraction which is included in the overall description-parameter concentration determinations.

Mixtures 9 through 12 contain different amounts of non-adsorbing materials and experimental effluent concentration-history profiles for these mixtures including the non-adsorbing constituent of influent and effluent concentrations are illustrated in Figures 5-9 through 5-12, respectively. In order to redefine the effluent concentration-history profile on an adsorbing-fraction concentration basis, the concepts of adsorption isotherm development for adsorber/non-adsorber systems given in Chapter 4 were used. The fraction of non-adsorbing concentration was determined from the adsorption isotherms, and thus the influent and effluent concentrations were evaluated on an adsorbing fraction basis.

The experimental effluent concentration-history profile data for the adsorbing fraction of Mixtures 9 through 12 are also given in Figures 5-9 through 5-12, respectively. The profiles predicted by the mathematic model are for the adsorbing fraction only and are also denoted by the solid lines in the respective Figures.

Examination of Figure 5-9 shows that there is good correspondence between the predicted profile and the experimental data for the adsorbing fraction of the complex mixture during initial stages of column operation for Mixture 9. After approximately 0.5 C_o concentration breaking through the adsorber bed, the experimental profile indicates much better adsorption than that predicted. At 55 hours of operation, the effluent to influent concentration ratio

FIGURE 5-9. EXPANDED-BED ADSORBER EFFLUENT CONCENTRATION-HISTORY PROFILE: MIX 9

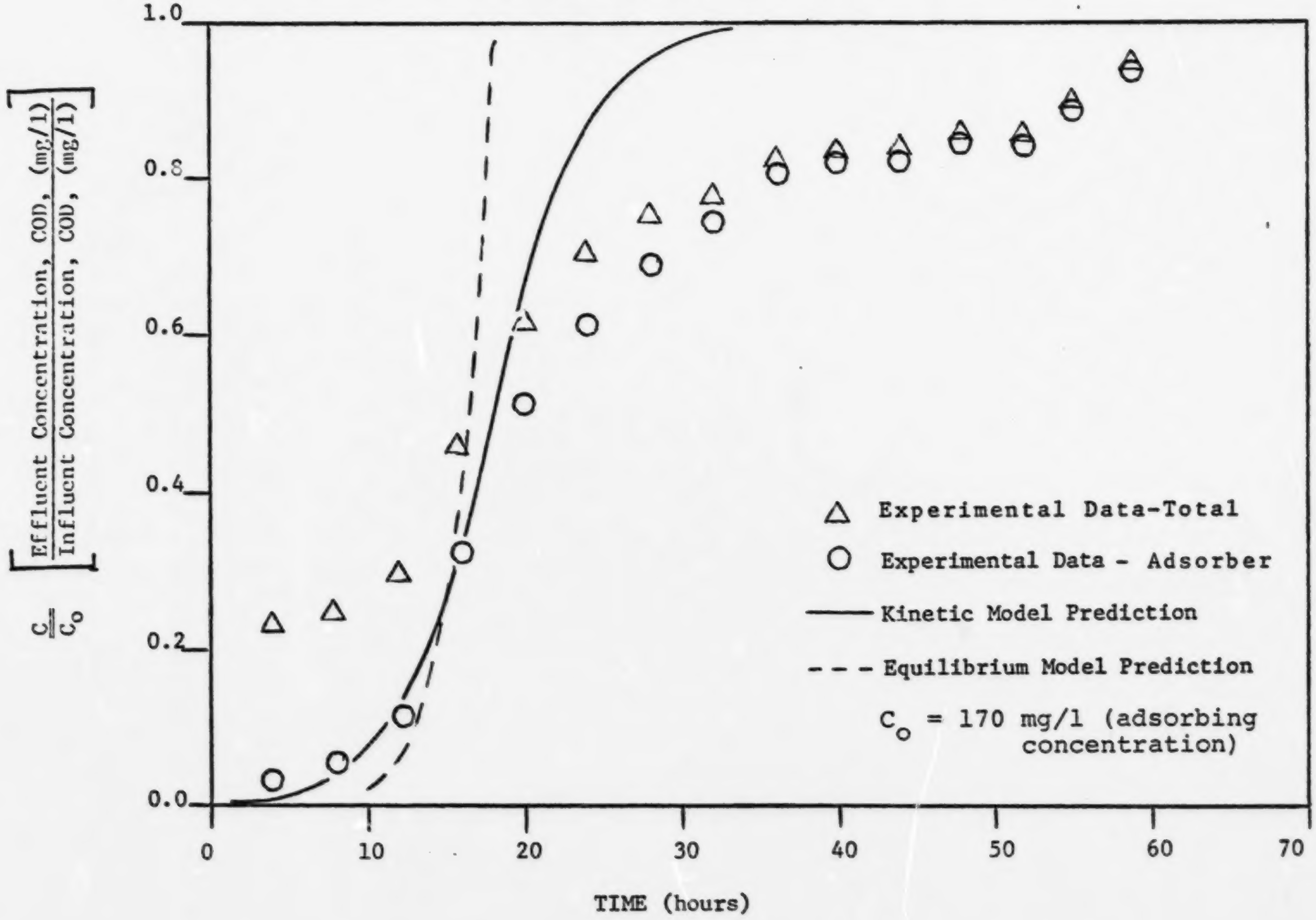

FIGURE 5-10. EXPANDED-BED ADSORBER EFFLUENT CONCENTRATION-HISTORY PROFILE: MIX 10

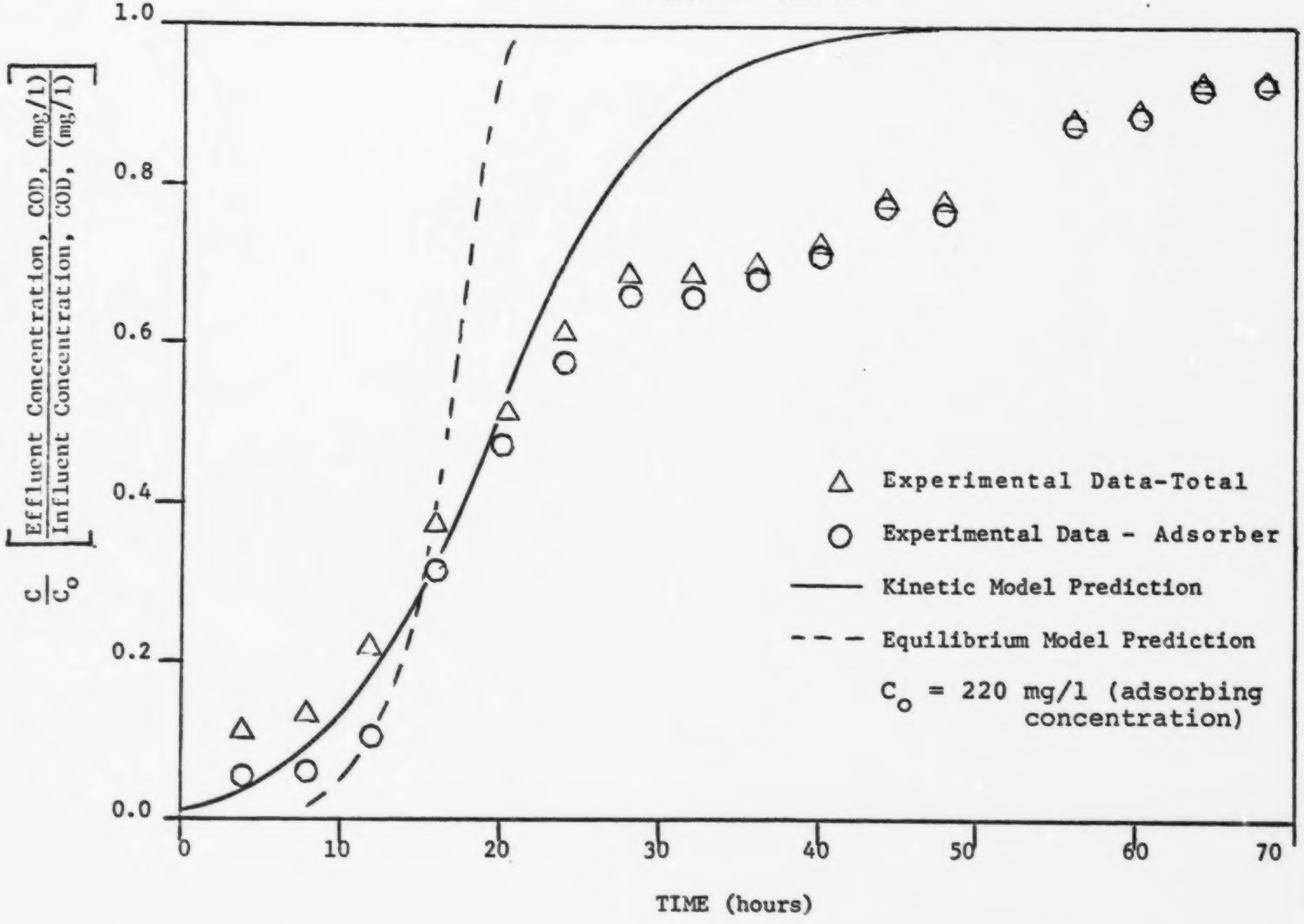

FIGURE 5-11. EXPANDED-BED ADSORBER EFFLUENT CONCENTRATION-HISTORY PROFILE: MIX 11

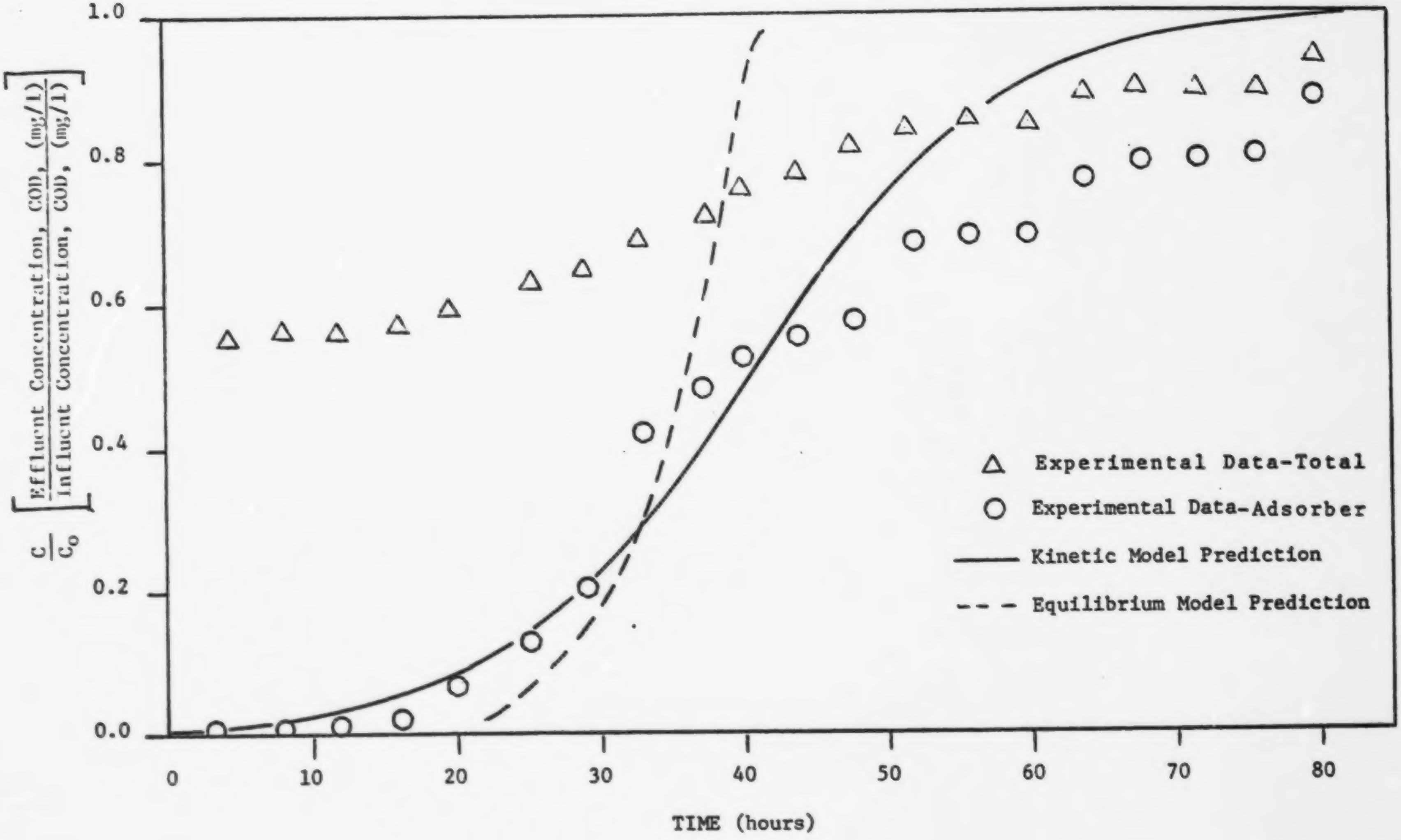

FIGURE 5-12. EXPANDED-BED ADSORBER EFFLUENT CONCENTRATION-HISTORY PROFILE: MIX 12

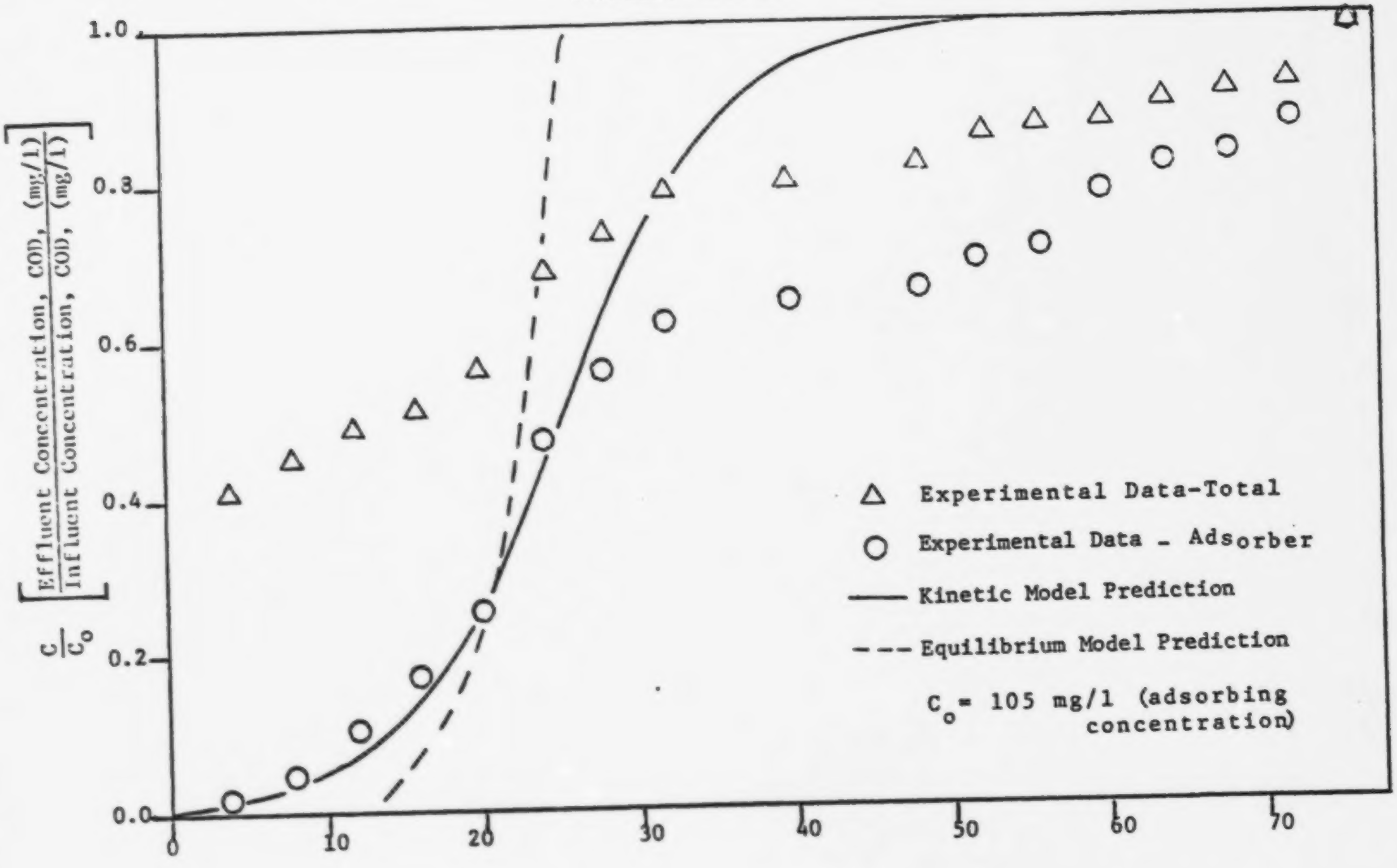

was 0.88, whereas complete saturation was predicted at 38 hours by the mathematic model.

The effluent concentration-history profiles for Mixture 10, given in Figure 5-10, indicates good correlation in the initial stages between the mathematic model predictions and the experimental data up to approximately 0.6 C_o effluent concentration. The pattern of better adsorption occurring in the experimental systems again is evident for Mixture 10. Adsorption capacity for the column system was predicted to obtain by 48 hours of operation, but in actuality the effluent/influent concentration ratio was only 0.77, indicating that the active carbon bed was still unsaturated.

Figure 5-11 provides the comparison of predicted to experimental profiles for Mixture 11. It is evident that good correlation between the mathematic model predictions and the experimental data for the initial periods of column operation, up to approximately 0.55 C_o, results. Beyond this effluent concentration, better adsorption than predicted was experienced in the adsorber bed. The experimental profile seems to have several distinct steps of rapid increase in concentration. A possible explanation for such steps is based on comparative adsorptivities of the active carbon for individual components of the mixture. The least adsorbable component breaks through first, and the remaining compounds continue to be essentially totally removed. As the capacity of the adsorbent for the next lower adsorbable compound is approached, there will be a faster increase in the concentration of that second compound in the effluent stream.

This pattern will continue for additional compounds with sufficiently different adsorption characteristics.

For Mixture 10, two such steps would be expected, but four seem to occur. If we assume that the second step is due to an increase in dodecyl sodium sulfate concentration, then examination of the behavior of that compound from experimental data given in Chapter 6 may account for the last two 'steps'. The experimental data defining the effluent concentration-history profile and the comparison to the mathematic model prediction for Mixture 12 is shown in Figure 5-12. The predicted profile describes the experimental data almost exactly up to approximately 0.55-0.6 C_o. As before, the experimental profile illustrates that better than predicted adsorption occurs in the adsorber bed column system during the following operation period.

The results of the adsorber/non-adsorber experimental profile determinations demonstrate that the technique developed in Chapter 4 utilizing the adsorption isotherm experiments to determine non-adsorbing fractions of overall description parameter concentration can be used to adequately redefine the complex mixture on an adsorbing fraction concentration basis. This adsorbing fraction can then be used to determine the concentration to serve as input to the mathematic model. The predicted profile for the adsorbing fraction resulting from use of this technique was successful in describing the experimental profiles for the experimental systems used in this research, within the limits discussed.

Correlation between the initial regions of effluent concentration-history profiles mathematically predicted and the corresponding mixture experimentally-generated data generally occurred for all systems investigated. After between approximately 0.5-0.8 C_o appeared in the effluent stream of the experimental adsorber bed systems, the effluent quality was experimentally better than predicted for all but one system. The mathematic model failed in prediction of this period of the effluent profile. No evidence of biological activity which could enhance solute removal and produce the better experimental adsorption was observed. The effect of this phenomena in the experimental systems reported herein was therefore negated as a contributing factor for the greater adsorption experienced in the experimental adsorber bed systems. The enhanced removal observed must then be due to adsorption effects not included in the mathematic model development.

COMPARISON OF MATHEMATIC MODELS

The mathematic model given by Equation 2-42 based on second-order kinetic formulations and material balance concepts has been shown to adequately predict the performance of expanded-bed adsorber columns for complex mixtures characterized as a single solute for effluent concentrations up to at least 0.5 C_o for all systems investigated. The failure of the mathematic model to adequately predict the full range of the adsorption column operation period, and the complexity of the mathematics involved, suggests the necessity of comparison of that model to a less complex mathematic model. If the latter formulations predict the experimentally-observed effluent concentration-history profiles as well (or better) than the more complex mathematic model, then it would be expedient to utilize the simpler form.

The equilibrium mathematic model of Michaels (73) was chosen for a comparison basis to the kinetic mathematic model. The details of this equilibrium model can be found in Appendix 4, with a computer program for solution of the predicted concentration-history profile. It is important to note that the Michaels equilibrium model requires the generation of an adsorption isotherm and determination of an overall mass-transfer rate constant. The experimental requirements for use of either of the two mathematic models to be compared is obviously the same.

The results of the solution to the Michaels equilibrium model predictions for effluent concentration-history profiles are illustrated by the dashed-lines in Figure 5-1 through 5-12 for tne respective mixture systems. For all cases investigated, the predicted profiles using the Michaels equilibrium model indicated better adsorption than experimentally observed in the initial periods of adsorption within the expanded-bed system, and a self-sharpening front leading to prediction of less adsorption after approximately 0.3 - 0.4 C_o concentration in the effluent stream. It is obvious, therefore, that the second-order kinetics mathematic model is more accurate in predicting the experimental effluent concentration-history profiles in comparison to the Michaels equilibrium model. Furthermore, although the mathematic formulation of the second-order kinetic model is more complex than that of the Michaels equilibrium model, the approximations for solution of Equation 2-42 result in an expression for the effluent concentration-history profile in terms of well-tabulated exponentials and error functions. The difficulty in solving the second-order-kinetic mathematic model is not much greater than the effort for solution of the Michaels equilibrium model.

The second-order-surface-reaction controlled kinetic mathematic model for prediction of expanded-bed adsorber performance is an adequate tool for predicting effluent concentration-history profiles for up to at least 0.5 C_o effluent concentration. The mathematic model generally fails to predict the remaining portion of the experimental profiles. Explanation of possible causes of the mathematic model failure are presented and discussed in Chapter 6.

CHAPTER 6

MIXTURE COMPONENT ANALYSES

The ultimate aim of a mathematic development and analysis of the adsorption process in a continuous flow system is to provide an expression for the dependence of effluent concentration on time. The concentration-history profiles predicted by the Keinath-Weber model exhibit a symmetric-sigmoidal shape. As we have seen, the experimental concentration-history profiles for the systems of solutes in this research follow the mathematically predicted curves throughout the initial stages of column operation, but begin to deviate after 0.6 - 0.8 influent concentration appears in the effluent. The experimental effluent concentration-history profile then exhibits better adsorption operation than that mathematically predicted. Although the critical region for design purposes lies within the initial portion of the breakthrough curve described by the mathematic model, it is of interest to discuss the deviations observed and to further investigate probable causes for these differences.

GENERAL CONSIDERATIONS

Klotz (60) presents a qualitative discussion on the types of effluent concentration-history profiles possible for single solute adsorption in columnar operation. Figure 6-1 is an illustration of three types of effluent concentration-history profiles. The curve labeled I in Figure 6-1 represents instantaneous adsorption on an infinitely fine-grained adsorbent. Adsorption represented by Curve I is visualized as being an instantaneous reaction wherein the sorbate

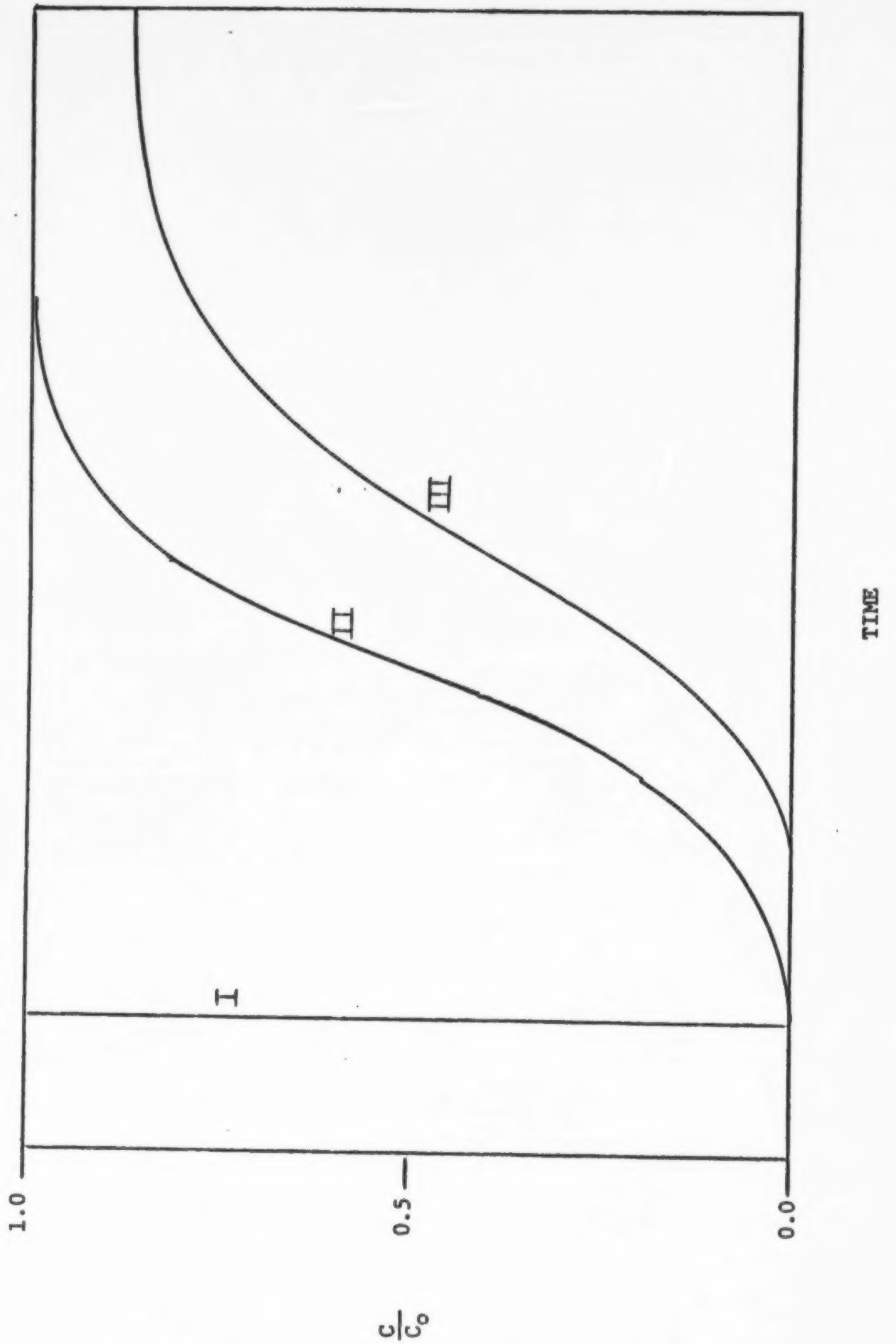

FIGURE 6-1. TYPES OF COLUMN EFFLUENT CONCENTRATION-HISTORY PROFILES

is completely removed from the solution fed to the column until that time when the adsorbent is completely saturated. At that time, the sorbate is no longer adsorbed and shows up immediately in the effluent in the same concentration as the feed concentration.

The curve represented by II in Figure 6-1 illustrates adsorption of a sorbate on finite-sized particles with a non-instantaneous reaction. The adsorption process must then be described by a rate controlling process. The resulting effluent concentration-history profile will be a symmetrical curve, as in Case II, only for certain simple rates of adsorption.

The curve represented by III in Figure 6-1 describes the case in which the adsorbent or its impregnant acts as a 'catalyst' for removal of the sorbate. Therefore the effluent concentration-history profile rises slowly, and if the 'catalyst' were to remain unpoisoned, the effluent concentration would never reach that of the influent. In reality, it would be expected that any catalytic effect would eventually be diminished, especially in cases involving a porous adsorbent. In such cases, the pore areas would eventually be filled with sorbate, and thus the immense surface area of the adsorbent originally available would be reduced to a small fraction equalling the outer surface area of a non-porous particle.

A complex mixture of sorbates classified as a single solute will exhibit a concentration-history profile composed of the sum of individual component breakthrough curves. The effluent concentration-history profiles of the individual components will differ from the profile generated by the same individual components in pure solution under otherwise identical operating conditions. This phenomenon has been demonstrated and discussed by Weber (114) and Weber and Morris (123). The competitive effects of the sorbates in a complex mixture upon the adsorptive capacity for any given component indicate a decreased capacity for the individual components, but a seemingly increased total capacity of adsorption. The adsorption properties responsible are postulated to be: 1) selectivity by adsorption sites for a given component; and, 2) variations in adsorption sites resulting in some sites being unavailable for a given component (91, 113).

Klotz (60) notes that an increase in capacity of an adsorbent is possible when a second slow reaction follows an initial fast reaction. This would result in a shifting of the concentration-time profile downward along the effluent/influent axis and extending it along the time axis. Such a situation can be visualized in a continuous flow column operation with the aid of Figure 6-2a and 6-2b. Figure 6-2a represents a hypothetical case of a column of adsorbent in expanded-bed operation which is exposed to a binary mixture of components A and B. Component A is more rapidly adsorbed than component B. During initial periods of operation, component A is totally removed by a fraction of the adsorbent bed. The adsorbent bed is exposed to component B throughout a greater depth. After a period of operation, component A has saturated a given depth of adsorbent bed, as in Figure 6-2b. That saturated fraction of the adsorbent bed still absorbs B, the slower reacting component, and the rest of the bed adsorbs both A and B.

FIGURE 6-2a. ILLUSTRATION OF CHROMATOGRAPHIC EFFECT

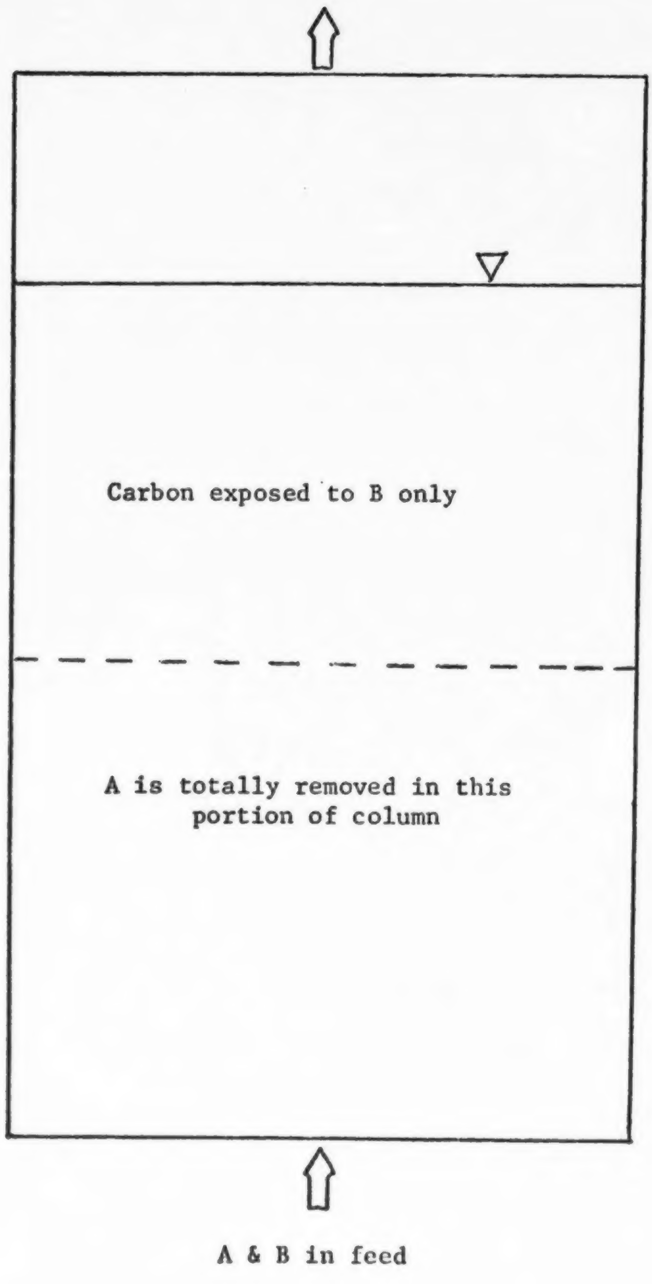
Carbon exposed to B only
A is totally removed in this portion of column
A & B in feed

FIGURE 6-2b. ILLUSTRATION OF CHROMATOGRAPHIC EFFECT

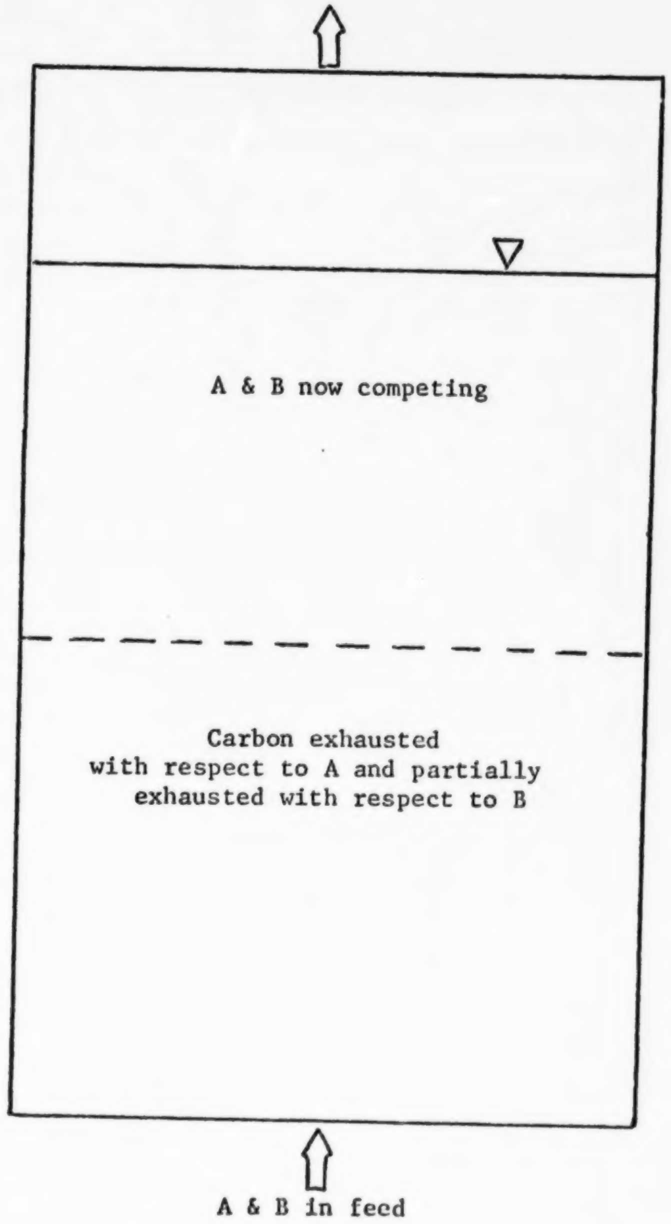
A & B now competing
Carbon exhausted
with respect to A and partially
exhausted with respect to B
A & B in feed

This hypothetical case illustrates the possibility of a chromatographic effect which results in varying mixture composition exposed to the adsorbent bed during different stages of operation. The 'averaging' procedure of identifying adsorption parameters for complex mixtures characterized as a single solute by a gross description parameter utilizing batch experiments does not duplicate chromatographic column conditions. All adsorbent particles in the batch experiments are exposed to the mixture components, as the mixture would be fed to the influent section of the flow-through adsorber. The adsorption behavior is dependent on the competitive adsorption processes of that mixture and the past history of the adsorbent. Any chromatographic effect produced in a flow through column operation will result in the adsorbent being exposed to many variations of component makeup of the feed mixture, and in the adsorbent being 'conditioned' for further adsorption in varying ways.

A further complication is that a clear statement of what is meant by capacity of an adsorbent is not as readily available in a flow through experiment as it is in the static case (60). In the latter situation, capacity refers to the amount adsorbed per unit of adsorbent after sufficient time has elapsed for equilibrium to have been attained. This definition may be inapplicable in cases involving complex mixtures, chromatographic separation effects, or 'catalytic' type effects.

EXPERIMENTAL INVESTIGATIONS

The concentration-time profiles of the complex mixtures resembled the non-symmetric case illustrated by Curve III in Figure 6-1. Based on the general considerations listed above, experiments were designed to determine the effects of the component sorbates and to provide possible explanation for the better adsorption characteristics observed with the experimentally generated effluent concentration-history profiles.

The experimental investigations undertaken consisted of developing the component sorbate behavior of complex mixtures in batch systems approximating column operation and in column operations simulating chromatographic separation effects. These experiments were carried out on two previously discussed binary mixtures, Mix 1 and Mix 2, and their respective components.

The batch experiments were designed to determine the behavior of the individual complex mixture components in pure solution, in the mixture, and in the presence of carbon previously equilibrated with the mixture concentration of the other component of the binary mixture. The procedure for the pure component and for the mixture followed that as given in Chapter 5 for similar experiments in rapidly-agitated mode. The additon of previously equilibrated carbon was achieved by performing a pure component experiment utilizing the second component, filtering out the carbon, and then introducing that carbon into the first pure component solution. The latter experiment then continued using the same procedure as for the pure component solution or the mixture.

The continuous flow column experiments were performed to generate the concentration-history profiles of the individual components of the mixture by analyzing the effluent concentration composition of the mixture. Pure solutions of the mixture component compounds in the same concentrations as in the mixtures were introduced to the adsorber beds to produce effluent concentration-history profiles for non-competitive adsorption of the compounds. After saturation of the adsorbent bed by one pure component, the adsorber was then exposed to the second component of the binary mixture, fed in the same concentration as in the mixture. The effluent concentration-history profile for this sequential loading was used in comparison to the profiles for the mixture solution and for the pure solution, and also to provide information by simulating chromatographic separation effects.

RESULTS OF BATCH EXPERIMENTS

The rapidly-agitated batch experiments provided concentration decay curves for the individual sorbates in the mixes studied. From these decay curves, analysis of the effects of sorbate interactions and of preconditioning of the adsorbate can be performed. The concentration-decay curves of individual components in pure solution, in the mixture, and in sequential loading cases were generated.

Phenol

The results of these investigations for phenol in Mix 1 and Mix 2 concentrations are shown in Figures 6-3 and 6-4, respectively. The results shown in these figures demonstrate a definite difference between the rate of decay of the pure component versus that of either the component behavior in the mixture or as the second compound added in the sequential loading experiment. The pure phenol was more rapidly removed from solution by the carbon than was the phenol in the presence of dodecyl sodium sulfate. The phenol solution subject to

FIGURE 6-3. COMPONENT RATE STUDIES FOR PHENOL: MIX 1

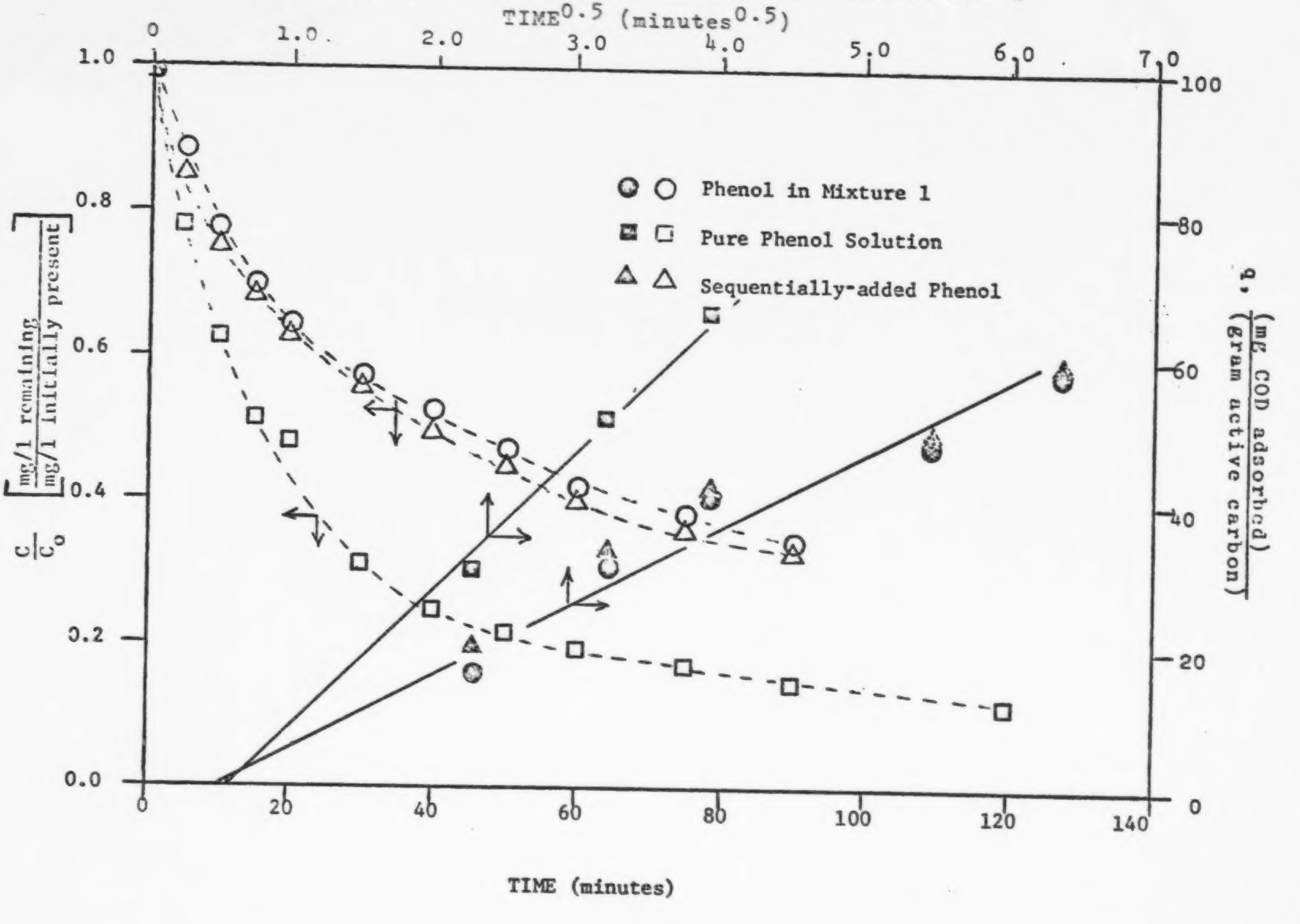

FIGURE 6-4. COMPONENT RATE STUDIES FOR PHENOL: MIX 2

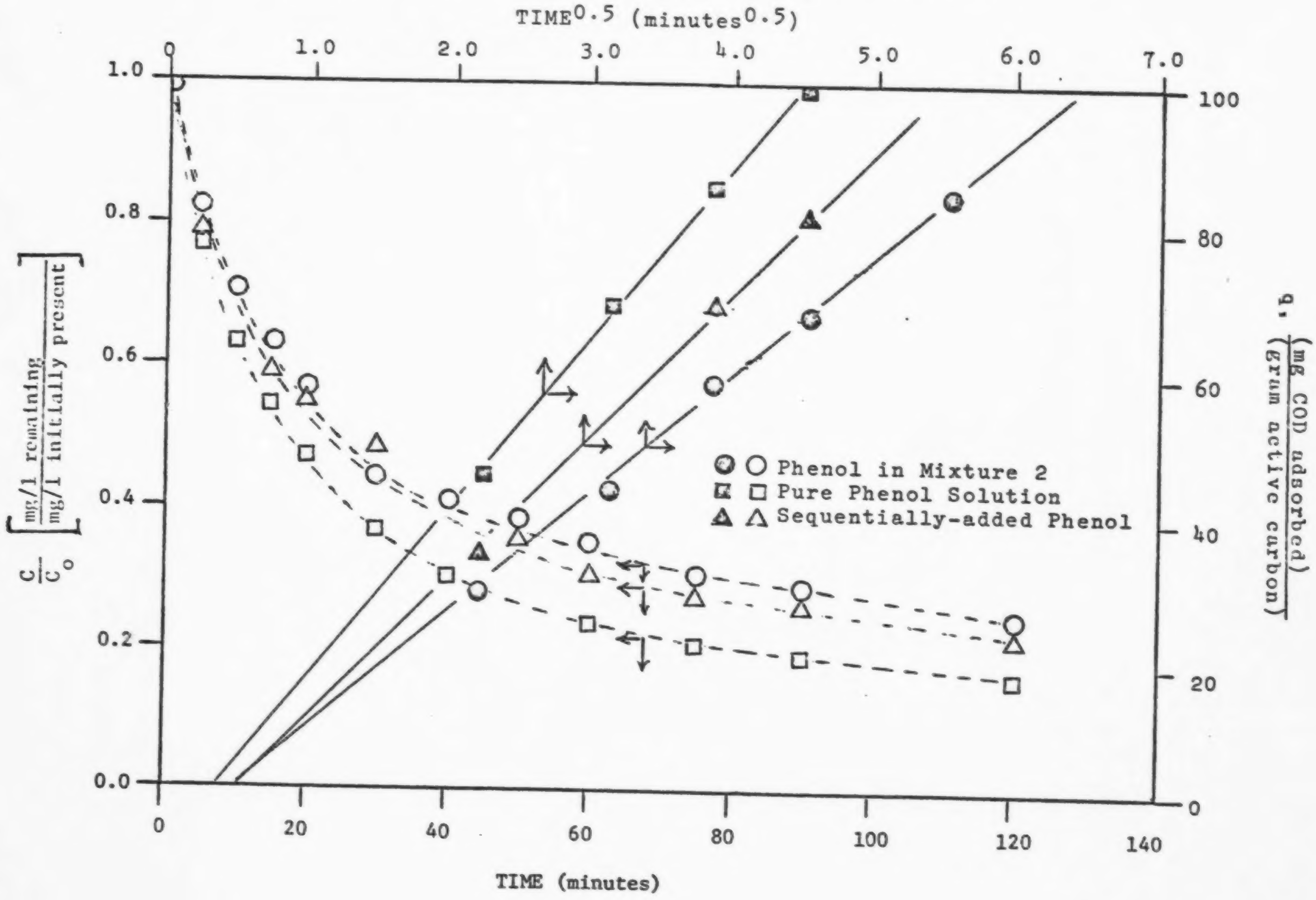

adsorption by carbon previously used to adsorb dodecyl sodium sulfate of the same concentration as in Mix 1 exhibited a decay curve just slightly more rapid than that for the phenol in the mixture. These results indicated that there was a definite interference for adsorption of phenol occurring in the mixture as opposed to the pure solution case. The sequential loading experimental results indicate that the adsorption interference is probably related to a competition by the sorbates for adsorption sites. Although the active carbon preconditioned by adsorption of dodecyl sodium sulfate was exposed to a pure solution of phenol sequentially added, the decay curve for phenol very closely followed that for removal of phenol in the case for the mixture. This indicates that the adsorbent is not as readily available to the added sorbate compound.

Figure 6-4 shows the concentration-decay of phenol in the concentrations for Mix 2. The same general decay pattern as that of the corresponding cases of Mix 1 was observed. The differences between the decay rates for Mix 2 were not as great as for Mix 1. This is probably due to the fact that there is less competition for adsorption between the phenol and the dodecyl sodium sulfate in Mix 2, because the phenol therein comprises a larger total of the mixture concentration than in Mix 1.

Dodecyl Sodium Sulfate

The concentration-decay curves for dodecyl sodium sulfate as generated in the rapidly-agitated batch experiments are shown in Figures 6-5 and 6-6 for Mix 1 and Mix 2 concentrations of dodecyl sodium sulfate, respectively. As in the decay curves for phenol

FIGURE 6-5. COMPONENT RATE STUDIES FOR DODECYL SODIUM SULFATE: MIX 1

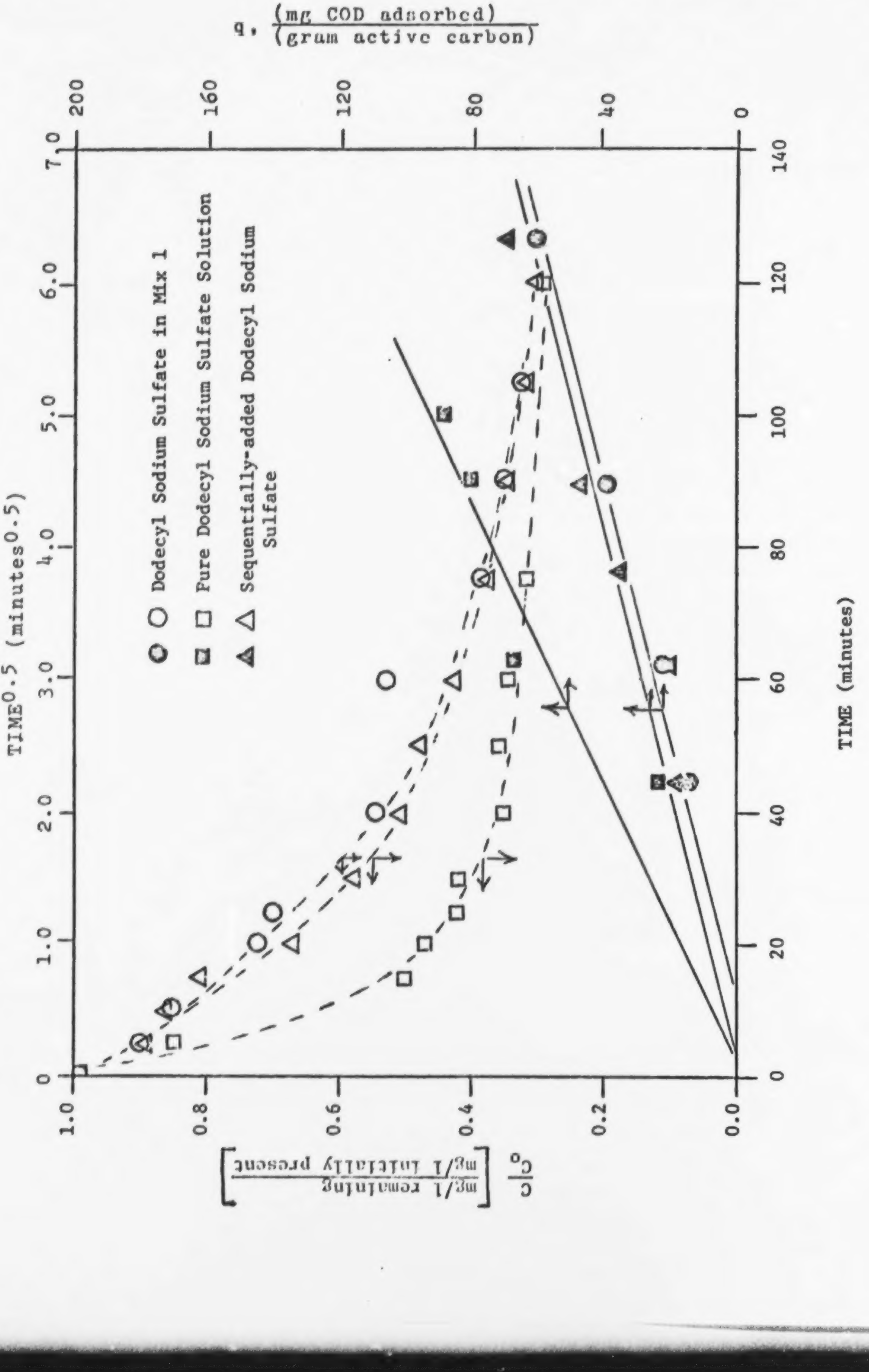

FIGURE 6-6. COMPONENT RATE STUDIES FOR DODECYL SODIUM SULFATE: MIX 2

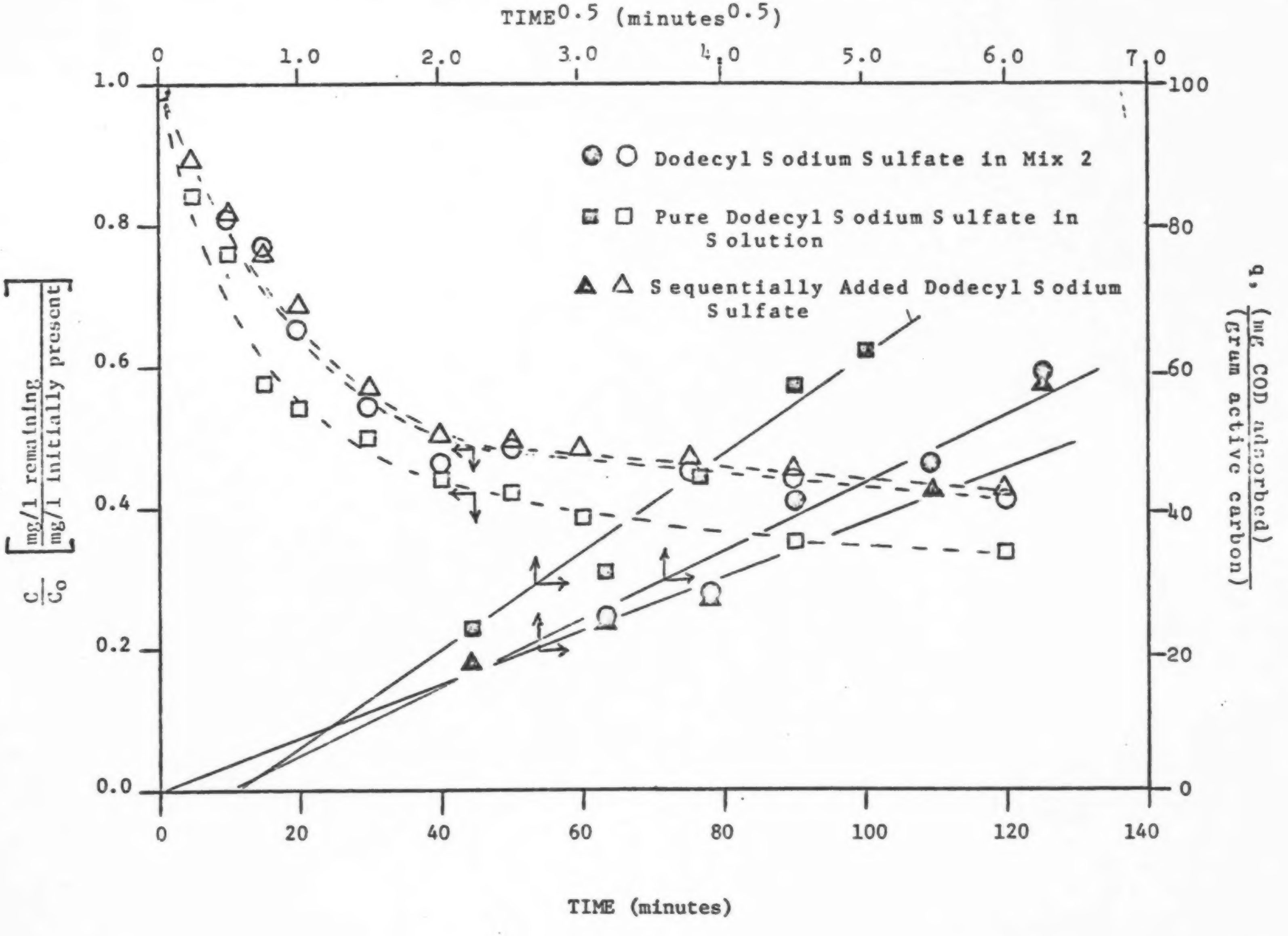

(Figures 6-3 and 6-4), the pure component solution of dodecyl sodium sulfate exhibited a more rapid decay than either that of that compound in the mixture or in the sequential loading experiment. This reinforces the argument for competitive interference effects for adsorption of a given compound in a complex mixture.

The adsorption of the dodecyl sodium sulfate in the sequential loading experiments resulted in decay curves closely resembling those for that compound in the mixture experiments. This suggests that the adsorbent had less availability to the added adsorbent. This same effect was noted in the phenol adsorption experiments.

The results of these batch experiments for competitive adsorption is in agreement with the earlier work of Weber and Morris (122) and Weber (113). The competitive effects of sorbates in complex mixtures result in different adsorption behavior of mixture components in comparison to pure component solutions.

CONCENTRATION-HISTORY PROFILES OF INDIVIDUAL COMPONENTS IN COMPETITIVE ADSORPTION

In order to investigate possible mechanisms leading to the discrepancies between the mathematic model prediction of the effluent concentration-history profile and the experimentally generated profile, individual component experiments were performed. The effluent concentration-history profiles illustrating the experimental versus mathematic model prediction for Mix 1 and for Mix 2 are shown in Figures 6-7 and 6-8, respectively. Experimental investigations were conducted to determine the adsorptive behavior of the individual components of these mixtures: 1) in pure component solution; 2) in the

FIGURE 6-8. EXPANDED-BED ADSORBER

EFFLUENT CONCENTRATION-HISTORY PROFILE: MIX 2

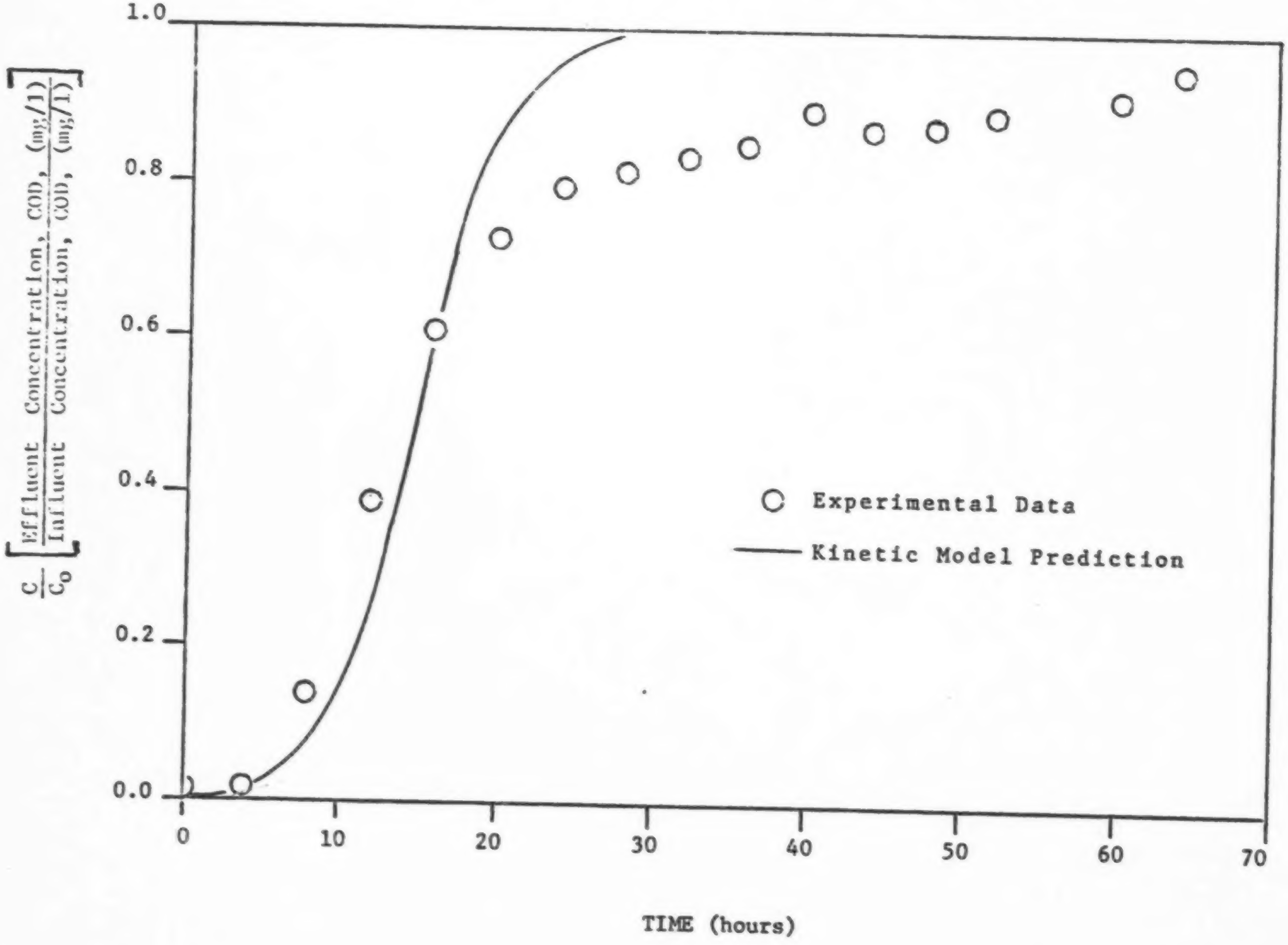

This page was missing from the report when received by NTIS. Repeated efforts to obtain a replacement page have been unsuccessful.

This report is being made available in its present form with the hope it will be of sufficient value to justify its announcement and distribution.

mixture; and 3) as the second compound in sequential loading.

PHENOL

Figure 6-9 shows the effluent concentration-time profiles for phenol in the concentration found in Mix 1 for the three cases of interest. Figure 6-10 represents the effluent concentration-history profiles for phenol in the concentration found in Mix 2. Because the isotherm parameters and mass-transfer parameters were readily available from previously performed experiments (Chapter 4) for the pure phenol solution case, the Keinath-Weber model was used to predict the effluent concentration-history profile for that case. The predicted profiles are indicated by the solid signoidal curve in Figures 6-9 and 6-10.

PHENOL: MIX 1

The comparison of the predicted profile with the pure component profile for phenol in Mix 1 concentration (135 mg/l COD) illustrates that the experimental profile is asymmetrical, with a flattening profile in the upper regions of the effluent concentration-history profile. This broadening shape for pure component column effluent concentration-history profiles can also be observed in the works of Weber and Morris (123) and others (1, 71).

The effluent concentration-history profile generated for phenol in the presence of dodecyl sodium sulfate, introduced as Mix 1 into the adsorption column, shows a more rapid appearance of phenol in greater quantities in the effluent than is observed for the pure solution case. The capacity for the phenol in the mixture solution decreased with the adsorption competition of dodecyl sodium sulfate.

FIGURE 6-9. COMPONENT EFFLUENT CONCENTRATION-HISTORY PROFILES IN EXPANDED BED OPERATION: PHENOL, MIX 1

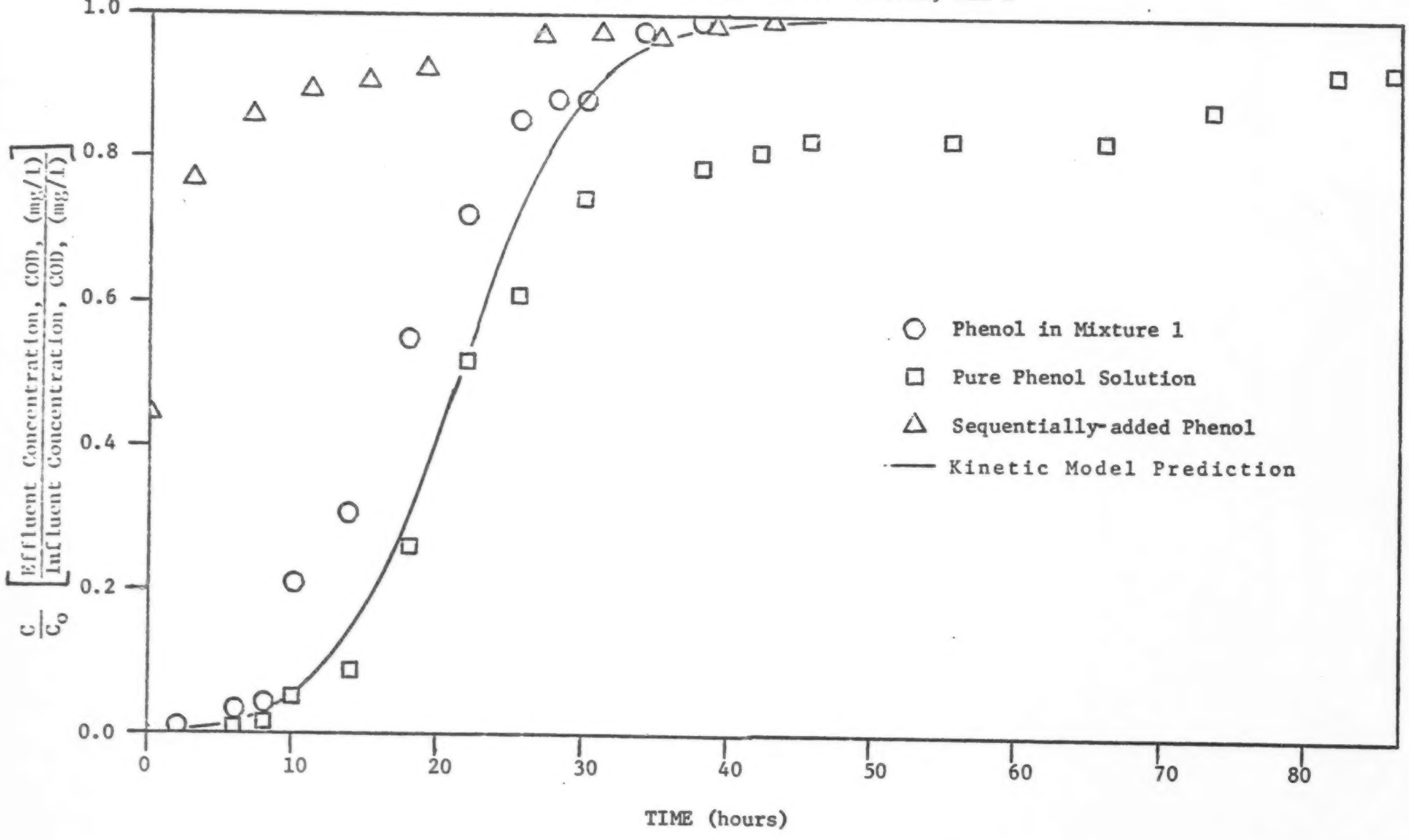

FIGURE 6-10. COMPONENT EFFLUENT CONCENTRATION-HISTORY PROFILES IN EXPANDED BED OPERATION: PHENOL, MIX 2

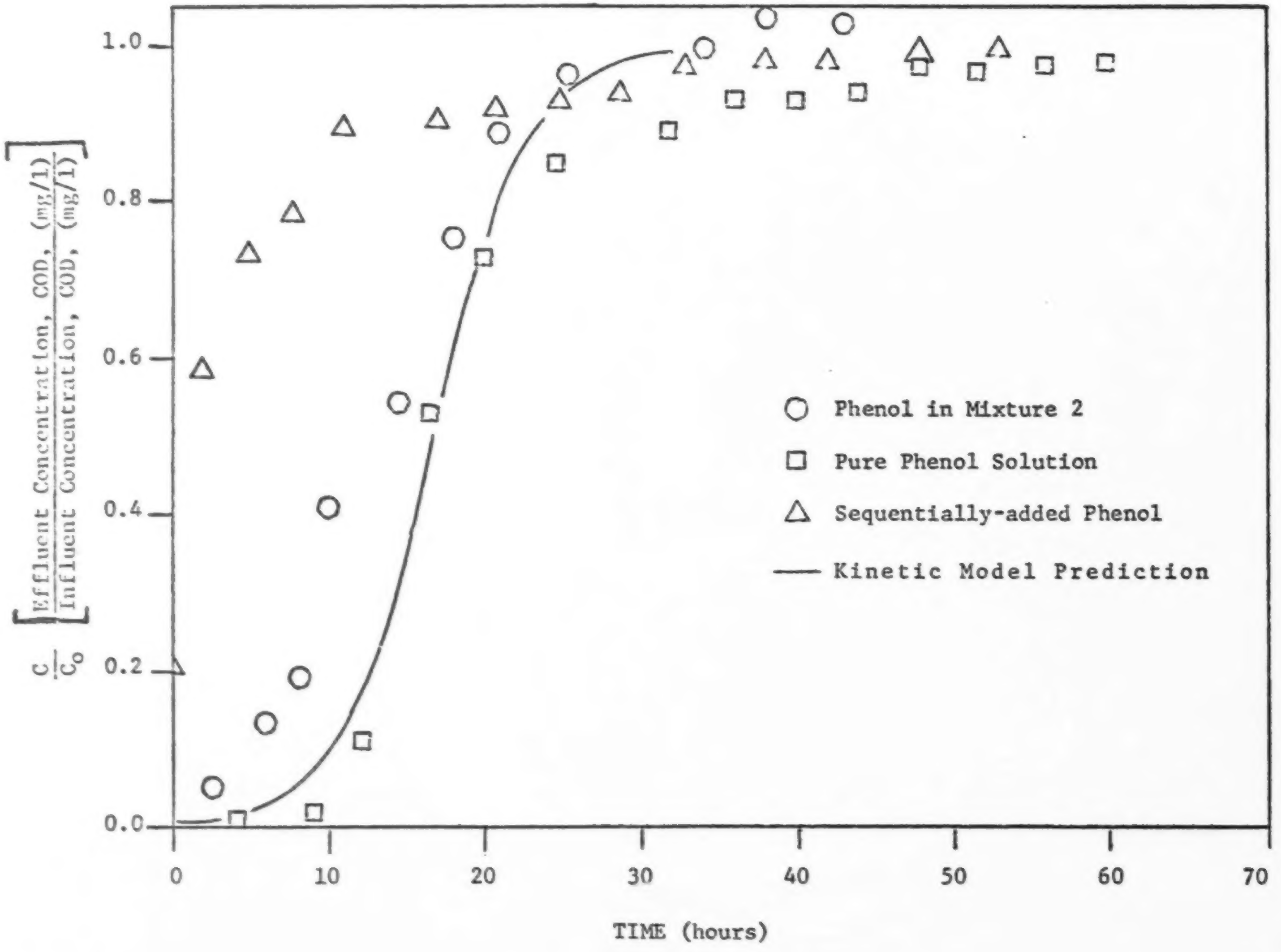

This effect is in agreement with earlier work on competitive adsorption (113, 123). The broadened effluent concentration-time profile of the pure component solution was not produced by the phenol in the mixture. The phenol effluent concentration-history profile assumed a more symmetrical shape when competing with the dodecyl sodium sulfate.

The effluent concentration-history profile resulting from the sequential loading of phenol into the adsorber bed previously saturated with dodecyl sodium sulfate of Mix 1 concentration resulted in a rapid saturation of the active carbon with phenol. The results of this experiment demonstrated that although the active carbon had no more capacity for the dodecyl sodium sulfate, there was still adsorption capacity for the phenol. This indicates that adsorption sites on the active carbon are not all available to the dodecyl sodium sulfate.

PHENOL: MIX 2

Figure 6-10 represents the experimentally generated and mathematically predicted effluent concentration-history profiles for phenol in Mix 2 concentrations. The mathematic prediction results in very good agreement with the pure component solution effluent-concentration-time profile experimentally obtained. The broadening effluent profile in the upper portion of the experimental curve is again observed for the pure phenol component solution.

The effluent concentration-history profile for phenol in the presence of the mixture concentration of dodecyl sodium sulfate indicates that competitive effects of the dodecyl sodium sulfate reduce the capacity for the phenol. However, in this case, the effluent/influent concentration ratio actually exceeds 1.0 for the phenol profile. Comparison of Figure 6-10 with Figure 6-8 indicates that the adsorber bed is not exhausted with respect to the total mixture concentration. These considerations point to displacement of previously adsorbed phenol by dodecyl sodium sulfate as an explanation for greater concentration of phenol in the effluent than in the influent.

The effluent concentration-history profile for phenol introduced to the adsorber previously saturated with dodecyl sodium sulfate in Mix 2 concentration resulted in rapid appearance of effluent concentrations approaching influent concentration values. Again, it appeared that the saturation capacity for dodecyl sodium sulfate did not preclude the adsorption of phenol.

DODECYL SODIUM SULFATE

The effluent concentration-history profiles for the dodecyl sodium sulfate component experimental investigations are shown in Figures 6-11 and 6-12 for Mix 1 and Mix 2 concentrations, respectively. The predicted profiles for the pure dodecyl sodium sulfate are illustrated by the solid sigmoid curves in these Figures.

DODECYL SODIUM SULFATE: Mix 1

The pure dodecyl sodium sulfate effluent concentration-history profile experimentally agreed with the mathematically predicted profile up to approximately 0.5 C_o. The experimental profile then began to flatten out and continued at a constant breakthrough value of approximately 0.8 C_o for twenty-five hours. Then the effluent

FIGURE 6-11. COMPONENT EFFLUENT CONCENTRATION-HISTORY PROFILES IN EXPANDED BED OPERATION: DODECYL SODIUM SULFATE: MIX 1

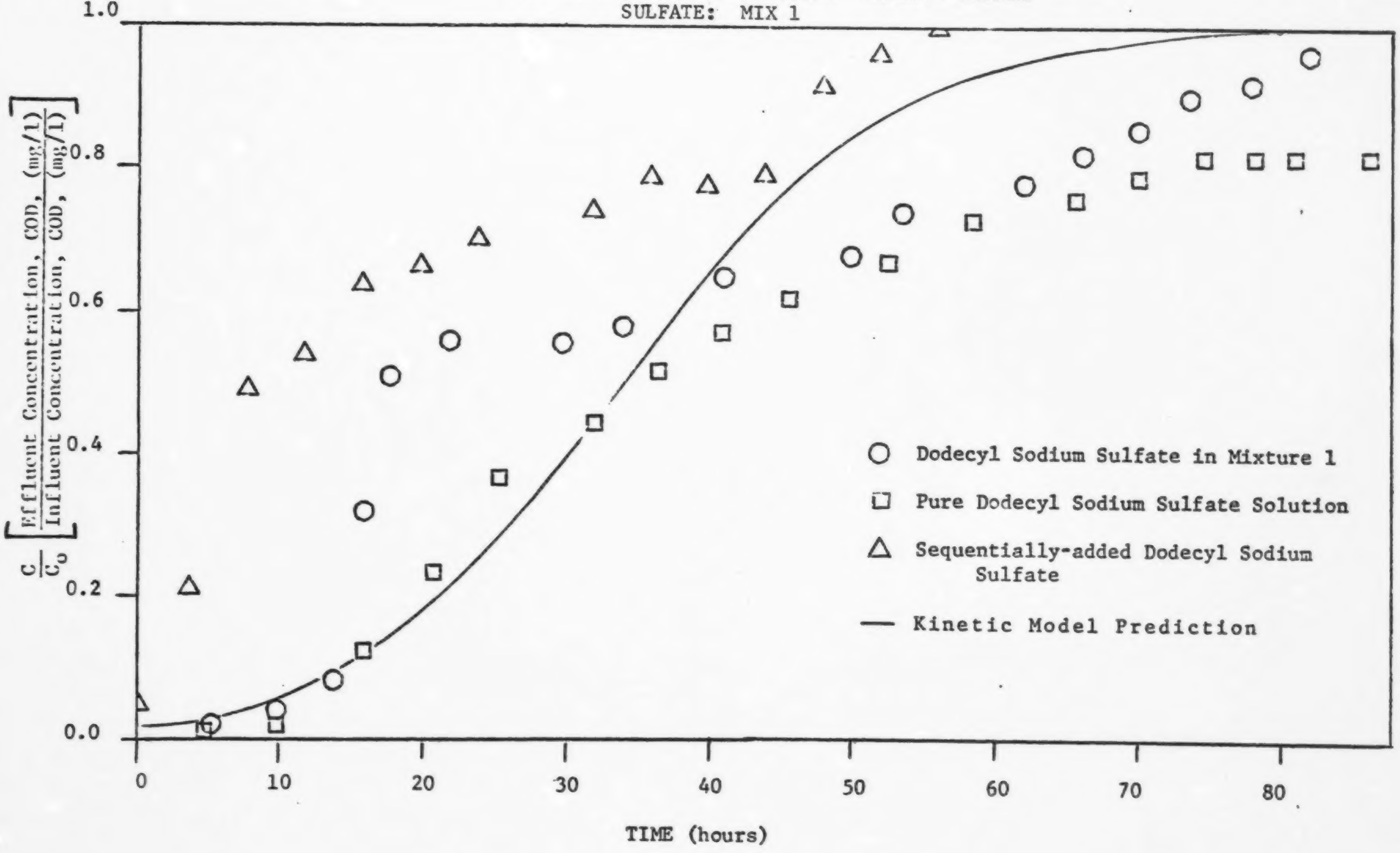

FIGURE 6-12. COMPONENT EFFLUENT CONCENTRATION-HISTORY PROFILES IN EXPANDED BED OPERATION: DODECYL SODIUM SULFATE: MIX 2

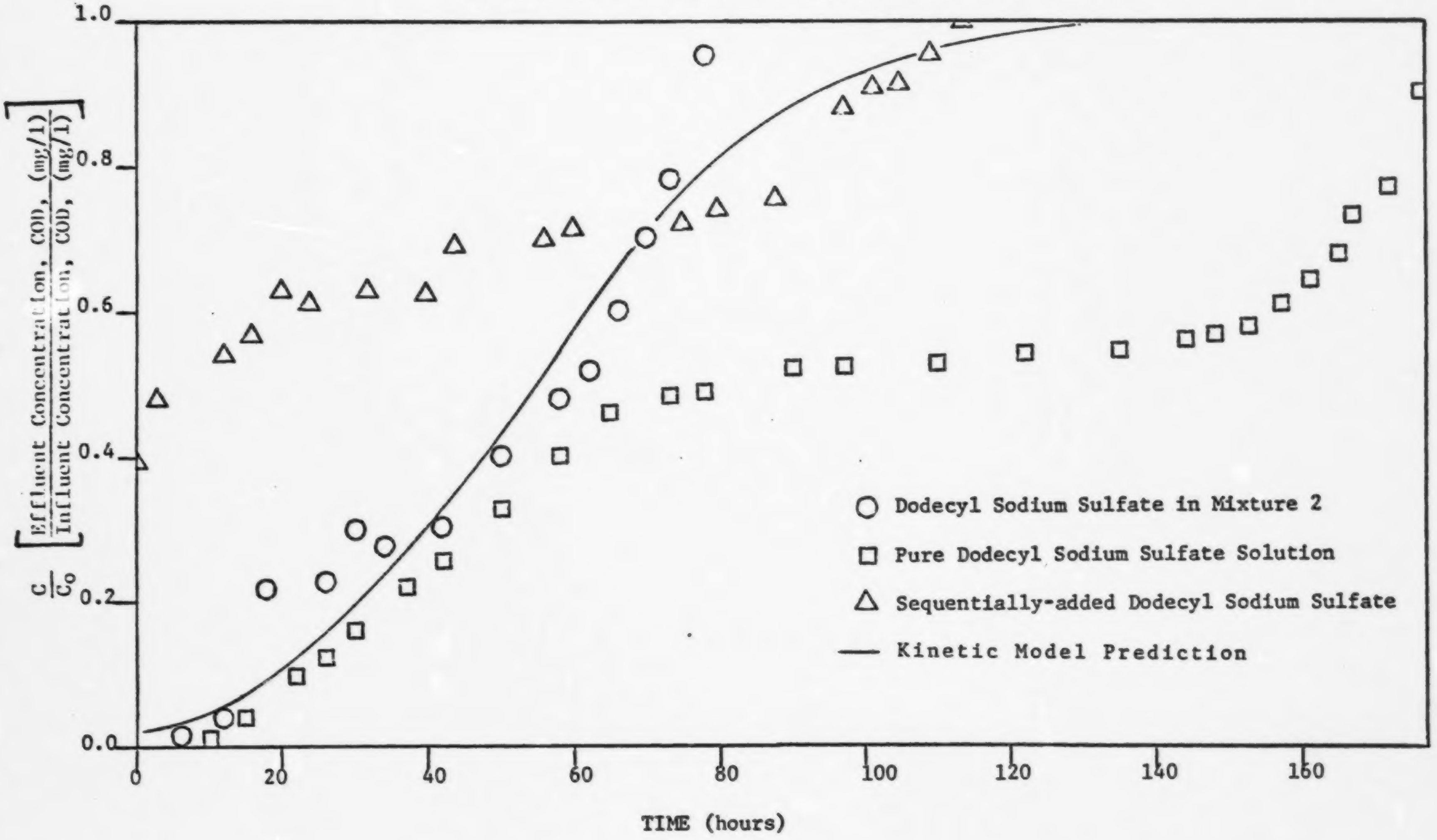

concentration rapidly increased to equal the influent concentration.

In the mixture with phenol competition for adsorption interacting with the dodecyl sodium sulfate adsorption processes, the profile for the dodecyl sodium sulfate showed slightly greater effluent concentrations than the pure solution case for the first fourteen hours of column operation. The effluent concentration rapidly increased within the next ten hours resulting in significant deviation from the pure dodecyl sodium sulfate component concentration-history profile for the dodecyl sodium sulfate in the mixture leveled off for the next ten hours at approximately 0.56 C_0, followed by a gradual increase in the effluent concentration until complete saturation of the adsorber bed was attained.

The sequential loading of dodecyl sodium sulfate following saturation of the adsorber by pure phenol solution in the concentration for Mix 1 yielded an effluent concentration-history profile similar to the sequential-loading experiments for phenol. The dodecyl sodium sulfate in this case exhibited less initial breakthrough and a more gradual rise in effluent concentration than did the similar case results for phenol. The sequentially loaded dodecyl sodium sulfate indicated a marked increase in the effluent concentration when compared to the profiles for the same influent concentrations in the mixture and in the pure solution experiments. There is, therefore, an indication that although the adsorber capacity for phenol was attained, adsorption of dodecyl sodium sulfate was still possible using that pre-conditioned active carbon.

DODECYL SODIUM SULFATE: MIX 2

The results for the lower concentration dodecyl sodium sulfate component investigations (Mix 2) were observed to be similar to those of the dodecyl sodium sulfate concentrations of Mix 1. The mathematically predicted profile was slightly higher than the experimentally generated profile throughout the initial range of development (0.4 - 0.5 C_o). The generated profile then began to flatten out and the effluent concentration increased only slightly from 0.52 to 0.56 C_o for the next sixty hours of column operation. The effluent profile then showed increasingly rapid additional sorbate in the effluent, with complete saturation being reached within an additional twenty-five hours.

The dodecyl sodium sulfate profile observed in the presence of phenol exhibited a more rapid saturation than the pure solution. The same general shape as in the pure solution case was observed, with an initial period of high percentage removal, a period of approximately constant percentage removal, and then rapid saturation of the adsorber bed by the dodecyl sodium sulfate. These profile regions for the mixture case were greatly condensed in comparison to the pure solution experimental results.

The sequentially-added dodecyl sodium sulfate resulted in an initial breakthrough of approximately 0.39 C_o appearing in the effluent. The effluent concentration gradually increased, exhibiting the same general pattern as in the previously discussed cases of pure and mixture component experiments. The adsorption of dodecyl sodium sulfate indicated that the preconditioned adsorber bed still had capacity for the added dodecyl sodium sulfate.

A comparison of the sequentially loaded effluent concentration-history profile with that of the mixture dodecyl sodium sulfate component indicates that saturation in the latter case was accomplished earlier in the column operation period. However, it must be noted that the sequentially loaded dodecyl sodium sulfate was added as a pure solution, and analyses of the effluent during the experimental period demonstrated that elution (or desorption) of phenol occurred. Therefore, adsorption sites previously occupied by phenol and also favorable to adsorption of dodecyl sodium sulfate may have been made available to the latter compound, resulting in the extended breakthrough curve.

Another possibility for the extended effluent concentration-history profile may have been due to displacement of the adsorbed phenol by the dodecyl sodium sulfate. Displacement phenomena have been observed in ion exchange (67, 74) due to greater affinity of the exchange sites for a given ion in competitive systems. An ion of lesser affinity previously sorbed is displaced by an ion of greater affinity. There is some evidence supporting displacement in the present systems (Figure 6-10, mixture case), but it is too meager to present a definitive statement of its existence. The sequential experiments do not provide displacement information because elution of phenol was found to occur without simultaneous dodecyl sodium sulfate adsorption, as will be illustrated in the next section.

ELUTION OF COMPOUNDS

The isotherm developments for the individual compounds indicated that the adsorption phenomena were reversible reactions. Therefore, it would be expected that a saturated adsorber bed would release an adsorbed compound when fed a solution not containing any of that compound. The assumption of reversibility was tested by analyzing the component sequential loading experimental effluent for presence of previously adsorbed compounds and by feeding sorbate free water to the saturated adsorber beds at the completion of the sequential loading experiments.

The results for the phenol elution experiments are shown in Figure 6-13 and for the dodecyl sodium sulfate experiments in Figure 6-14. The time of the first sample was taken as that time calculated for one bed volume to pass through the column after the change in feed solution conditions. The results show an initially high ratio of effluent concentration to the previously-fed influent concentration which then rapidly decreased as component-free solution was introduced to the column system.

The results of the elution experiments showed that a greater amount of adsorbed compound was removed in the sequentially loaded experiments for the cases in which that compound was introduced to the column first. To suggest displacement of the initially adsorbed compound by the following compound as the reason for this is premature because the solid-phase adsorbed concentration for the case of the compound initially fed was always higher than when the compound was

FIGURE 6-13. DESORPTION OF PHENOL

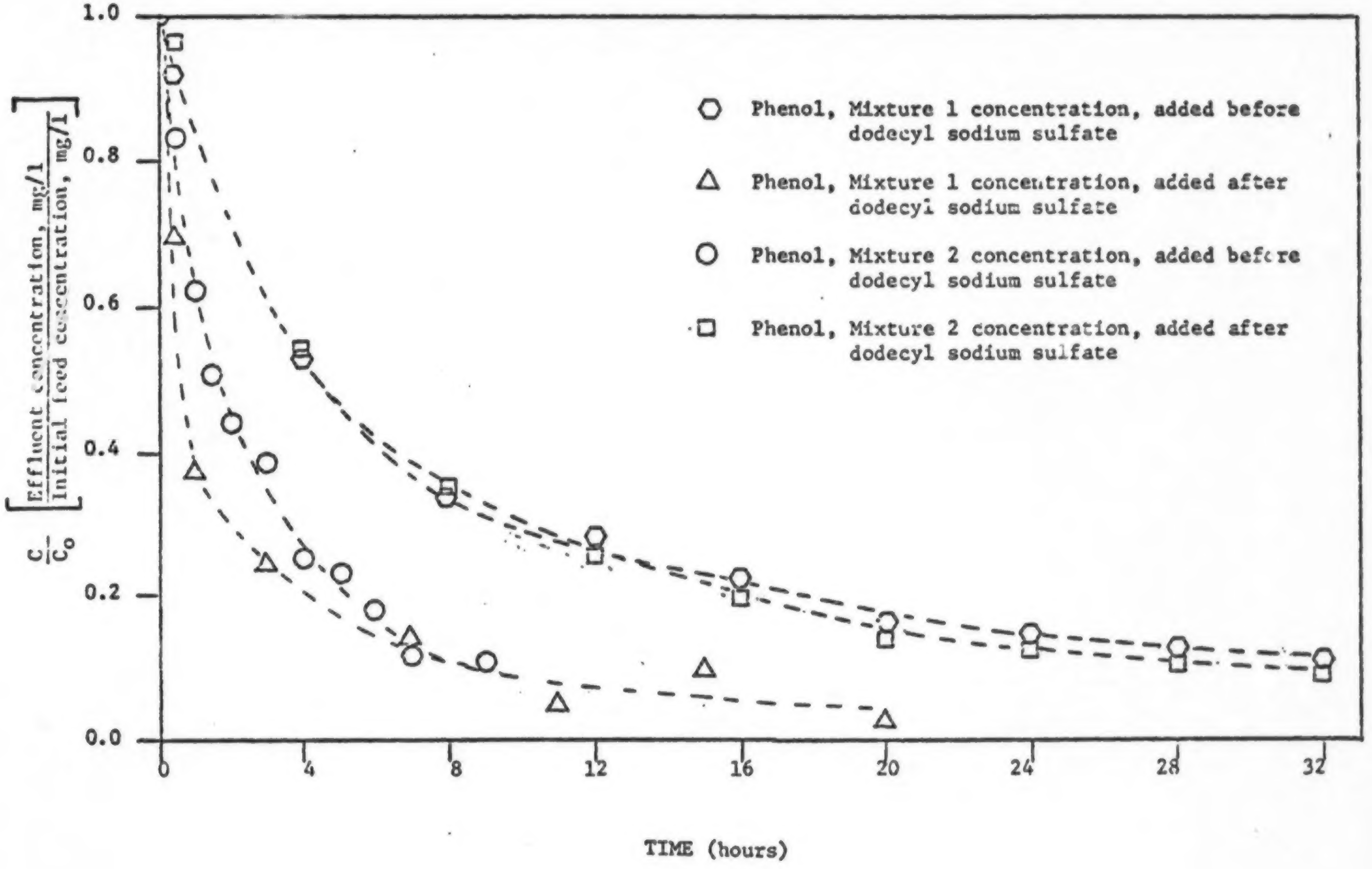

FIGURE 6-13. DESORPTION OF PHENOL

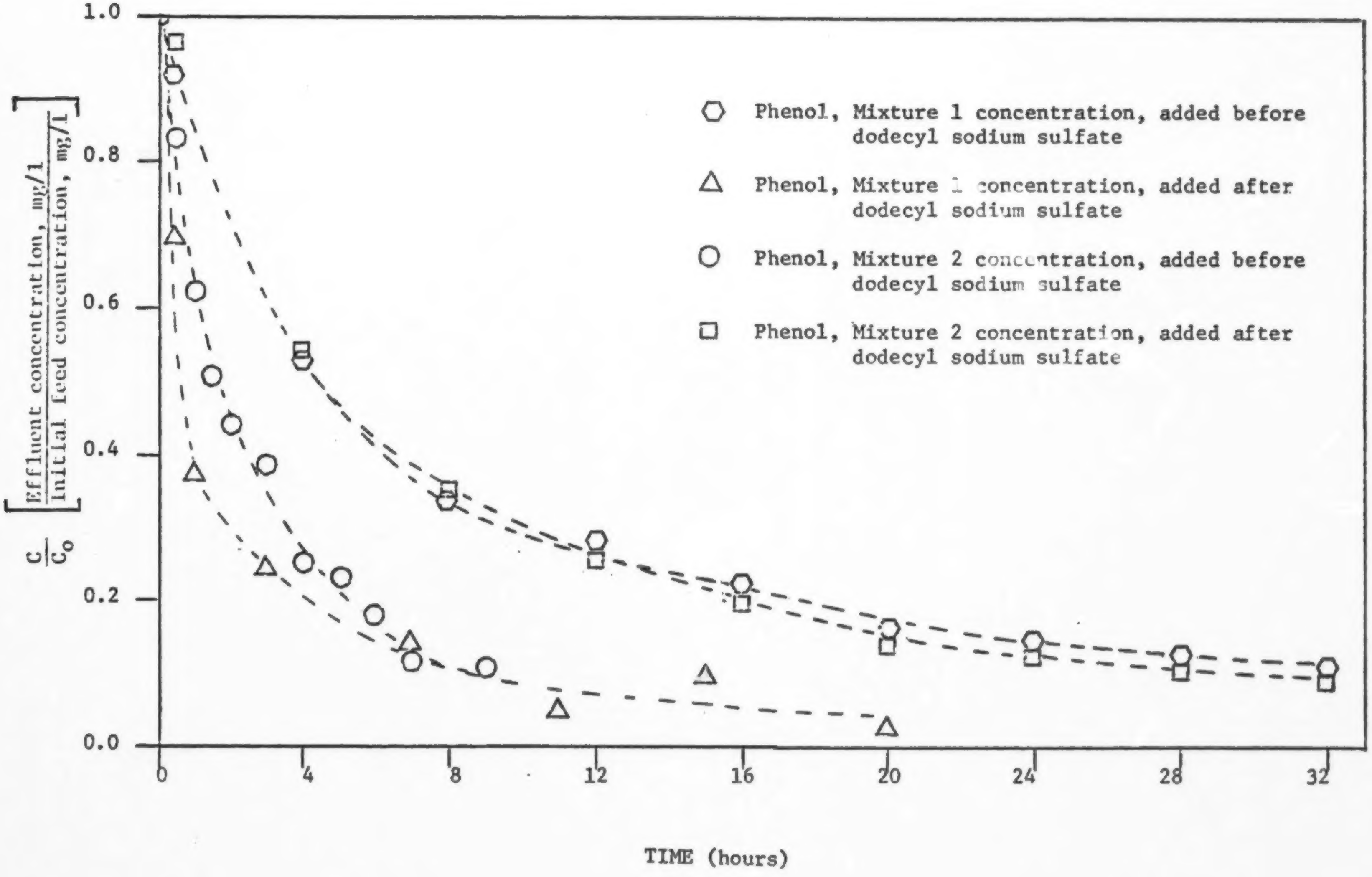

introduced to the preconditioned active carbon. Further comparative studies are necessary to define displacement hypotheses.

Examination of Figure 6-13 illustrates that the adsorbed material is held by the active carbon and does not readily desorb. This hysterisis effect has been noted by other investigators (92) and indicates that the extent of reversibility is limited.

DISCUSSION OF COMPONENT ANALYSES RESULTS

Mass-Transport Considerations

The general qualitative discussion after Klotz (60), as noted earlier, states that a symmetric effluent concentration-history profile obtains for cases in which a simple rate law governs the adsorption process. The linear driving-force concepts discussed in Chapter 2 result in a rate law yielding a mathematically predicted symmetrical profile. This mathematic prediction method was used in this research to determine its applicability to complex mixtures classified as a single sorbate. The demonstrated inability of the mathematic model to adequately describe the upper regions ($> 0.5\ C_o$) of the breakthrough curves after good correlation for the initial periods of adsorber column operation demonstrated a fundamental deficiency in the mathematic model.

The component analyses experiments for the pure solutions provided further evidence that the observed effect of flattening in the upper regions of the effluent concentration-history profiles was not due solely to the fact that a mixture of compounds was being analyzed as a single component. The possibility that some compounds in the multicomponent mixtures were being almost entirely removed while others had completely satisfied their respective adsorption capacities in the adsorber beds could also produce this effect. The pure compounds generated experimental asymmetric effluent concentration-history profiles similar to those of the mixtures. Therefore, the problem does not lie in the experimental system but in the mathematic model.

The mathematic model limitations may be due to several factors. The most obvious problem is the use of the simplified linear-driving force relationships for description of diffusional mass-transfer rate processes related to second-order kinetics. As shown by Helfferich (37), more 'rigorous' treatment of sorption rate processes demonstrates generally that no 'order' can be given for sorption rate processes. The momentary rate cannot generally be related to average concentrations within the particle, but depends upon the shape of the non-steady concentration profiles within the particles. Thus, the range of validity of any mathematic model will depend on the extent to which the averaging technique approximates the actual situation.

The concept of constant and additive diffusion resistances is also questionable. The diffusion resistances may be a function of concentration. The approach in which diffusion rate laws or close approximations of diffusion rate laws are used has more appeal than the use of the simplifying linear-driving force or kinetic reaction-rate theories (37). However, in all such approaches (e.g. 105, 111), the assumption of a constant effective diffusion coefficient has been used, making the superiority of such diffusion rate law treatment over the simplified concepts questionable (37).

The dependence of the diffusion coefficients on the concentration of the external solution exhibits interesting effects (37). Since intraparticle diffusion must take place in the pore fluid, this fluid is the medium of interest. In ion exchange, when the solution concentration is increased, the free water content of the ion-exchange resin decreases, and a corresponding decrease in the diffusion coefficient would be expected. However, the diffusion coefficient of counter-ions increases. This phenomena is linked to greater mobility of the counter-ions in the sorbed phase.

Another possible explanation can be derived from the work of Deryagin (18) and others (8, 64). In capillary tubes, water has been observed to take on a more orderly arrangement, and to exhibit different chemical and physical properties than the bulk solution water. The presence of this 'polywater' (64) in porous media could greatly alter intraparticle diffusional characteristics. The concentrations of interest within the pores may then be of larger values than the corresponding bulk-solution concentrations. The characterization of such a phenomena within the framework of a mathematic model for prediction of adsorber performance would probably be best accomplished by means of a varying diffusion coefficient.

SECONDARY ADSORPTION PHENOMENA

The mathematic model utilized in this research was based on the Langmuir adsorption isotherm development. Two basic assumptions inherent in the Langmuir formulation are: 1) monolayer adsorption; and 2) uniform energies of adsorption on the surface. The Langmuir expression is often utilized to approximate multilayer adsorption as occurring in a uniform manner. However, the original surface characteristics favoring adsorption will be masked as surface coverage is completed. Therefore a new adsorption mechanism must be used to describe any additional adsorption. Furthermore, the equilibrium concentration used in the Langmuir formulation is taken to be the external bulk concentration, but since the majority of the adsorption surfaces are internally located within the adsorbent particle, the fluid concentration of interest must be that of the pore-fluid. If the equilibrium concentration within the pore-fluid is significantly different from the bulk solution equilibrium concentration, then the pore-fluid concentration should be the one used in equilibrium analyses. Of course, this intraparticle fluid concentration is not readily defined.

The assumption of uniform adsorption energies is only an approximation. Investigations (91) on the surface characteristics of carbon indicate that various active groups are present. Experimental results for the component analyses presented earlier in this section allude to the presence of adsorption sites not available to all compounds, thus indicating non-uniform adsorption surface energies. Even with the obvious conflict with actual adsorption conditions, the Langmuir adsorption isotherm development can be used to represent practical ultimate capacities for adsorption and a mathematic representation of observed equilibrium relationships (115).

The adsorption behavior in the column studies for removal of dodecyl sodium sulfate indicated the presence of another type of secondary adsorption behavior which is not accounted for in adsorption equilibria relationships. This represents the formation of micelles of the surfactant with the adsorbed solid phase. Micelles may be formed in solution when the critical micelle concentration (cmc) is reached (2). The micelles are aggregations of long chain electrolytes into fairly large units. The formation of micelles can be visualized in adsorption processes due to the effects of removing sorbates from a large volume of solution and concentrating them at the solid-liquid interface. The cmc can be approached and micelle formation can then occur. This formation of micelles would lead to much greater 'adsorption capacities' than otherwise would be expected. Sufficient buildup of sorbate material in the pores could actually block the pores, accounting for the sudden change in removal properties and rapid increase in effluent concentration as illustrated in Figures 6-11 and 6-12.

REFERENCES

1. Abrams, I. M., and Lewon, S. M., "Removal of ABS From Water by Chloride Cycle Anion Exchange", *Jour. AWWA* *54*, 537 (1962).

2. Adamson, A. W., *Physical Chemistry of Surfaces*, p. 568, Interscience Publishers, New York (1967).

3. Acrivos, A., "On the Combined Effect of Longitudinal Diffusion and External Mass Transfer Resistance in Fixed Bed Operations", *Chem. Eng. Sci*. *13*, 1 (1960).

4. American Public Health Association, *Standard Methods for the Examination of Water and Wastewater*, Twelfth Edition, American Public Health Association, Inc., New York (1967).

5. Amundson, N. R., "A Note on the Mathematics of Adsorption in Beds", *J. Phys. and Colloid Chem*. *48*, 1153 (1952).

6. Amundson, N. R., "Solid-Fluid Interactions in Fixed and Moving Beds-Fixed Beds with Large Particles", *Ind. Eng. Chem*. *48*, 35 (1956).

7. Aris, R., And Amundson, N. R., "Some Remarks on Longitudinal Mixing or Diffusion in Fixed Beds", *AIChE J*., *3*, 280 (1957).

8. Bellamy, L. J., Osborn, A. R., Lippincott, E. R., and Bandy, A. R., "Studies of the Molecular Structure and Spectra of Anomalous Water, " *Chem. Ind.* *21*, 686 (1969).

9. Bishop, D. F., O'Farrell, T. P., and Stamberg, J. B., "Physical-Chemical Treatment of Wastewater", *J. Water Poll. Control Fed*. *44*, 361 (1972).

10. Bird, R. B., Stewart, W. E., and Lightfoot, E. N., *Transport Phenomena*, John Wiley and Sons, Inc., New York (1960).

11. Bohart, G. S., and Adams, E. Q., "Behavior of Charcoal With Respect to Chlorine", *J. Chem. Soc*. *42*, 523 (1920).

12. Bowen, D. H. M., "Effluents Are Tasting Better and Better", Editorial, *Environmental Science and Technology* *5*, 97 (1971).

13. Boyd, G. E., Myers, L. S. Jr., and Adamson, A. W., "The Exchange Adsorption of Ions From Aqueous Solutions by Organic Zeolites", *J. Am. Chem. Soc.* *69*, 2836, 2849 (1947).

14. Chilton, T. H., and Colburn, A. R., "Distillation and Absorption in Packed Beds", Ind. Eng. Chem. 27, 255 (1935).

15. Cohen, J. M., "Physical and Chemical Methods", Literature Review, J. Water Poll. Control Fed. 43, 1092 (1971).

16. Chu, J. C., Kalil, J., and Wetteroth, W. A., "Mass Transfer in a Fluidized Bed:, Chem. Eng. Progr. 49, 141 (1953).

17. Dedrick, R. L., and Beckman, R. B., "Kinetics of Adsorption by Activated Carbon from Dilute Aqueous Solution", Chem. Eng. Progr., Symp. Ser. 74, 63, 68 (1967).

18. Deryagin, B. V., and Churaev, N. V.,"Do We Know Water?", Priroda 4, 16 (1968).

19. De Vault, D. J., "The Theory of Chromatography", J. Am. Chem. Soc. 65, 532 (1943).

20. Di Giano, F. M., and Weber, W. J., Jr., "Mathematic Modeling of Sorption Kinetics in Finite and Infinite Batch Systems", Tech. Publication, Research Project WP-00706, Fed. Water Poll. Control Admin., U. S. Dept. of Interior (April 1969).

21. Ditkin, V. A., and Prudnikov, A. P., Operation Calculus in Two Variables and Its Application, Volume 24, International Series of Monographs on Pure and Applied Mathematics, I. N. Sneddon, S. Ulan, and M. Stark, editors, Pergammon Press Inc., New York (1962).

22. Ditkin, V. A., and Prudnikov, A. P., Integral Transforms and Operational Calculus, translated by D. E. Brown, Pergammon Press Ltd., London (1965).

23. Edeskuty, F. J., and Amundson, N. R., "Mathematics of Adsorption. IV. Effect of Intraparticle Diffusion in Agitated Static Systems", J. Phys. Chem. 56, 148 (1952).

24. Frantz, J. F., "Design for Fluidization", Chem. Eng., Sept. 17, 1962, 161 (1962).

25. Frantz, J. F., "Minimum Fluidization Velocities and Pressure Drop in Fluidized Beds", Chem. Eng. Progr., Symp. Ser. 62, 21 (1966).

26. Furnas, C. C., "Heat Transfer From a Gas Stream to a Bed of Broken Solids", Trans. Am. Inst. Chem. Engrs. 24, 142 (1930).

27. Getman, F. H., and Daniels, F., Outlines of Theoretical Chemistry, Sixth Edition, John Wiley and Sons, Inc., New York (1937).

28. Glueckauf, E., "Theory of Chromatography", J. Chem. Soc., 1312 (1947).

29. Glueckauf, E., and Coates, J. I., "Theory of Chromatography", J. Chem. Soc., 1315 (1947).

30. Goldstein, S., "The Mathematics of Exchange Processes in Fixed Columns", Proc. Roy. Soc. London , A219, 151 (1953).

31. Gray, A., Mathews, G. B., and Mac Robert, T. M., A Treatise on Bessel Functions, Mac Millan and Co., Ltd., London (1931).

32. Griffin, R. P., and Dranoff, J. S., "The Rate of Glycerol Adsorption by Ion Exchange Resins", AIChE J. 9, 283 (1963).

33. Hager, D. G., and Reilly, P. B., "Clarification-Adsorption in the Treatment of Municipal and Industrial Wastewaters", J. Water Poll. Control Fed. 42, 794 (1970).

34. Hall, K. R., Eagleton, L. C., Acrivos, A., and Vermeulen, T., "Pore- and Solid-Diffusion Kinetics in Fixed-Bed Adsorption Under Constant-Pattern Conditions", Ind. Eng. Chem., Fundamentals 5, 212 (1966).

35. Hanratty, T. J., and Bandukwala, A., "Fluidization and Sedimentation of Spherical Particles", AIChE J. 3,293 (1957).

36. Heaton, R., "It's Reuse in the Rockies", Water and Wastes Engr. 9, 32 (1972).

37. Helfferich, F., Ion Exchange, McGraw-Hill Book Co., Inc., New York (1962).

38. Hiester, N. K., Radding, S. B., Nelson, R. L., Jr. and Vermeulen, T., "Interpretation and Correlation of Ion Exchange Column Performance Under Nonlinear Equilibria", AIChE J. 2, 405 (1956).

39. Hiester, N. K., and Vermeulen, T., "Saturation Performance of Ion Exchange and Adsorption Columns", Chem. Eng. Prog. 48, 505 (1952).

40. Hodgman, C. D., C.R.C. Standard Mathematical Tables, Twelfth Edition, Chemical-Rubber Co., Cleveland, Ohio (1963).

41. Hodgman, C. D., Weast, R. C., and Selby, S. M., Handbook of Chemistry and Physics, Forty-Third Edition, The Chemical Rubber Publishing Co., Cleveland, Ohio (1961).

42. Hollis, M. D., "Water Resources and Needs for Pollution Control", J. Water Poll. Control Fed. 32, 3, 225 (March 1960).

43. Hopkins, C. B., Weber, W. J., Jr., and Bloom, R., Jr. "Comparison of Expanded-Bed and Packed-Bed Adsorption Systems", Robert A. Taft Water Research Center, Rep. 1968 TWRC-2.

44. Hougen, O. A., and Marshall, W. R., Jr., "Adsorption from a Fluid Stream Flowing Through a Stationary Granular Bed", Chem. Eng. Prog. 43, 197 (1947).

45. Hougen, O. A., and Watson, K. M., Chemical Process Principles - Part Three Kinetics and Catalysis, pp. 982-987; Wiley, New York (1964).

46. Hunter J. V., and Heukelekian, H., "The Composition of Domestic Sewage Fractions", J. Water Poll. Control Fed. 37, 1142 (1965).

47. Jahnke, E., Emde, F., and Losch, F., Tables of Higher Functions, Sixth Edition, McGraw-Hill Book Co., Inc., New York (1960).

48. Johnson, R. L., Lowes, F. J., Jr., Smith, R. M., and Powers, T. J., "Evaluation of the Use of Activated Carbons and Chemical Regenerants in Treatment of Waste Water", Public Health Service Publication No. 999-WP-13. Number 11 in the series of Advanced Waste Treatment Research Publications.

49. Joyce, R. S., and Sukenik, V. A., "Feasibility of Granular, Activated-Carbon Adsorption for Waste-Water Renovation", Public Health Service Publication No. 999-WP-12. Number 10 in the series of Advanced Waste Treatment Research Publications.

50. Joyce, R. S., and Sukenik, V. A., "Feasibility of Granular, Activated-Carbon Adsorption for Waste-Water Renovation. 2.", Public Health Service Publication No. 999-WP-28. Number 15 in the series of Advanced Waste Treatment Research Publications.

51. Joyce, R. S., Allen, J. B., and Sukenik, V. A., "Treatment of Municipal Wastewater by Packed Activated Carbon Beds", J. Water Poll. Control Fed. 38, 813 (1966).

52. Juda, W., and Carron, M. J., "Equilibrium and Velocity of the Sodium-Hydrogen Exchange on Carbonaceous Exchangers in Contact With Chloride Solutions", J. Am. Chem. Soc. 70, 3295 (1948).

53. Kaplan, W., Advanced Calculus , Addison-Wesley Pub. Co., Inc. Reading, Mass., p. 86 (1952).

54. Kasten, P. R., and Amundson, N. R., "Analytical Solution for Simple Systems in Moving Bed Adsorbers: Effect of Intraparticle Diffusion", Ind. Eng. Chem. 44, 1704 (1952).

55. Kasten, P. R., Lapidus, L., and Amundson, N. R., "Mathematics of Adsorption in Beds. V. Effect of Intraparticle Diffusion in Flow Systems in Fixed Beds", J. Phys. Chem. 56, 683 (1952).

56. Keinath, T. M., and Weber, W. J., Jr., "A Mathematic Model for Prediction of Concentration-Times Profiles for Design of Fluid-Bed Adsorbers", Tech. Publication Research Project WP-00706, Fed. Water Poll. Control Adm., U. S. Dept. of Interior (April 1968).

57. Keinath, T. M., and Weber, W. J., Jr., "A Predictive Model for the Design of Fluid-Bed Adsorbers", J. Water Poll. Control Fed. 40, 743 (1968).

58. Keinath, T. M., and Weber, W. J., Jr., "Simulation of Heterogeneous Sorption of Organic Contaminants in Waste-Water for Process Control of Fluidized-Bed Adsorbers", presented at the 43rd Annual Conference of the Water Pollution Control Federation, October 4-9, 1970, Boston, Mass.

59. King, C. J., "Mass Transfer During Short Surface Exposures in Countercurrent Flow", Ind. Eng. Chem., Fund. 4, 125 (1965).

60. Klotz, I. M., "The Adsorption Wave", Chemical Reviews 39, 241 (1946).

61. Lapidus, L., and Amundson, N.R., "Mathematics of Adsorption in Beds. VI. The Effect of Longitudinal Diffusion in Ion Exchange and Chromatographic Columns", J. Phys. Chem. 56, 984 (1952).

62. Le Bas, G., The Molecular Volumes of Liquid Chemical Compounds, from the Point of View of Kopp, Longmans, Green and Co., London (1915).

63. Lewis, E. W., and Bowerman, E. W., "Fluidization of Solid Particles in Liquids", Chem. Eng. Progr. 48, 603 (1952).

64. Lippincott, E. R., Stromberg, R. R., Grant, W. H., and Cessac, G. L., "Polywater", Science 164, NO. 3887, 1482 (27 June 1969).

65. Lyskj, I., Nelson, K. H., and Webb, S. R., "Analysis of Multicomponent Organic Mixtures in Aqueous Systems by Pyrolysis", Water Research 4, 157 (1970).

66. Mantell, C. L., Adsorption, Second Edition, McGraw-Hill Book Co., New York, p. 8 (1951).

67. Marinsky, J. A., Ion Exchange, A Series of Advances, Volume 1, Marcel Dekker, Inc., New York (1966).

68. Masamune, S., and Smith, J. M., "Adsorption Rate Studies - Significance of Pore Diffusion", AIChE J. 10, 246 (1964).

69. Masamune, S., and Smith, J. M., "Transient Mass Transfer in a Fixed Bed", Ind. and Engl. Chem. Fund. 3, 179 (1964).

70. Masamune, S., and Smith, J. M., "Adsorption Rate Studies - Interaction of Diffusion and Surface Processes", AIChE J. 11, 34 (1965).

71. Masamune, S., and Smith, J. M., "Adsorption of Ethyl Alcohol on Silica Gel", AIChE J. 11, 41 (1965).

72. McCollum, P. A., and Brown, B. F., Laplace Transform Tables and Theorems, Holt, Rinehart, and Winston, New York (1965).

73. Michaels, A. S., "Simplified Method of Interpreting Kinetic Data in Fixed-Bed Ion Exchange", Ind. Eng. Chem. 44, 1922 (1952).

74. Midkiff, W. S., and Weber, W. J., Jr., "Reactions of a Strongly Basic Ion Exchange Resin with Dilute Aqueous Solutions in a Column System", Tech. Publication, Research Project A-013-MICH, Office of Water Resources Research, U. S. Dept. of the Interior (Nov. 1969).

75. Moilliet, J. L., and Collie, B., Surface Activity, p. 54-96, D. Van Nostrand Co., New York (1965).

76. Morris, J. C., and Weber, W. J., Jr., "Preliminary Appraisal of Advanced Waste Treatment Processes", Public Health Service Publications No. W62-24. Number 2 in the series of Advanced Waste Treatment Research Publications.

77. Morris, J. C., and Weber, W. J., Jr., "Adsorption of Biochemically Resistant Materials from Solution. 1.", Public Health Service Publications No. 999-WP-11. Number 9 in the series of Advanced Waste Treatment Research Publications.

78. Morris, J. C., and Weber, W. J., Jr., "Adsorption of Biochemically Resistant Materials from Solution. 2.", Public Health Service Publication No. 999-WP-33. Number 16 in the series of Advanced Waste Treatment Research Publications.

79. O'Farrell, T. P., Dolloff, F., Bishop, D. F., and Bennet, S. M., "Advanced Waste Treatment at Washington, D. C.", Chem. Eng. Prog. Symposium Series 65, 251 (1967).

80. Parkhurst, J. D., Dryden, F. D., McDermott, G. N., and English, J., "Pomona Activated Carbon Pilot Plant", J. Water Poll. Control Fed. 39, Part 2, R 70 (1967).

81. Peterson, J. O., and Lee, G.F., "Sorption Capacity Estimation for Activated Carbon Packed Columns", Water Research 5, 717 (1971).

82. Resnick, W., and White, R. R., "Mass Transfer in Systems of Gas and Fluidized Solids", Chem. Eng. Progr. 45, 377 (1949).

83. Richardson, J. F., and Zaki, W. N., "Sedimentation and Fluidization: Part I", Trans. Inst. Chem. Engrs. 32, 35 (1954).

84. Rizzo, J. L., and Schade, R. E., "Secondary Treatment with Granular Activated Carbon", Water and Sewage Works 116, 307 (1969).

85. Rose, J. L., "Advanced Waste Treatment in Nassau County, N.Y.", Water and Wastes Engineering 7, 38 (1970).

86. Rosen, J. B., "Kinetics of a Fixed-Bed System for Solid Diffusion into Spherical Particles", J. Chem. Phys. 20, 387 (1952).

87. Rosen, J. B., "General Numerical Solution for Solid Diffusion into Fixed Beds", Ind. Eng. Chem. 46, 1590 (1954).

88. Ross, L. W., Carlson, G. R., and Cheng, C. Y., "Economic Study for Wastewater Treatment Plant Expansion", Public Works 100, No. 9, 130 (1969).

89. Schumann, T. E. W., "Heat Transfer: A Liquid Flowing Through a Porous Prism", Journal Franklin Institute 208, 405 (1929).

90. Schlichting, H., Boundary Layer Theory , McGraw-Hill Book Co., New York (1960).

91. Snoeyink, V. L., and Weber, W. J., Jr., "The Surface Chemistry of Active Carbon - A Discussion of Structure and Surface Functional Groups", Environ. Sci. Tech. 1, 228 (1967).

92. Snoeyink, V. L., Weber, W. J., Jr., and Mark, H. B., "Sorption of Phenol and Nitrophenol by Active Carbon", Environ. Sci. Tech. 3, 918 (1969).

93. Snoeyink, V. L., and Weber, W. J., Jr., "Reaction of the Hydrated Proton with Active Carbon", in Adsorption from Aqueous Solution, Advances in Chemistry Series, American Chemical Society, No. 79, (1968).

94. Sommerfeld, A., Partial Differential Equations in Physics, translated by E. G. Straus, Academic Press, Inc., New York (1949).

95. Stephen, D. G., "Renovation of Municipal Wastewater for Re-Use", AIChE Symposium Series 9, (1965).

96. Stephen, D. G., and Schaffer, R. B., "Wastewater Treatment and Renovation Status of Process Development", J. Water Poll. Control Fed. 42, Part 1, 399 (1970).

97. Stephen, D. G., and Weinberger, L. W., "Wastewater Reuse: Has it Arrived?", J. Water Poll. Control Fed. 40, 529 (1968).

98. Summary Report - The Advanced Waste Treatment Research Program; June 1960 - December 1961, SEC TR W62-9, U. S. Dept. of Health, Education and Welfare, (May 1962).

99. Thomas, H. C., "Heterogeneous Ion Exchange in a Flowing System", J. Amer. Chem. Soc. 66, 1664 (1944).

100. Thomas, H. C., "Chromatography: A Problem in Kinetics", Ann. N. Y. Acad. Sci. 49, 161 (1948).

101. Thomas, H. C., "Solid Diffusion in Chromatography", J. Chem. Phys. 19, 1213 (1951).

102. Thomas, H. C., "The Kinetics of Ion Exchange", in Ion Exchange, edited by F. C. Nachod, Academic Press, Inc., New York (1949).

103. Tien, C., " A Simplified Method for Determination of Solid Diffusion Coefficient with Non-Linear Adsorption Isotherm", Can. J. Chem. Engr. 38, 25 (1960).

104. Tien, C., and Thodos, G., "Ion Exchange Kinetics for Systems of Non-Linear Equilibrium Relationships", AIChE J. 5, 373 (1959).

105. Tien, C., and Thodos, G., "Ion Exchange Kinetics for Systems of Linear Equilibrium Relationships", AIChE. J. 6, 364 (1960).

106. Tien, C., and Thodos, G., "Ion Exchange Kinetics: The Removal of Oxalic Acid from Glycol Solutions", Chem. Eng. Sci. 13, 120 (1961).

107. Treybal, R. E., Mass Transfer Operations, Second Edition, McGraw-Hill Book Co., New York (1968).

108. Vassiliou, B., and Dranoff, J. S., "The Kinetics of Ion Exclusion", AIChE J. 8, 248 (1962).

109. Vermeulen, T., "Theory for Irreversible and Constant-Pattern Solid Diffusion", Ind. Eng. Chem. 45, 1664 (1953).

110. Vermeulen, T.,"Separation by Adsorption Methods", in Volume II, in Advances in Chemical Engineering, Academic Press New York (1958).

111. Vermeulen, T. and Huffman, E. H., "Ion Exchange Column Performance", Ind. Eng. Chem. 45, 1658 (1953).

112. Weber, T. W., and Meyer, O. A., "Nonisothermal Adsorption in Fixed Beds", AIChE J. 13, 457 (1967).

113. Weber, W. J., Jr., "Competitive Interactions in Adsorption from Dilute Aqueous Bi-Solute Solutions", J. Appl. Chem. 14, 565 (1964).

114. Weber, W. J., Jr., "Fluid-Carbon Columns for Sorption of Persistent Organic Pollutants", in Advances in Water Pollution Research. Proceedings of the Third International Conference on Water Pollution Research, Water Pollution Control Federation, Washington, D. C., Volume 1, 253 (1967).

115. Weber, W. J., Jr., Physicochemical Processes for Water Quality Control, John Wiley and Sons, Inc., New York (1972).

116. Weber, W. J., Jr., Bloom, R., Jr., and Hopkins, C. B., "Expanded-Bed Active-Carbon Adsorption for Waste Water Treatment", Water Res. Symp. 3, 294 (1970).

117. Weber, W. J., Jr., Friedman, L. D., and Bloom, R., Jr., "Biologically-Extended Physicochemical Treatment", Paper submitted for the Sixth Conference of the International Association of Water Pollution Research, Jerusalem, 18-24 June 1972.

118. Weber, W. J., Jr., and Gould, J. P., "Sorption of Organic Pesticides from Aqueous Solution", Adv. Chem. Ser. 60, 280 (1966), Amer. Chem. Soc. Publications, Washington, D. C.

119. Weber, W. J., Jr., Hopkins, C. B., and Bloom, R., Jr., "Physicochemical Treatment of Wastewater", J. Water Poll. Control Fed. 42, 1, 83 (January 1970).

120. Weber, W. J., Jr. and Keinath, T. M., "Mass Transfer of Perdurable Pollutants from Dilute Aqueous Solution in Fluidized Adsorbers", Chem. Eng. Progr., Symp. Ser. 74, 63, 79 (1967).

121. Weber, W. J., Jr., and Morris, J. C., "Kinetics of Adsorption on Carbon from Solution", ASCE, SED, SA2, 31 (1963).

122. Weber, W. J., Jr., and Morris, J. C., "Equilibria and Capacities for Adsorption on Carbon", ASCE, SED, SA3, 79 (1964).

123. Weber, W. J., Jr., and Morris, J. C., "Kinetics of Adsorption in Columns of Fluidized Media", J. Water Poll. Control Fed. 37, 425 (1965).

124. Weber, W. J., Jr., and Rumer, R. R., "Intraparticle Transport of Sulfonated Alkylbenzenes in a Porous Solid: Diffusion with Nonlinear Adsorption", Water Resources Research 1, 361 (1965).

125. Wen, C. Y. and Yu, Y. H., "Mechanics of Fluidization", Chem. Eng. Progr. , Symp. Ser. 62, 100 (1966).

126. Weisz, P. B., "Sorption- Diffusion in Heterogeneous Systems; Part 1. - General Sorption Behavior and Criteria", Faraday Society Transactions, 63, 1801 (1967).

127. Weisz, P. B., "Sorption - Diffusion in Heterogeneous Systems; Part 3. - Experimental Models of Dye Sorption", Faraday Society Transactions, 63, 1815 (1967).

128. Wilke, C. R., and Chang, P., "Correlation of Diffusion Coefficients in Dilute Solutions", J. AIChE 1, 264 (1955).

129. Williamson, J. N., Heit, A. H., and Calmon, O., "Evaluation of Various Adsorbents and Coagulants for Waste-Water Renovation", Public Health Service Publication No. 999-WP-14. Number 12 in the series of Advanced Waste Research Publications.

130. Zanitsch, R. H., and Morand, J. M., "Tertiary Treatment of Combined Wastewater With Granular Activated Carbon", Water and Wastes Engr. 7, 58 (1970).

APPENDIX 1

LAPLACE TRANSFORM

The solution of the equation describing the performance of an adsorber column (Equation 2-23) with appropriate boundary conditions (Equation 2-27) may be obtained through application of the Laplace transform for two variables (21,22). In general for an equation

$$\frac{\partial\Phi(x,y)}{\partial x\partial y} - AB\Phi(x,y) = 0 \qquad \text{(A1-1)}$$

with boundary conditions

$$\begin{aligned} \Phi(0,0) &= 1 \\ \Phi(x,0) &= e^{Bx} \\ \Phi(0,y) &= e^{\alpha y} \\ \alpha &= C_1C_0 + A \end{aligned} \qquad \text{(A1-2)}$$

The transform may be given in terms of p and q as

$$pqF(p,q) - pq(F(0,q)) - pq(F(p,0)) + pq(F(0,0)) - ABF(p,q) = 0 \qquad \text{(A1-3)}$$

$$pqF(p,q) - \left[pq\cdot q \int_0^\infty e^{-q\eta}\,\Phi(0,\eta)\,d\eta\right] - \left[pq\cdot p \int_0^\infty e^{-p\xi}\Phi(\xi,0)\,d\xi\right] + pq - ABF(p,q) = 0 \qquad \text{(A1-4)}$$

Simplifying Equation A1-4 yields

$$pqF(p,q) - \left[pq^2 \int_0^\infty e^{-(q-\alpha)\eta}\,d\eta\right] - \left[p^2q \int_0^\infty e^{-(p-B)\xi}\,d\xi\right] + pq - ABF(p,q) = 0 \qquad \text{(A1-5)}$$

In terms of $F(p,q)$, Equation A1-5 may be simplified to

$$F(p,q) = \frac{pq}{pq-AB} + \frac{\alpha pq}{(pq-AB)(q-\alpha)} + \frac{pqB}{(pq-AB)(p-B)} \tag{A1-6}$$

Since $\Phi(x,y) = \mathcal{L}^{-1}\{F(p,q)\}$

$$\Phi(x,y) = \mathcal{L}^{-1}\left\{\frac{pq}{pq-AB}\right\} + \mathcal{L}^{-1}\left\{\frac{\alpha pq}{(pq-AB)(q-\alpha)}\right\}$$

$$+\mathcal{L}^{-1}\left\{\frac{pqB}{(pq-AB)(p-B)}\right\} \tag{A1-7}$$

Also noting

$$\mathcal{L}^{-1}\ \{F(p,q) \cdot f(q)\} = \int_0^y f(x,\eta)\ f\ (x,\ y-\eta)\ d\eta$$

$$\mathcal{L}^{-1}\ \{F(p,q) \cdot f(p)\} = \int_0^x f(\xi,y)\ f\ (x-\xi,y)\ d\xi \tag{A1-8}$$

From inverse transform tables we may find, therefore, that

$$\Phi(x,y) = J_0\{2i\sqrt{ABxy}\} + \int_0^x Be^{B\xi}\ J_0\{2i\sqrt{ABy(x-\xi)}\}\ \ d\xi$$

$$+ \int_0^y \alpha e^{\alpha\eta}\ J_0\{2i\sqrt{ABx(y-\eta)}\}\quad d\eta \tag{A1-9}$$

APPENDIX 2

COD DETERMINATION USING TECHNICON® AUTOANALYZER

The schematic representation of the automated chemical oxygen demand concentration analyzer apparatus is given in Figure A2-1. The tubing sizes are given in parentheses as inside diameter in inches, and the nominal flow rates in brackets are expressed as milliliters per minute. Tubing was tygon except those indicated by an asterisk (*), in which case acidflex tubing was used. Pumping of reagents and samples was done using a Technicon Single Speed Proportioning Pump. The heating bath coil consists of 130 feet of 5 mm outside diameter glass coil tubing.

The digestion mix was composed of 6.0 percent by volume of 0.25 N potassium dichromate solution to which 0.12 grams of sulfamic acid was added per liter of the potassium dichromate stock solution, 6.5 percent distilled water and 87.5 percent reagent grade concentrated sulfuric acid in which 11.0 grams of reagent grade silver sulfate was dissolved per 9.0 pound bottle of acid. The mercuric reagent consisted of 8.0 grams of mercuric ion (11.8 grams of mercuric sulfate) per liter of solution of 100.0 milliliter of concentrated reagent sulfuric acid per liter dissolved in distilled water.

The digested mix and sample passed through a 50 mm tubular flow cell in a Technicon Colorimeter containing a 620 mμ optical filter for determining decrease in the concentration of dichromate.

FIGURE A2-1. CHEMICAL OXYGEN DEMAND

AUTO ANALYZER SYSTEM

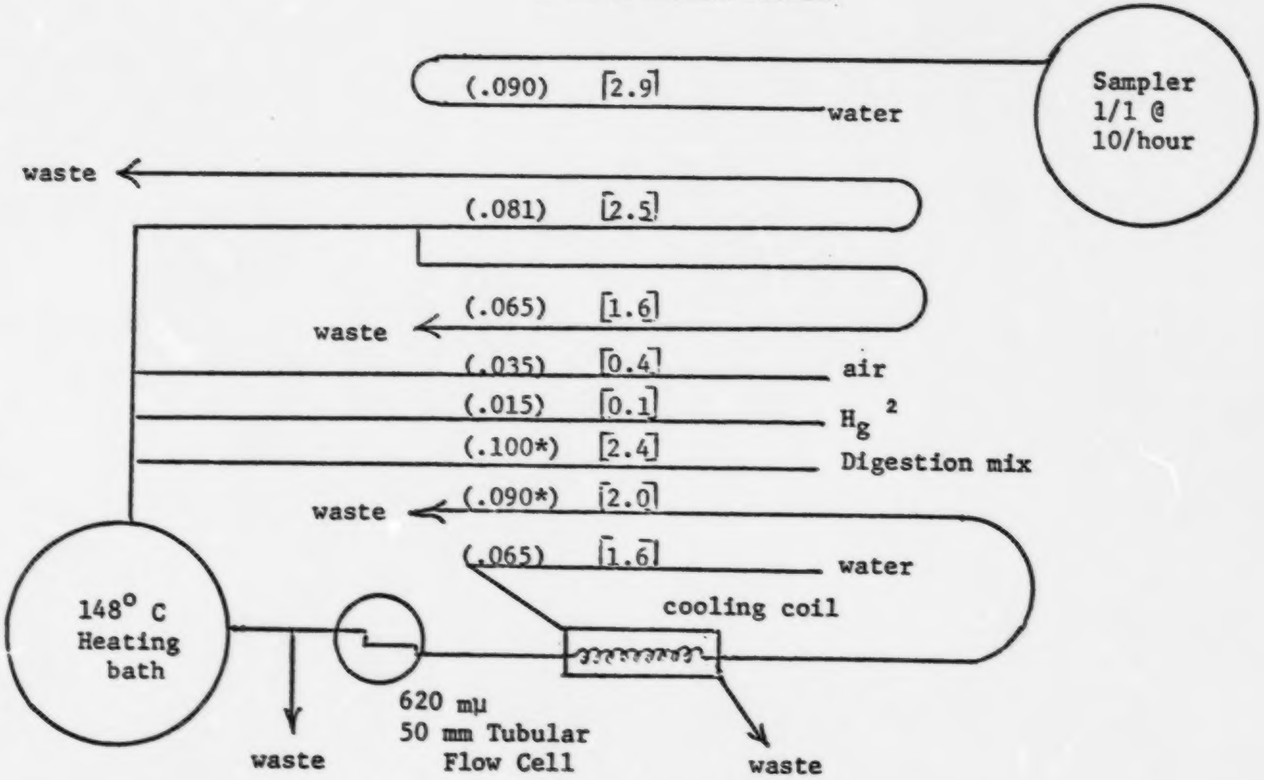
Sampler
1/1 @
10/hour
(.090) [2.9] water
waste
(.081) [2.5]
(.065) [1.6]
waste
(.035) [0.4] air
(.015) [0.1] H_g 2
(.100*) [2.4] Digestion mix
waste
(.090*) [2.0]
(.065) [1.6] water
cooling coil
148° C
Heating
bath
waste
620 mμ
50 mm Tubular
Flow Cell
waste

A calibration curve using glucose as a standard measurement was used to correlate the COD concentration with the decrease in dichromate color intensity. It was assumed that the theoretical COD of glucose equalled the actual measured COD, thus for each mg/l of glucose in solution, 1.067 mg/l of COD resulted.

APPENDIX 3

COMPUTER PROGRAM FOR KINETIC MODEL

The outline for digital computer solution of the second-order kinetic mathematic model is presented below.

1. Input necessary model parameters.
2. Calculate constants used in solution.
3. Set initial values for time and effluent concentration.
4. Numerically increment time and solve for effluent concentration to influent concentration ratio using approximations for $\Psi(Bv, A(V-v\varepsilon))$ and $\Psi(\alpha(V-v\varepsilon), \beta v)$ as given by Equation 2-45, and for $I_0(2\sqrt{ABv(V-v\varepsilon)}$ by Equation 2-46 in Equation 2-42.
5. Check incremental change in C/C_0 ratio, and if within limits, stop. Otherwise continue to increment time until incremental change is within limits.

The computer program for solution of the kinetic model is given below.

```
C     PROGRAM FOR SOLVING THE  KINETIC MATHEMATIC MODEL:
C     SOLUTION USING APPROXIMATIONS FOR BESSEL FUNCTIONS
C     AND INTEGRALS
      DOUBLE PRECISION CI,Q,R,DG,KAP,K,A,B,C1,B1.B2,ALPH,
     1GAM,GAM1,GAM2,E1,E2,BF,PSI1,PSI2,PHI,C,V2,V,ALPH1,
     2ALPH2,A1,A2,AB1,KFA,KSA
      COMMON CI,Q,K,A,B,C1,B1,B2,ALPH,GAM,GAM1,GAM2,V,BI,
     1RHO,F,EPS,KFA,KSA,R,DG,KAP
      NAMELIST / CODAT / F,DELT1,N2,EPSIL,RHO,V,EPS
      NAMELIST / DATA /Q,BI,CI,KFA,KSA,MIX
      READ (5,CODAT)
  301 READ (5,DATA,END=999)
      DELT=DELT1*60.
      WRITE (6,123) MIX
      WRITE (6,102)Q,BI,RHO,EPS,V,KFA,KSA
      WRITE (6,103) DELT1,EPSIL
      TIME=0.0
      CNEW=0.0
      CALL COMCON
C     WRITE VALUES FROM COMCON
      WRITE (6,111) R,DG,KAP,K,A,B,C1,B1
      WRITE (6,101) F,CI
      WRITE (6,104)
      M1=1
      DO 30 I=M1,N2
      TIME=I*DELT
      TIME1=I*DELT1
      V2=F*TIME-V*EPS
      A1=DSQRT(A*V2)
      A2=DSQRT(A1)
      AB1=A1*B1
      E1=DEXP(A*V2+B*V)
      BF=(DEXP(2*AB1))/(2*(DSQRT(3.143*AB1)))
      PSI1=E1*(1.-DERF(A1-B1))/2-(B2/(A2+B2))*BF
      ALPH1=DSQRT(ALPH*V2)
      ALPH2=DSQRT(ALPH1)
      E2=DEXP(ALPH*V2+GAM*V)
      PSI2=E2*(1.-DERF(GAM1-ALPH1))/2.-(ALPH2/(ALPH2+GAM2))*BF
      PHI=BF+PSI1+PSI2
      C=1.-PSI1/PHI
      WRITE (6,106) TIME1,PSI1,PSI2,PHI,C
      CC=(C-CNEW)/ C
      IF(ABS(CC)-EPSIL)40,40,36
   36 CNEW=C
   30 CONTINUE
   40 CONTINUE
      GO TO 301
  999 CALL EXIT
```

```
123 FORMAT (/,'MIX =',I3)
101 FORMAT(1H1,9X!FLOW RATE F = ',F10.4,1X,'CC/MIN',/10X,
   1'INITAIL CONCENTRATION CI = ',E12.4,1X,'GRAMS/CC')
102 FORMAT(//10X,LANGMUIR CONSTANT Q = ',E12.4,1X,'GRAMS/
   1GM',/10X!LANGMUIR CONSTANT B = ',E12.4,1X,'CC/GRAM',
   2/10X,' DENSITY OF BED = ',F10.4,/10X,'POROSITY OF BED
   3 = ',F12.4,/10X,'VOLUME OF BED = ',F10.4,1X,'CC',/10X
   4,'KFA = ',F10.4,1X,'PER MIN',/10X!KSA = ',F10.4,1X,'
   5PER MIN')
103 FORMAT(//10X,'TIME STEP = ',F10.4,1X,'HOURS',/10x,'EP
   1SIL = ',F10.4)
111 FORMAT(//10X,'R = ',E12.4,10X,'KAP = ',E12,4,/10X,'K =

   1 ',E12.4,/ 10X,'A = ',E12.4,/10X,'B = ',E12.4,/10X,
   2 'C1 = ',E12.4,/10X,'B1 =',E12.4)
104 FORMAT (//10X,'TIME',15X,'PSI1',15X,'PSI2',15X,'PHI',
   115X,'C/CI')
106 FORMAT (12X,F10.5,8X,E12.4,8X,E12.4,8X,E12.4,8X,F10.4)
    STOP
    END
```

```
      SUBROUTINE COMCON
      DOUBLE PRECISION CI,Q,R,DG,KAP.K,A,B,C1,B1,B2,ALPH,
     1GAM,GAM1,GAM2,E1,E2,BF,PSI1,PSI2,PHI,C,V2,V,ALPH1,
     2ALPH2,A1,A2,AB1,KFA,KSA
      COMMON CI,Q,K,A,B,C1,B1,B2,ALPH,GAM,GAM1,GAM2,V,BI,
     1RHO F,EPS,KFA,KSA,R,DG,KAP
      R=1./(1.+BI*CI)
      DG=(Q*BI*RHO)/(EPS*(1.+(BI*CI)))
      KAP=2./((1.+R)*(1./KFA+1./(KSA*DG)))
      K=(KAP*EPS)/(Q*RHO)
      A=K/(F*BI)
      B=(K*Q*RHO)/F
      C1=K/F
      B1=DSQRT(B*V)
      B2=DSQRT(B1)
      ALPH=(C1*CI)+A
      GAM=(K*Q*RHO)/(F*(1.+BI*CI))
      GAM1=DSQRT(GAM*V)
      GAM2=DSQRT(GAM1)
      RETURN
      END
```

APPENDIX 4

MICHAELS EQUILIBRIUM MATHEMATIC MODEL

The Michaels equilibrium mathematic model is a simplification of adsorption behavior in adsorber beds used to predict effluent concentration-history profiles. This model is limited to isothermal adsorption from dilute feed mixtures for those cases in which the equilibrium adsorption isotherm is of the favorable type. The adsorption zone must be constant in length as it moves through the adsorption column and must be small relative to the overall length of the adsorber bed. The Michaels equilibrium model was developed for fixed beds, but may be extended to expanded beds if one assumes the expanded system approximately equals an inverted packed system of higher porosity. The relative positions of adsorber particles are assumed to remain constant and the adsorption zone is also assumed to be of constant height in the expanded bed.

With reference to Figure A4-1, an idealized effluent concentration-history profile, one may follow the Michaels development in the ensuing manner. The idealized profile results from the flow of the sorbate through the adsorber bed at a volumetric flow rate of F(cc/min) and an influent concentration C_o(g/cc). The total adsorption-treated effluent after any time is given as V_e (cc). The breakpoint concentration C_b(g/cc) is arbitratily chosen at some low value, and the adsorber bed is considered exhausted at

FIGURE A4-1. IDEALIZED EFFLUENT CONCENTRATION-HISTORY PROFILE

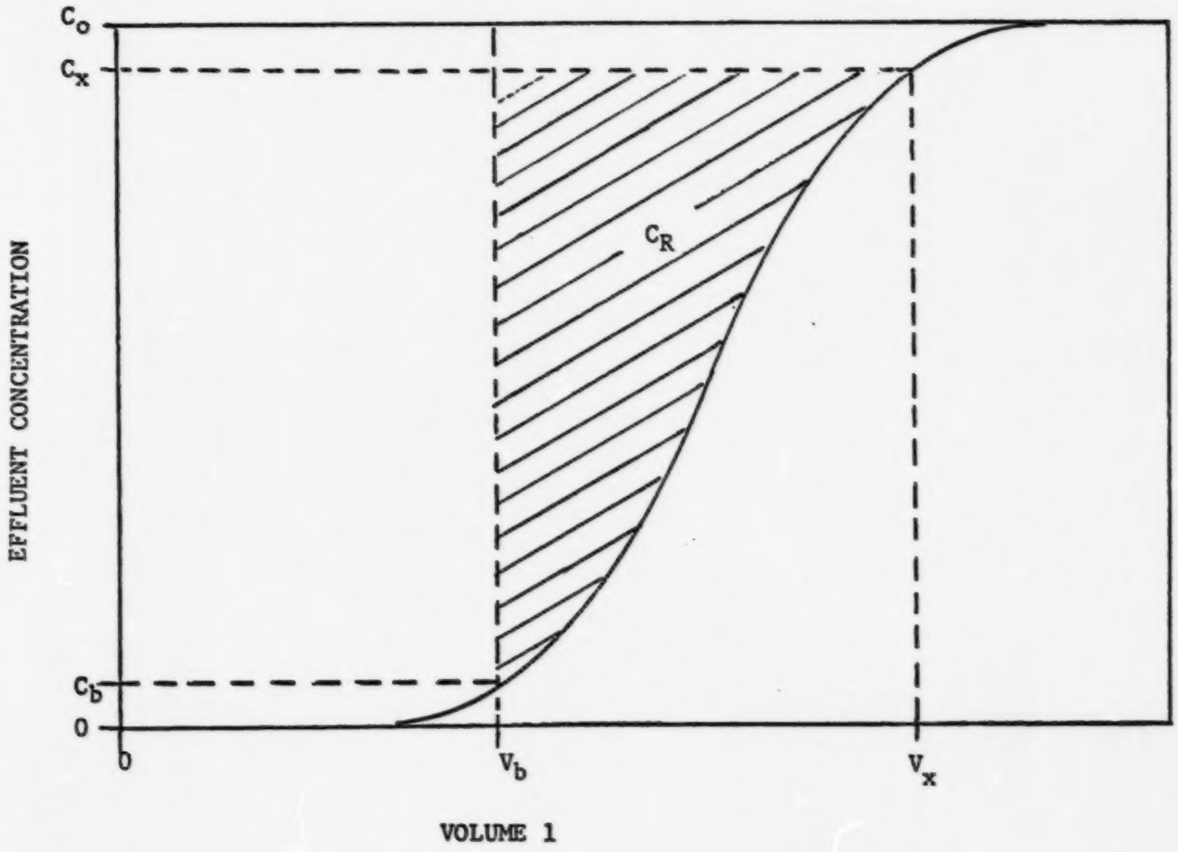

some arbitrary effluent concentration value, C_x(g/cc), chosen close to the influent concentration C_o. The total quantity of effluent passing through the adsorber bed up to breakpoint, V_b and the nature of the effluent profile between V_b and the volume of the total effluent treated up to exhaustion, V_x, are the two primary considerations of interest.

The total effluent flowing through the adsorber bed during the appearance of the primary adsorption zone in the effluent concentration-history profile is given as

$$V_a = V_x - V_b \qquad \text{(A4-1)}$$

The time, t_h, for the adsorption zone to move its own height, h, through the column is given by

$$t_h = \frac{V_a}{F} \qquad \text{(A4-2)}$$

The total time, t_x, required for the formation of the primary adsorption zone to establish itself, to move through the adsorber bed of length H, and to pass out of the bed, is given by

$$t_x = \frac{V_x}{F} \qquad \text{(A4-3)}$$

If the time required for formation of the adsorption zone is given by t_f, then the depth and time ratios for the adsorber bed and primary adsorption zone may be equated as

$$\frac{h}{H} = \frac{t_h}{t_x - t_f} \qquad \text{(A4-4)}$$

The quantity of sorbate removed from the solution in the primary adsorption zone from breakpoint to exhaustion is represented by the shaded area in Figure A4-1. This may be evaluated by

$$C_R = \int_{V_b}^{V_x} (C_o - C)\,d\,V_e \qquad \text{(A4-5)}$$

The total capacity of the adsorber bed within the primary adsorption zone at breakpoint would be the product V_aC_o. Thus the fractional capacity, f, of the adsorbent when the primary zone is still within the bed, may be given at breakpoint as

$$f = \frac{C_R}{V_aC_o} = \frac{\int_{V_b}^{V_x} (C_o - C)\,dV_e}{V_aC_o} = \int_0^1 \left(1 - \frac{C}{C_o}\right) d\left(\frac{V_e - V_b}{V_a}\right) \qquad \text{(A4-6)}$$

As f approaches 0, the adsorbent bed becomes essentially saturated, and hence the time of formation of the primary adsorption zone will be equal to the time required for the zone to descend a distance equal to its own height. As f approaches 1.0, the adsorber within the bed contains essentially no solid, so that the formation time must be very short, essentially zero. The zone formation time may then be given by

$$t_f = (1-f)t_h \qquad \text{(A4-7)}$$

From Equations A4-4 and A4-7, we get

$$\frac{h}{H} = \frac{t_h}{t_x + t_h(f-1)} \qquad \text{(A4-8)}$$

or in terms of effluent volumes

$$\frac{h}{H} = \frac{V_a}{V_b + f(V_a)} \tag{A4-9}$$

When the entire adsorber bed is in equilibrium with the influent concentration, the amount of sorbate, S_s, which will have accumulated in the bed will be equal to the amount adsorbed per unit amount of adsorbent, q_∞, times the total amount of adsorbent. For a bed of unit cross sectional area, and height, H,

$$S_s = \rho q_\infty H \tag{A4-10a}$$

in which ρ is the density of the expanded bed. At breakpoint, the adsorption zone of height, h, is still in the adsorber bed, but the rest of the column is essentially saturated. The length of the saturated zone is H-h, and the total amount of solute, S_b, accumulated on the adsorbent at breakpoint is

$$\begin{aligned} S_b &= q_\infty \rho \left[(H-h) + (1-f)h\right] \\ &= q_\infty \rho (H-fh) \end{aligned} \tag{A4-10b}$$

Thus the degree of saturation, S, is given by

$$S = \frac{H-fh}{H} \tag{A4-11}$$

In the adsorber bed, the adsorption zone moves through the solid. Consider instead that the solid moves through the column countercurrent to the fluid such that the adsorption zone remains stationary (Figure A4-2). The solid leaving the column is in equilibrium with the influent solution, and all sorbate has been

FIGURE A4-2. IDEALIZED

COUNTER CURRENT ADSORPTION

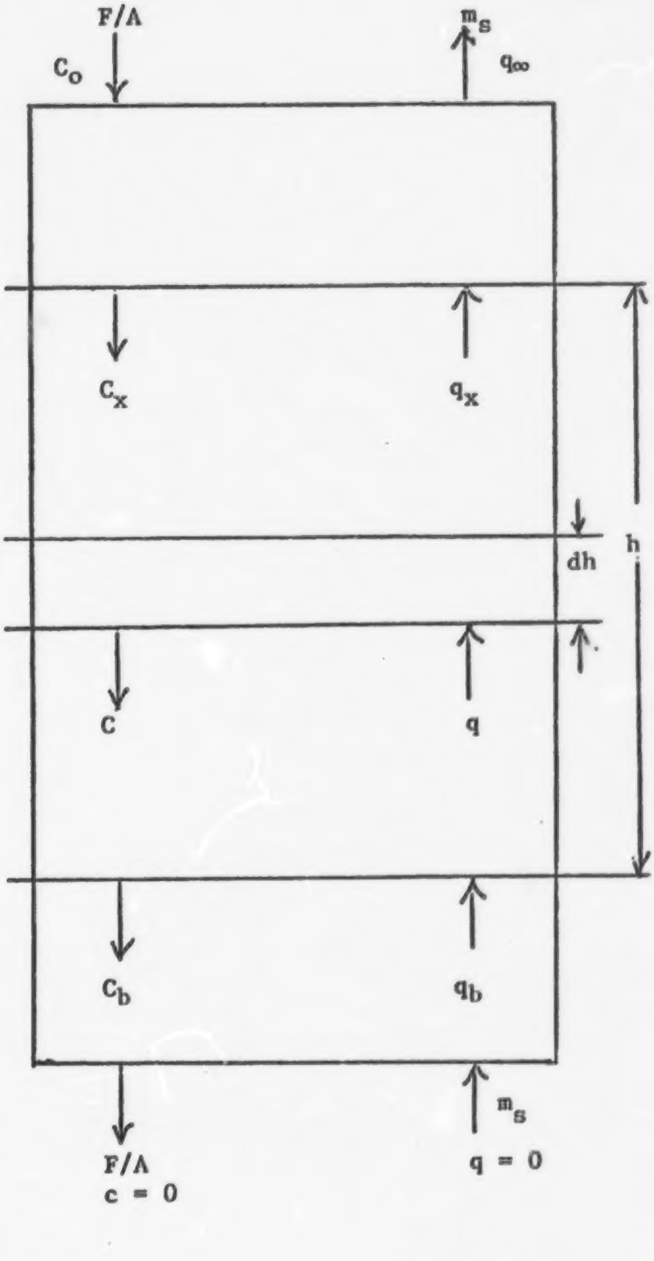
F/A
C_o
m_s
q_∞
C_x
q_x
dh
h
C
q
C_b
q_b
m_s
F/A
c = 0
q = 0

removed from the effluent. (This would require an infinitely long column, but we will be concerned with the concentrations at the levels corresponding to the extremities of the adsorption zone). The operating line over the entire column, assuming all sorbate is removed from solution, is

$$FC_o = Am_s q_\infty \tag{A4-12}$$

in which A is the cross sectional bed area (cm^2), and m_s is the superficial rate of saturation of the adsorbent (gram adsorbate saturated per minute per cm^2). For the most common case in which the operating line passes through the origin of a plot of C versus q, (see Figure A4-3), the concentration of sorbate in solution and in the adsorbed phase are related by

$$FC = Am_s q \tag{A4-13}$$

Over a differential height of adsorber bed, dh_1, the rate of transfer of sorbate may be expressed as

$$\frac{F}{A} dC = Ka(C-C_e)dh_1 \tag{A4-14}$$

in which Ka is the overall mass transfer coefficient. For the adsorption zone, one can write from Equation A4-14, assuming Ka is constant,

$$\frac{hKaA}{F} = \int_{C_b}^{C_x} \frac{dC}{(C-C_e)} \tag{A4-15}$$

FIGURE A4-3. ADSORPTION ISOTHERM

AND OPERATING LINE

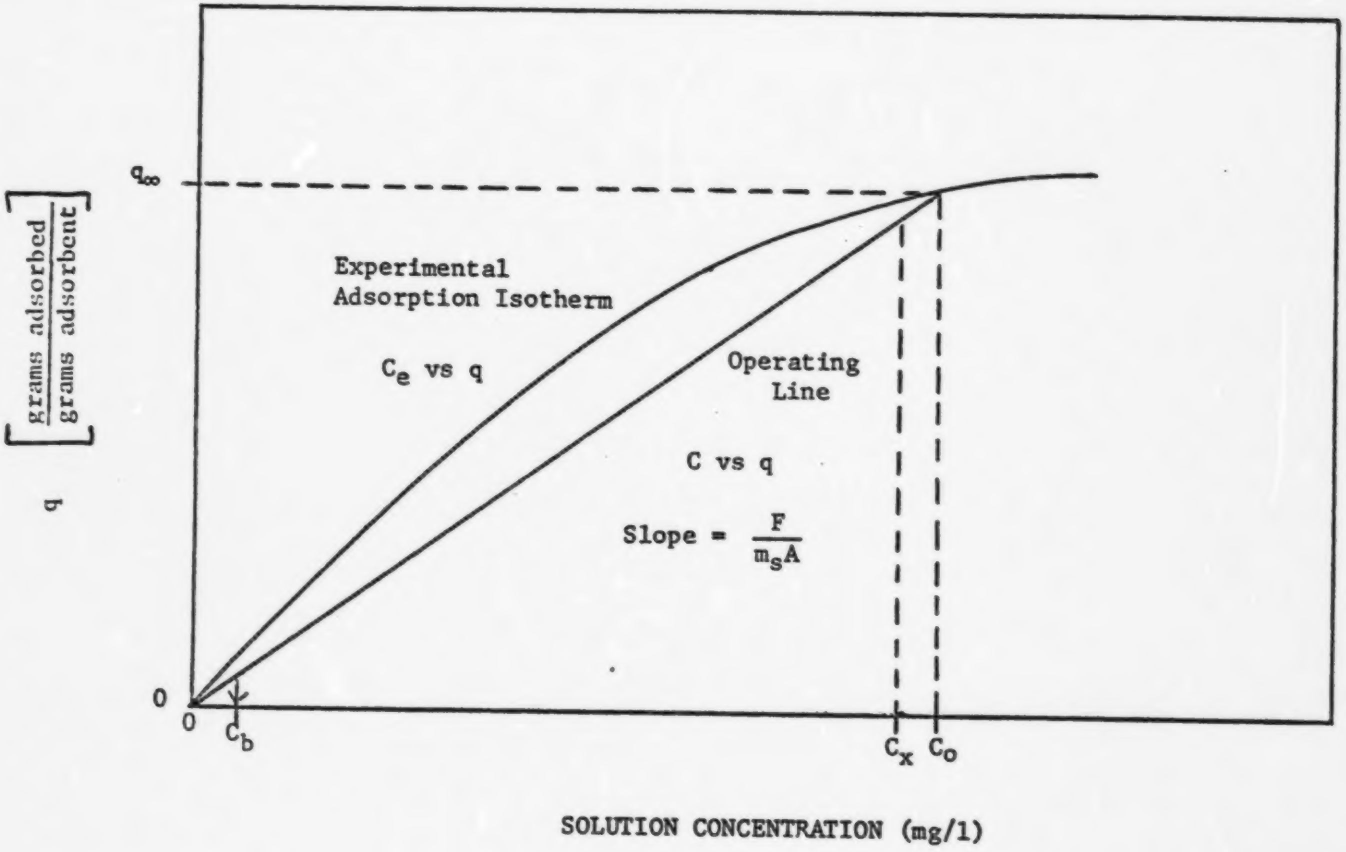

For any value of h, less than h, corresponding to a concentration $C_b < C < C_x$, the following relationship may be given:

$$\frac{h_1}{h} = \frac{V_e - V_b}{V_a} = \frac{\int_{C_b}^{C} \frac{dC}{(C-C_e)}}{\int_{C_b}^{C_x} \frac{dC}{(C-C_e)}} \qquad (A4\text{-}16)$$

Graphical integration of Equation A4-16 results in prediction of the effluent concentration-history profile for the adsorber bed. The use of an overall transfer coefficient, Ka, for the equilibrium model may be represented by a series addition of resistances to film diffusion and pore-surface diffusion such that

$$Ka = \left[\frac{1}{k_f a} + \frac{1}{k_s a D_G}\right]^{-1} \qquad (A4\text{-}17)$$

COMPUTER PROGRAM SOLUTION FOR THE MICHAELS EQUILIBRIUM MODEL

Outline

1. Define equilibrium distribution of sorbate by Langmuir adsorption isotherm.
2. Choose limits of effluent concentration-history profile; e.g. $C_b = 0.05\ C_o$ and $C_x = 0.95\ C_o$.
3. Calculate slope of operating line.
4. Incrementing operating line concentration, determine corresponding q and thus calculate corresponding equilibrium concentration.
5. Calculate concentration differences between corresponding concentrations and numerically integrate $\int_{C_b}^{C} (C-C_e)^{-1} dC$.
6. Determine height of adsorption zone from Equation A4-15 and $\int_{C_b}^{C_x} (C-C_e)^{-1} dC$ found in step 5.

7. Divide individual numerical integrations in step 5 by $\int_{C_b}^{C_x} (C-C_e)^{-1} dC$, corresponding to solution of Equation A4-16).

8. Determine fractional capacity remaining at breakthrough by numerical integration of Equation A4-6.

9. Determine degree of saturation (Equation A4-11) at breakpoint.

10. Calculate time to breakpoint.

11. Calculate total time for exhaustion.

12. Calculate time for breakthrough curve to pass through column, and then determine time at which incremented concentrations appear.

```
C     PROGRAM FOR SOLVING MICHAELS EQUILIBRIUM MODEL
      REAL KFA,KSA,KAP,MS
      DIMENSION C(50),CCO(50),Q(50),CE(50),CDIF(50),AINT(50),
     1SUMINT(50),VRAT(50),TBED(50),TTOTAL(50),DVRAT(50)
      NAMELIST / DATA / QMAX,B,CO,KFA,FLOW,H,MIX,RHOB,RCOL,
     1KSA,WTCARB,EPS
   10 READ (5,DATA,END=999)
      WRITE (6,201)
      CB=0.05*CO
      SUM=0.0
      PI=3.1416
      AREA=PI*RCOL**2.
      QINF=QMAX*B/(1.+B*CO)
      A=QMAX*B/(1.+B*CO)
      MS=FLOW/(A*AREA*RHOB)
      DG=QINF*RHOB/(CO*EPS)
      KAP=1./((1./KFA)+ (1./(DG*KSA)))
      WRITE (6,200)MIX,QMAX,B,CO,KFA,FLOW,H,RHOB,RCOL
      N=19
      DO 7 I=1,N
      C(I)=CB*I
      CCO(I)=C(I)/CO
      Q(I)=A*C(I)
      CE(I)=Q(I)/(B*(QMAX-Q(I)))
      CDIF(I)=1./(C(I)-CE(I))
    7 CONTINUE
      AINT(1)=0.0
      SUMINT(1)=0.0
      DO 1 I=2,N
      DC=CB
      AINT(I)=DC*CDIF(I)
      SUMINT(I)=SUM+AINT(I)
    1 SUM=SUMINT(I)
      WRITE(6,203) SUMINT(N)
      DEL=FLOW*SUM/(AREA*KAP)
      DO 2 I=1,N
      VRAT(I)=SUMINT(I)/SUM
    2 CONTINUE
      SUMF=0.0
      DO 17 I=1,N
      DVRAT(I)=VRAT(I)-VRAT(I-1)
   17 SUMF=(1.-CCO(I))*DVRAT(I)+SUMF
      F=SUMF
      SAT=(H-F*DEL)/H
      TBP=QINF*SAT*WTCARB/(CO*FLOW*60.)
      VB=TBP*FLOW*60.
      VX=WTCARB*QINF*(1.-SAT)/CO +VB
      TX=VX/(FLOW*60.)
      DO 5 I=1,N
      TBED(I)=(TX-TBP)*VRAT(I)
```

```
  5 TTOTAL(I)=TBP+TBED(I)
    TFI=(1.-F)*TBED(N)
    WRITE (6,220) TFI
    WRITE (6,222) F,SAT,TBP,VX,TX
    WRITE (6,202) MS,DEL,TBP,(I,C(I),CE(I),O(I),CDIF(I),
   1SUMINT(I),VRAT(I),TBED(I),CCO(I),TTOTAL(I),I=1,N)
    GO TO 10
999 CALL EXIT
201 FORMAT ('1')
200 FORMAT (//4X,'MIX = ',I2,/10X,'QMAX= ',E10.5,/10X,
   1'B = ',E10.5,/10X,'CO = ',E10.5,/'KFA = ',E10.5,/10X,
   2'FLOW = ',E10.5,/10X,'H = ',E10.5,/10X,'RHOB = ',E10.
   35,/10X,'RCOL = ',E10.5)
202 FORMAT ('MS = ',E10.5,/'DEL = ',E10.5,/'TBREAK = ',
   1F10.5,/3X,'I',4X.'C',10X,'CE',10X,'O',10X,'CDIF',10X,
   2'SUMINT',10X,'VRAT',10X,'TBED',10X,'CCO',10X,'TTOTAL'
   3,//(I4,9E13,6))
203 FORMAT (//4X,'SUMINT(N)' = ',E10.5)
204 FORMAT(//4X,'MS = ',E10.5,/4X,'A = ',E10.5)
220 FORMAT (///4X,'TFI = ',E10.5)
222 FORMAT (//4X,'F = ',E10.5,/4X,'SAT = ',E10.5,/4X,'TBP
   1= ',E10.5,/4X,'VX = ',E10.5,/4X,'TX = ',E10.5)
    END
```